Effects of Zirconia Nanoparticles on the Physico-Mechanical Properties of High-Impact Heat-Cured Acrylic Resin Denture Base

A thesis submitted to the University of Manchester for the degree of

Doctor of Philosophy

Faculty of Biology, Medicine and Health

2020

Saleh Imhammed Hassan Zidan

School of Medical Sciences

Division of Dentistry

Table of Contents

Table of Contents ______ 2

List of Figures ______ 9

List of Tables ______ 13

List of Abbreviations, Symbols and Units ______ 15

Abstract ______ 17

Declaration ______ 19

Copyright Statement ______ 20

The Author ______ 21

Dedication ______ 23

Acknowledgements ______ 24

Chapter 1: General Introduction and Literature Review ______ 25

1.1. INTRODUCTION ______ 26

1.2. DEVELOPMENT OF ACRYLIC RESINS DENTURE BASE MATERIALS ______ 27

1.3. CLASSIFICATION OF ACRYLIC RESINS DENTURE BASE MATERIALS ______ 27

1.3.1. Heat-Cured Poly methyl methacrylate ______ 27
1.3.2. Self-Cured polymethyl methacrylate ______ 28
1.3.3. Microwave polymerized poly methyl methacrylate ______ 28
1.3.4. Visible Light-activated acrylic resin ______ 28

1.4. HEAT-CURED ACRYLIC RESINS ______ 29

1.4.1. Composition of heat-cured acrylic resin denture bases ______ 29
1.4.2. Polymerisation reaction ______ 31
1.4.3. Processing of heat-cured acrylic resin ______ 32
1.4.4. Effect of curing cycles on acrylic resin denture bases ______ 32

1.5. ALTERNATIVE POLYMERS ______ 33

1.6. REINFORCEMENT OF ACRYLIC RESINS DENTURE BASE MATERIALS ______ 34

1.7. APPLICATION OF ACRYLIC RESINS IN DENTISTRY ______ 37

1.8. PROPERTIES OF HEAT-CURED ACRYLIC RESIN DENTURE BASE ______ 38

1.8.1. Mechanical properties ______ 38

1.8.2. Physical properties 40

1.8.3. Biocompatibility properties 41

1.8.4. Comparison properties of different types of heat-cured acrylic resins. 41

1.9. JUSTIFICATION FOR HIGH IMPACT HEAT-CURED ACRYLIC RESINS 43

1.10. DEVELOPMENT OF ZIRCONIA IN DENTISTRY 46

1.10.1. Phases structure of zirconia 46

1.10.2. Types of zirconia used in dentistry 48

1.10.3. Application of zirconia in dentistry 49

1.11. PROPERTIES OF ZIRCONIA 49

1.11.1. Mechanical and physical properties of yttrium stabilised zirconia (Y-TZP) 49

1.11.2. Biocompatibility properties of zirconia 50

1.12. THE CLINICAL PROBLEM 50

1.13. NOVELTY 52

Chapter 2: Aims and Objectives 53

2.1. AIM 54

2.2. OBJECTIVES 54

2.3. CHAPTER OUTLINE 55

Chapter 3: Methodology 56

3.1. INTRODUCTION 57

3.2. PREPARATION AND CHARACTERIZATION OF RAW MATERIALS 57

3.2.1. Characterisation of ZrO_2 and HI PMMA powders 57

3.2.2. Silanisation of zirconia nanoparticles 57

3.2.3. Assessment of silanised and non-silanised zirconia 58

3.2.4. Selection of concentration of ZrO_2 to HI PMMA resin-Pilot study 58

3.3. PREPARATION OF SPECIMENS 60

3.3.1. Mixing of Zirconia with PMMA 60

3.3.2. Packing and curing 60

3.4. ASSESSMENT OF MECHANICAL PROPERTIES 61

3.4.1. Flexural strength, flexural modulus 61

3.4.2. Fracture toughness 63

3.4.3. Impact strength 64

3.4.4. Surface hardness 65

3.5. ASSESSMENT OF PHYSICAL PROPERTIES 66

3.5.1. Sorption and solubility 66

3.5.2. Measurement of colour stability 68

3.6. ASSESSMENT OF POLISHABILITY 70

3.6.1. Roughness measurement machine-Talysurf CLI 1000 70

3.6.2. Specimen surface preparation 71

3.6.3. Roughness measurement 72

3.7. EVALUATION OF TENSILE BOND STRENGTH 73

3.7.1. Preparation of acrylic resin teeth 73

3.7.2. Preparation of the moulds and specimens 74

3.7.3. Evaluation of tensile bond strength (TBS) 77

3.8. EVALUATION OF EQUIVALENT FLEXURAL STRENGTH 78

3.8.1. Preparation of wax denture 78

3.8.2. Preparation of denture base specimens 80

3.8.3. Measurement of fatigue loading using a chewing simulator 81

3.8.4. Evaluation of equivalent flexural strength 82

Chapter 4: Chemical Characterisation of Silanised Zirconia and its Effects on the Properties of PMMA-Zirconia Nanocomposites 85

4.1. ABSTRACT 86

4.2. INTRODUCTION 87

4.3. MATERIALS AND METHODS 88

4.3.1. Materials 88

4.3.2. Specimen preparation 89

4.3.3. Materials Characterization 91

4.3.4. Mechanical tests 91

4.3.5. Imaging of particles and fractured surface 92

4.3.6. Statistical analysis of test results 92

4.4. RESULTS 93

4.4.1. Surface morphology analysis of particles 93

4.4.2. Chemical analysis of particles 93

4.4.3. Analysis of zirconia functionalising by silane 94

4.4.4. Flexural strength and modulus 97

4.4.5. Vickers Hardness 98

4.4.6. Fractured surface analysis 100

4.5. DISCUSSION 100

4.6. CLINICAL IMPLICATIONS 104

4.7. CONCLUSION 104

Chapter 5: Investigating the Mechanical Properties of ZrO_2-Impregnated PMMA Nanocomposite for Denture-Based Applications 105

5.1. ABSTRACT 106

5.2. INTRODUCTION 107

5.3. MATERIAL AND METHODS 109

5.3.1. Materials 109

5.3.2. Specimen Preparation 109

5.3.3. Mechanical Characterization of the Nanocomposite 111

5.3.4. Scanning Electron Microscopy (SEM) Examination 114

5.3.5. Statistical Analyses 114

5.4. RESULTS 115

5.4.1. Visual Analysis 115

5.4.2. Mechanical Tests 115

5.4.3. Microstructural Characteristics 118

5.5. DISCUSSION 119

5.6. CONCLUSION 123

Chapter 6: Physical Properties of Zirconia-Impregnated PMMA Nanocomposite 125

6.1. ABSTRACT 126

6.2. INTRODUCTION 128

6.3. MATERIALS AND EXPERIMENTAL METHOD 130

6.3.1. Materials 130

6.3.2. Preparation of Specimens 131

6.3.3. Sorption and solubility test procedures 132

6.3.4. Colour measurement procedure 134

6.3.5. Statistical analyses 135

6.4. RESULTS 136

6.4.1. Solubility and sorption analysis 136

6.4.2. Colour change 140

6.5. DISCUSSION 145

6.6. CLINICAL IMPLICATIONS 153

6.7. CONCLUSION 153

Chapter 7: Polishability of Zirconia Impregnated PMMA Nanocomposite 154

7.1. ABSTRACT **155**

7.2. INTRODUCTION **156**

7.3. MATERIALS AND EXPERIMENTAL METHOD **158**

7.3.1. Materials 158
7.3.2. Preparation of Specimens 158
7.3.3. Surface roughness measurements 161
7.3.4. Imaging of particle surface morphology 162
7.3.5. Statistical analyses 162

7.4. RESULTS **162**

7.4.1. Analysis of surface roughness 162
7.4.2. Particle surfaces analysis 165
7.4.3. Specimen surfaces analysis 169

7.5. DISCUSSION **171**

7.6. CLINICAL IMPLICATIONS **174**

7.7. CONCLUSION **174**

Chapter 8: Tensile Bond Strength between Denture Teeth and Zirconia Impregnated PMMA Nanocomposite 176

8.1. ABSTRACT **177**

8.2. INTRODUCTION **179**

8.3. MATERIALS AND EXPERIMENTAL METHOD **182**

8.3.1. Tooth and denture base materials 182
8.3.2. Surface treatment of zirconia nanoparticles 182
8.3.3. Preparation of denture teeth 183
8.3.4. Preparation of specimens 184
8.3.5. Tensile bond strength (TBS) test 185
8.3.6. Examination of fractured specimens 187
8.3.7. Statistical analyses 188

8.4. RESULTS **188**

8.4.1. Tensile bonding strength 188
8.4.2. Fractured sample analysis 192

8.5. DISCUSSION **193**

8.6. CLINICAL IMPLICATIONS **198**

8.7. CONCLUSION **198**

Chapter 9: Equivalent Flexural Strength for Complete Removable Dentures made of Zirconia Impregnated PMMA Nanocomposites 200

9.1. ABSTRACT 201

9.2. INTRODUCTION 202

9.3. MATERIALS AND EXPERIMENTAL METHOD 204

9.3.1. Materials 204
9.3.2. Preparation of complete removable dentures 204
9.3.3. Mechanical strength test 207
9.3.4. Qualitative fractured surface analysis 209
9.3.5. Statistical analysis 209

9.4. RESULTS 210

9.4.1. Weight and visual analysis of denture specimens 210
9.4.2. Cyclic Fatigue loading 211
9.4.3. Equivalent Flexural strength 211
9.4.4. Failure modes of complete dentures 213
9.4.5. Fractured specimen analysis 215

9.5. DISCUSSION 219

9.6. CLINICAL IMPLICATIONS 223

9.7. CONCLUSION 223

Chapter 10: Summary, Conclusions and Future Work 224

10.1. INTRODUCTION 225

10.2. Selection of the methods 225

10.3. SUMMARY OF THE KEY FINDINGS 226

10.3.1. Chemical properties 226
10.3.2. Mechanical properties 227
10.3.3. Physical properties 228
10.3.4. Polishability 230
10.3.5. Tooth bonding 231
10.3.6. Mastication simulation 232

10.4. CONCLUSIONS 232

10.5. FUTURE WORK AND RECOMMENDATIONS 234

References 236

Appendix 255

Cluster formation 255

PUBLISHED PAPER FROM CHAPTER 5 AND CHAPTER 9 255

Word Count: 58, 946

List of Figures

Figure 1.1. Chemical structure of polymethyl methacrylate (PMMA) (drawn by ChemDraw software, version 12)...........30

Figure 1.2. Chemical structure of methyl methacrylate (MMA) (drawn by ChemDraw software, version 12)...........30

Figure 1.3. Comparison of fracture toughness between HI PMMA and conventional PMMA resins (Graphs drawn by Granta EduPack software)...........44

Figure 1.4. Comparison of elastic modulus and strength between HI PMMA and conventional PMMA resins (Graphs drawn by Granta EduPack software)...........45

Figure 1.5. Comparison of flexural strength between HI PMMA and conventional PMMA resins (Graphs drawn by Granta EduPack software)...........45

Figure 1.6. Zirconium oxide (ZrO_2) in a natural form (Vagkopoulou et al., 2009)...........47

Figure 1.7. Crystal structure of monoclinic (a) tetragonal (b) and cubic zirconia (c) (Volpato et al., 2011). 47

Figure 2.1. Presents details of chapters within the thesis with a brief description...........55

Figure 3.1. Steps of the silanisation procedure of zirconia nanoparticles with silane couple agent...........58

Figure 3.2. Design of three different moulds according to the type of tests undertaken, (A) flexural strength and surface hardness (B) impact strength and (C) fracture toughness...........61

Figure 3.3. Photograph detailing the set-up of the Zwick universal testing machine and specimen (65 mm ×10 mm × 2.5 mm) placed between bending supports with a gap of 50 mm...........62

Figure 3.4. Photograph illustrating a sample undergoing fracture toughness testing on the Zwick universal testing machine. Crack propagation through the sample can be observed...........64

Figure 3.5. A micro-hardness testing instrument with diamond Vickers indenter in action to indent the top surface of specimen (inset)...........66

Figure 3.6. Design of two moulds used for preparation of specimens: (A) sorption and solubility and (B) colour stability and surface roughness...........68

Figure 3.7. Pictures illustrating Minolta Chroma Meter instrument. Measurement of colour change of specimen performed in the holder of Chroma Meter (inset)...........70

Figure 3.8. Diagram from profilometer of surface roughness instrument Talysurf CLI 1000 representing the working principle of the chromatic length aberration (CLA) confocal point gauge through measurement. (Precision, 2009)..........71

Figure 3.9. The surface roughness profilometer instrument set up. Specimen was placed on a precision X/Y stage for measuring using of non-contact method (inset)...........72

Figure 3.10. Photographs illustrating the tooth preparation for TBS tests (a) Different types of grooved anterior teeth and (b) a sample groove dimensions of a canine tooth..........73

Figure 3.11. Photograph of the metal grip former used in fabricating TBS test specimen...........74

Figure 3.12. Photograph of (A) Wax base with teeth and (B) wax base specimen in the flask..........75

Figure 3.13. Photographs illustrating the steps involved in duplicating the wax specimen in the grip former by Addition cured 2-part silicone putty: (A) creating silicone putty duplication mould (B) placing maxillary anterior teeth in the duplication mould, (C) placing duplication mould containing teeth in the grip former and pouring denture wax and (D) removing final wax specimen from the silicone putty mould. 76

Figure 3.14. Photograph of the jig used to displace teeth from the test specimens 77

Figure 3.15. Bonding strength test set-up under tensile loading condition using Hounsfield universal testing machine... 78

Figure 3.16. Photograhs illustrating (A) Silicone mould poured with high-strength plaster stone, (B) Silicone mould and maxillary edentulous master cast. 79

Figure 3.17. Photographs detailing (A) Maxillary master cast with teeth set on occlusion rim fixed on articulator and (B) Wax denture on a cast placed into dental plaster contained within a flask. 79

Figure 3.18. Chewing simulator instrument with denture base specimen fixed to the chamber base on the cast for mastication simulation under fatigue cyclic loading (inset)... 82

Figure 3.19. Photograph demonstrating (A) Sticking emery paper on the palatal surface with a hole at the point of loading, (B) applying bending load on palatal surface of denture specimen in Hounsfield universal testing machine... 83

Figure 3.20. Photograph showing the denture thickness measurement using a micrometer at the point of loading during bending test.. 84

Figure 4.1. Photographs illustrating non-treated and silane treated zirconia nanoparticles mixed in (A, B) monomer (MMA) and (C, D) water. 90

Figure 4.2. SEM illustrating the surface morphology and size distribution of (a) HI PMMA with rubber and (b) Zirconia particles 93

Figure 4.3. SEM images and EDX spectra representing (A & B) rubber particles into PMMA powder, (C & D) PMMA particles and (E & F) zirconia nanoparticles.. 94

Figure 4.4. FTIR spectra showing (black curve, top) silane coupling agent (γ-MPS), (red curve, middle) zirconia nanoparticles after treatment with silane (γ-MPS) and (blue curve, bottom) zirconia nanoparticles without silane 96

Figure 4.5. Illustration showing the chemical bonding of silane (MPS) with zirconia (ZrO_2) nanoparticles . 97

Figure 4.6. Bar charts showing the effect of treating zirconia nanoparticles on the flexural strength of PMMA+ zirconia nanocomposites. 98

Figure 4.7. Bar chart showing the effect of treating zirconia nanoparticles on the flexural modulus of the PMMA+ zirconia nanocomposites. 99

Figure 4.8. Bar chart showing the effect of treating zirconia nanoparticles on the hardness of the PMMA+ zirconia nanocomposites.. 99

Figure 4.9. SEM micrographs detailing the fractured surfaces of (A) pure HI PMMA (B) PMMA-Zirconia nanocomposite with non-treated zirconia and (C) PMMA-zirconia nanocomposite with silane-treated zirconia 100

Figure 5.1. (A) Photograph illustrating the impact test machine and (B) position of sample in the machine before the test. 113

Figure 5.2. SEM images showing particle size and shape distributions of (A) PMMA powder and (B) zirconia nanoparticles.. 115

Figure 5.3. Vickers hardness median (kg/mm^2) after 0, 7, and 45 days of water immersion........................ 117

Figure 5.4. Representative SEM images of the fractured surfaces of impact strength test specimens at two different magnifications (1 at 10K and 2 at 50K for the control group (A) 0 wt.%, (B) 5 wt.% and (C) 10 wt.% added zirconia, respectively). 119

Figure 6.1. Line graph illustrating the mass change of specimens from six groups immersed in distilled water over 180 days 136

Figure 6.2. Line graph illustrating the mass change of specimens from six groups immersed in artificial saliva over 180 days 137

Figure 6.3. Bar chart demonstrating the mean sorption values of specimens after immersing for 90 days in distilled water and artificial saliva 139

Figure 6.4. Bar chart demonstrating the mean solubility values of specimens after immersing for 180 days in distilled water and artificial saliva 139

Figure 6.5. Photograph showing the colour changes in the control group (0 wt.%) and group containing 3 wt.% of ZrO_2 (A) before immersion in DW or AS, (B) after immersing for 180 days in DW and (C) after immersing for 180 days in AS. 140

Figure 6.6. Photographs showing the colour changes in the samples before and after 180 days' immersion in different solutions. 141

Figure 6.7. Line graph showing the colour change according to NBS unit system in specimens immersed in DW, Steradent (STD) and Milton (MIL) for 180 days... 145

Figure 7.1. Photograph demonstrating specimens with different wt.% of zirconia in HI PMMA acrylic resin after polishing for two minutes. 160

Figure 7.2. Photograph demonstrating the surface profile measurement of the denture base specimens with Talysurf CLI 1000 surface profiling system. 161

Figure 7.3. Box plot graph showing surface roughness of denture base materials before and after polishing (one and two minutes). 165

Figure 7.4. Particle surface morphologies of (A) PMMA and (B) Zirconia.. 166

Figure 7.5. Representative 2D and 3D surface images for the tested specimens in groups containing 0 wt.% and 3 wt. % of zirconia before and after polishing 167

Figure 7.6. Representative 2D and 3D surface images for the tested specimens in groups containing 5 wt.% and 10 wt. % of zirconia before and after polishing 168

Figure 7.7. Representative SEM micrographs of the tested specimens in the groups containing (0 wt.%, 1.5 wt.% and 3 wt.% of zirconia) before and after polishing (two-minute). 170

Figure 7.8. Representative SEM micrographs of the tested specimens in the groups containing (5 wt.%, 7 wt.% and 10 wt.% of zirconia) before and after polishing (two-minutes). 171

Figure 8.1. Photograph of (a) Different types of grooved anterior teeth and (b) a sample groove dimensions of a canine tooth. 183

Figure 8.2. Photographs illustrating the steps of duplication of wax specimen in the grip former by Addition cured 2-part silicone putty: (A) creating silicone putty duplication mould (B) placing maxillary anterior teeth in the duplication mould, (C) placing duplication mould containing teeth in the grip former and pouring denture wax and (D) removing final wax specimen from the silicone putty mould..................................... 185

Figure 8.3. Schematic diagram of prepared specimen with different dimensions (adapted from (Kurt et al., 2012))......186

Figure 8.4.Photogrpah of the jig used for pulling teeth from the test specimen.......186

Figure 8.5. Photograph illustrating the bonding strength test set-up under tensile loading condition using Hounsfield universal testing machine......187

Figure 8.6. Line graph showing the representative force vs extension graphs for different test groups during TBS tests......189

Figure 8.7. Bar chart showing the mean and standard deviation of TBS values between anterior teeth (central, lateral and canine) and denture base nanocomposites.......190

Figure 8.8. Bar chart showing the modes of tooth failures in the studied groups.......191

Figure 8.9. Correlation between zirconia nanoparticle concentrations and tensile bond strength for canine teeth.......191

Figure 8.10. Photographs of (A) Canine tooth with groove (dotted boxes highlight the failed area), (B) broken canine tooth from groove root (C) part of the denture base with broken parts of tooth from the groove (dotted areas in B and C highlight matching broken surfaces in tooth and HI PMMA nanocomposite body) and (D) filling of tooth groove by denture base material.......192

Figure 8.11. SEM images of fracture surfaces: (A) mixed cohesive failure with part of denture base material on tooth surface (B) mixed cohesive failure with layer of denture base material on tooth surface and (C) cohesive failure within tooth showing cracks and their propagation on the fractured tooth surfaces.......193

Figure 9.1. Photographs showing (A)Test set-up for mastication simulation under fatigue cyclic loading and (B) schematic diagram of mastication fatigue loading......207

Figure 9.2. (A) Applying bending load on palatal surface of denture specimen in Hounsfield universal testing machine, (B) schematic diagram of loading condition.......209

Figure 9.3. Photographs showing dentures from different specimen groups (a) control group (0 wt.% zirconia) (b) 3 wt.% zirconia and (c) 5 wt.% zirconia.......210

Figure 9.4. Line graph illustrating typical bending load vs deflection curves without fatigue loading for pure HI PMMA and zirconia reinforced nanocomposites.......212

Figure 9.5. Bar chart showing equivalent flexural strengths of complete dentures with and without fatigue cyclic loading.......212

Figure 9.6. Photographs showing the failure modes observed in the dentures during the bending tests: Midline fracture, Localised fracture and Crack.......214

Figure 9.7. Complete denture failure modes with and without fatigue cyclic loading......216

Figure 9.8. Fractured surfaces of denture specimens with fatigue cyclic loading during bending tests at different magnifications.......217

Figure 9.9. Fractured surfaces of dentures with fatigue cyclic loading during bending tests showing surface characteristics at 25,000×. Arrows indicate voids and circles indicate voids filled by zirconia particles.......218

Figure 10.1. Characterisation summary of HI PMMA+ zirconia nanocomposite.......225

List of Tables

Table 1.1. Typical chemical constituents of powder component of a heat-cured resin (Bonsor and Pearson, 2013). 31

Table 1.2. Chemical constituents of the monomer component of a denture base resin (Bonsor and Pearson, 2013). 31

Table 1.3. Several key properties of conventional acrylic resins denture base and high impact rubber reinforced acrylic (Ayad et al., 2008; Craig et al., 2004; Miettinen and Vallittu, 1996; Vojdani et al., 2012; Zappini et al., 2003, Asar et al., 2013). 42

Table 1.4. Results of fracture toughness of seven heat-cured acrylic denture bases in mean values and SDs (Zappini et al., 2003). 43

Table 1.5. Mechanical and physical properties of zirconia (Madfa et al., 2014; Mihai et al., 2014). 50

Table 3.1. Raw materials used in this research. 57

Table 3.2. Weight percentage of silanised zirconia in combination with acrylic resin powder as well as monomer content of the specimen groups. 59

Table 3.3. Mean (MPa) and Standard deviation (SD) values of flexural strength for specimens of a pilot study on HI PMMA-ZrO_2 *nanocomposites with concentrations (1.5%, 10% and 15wt% of* ZrO_2*).* 59

Table 3.4. Weight percent zirconia in combination with acrylic resin powder as well as monomer content of the specimen groups. 61

Table 3.5. Composition of artificial saliva (Williams et al., 2001) 68

Table 3.6. Weight percent zirconia in combination with acrylic resin powder as well as monomer content of the specimen groups. 76

Table 4.1. Weight percent zirconia in combination with acrylic resin powder as well as monomer content of the specimen groups. 90

Table 4.2. Bond type and wavelength of Silane coupling agent, 3-trimethoxysilyl propyl methacrylate (γ-MPS) and silanized zirconia nanoparticles. 95

Table 4.3. Mean and standard deviation (SD) values of flexural strength, flexural modulus and Vickers hardness for the test groups. 98

Table 5.1 Weight percent zirconia in combination with acrylic resin powder as well as monomer content of the specimen groups. HI: High impact; PMMA: Poly-methyl methacrylate; MMA: methyl methacrylate. .. 110

Table 5.2. Mean (MPa) Standard deviation (SD) values of flexural strength, flexural modulus and fracture toughness as well as median of impact strength (kJ/m^2*) Interquartile range (IQR) for the test groups.* 116

Table 5.3. Vickers hardness (kg/mm^2*) (median and interquartile range) after 0, 7 and 45 days of water immersion.* 118

Table 6.1. Materials and denture cleaners used in this study 131

Table 6.2. Weight percent zirconia in combination with acrylic resin powder as well as monomer content of the specimen groups. 132

Table 6.3. Composition of artificial saliva (Williams et al., 2001) 134

Table 6.4. Critical marks of colour difference according to the National Bureau of Standards (Hong et al., 2009)............ 135

Table 6.5. Mean and standard deviation values of sorption (µg/mm^3) and percentage of sorption (%) after 90 days of storage in distilled water; solubility (µg/mm^3) and its percentage (%) values after 180 days.......... 138

Table 6.6. Mean and standard deviation values of sorption (µg/mm3) and percentage of sorption (%) after 90 days of storage in artificial saliva; solubility (µg/mm^3) and its percentage (%) values after 180 days........ 138

Table 6.7. Mean & SD baseline colour measurements after 24 hours' immersion in distilled water. 141

Table 6.8. Median values and Interquartile Range (IQR) of colour change and National Bureau of Standards (NBS) unit for specimens (control 0%, 1.5%, 3%, 5%, 7% and 10 wt.% of zirconia) immersed in distilled water, Steradent and Milton over time............ 142

Table 6.9. The median colour change values and statistical differences of specimens following immersion in STD and MIL compared to DW over time............ 143

Table 6.10. Colour change values after 180 days according to NBS unit system............ 144

Table 7.1. Materials used in making PMMA-zirconia nanocomposites............ 158

Table 7.2. Weight percent of zirconia in combination with acrylic resin powder as well as monomer content in the specimen groups............ 159

Table 7.3. 2D Surface roughness values for different denture base materials before and after polishing at different polishing times............ 163

Table 7.4. 3D Surface roughness values for different denture base materials after polishing at different polishing times............ 163

Table 8.1. Materials used in this study............ 182

Table 8.2. Weight percent zirconia in combination with acrylic resin powder as well as monomer content of the specimen groups............ 183

Table 8.3. Mean and Standard deviation (SD) of tensile bond strength values (N) with a count of teeth failure types............ 189

Table 9.1. Materials used in making complete removable dentures 205

Table 9.2. Weight percent zirconia in combination with acrylic resin powder as well as monomer content of the specimen groups............ 205

Table 9.3. Weight of complete dentures made of pure PMMA and zirconia impregnated PMMA 210

Table 9.4. Maximum force (N) and mean & SD of values the equivalent flexural strength (MPa) before and after fatigue cyclic loading for the test groups. 213

Table 9.5. Failure modes of complete dentures with and without fatigue cyclic loading............ 214

Table 10.1. Summary table of test results of HI PMMA zirconia nanocomposite compared to the HI PMMA (control group). 233

List of Abbreviations, Symbols and Units

PMMA	Polymethyl methacrylate
MMA	Methyl methacrylate
HI	High impact heat-cured acrylic resin
TBS	Tensile bond strength
UHMPE	Ultra-high modulus polyethylene
SENB	Single-edge notched bend
K_{IC}	Fracture toughness
Y-TZP	Yttrium tetragonal zirconia poly crystal
Mg-PSZ	Magnesium partially stabilized zirconia
ZTA	Zirconia-toughened alumina
HVN	Vickers hardness number
SEM	Scanning electron microscope
EDX	Energy Dispersive X-ray
FTIR	Fourier Transform Infrared Spectroscopy
ISO	International Organization for Standardization
W_{SP}	water sorption
W_{SL}	water solubility
STD	Steradent (dental cleaner)
MIL	Milton
DW	Distilled water
AS	Artificial saliva
NBS	American National Bureau of Standards
γ-MPS	3-trimethoxysilyl propyl methacrylate
C=C	Carbon double bond
IQR	Interquartile range
RPM	Rapid speed mixing
SD	Standard deviation
GPa	Gigapascal
MPa	Megapascal
Kv	Kilovolt
°C	Centigrade
d	Day
h	Hour
Sec	Second(s)
nm	Nanometer
µm	Micrometer

mm	Millimeter
wt%	Percentage content by weight
cm^{-1}	Wavelength unit
P/L	Powder to monomer ratio
ml	Millilitre
g	Gram
mg	Milligram
g/l	Gram per litre
$\mu g/mm^3$	Microgram per cubic millimetre
Hz	Frequency or cycles per second
$\boldsymbol{a_{iN}}$	Charpy impact strength
ΔE	Colour change
p	Estimated probability
pH	Potential hydrogen
Ra	Average surface roughness (Line)
Sa	Average surface roughness (Area)
WOF	The work of fracture toughness

Abstract

Polymethyl methacrylate (PMMA) has been commonly used as a material for fabricating denture base since 1937. However, this material displays relatively poor mechanical and physical properties under clinical application. To address the mechanical properties issues, PMMA heat-cured acrylic resin denture base was reinforced with rubber to form a new high-impact version of PMMA resin with improved impact strength. However, this has negatively affected the flexural and fatigue properties. The aim of the present research was to develop and characterise new denture base nanocomposites made of high-impact (HI) heat-cured PMMA resin impregnated with different concentrations of zirconia nano fillers, and to assess their mechanical and physical properties.

Initially, PMMA resin reinforced with silanised and non-silanised zirconia (ZrO_2) nanoparticles at a concentration of 3wt.% was evaluated. It was found that the PMMA resin with silanised zirconia showed a significant increase ($p<0.05$) in flexural strength and surface hardness. Subsequently, the mechanical properties (flexural strength, fracture toughness, impact strength, and hardness) of HI PMMA denture base acrylic resin impregnated with different concentrations of zirconia nanoparticles (0% (control), 1.5 wt%, 3 wt%, 5 wt%, 7 wt%, and 10 wt%) were further evaluated. HI PMMA-zirconia nanocomposites significantly improved flexural strength, flexural modulus, fracture toughness and surface hardness with an optimum concentration of approximately 3wt%–5 wt% zirconia.

Sorption and solubility were assessed after six months storage in distilled water and artificial saliva. Colour stability was also assessed after exposure of the specimens to distilled water and different denture cleaners (Steradent and Milton) for six months. The nanocomposite at 3 wt% of zirconia displayed the lowest sorption and solubility in both media. In addition, the colour change for the nanocomposite group containing upto 3 wt% zirconia was clinically acceptable.

The polishability of the PMMA-zirconia nanocomposite was assessed by measuring surface roughness at different polishing times (one-minute and two minutes) with conventional laboratory polishing techniques. The nanocomposite at low concentrations (1.5 wt.%, 3 wt.% and 5 wt.%) did not affect the surface finish negatively after conventional polishing employed for fabricating the denture base as the surface roughness remained below the clinically acceptable limit (0.2 µm).

Tensile bond strength (TBS) between anterior acrylic teeth and PMMA-zirconia nanocomposite was evaluated by following a British Standard testing procedure. It was found that the nanocomposites at high concentration (7 wt% and 10 wt %) significantly ($p<0.05$) reduced the bonding strength.

The equivalent flexural strength of complete removable dentures made of HI PMMA zirconia nanocomposite was assessed with and without fatigue cycling. Denture specimens made of 5 wt.% zirconia nanocomposites significantly improved equivalent flexural strength without fatigue loading.

Both fundamental material tests (chemical, mechanical and physical) and functional tests (polishability, bond strength and equivalent flexural strength) on PMMA-zirconia nancomposite for the fabrication of denture bases indicated that an optimum concentration of approximately 3 wt% to 5 wt% of zirconia can improve the functional life of the denture base in clinical applications.

Declaration

I declare that that no portion of the work referred to in the thesis has been submitted in support of an application for another degree or qualification of this or any other university or other institute of learning.

Student Name: Saleh Imhammed Hassan Zidan

Student ID: 9604648

Copyright Statement

i. The author of this thesis (including any appendices and/or schedules to this thesis) owns certain copyright or related rights in it (the “Copyright”) and s/he has given The University of Manchester certain rights to use such Copyright, including for administrative purposes.

ii. Copies of this thesis, either in full or in extracts and whether in hard or electronic copy, may be made only in accordance with the Copyright, Designs and Patents Act 1988 (as amended) and regulations issued under it or, where appropriate, in accordance with licensing agreements which the University has from time to time. This page must form part of any such copies made.

iii. The ownership of certain Copyright, patents, designs, trademarks and other intellectual property (the “Intellectual Property”) and any reproductions of copyright works in the thesis, for example graphs and tables (“Reproductions”), which may be described in this thesis, may not be owned by the author and may be owned by third parties. Such Intellectual Property and Reproductions cannot and must not be made available for use without the prior written permission of the owner(s) of the relevant Intellectual Property and/or Reproductions.

iv. Further information on the conditions under which disclosure, publication and commercialisation of this thesis, the Copyright and any Intellectual Property and/or Reproductions described in it may take place is available in the University IP Policy (see http://documents.manchester.ac.uk/DocuInfo.aspx?DocID=24420), in any relevant Thesis restriction declarations deposited in the University Library, The University Library’s regulations (see http://www.library.manchester.ac.uk/about/regulations/) and in The University’s policy on Presentation of Theses.

The Author

I graduated from the college of Medical Dental Technology at University of Misurata-Libya in 1997. I worked as a Dental Technician in Dental Compound Clinic Sabha, Libya, between 1998 and 2006. I was awarded a scholarship from the Ministry of Higher Education in Libya to complete my postgraduate study. I joined a one-year full-time Master degree course in Dental Material Science at University of Queen Marry, London in 2007. I worked as a teaching staff member in the department of Dental Materials in the School of Dentistry at the University of Sebha-Libya between 2009 and 2014. I decided to complete my PhD in Dental Materials Science. Further encouragement was received from one of my best friends from Iraq. I was really interested in dental materials because I would like to develop new materials that will be useful to a dental clinic. I was awarded another scholarship by the Ministry of Higher Education to study PhD. In April 2016, I enrolled for PhD research program (Doctor of Biomaterials Science and Dental Technology) at the University of Manchester, UK.

Publications-Conference

I have presented aspects of my research at the following conferences/meetings:

1. Title: Effects of zirconia-nano-filler on mechanical properties of heat-cured denture base.

- General Conference & Exhibition, Manchester, University of Manchester in June 2017.
- Event of school of Dentistry University of Manchester in March (2018)

2. Title: Investigating the effects of Zirconia nano-filler on mechanical properties of high impact heat-cured acrylic resin denture base.

- Poster at Conference of the Academy of Dental Materials (ADM) annual meeting in Nuremberg (Germany) in October (2017).

3. Title: Evaluating the Effects of Silane Treated Filler on the Properties of Zirconia-PMMA Nanocomposite for Denture Base.

- Poster at Second Annual Doctoral Academy PhD Conference, Manchester faculty of biology, medicine and health University of Manchester in June (2018).
- Poster at IADR Conference, General Session & Exhibition, London (UK), July (2018).

4. Title: Effects of Silane Treated Filler on the Properties of Zirconia-PMMA Nanocomposites.

- Oral presentation at Event of school of Dentistry University of Manchester June (2018).

5. Title: Fracture surface and clustering behaviour of zirconia reinforced high impact acrylic resin.

- Poster presented at European Dental Materials Conference (EDMC) in Brussels (Belgium) in August (2019).

Publications - International Journal

1. Zidan, S., Silikas, N., Alhotan, A., Haider, J. & Yates, J. (2019). 'Investigating the Mechanical Properties of ZrO_2-Impregnated PMMA Nanocomposite for Denture-Based Applications', Materials, 12(8), p. 1344. https://doi.org/10.3390/ma12081344

2. Zidan, S.; Silikas, N.; Haider, J.; Alhotan, A.; Jahantigh, J.; Yates, J. Evaluation of Equivalent Flexural Strength for Complete Removable Dentures Made of Zirconia-Impregnated PMMA Nanocomposites. Materials 2020, 13, 2580. https://doi.org/10.3390/ma13112580

Publication in Progress

1. Assessing Tensile Bond Strength between Denture Teeth and nano-Zirconia Impregnated PMMA Denture Base – planned to be submitted in Journal of Materials Science and Engineering
2. Chemical Characterisation of Silianised Zirconia and its Effects on the Properties of PMMA-Zirconia Nanocomposites – planned to be submitted in Dental Materials
3. Physical Properties of Zirconia-Impregnated PMMA Nanocomposite – planned to be submitted in Dental Materials Journal
4. Polishability of Zirconia Impregnated PMMA Nanocomposite – planned to be submitted in Journal of Dentistry

Dedication

“Say: My Lord, increase me in knowledge”

IN THE NAME OF ALLAH

And with His blessing

The All-Knowing, The Most-Wise

All praises are due to ALLAH for his merciful guidance throughout my life and gave me good heath to achievement this thesis.

I would like to dedicate my work to my beloved parents and grandfathers and grandmothers, the spring of love, who have raised me on passion and dedication for acquiring knowledge.

This thesis is also dedicated to my loving wife and my children and my brothers and sisters and all my uncles and aunts who were always there for me whenever I need.

Finally, I would also like to dedicate this work to my close friends, thank you for supporting and encourage me during my study.

Acknowledgements

I would like to express my sincerest gratitude and appreciation to my supervisors, Prof. Julian Yates, Prof. Nick Silikas and Dr Julfikar Haider for their guidance and support throughout my PhD study. This thesis would not have been possible without their tremendous effort and guidance in their capacity as supervisors. I really enjoyed working under their supervisions, as they have supported me with a lot of advice when I needed help to make this project successful. I would also like to thank Prof. Julian Satterthwaite for his advice as my academic advisor as well as Prof. David Watts for his invaluable advice.

I would like to acknowledge Mr. Brian Daber and Mr. Paul Murphy for their great assistance and help throughout my study. My thanks are also extended to a group of post-doctoral students at the Division of Pharmacy at University of Manchester during silanization procedure. My sincere thanks go to Mr. Michael Green for mechanical and functional testing and manufacturing of the jigs and fixtures and Dr. Hayley Andrews for SEM imaging, EDX and FTIR studies at the Faculty of Science and Engineering, Manchester Metropolitan University. Also, I would to thank Mr. Gary Pickles from School of Materials, University of Manchester.

Throughout my PhD, I would like to give special thanks to my dear colleagues who have supported and helped me during the use of laboratory equipment as well as to analyse specific data. I wish to give them all the credits they deserve.

I am also grateful to Mrs. Joy Stewart for giving me support and advice during my study. Mr. Lea at the library team of Endnote, University of Manchester for his time and effort for manging thesis references.

Last but not least, it is my great pleasure to thank the Ministry of Higher Education of Libya for providing financial support throughout my PhD study.

Chapter 1: General Introduction and Literature Review

1.1. INTRODUCTION

There are many people around the world with missing teeth; significant numbers of them wear partial or full dentures or have crowns or bridges. In addition to this, some may even have implant retained prostheses. In order to maintain function, appearance and oral health, these patients may want to replace their missing teeth. The way in which this is done is dependent on the clinical picture presented to the treating clinician. If patients desire, for, or have no alternative but to wear a denture, they may wish to know about the material used for a dental prosthesis and whether it has adequate qualities for the role. This may include the material used for both the base of the denture and the teeth. Denture base resin is the part of the denture that rests on the supporting tissues and to which artificial teeth are attached (McCabe and Walls, 2009).

The prosthetic replacement of teeth is not new; the construction of dental prostheses has been documented in Egypt as early as 2500 BC. Use of artificial teeth in dentures has also been reported. Throughout the centuries, teeth have been removed from the deceased and collected from poor and deprived people who were forced to sell them. In addition to human teeth, animal teeth including hippopotamus teeth or elephant ivory were also used, which were then cut to the appropriate size and shape prior to use (Johnson, 1959). The early dental protheses were carved from naturally occurring materials, with ivory, bone and wood all being employed (Elshereksi et al., 2014). Other examples of removable prostheses have also been discovered. Upper and lower complete denture made from Ox femur in the early 1500 BC has been discovered in Switzerland. They were fabricated from two arch-shaped templates of bone joined at the posterior edge to form a “hinge”. However, this prosthesis appear to have been constructed more for aesthetic reasons than function (Murray and Darvell, 1993). The Etruscans (circa 700 BC) also fabricated partial dentures from carved bone and ivory. These were then attached to the existing teeth using gold wires or bands (Anusavice, 2013).

The late 18th century saw the creation of the first porcelain complete denture. The use of porcelain resulted in a product with low solubility and low water absorption, however, this came with the drawbacks of being brittle and difficult to grind (Elshereksi et al., 2014). Porcelain dentures did not improve in quality until the commercial manufacture of dentures in the mid-19th century led to new companies competing to produce teeth with natural shades and translucency (Johnson, 1959). Around this time vulcanite, a form of vulcanised rubber, was employed in the manufacture of denture bases. These dark-red bases were cheaper to produce, however they were difficult to pigment as well as posing hygiene concerns due to absorption of saliva (Elshereksi et al., 2014).

Further advancement was made by Taggert in 1907, who developed a method for producing cast inlays. Development of cast alloys allowed their use in prostheses later in the 20th century. Many types of metals and alloys are now available for removable, all-metal and metal-ceramic dentures, also being used for inlays, onlays, crowns and frameworks (Anusavice, 2013).

In 1937 Dr Walter Wright introduced PMMA as a denture base material (John et al., 2001). While methods of storage, packing and curing posed problems at the time, the material was so well-received by dentists that within a decade 98% of denture bases incorporated PMMA (Elshereksi et al., 2014; John et al., 2001; Johnson, 1959).

1.2. DEVELOPMENT OF ACRYLIC RESINS DENTURE BASE MATERIALS

Acrylic resin, or polymethyl methacrylate (PMMA), has been the most widely documented and used material in prosthetic dentistry since 1937 (Ayad et al., 2008). It is used for the manufacture of dentures and teeth and has enormous advantages over other materials, including chemical stability in the oral environment, acceptable aesthetics and accurate fit. In addition, it is relatively easy to fabricate and process in the laboratory and clinically amenable to manipulation, adjustment and repair. Furthermore, it only requires relatively cheap processing equipment (Ahmed and Ebrahim, 2014). The mechanical and physical properties of acrylic resins (polymethyl methacrylate) are also better than polystyrene resin, nylon, epoxy resin and polypropylene. However, acrylic resins typically have low strength, and fracture relatively easily (Alhareb and Ahmad, 2011).

1.3. CLASSIFICATION OF ACRYLIC RESINS DENTURE BASE MATERIALS

Acrylic resins used for denture base can be classified in different ways. These primarily relate to the different methods of curing: the application of heat, chemical reaction (self-curing), by light, or using microwave energy (Ferracane, 2001).

1.3.1. Heat-Cured Poly methyl methacrylate

The most common method of curing for PMMA is heat-polymerisation, usually with the use of a heated water-bath (Bural et al., 2011). There are two suggested methods of heat-polymerisation. The first is a long process, whereby products are maintained at a constant temperature of 74º C for 9 hours. The second method finishes the slow heating with the inclusion of a boiling phase for 30 minutes (short-term) or an hour (long-term)(Bural et al., 2011; Honorez et al., 1989). Heat-curing of PMMA results in a stronger denture base material than light- and chemical-cured, with the additional benefits of higher colour stability and lower levels of residual monomer (Elshereksi et al., 2014).

1.3.2. Self-Cured polymethyl methacrylate

This curing method is referred to as either autopolymerisation, cold cure or chemical cure. While it has the same chemical composition as heat-cured acrylic, the powder component contains beads of polymer which have a lower molecular weight when compared with those present in heat-cured PMMA. Moreover, it requires chemical polymerisation that is initiated by amine molecules. It offers a reduced curing time and can be used for repairs or immediate denture fabrication. Nevertheless, it has drawbacks that include higher levels of residual monomer that can lead to lower strength, polymerisation shrinkage, and reduced colour stability when compared to heat-cured acrylic resins. Because of these issues, it is generally accepted that acrylic dentures made by heat-polymerisation have superior mechanical, chemical and physical properties than those made by chemical polymerisation (Ferracane, 2001; Van Noort, 2007).

1.3.3. Microwave polymerized poly methyl methacrylate

The first reported use of microwave energy to cure denture base materials was by Nishii in 1968. Subsequently, Kimura developed the curing of poly-methyl methacrylate in a very short time by this technique (Singh et al., 2013). Microwave polymerisation involves inducing molecules to move in an electromagnetic field. This promotes intermolecular collision, causing generation of heat energy that is subsequently absorbed by the resin (Spartalis et al., 2015). Microwave curing allows for a shorter and cleaner process and results in a denture base that is well-adapted to the dental cast (Ferracane, 2001). This method has received limited clinical acceptance, however, despite the aforementioned advantages (Spartalis et al., 2015).

1.3.4. Visible Light-activated acrylic resin

Light-cured denture base resins were presented to the marketplace in the 1980s and were free of methyl methacrylate monomer. This type of resin can be and is used as an alternative to heat and self-cured PMMA. Investigators first reported light-activated

Urethane dimethacrylate (UDMA) denture base polymer, known as Triad (Ali et al., 2008). This light activated system had low bacterial adherence, simple manipulation and processing as well as being accepted and well tolerated by patients. Furthermore, it could bond to other denture base resins and therefore lend itself to repair adjustments of existing dentures. Nonetheless, the application of this system was limited due to its brittleness and low impact resistance. As a result of the latter, several studies have been undertaken to develop new light- and heat- activated denture base materials. Recently, studies have shown that the impact strength and flexural strength of these new light- and heat-cured materials have been favourable and higher than the older light-cured acrylic denture base materials (Ali et al., 2008).

1.4. HEAT-CURED ACRYLIC RESINS

Heat-cured acrylic resin is the most popular material for fabrication of denture bases (Salim et al., 1992). It has been reported that approximately 98% of denture bases made are with heat-cured resin as it is a hard material that is resilient enough to hold the teeth in occlusion during mastication. Heat-cured denture base resin should meet all ideal property requirements, so that an ideal prosthesis can be made (Elshereksi et al., 2014).

1.4.1. Composition of heat-cured acrylic resin denture bases

Heat-cured denture bases resin is made from powdered polymethyl methacrylate (PMMA) (Figure 1.1) and methyl methacrylate (MMA) (Figure 1.2). This composition is named conventional heat-cured (Bonsor and Pearson, 2013). The powder consists of small spheres called beads or pearls and is granular in some products. The powder can easily dissolve in monomer and, in resins that are processed by heat, has a mean particle size of approximately 150µm. Table 1.1 and Table 1.2 show the components of polymethyl methacrylate and methyl methacrylate, along with their advantages (Bonsor and Pearson, 2013).

High impact acrylic resin has a similar composition to conventional heat-cured resin and is also known as “high strength” acrylic resin (Ferracane, 2001). This variation involves the addition of butadiene-styrene rubber copolymers to the polymethyl methacrylate powder. This results a resin that consists of a matrix of PMMA with an interpenetrating network of rubber. These rubber-reinforced, or “high impact”, resins have the advantage of being able to absorb greater amounts of energy before fracture than the standard resins (Jagger et al., 1999; Sasaki et al., 2016). However, the flexural strength, modulus of elasticity and fatigue resistance are decreased in comparison to conventional heat-cured PMMA (Jagger et al., 2003).

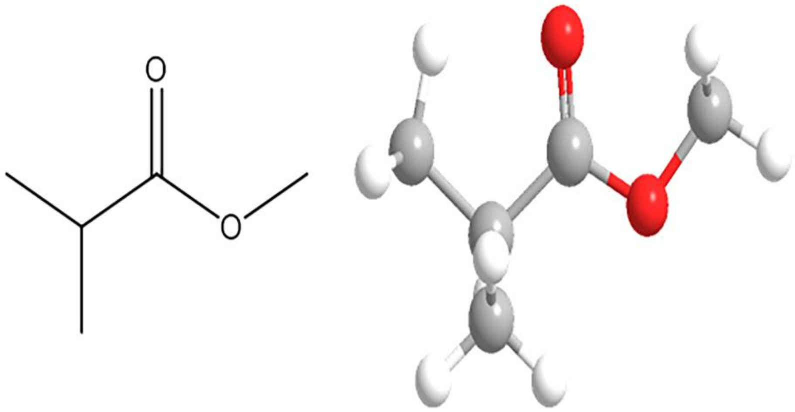

Figure 1.1. Chemical structure of polymethyl methacrylate (PMMA) (drawn by ChemDraw software, version 12).

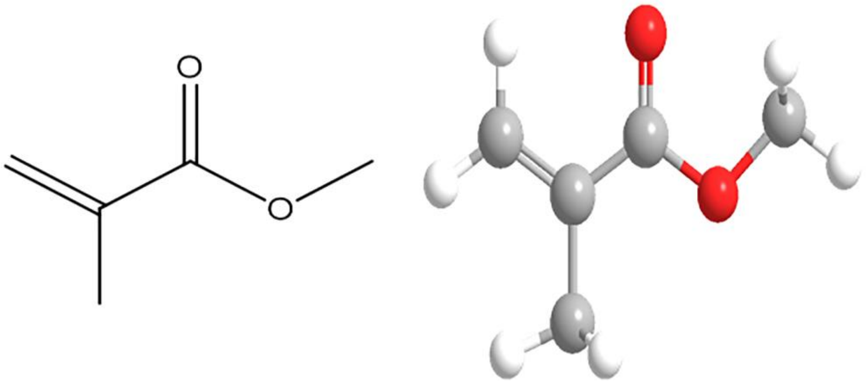

Figure 1.2. Chemical structure of methyl methacrylate (MMA) (drawn by ChemDraw software, version 12).

Table 1.1. Typical chemical constituents of powder component of a heat-cured resin (Bonsor and Pearson, 2013).

Composition	Percentage %	Reason for inclusion
Poly methyl methacrylate	95-98	Principal component
Benzoyl peroxide	1	Initiator
Titanium dioxide or Zinc oxide	< 0.5	Increases opacity to match the translucency of the oral soft tissues
Inorganic pigments: Mercuric sulphide Cadmium sulphide Ferric oxide	1	Varies colour, respectively: Red Yellow Brown
Dibutyl phthalate	< 0.5	Plasticizer
Dyed synthetic fibres-nylon or acrylic	< 0.5	Simulate anatomical structures such as capillaries within the denture base material

Table 1.2. Chemical constituents of the monomer component of a denture base resin (Bonsor and Pearson, 2013).

Composition	Percentage %	Reason for inclusion
Methyl methacrylate	97	Monomer
Hydroquinone	0.003 -0.1	Inhibitor - prevents monomer polymerizing during storage
Ethylene glycol dimethacrylate (substituted for the main monomeric component)	2 -14	Cross-linking agent
Dibutyl phthalate, butyl and octyl methacrylate	< 0.5	Plasticizer

1.4.2. Polymerisation reaction

As detailed previously, the polymerisation of PMMA can be induced by using a water bath to heat the polymer-monomer mixture (Bartoloni et al., 2000). The length of the polymeric chain increases with heat until all the monomer is converted into polymer (Spartalis et al., 2015). The active free radicals react with the double bond of the methyl methacrylate monomer molecules, converting them to single bonds (Barron et al., 1992). When the monomer molecules become activated, the polymerisation reaction can occur with the addition of further monomer units and an elongation of the polymer chain occurs. The reaction continues until either the monomer becomes unavailable or the activated molecule becomes inactive and forms the final polymer (Bartoloni et al., 2000). Within the powder, benzoyl peroxide acts as an initiator that reacts and separates into active free radicals by heating. The processing temperature should be approximately 74 ^{o}C to get reasonable rates of separation and polymerisation. The aim of conventional curing is to utilise all monomer in the formation of the polymeric chain without porosity (Bartoloni et al., 2000).

1.4.3. Processing of heat-cured acrylic resin

There are two techniques for the fabrication of denture base resins: (1) compression moulding technique and (2) injection moulding technique. Both techniques are used in laboratories depending on the preferences of dental technicians or availability of equipment. The injection moulding technique is faster than the compression moulding processing and, moreover, reduces polymerisation shrinkage and material porosity. However, it is a complicated procedure and requires specialist flasks and equipment. For this reason, many dental technicians prefer the compression moulding technique (Hatrick, 2011).

1.4.4. Effect of curing cycles on acrylic resin denture bases

1.4.4.1. Porosity

Porosity is a factor that affects the mechanical, physical and hygienic properties of processed denture bases. It has been reported that porosity within the acrylic resin can produce high internal stresses and increase the vulnerability to distortion and warping of the denture base. Porosity can be caused by air entrapment during mixing, excess or residual monomer, monomer contraction through the polymerisation process and monomer vaporization during the heat reaction (Singh et al., 2013). Furthermore, Jerolimov et al. concluded that porosity was dependent on the rate of polymerisation and the efficiency of heat dissipation. It is believed that on occasions the significant heat produced during polymerisation cannot be dissipated quickly enough, especially in the thicker regions, which then causes local vaporization of monomer within the mixture and gaseous porosity is formed within the denture base (Jerolimov et al., 1989).

1.4.4.2. Crazing

The effect of the rising temperature on the heat-curing of denture bases can lead to internal stresses and strains that can result in crazing. Polymerisation must be undertaken slowly to prevent these processing issues (Van Noort, 2007). Bonsor et al. detailed that "crazing is the presence of fine cracks on the surface of the acrylic" and that "they represent localized areas of plastic deformation of the polymer caused by stress relief of internal strain". The areas involved are filled with microscopic voids that cannot withstand the inherent stresses associated with polymerisation. As such, cracks can be formed in the areas of the denture base that are thin, unsupported or where there are processing voids. Under increased loads such as mastication the crack can then propagate and cause fracture of the denture (Bonsor and Pearson, 2013).

1.4.4.3. Allergy

It has been recommended that acrylic denture bases should be immersed in water for 24 hours after processing to remove any residual monomer that can cause irritation of the oral tissue mucosa (Ferracane, 2001). In addition to potential irritation, inflammation and allergic responses, leaching of residual monomer may also plasticise the denture base, impairing the mechanical properties (Çelebi et al., 2008). In addition, the processing should be completed accurately and in accordance with the manufacturer's instructions so that the quantity of monomer added for the polymerisation is appropriate (Ferracane, 2001).

1.5. ALTERNATIVE POLYMERS

Various studies have sought to develop polymethyl methacrylate denture base resins and improve their mechanical properties including strength, stiffness and abrasion resistance, in addition to attempting to achieve radio-opacity. Some of the polymers proposed for use in denture base include polyamides, epoxy resin, vinyl acrylic and polystyrene (Jagger et al., 1999). Polyamide has been found to have some mechanical advantages, however, is prone to staining, absorption of fluids and loss of smoothness (Macgregor et al., 1984). Nasution and Arksornnukit compared several mechanical properties of PMMA and polyamide and found that PMMA had the higher elastic modulus and nano-hardness (Nasution and Arksornnukit, 2017). Epoxy resin, in general, possesses good hardness, strength and toughness and has low polymerisation shrinkage, however, like polyamide, it suffers from high water absorption, staining with the addition of air entrapment during processing (Smith, 1962).

1.6. REINFORCEMENT OF ACRYLIC RESINS DENTURE BASE MATERIALS

During the last 30 years attempts have been made to improve the properties of acrylic resin denture base materials by reinforcement with additional materials (Jagger et al., 1999). Vallitu hypothesised that the inclusion of metal wires of sufficient rigidity may reduce dimensional changes of PMMA during polymerisation (Vallittu, 1996). Carroll and Von Fraunhofer reported in the literature that the reinforcement of PMMA denture bases with stainless steel wire resulted in improved strength (Carroll and Von Fraunhofer, 1984). Furthermore, Yu et al. fabricated complete dentures reinforced with glass fibre mesh or metal and they found a significant increase in fracture resistance with the inclusion of glass fiber mesh over the metal and non-reinforced control. This increase in strength was attributed to better bonding between the glass fiber mesh and polymer resin (Yu et al., 2015).

Studies have explored other materials used for reinforcement, including rubber, fibres, metal fillers and zirconia; all have provided different outcomes (Jagger et al.,1999; John et al., 2001). Studies have investigated additions of aramid fibre, carbon fibre (Vallittu and Lassila, 1992), ultra-high modulus polyethylene (UHMPE) fibre (Köroğlu et al., 2009) and glass fibre (Kim et al., 2012; Vallittu et al., 1994a) to polymethyl methacrylate denture base materials. Carbon and aramid fibres were not clinically acceptable due to difficulties in polishing and poor aesthetics (Kim et al., 2012). Ultrahigh-molecular-weight polyethylene fibre appears not to have a good adhesion-bond strength within poly-methyl methacrylate and therefore no significant increase in the flexural properties was demonstrated (Köroğlu et al., 2009). Vallittu et al. conducted a study to investigate transverse strength using heat-cured PMMA denture bases reinforced with a high concentration of continuous glass fibre. Glass fibre exists in three forms including woven, loose and continuous. Additionally, silane compounds have been added to enhance adhesion between polymer resin and glass fibre, so that it can improve its mechanical strength. Studies have shown that an increase in the transverse strength significantly reduced fatigue weakening in PMMA reinforced with continuous glass fibers (Vallittu et al., 1994a). Kim and Watts investigated the effect of E-glass fibre-reinforcement on the impact strength of complete dentures, finding that impact strength more than doubled when reinforced with woven E-glass fibre (Kim and Watts, 2004).

In a study conducted by Vallittu and Lassila investigating the effect of different quantities of continuous glass fibres in heat-cured polymethyl methacrylate matrix on fracture resistance, it was determined that a higher concentration of glass fibre improved the fracture resistance of PMMA (Vallittu et al., 1994a). However, Pan et al. detailed that the orientation of fibres in the resin matrix was technically difficult to predict and a random distribution could result in some defects within the material (Pan et al., 2013). Furthermore, the technicians found the handling and processing of fibres difficult during denture preparation (Jagger et al., 1999).

A study investigated a high impact acrylic resin reinforced with zirconia and its effect on impact strength, transverse strength, surface hardness, water sorption and solubility, using different quantities of zirconia: 5% and 15%. The findings of the study determined that the transverse strength was increased by increasing the percentages of filler content. In contrast, no significant improvement was observed in impact strength, surface hardness, water sorption and solubility (Ayad et al., 2008).

Another study has also been reported investigating mixtures of metal oxides such as TiO_2, ZrO_2 and Al_2O_3 micro particles in heat-cured acrylic resin to determine the effect of their inclusion on fracture toughness, impact strength, water sorption and solubility of heat-cured acrylic resin. The findings showed that metal oxides did appear to enhance the fracture toughness and impact strength of the hybrid material whilst at the same time reducing the water sorption and solubility of the material. The authors therefore concluded that the use of zirconia, when compared to other metal oxide powders, can be useful in enhancing some properties, including denture fracture resistance, and reducing some undesirable physical changes resulting from uptake of oral fluids (Asar et al., 2013).

One study reported somewhat improved flexural strength, fracture toughness and hardness of reinforced PMMA resin with concentrations of zirconia at 1.5%, 3%, and 5%, while a concentration of 7 wt.% showed the greatest improvement (Ahmed and Ebrahim, 2014).

Researchers have also investigated the differences between the reinforcement of denture base acrylic resin with zirconia nanoparticles and nanotubes. ZrO_2 nanotubes were prepared by anodization, which requires a solution containing formamide and glycerine with zirconia foils acting as the anode and platinum as the cathode. The purpose was to improve the mechanical properties of ZrO_2 nanotubes. Findings suggested that ZrO_2 nanotube-reinforced acrylic had a large surface area and porous structures after the anodization process, which improved the mechanical properties of acrylic resin.

Consequently, the flexural strength of acrylic reinforced with ZrO_2 nanotubes was higher than that reinforced with ZrO_2 nanoparticles (Yu et al., 2014).

Karci et al. sought to evaluate the effect of incorporating varying concentrations of metal oxides on the flexural strength of different acrylic resins. They added TiO_2, SiO_2 and Al_2O_3 at varying weight percentages (1%, 3% and 5%) to three different resins (heat-cure, self-cure and microwave cure PMMA). The greatest increase in flexural strength was noted at 1%, with the flexural strength reducing below that of the control in the 3% and 5% groups (Karci et al., 2019).

Moslehifard et al. examined the effect of adding titanium oxide nanoparticles on the compressive, flexural and impact strengths of PMMA. SEM imaging provided evidence that nanocomposites comprising of 1 wt.% TiO_2 had fewer micro-crack and pores. Addition of 1 wt.% titanium oxide also resulted in an increase in the impact strength of the heat cured PMMA, although this was not significant (Moslehifard et al., 2019). In accordance with Karci et al (2019), they observed a decrease in flexural and impact strength at the concentrations of nanoparticles over 1 wt%.

A literature review conducted by Gad et al., on the effects of the addition of titanium oxide nanoparticles to PMMA reported there was little agreement across studies on the benefits of the material's inclusion. The lack of consensus was attributed to the varying methodologies employed by the studies, the different manners of adding the nanoparticles and the varying nanoparticle sizes. However, one common theme was documented: lower percentages (1-2 wt%) of nano-fillers tended to improve properties while concentrations over 5 wt.% weaken the strength of the composite (Gad and Abualsaud, 2019a).

Nanodiamonds have also been used in experimental composites. Mangal et al. added varying amounts of nanodiamonds to PMMA and tested the flexural strength, elastic modulus, hardness and surface roughness in comparison to zirconia-reinforced (5 wt.%) and pure PMMA. All nanodiamond composites exhibited significantly higher flexural strengths and elastic modulus than the zirconia and pure PMMA. Higher levels (0.3 wt.% and 0.5 wt.%) of nanodiamonds also resulted in significantly improved surface hardness values compared to the pure PMMA (Mangal et al., 2019).

Composites employing more than one reinforcing agent are named hybrids. Zhang et al. investigated the hybrid effects of the incorporation of zirconia nanoparticles and alumina borate whiskers (ABW) on PMMA denture bases. They found a significant improvement in the flexural strength of all silanised hybrid groups, with the highest being the group with the combination of 2% ZrO_2 and 4% ABW(Zhang et al., 2014). Further hybrids have been explored by Gad et al., who explored the effects on flexural and impact strength of the reinforcement of PMMA with zirconia and glass fibres at different ratios. Nano-ZrO_2/GF were as follows containing (wt.%) 5%–0%, 4%–1%, 3%–2%, 2.5%–2.5%, 2%–3%, 1%–4%, and 0%–5%. Addition of the hybrid fillers significantly improved the flexural and impact strengths of PMMA, with the highest values being found in the 2.5:2.5 ratio of zirconia to glass (Gad et al., 2019b). The addition of zirconia has been documented to improve the flexural strength of PMMA, with the concentration of zirconia having a greater effect on the mechanical properties than size and silanisation of the particles (De Souza Leão et al., 2019).

Given the limited availability of published data, it can be concluded that there are a few studies that have investigated the properties of high impact acrylic resin reinforced with zirconia nanoparticles. Consequently, more research should be undertaken to investigate the addition of different concentrations of zirconia nano-fillers using highly standardised experimental techniques in order to characterise this novel combination and to see if (high impact) acrylic resin reinforced with zirconia will have superior properties to other similar materials.

1.7. APPLICATION OF ACRYLIC RESINS IN DENTISTRY

Acrylic resins have seen in many applications since their introduction to dentistry. They have been used for denture bases, artificial teeth, crowns, bridges and impression trays (Kim and Watts, 2004). Moreover, other applications include the relining of denture bases, rebasing, repairing of denture fractures, fabrication of orthodontic appliances, as well as maxillofacial materials (Goiato et al., 2015). Although adequate for some functions, the mechanical properties of existing acrylics do limit their use in some areas of dentistry. Given their excellent aesthetic and colour qualities and ease of processing, their application in areas of dentistry that may requires increased resistance to general “wear and tear” would be extremely beneficial. Therefore, optimising the properties of these acrylic materials so that they can be used in situations where high impacts and stresses are anticipated would be invaluable. Thus, investigating the properties of PMMA reinforced with zirconia nano-fillers may allow important improvements to be made.

1.8. PROPERTIES OF HEAT-CURED ACRYLIC RESIN DENTURE BASE

1.8.1. Mechanical properties

1.8.1.1. Flexural strength

One of the most important properties of polymer material is flexural strength, measured by stiffness and resistance to fracture (Jagger et al., 2002). Flexural strength is defined as the maximum stress that a material can withstand before breaking (Ferracane, 2001). The flexural strength of a material is vital during the mastication of a denture base inside the mouth. When a combination of compressive, tensile and shear strength increases, the denture base is deformed under the high load as result of flexural and fatigue failure (John et al., 2001; Li et al., 2016; Vallittu et al., 1994b). The three-point bend test is suitable for evaluating the type of stress that is applied to the prosthesis during chewing. Consequently, this test is used to assess the flexural strength of denture base resin materials (Gungor et al., 2017). Many mechanical tests that record a stress-strain curve can also be used to calculate the modulus of elasticity for the material (Ilie et al., 2017). This elastic modulus is an indication of the stiffness of a material, measured from the slope of the elastic region of the stress-strain curve (Anusavice, 2013).

1.8.1.2. Fracture toughness

The fracture of a denture base is one of the main causes of failure of denture base acrylic resin in the mouth. One of the most important measurement to assess the suitability of a dental polymer is fracture toughness, which is defined ‘the ability of a material to resist crack propagation’ (Al-Haddad et al., 2014; Hamza et al., 2004). Al-Haddad et al. described the fracture toughness as the “critical stress intensity factor (K_{IC}) that provides information on crack propagation which is the main cause of acrylic fracture” (Al-Haddad et al., 2014). There are a variety of tests that can measure fracture toughness. One of the measurement methods recommended is a three-point bend, also called ‘single-edge notched bend’ (SENB). The test requires small geometries to accomplish plane strain (Williams and Cawood, 1990).

1.8.1.3. Impact strength

Impact strength of denture base resin has been defined as “the energy required to fracture a material under the impact force” (Anusavice, 2013). Machado et al. stated impact strength is a measure of the energy needed to initiate and propagate a crack through the material.

Therefore, it can reflect the contact force of stress required to cause a fracture in a denture base under conditions such as accidental dropping (Machado et al., 2012). The most common clinical failures of denture base resins are from impact and fatigue failures and are most likely to occur on the midline of a denture due to the low levels of resistance to impact and flex (Thomas et al., 2015).

The impact strengths of denture base resins can be evaluated by two methods: the Charpy and Izod impact tests. With the Charpy test, a specimen is placed horizontally, supported at both ends and struck in the middle with a weighted pendulum. However, in the Izod impact test a specimen is held vertically, supported at one end and struck at the other end (Faot et al., 2006).

In the Charpy method, the centre of the sample is fractured by a swinging pendulum. It is possible to calculate the energy lost (in Joules) during fracture by comparing the length of the swing after impact with a free swing during which impact does not occur (Anusavice et al., 2012).

1.8.1.4. Fatigue strength

Fatigue is the loss of strength resulting from application of stress over a period of time (Vallittu et al., 1994b). Damage produced by cyclic loading during mastication can accumulate over time, leading to failure (Ilie et al., 2017). Fatigue is likely to begin at areas with high stress concentration. Stresses are concentrated in areas when there is a change in the surface contour, such as notches, internal and surface flaws, voids, bubbles or scratches (Kelly, 1969). Fatigue strength can be measured by applying cyclic loading for a designated number of cycles. The amount of force applied is varied until the material factures at the end of the cycles (Ilie et al., 2017).

1.8.1.5. Hardness

Hardness is the measures of resistance a material poses to indentation, cutting, scratching and abrasion (Van Noort and Barbour, 2013). It is vital in enabling resins to resist forces generated by chewing or cleaning of dentures (Farina et al., 2012). Common methods of testing surface hardness of a material involve pushing an indenter into the surface of the material of a period of time and then measuring the size of the resultant indentation. Different tests involve different shapes of indenter (Vickers – pyramid, Rockwell – cone, Brinell – ball) (Van Noort and Barbour, 2013).

1.8.1.6. Tensile bonding strength

Tensile strength is the maximum tension force a material can undergo before fracture (Combe et al., 1999). It is vital to the integrity of dentures as it prevents debonding of denture teeth from the base and can be affected by excessive loading, incomplete polymerisation, fatigue and poor manufacturing (Matos et al., 2018). It is measured by application of a constant load in a tensile tester and measurement of the resultant elongation (Van Noort and Barbour, 2013).

1.8.2. Physical properties

1.8.2.1. Water sorption and solubility

PMMA tends to absorb water over time. This is a result of the polar properties of the molecules in the resin (Miettinen and Vallittu, 1996). This intake of water can negatively affect the mechanical and physical properties of the material, increase the roughness and causing unpleasant smells (Umemoto and Kurata, 1997). The solubility of polymers represents the amount of residual monomer and other soluble material in the polymer (Rahal et al., 2004). As water penetrates the resin matrix it dissolves the unreacted monomer in addition to causing plasticisation that weakens the polymer (Malacarne et al., 2006).

1.8.2.2. Colour stability

Colour stability is vital for the aesthetics of denture bases, ensuring that they match the colour of the soft tissues in the mouth (Altıncı and Durkaya, 2016). Colour changes can be either intrinsic, resulting from matrix changes as the material ages, or extrinsic, whereby the material is stained by food, drink, smoking and cleaners (Goiato et al., 2014). Other extrinsic factors affecting the colour of PMMA are disinfectants and cleaning solutions, and thermal changes causes by drinks and foods of different temperatures (Altıncı and Durkaya, 2016; Goiato et al., 2013a).

1.8.2.3. Surface roughness

Surface roughness affects patient comfort, staining and oral health (Gungor et al., 2014). Surface roughness affects the hygiene of the denture base, as roughness aids the adhesion of microorganisms to the denture base. These adhered bacteria can also be difficult to remove by standard oral hygiene methods (Oliveira et al., 2008). This can lead to plaque formation, fungal infections, denture stomatitis, angular cheilitis, as well as caries (Ozyegin et al., 2012; Ozyilmaz and Akin, 2019). In order to deter the adhesion of these microorganisms, the roughness of PMMA after polishing should not exceed 0.2 μm (Onwubu et al., 2018).

1.8.3. Biocompatibility properties

According to Jorge et al. biocompatibility defined " the acceptance (or rejection) of artificial material by the surrounding tissues and by the body as whole" (Jorge et al., 2007). *In vitro* and in vivo studies conducted by Vasiliu investigated the effect of denture acrylic on intra-oral soft tissues in mice. Denture resin appeared biocompatible and did not cause irritation or damage to the oral mucosa. However, it is acknowledged that the monomers are toxic and irritant at high concentrations. However, after complete polymerisation by heat the residual levels of monomer are negligible and not harmful to the surrounding tissues. Clearly, if the polymerisation process is undertaken slowly under the appropriate temperatures, then any remaining monomer will be negligible (Vasiliu et al., 2016).

An *in vitro* study by Goiato et al evaluated the cytotoxicity of heat-cured acrylic resin denture base, cold-cured acrylic resin and their components. The test was achieved with extracts of acrylic resin and measured the material's biocompatibility by its action on cell cultures. The finding of the study determined that the heat-polymerised acrylic resin was not cytotoxic, however, the auto-polymerisation acrylic resin is more cytotoxic compared to heat-polymerised. The effect of the cytotoxicity was observed dependent on the amount of residual monomers (Goiato et al., 2015).

1.8.4. Comparison properties of different types of heat-cured acrylic resins.

It has been demonstrated that there are differences in the properties of conventional (normal impact) and high impact denture base resin as shown in Table 1.3. The high impact denture base resin contains the same components as conventional heat-cured resin, with the reinforcement with butadiene-styrene, which is distributed in the poly-methyl methacrylate matrix. The impact strength, fracture toughness, surface hardness and transverse deflection properties of high impact denture bases are higher than conventional acrylic denture bases. However, the modulus of elasticity during flexing is decreased when compared to conventional heat-cured denture resins. It has been reported that one of the advantages of reinforced denture bases is reduced water sorption. In contrast, the colour stability of high impact dentures when compared to conventional resin is slightly altered, but it appear to have no relevance in clinical applications (Ayad et al., 2008; Craig et al., 2004; Miettinen and Vallittu, 1996; Vojdani et al., 2012; Zappini et al., 2003).

A study conducted by Zappini et al. tested seven different brands of heat-cured denture base resin to determine the impact strength and fracture toughness. Two conventional and five high-impact acrylics were investigated. GC Luxon, Lvocap plus, Lucitone 199, and Trevalon high impact resins were shown to have higher values of toughness when compared to the conventional heat-cured acrylic denture bases as shown in Table 1.4 (Zappini et al., 2003).

Table 1.3. Several key properties of conventional acrylic resins denture base and high impact rubber reinforced acrylic (Ayad et al., 2008; Craig et al., 2004; Miettinen and Vallittu, 1996; Vojdani et al., 2012; Zappini et al., 2003, Asar et al., 2013)

Properties	**Conventional Acrylic**	**Rubber- Reinforced Acrylic**
Flexural strength (MPa)	85.10	69.77
Transverse deflection (mm) @ 3500 gm @ 5000 gm	2.0 4.1	2.4 5.0
Elastic modulus (MPa)	2000	1780
Impact strength (Charpy) (KJ/m^2)	1.36	2.71
Fracture toughness (MPa m$^{1/2}$)	1.44	2.56
Surface hardness (VH) (Kg/mm^2)	14.33	16.60
Water Sorption (mg/cm^2)	0.60	0.55
Water solubility (µg/mm^3)	1.8	1.15
Colour stability (24 hr in Ultraviolet Light)	No change	Slight change (clinically insignificant)

Table 1.4. Results of fracture toughness of seven heat-cured acrylic denture bases in mean values and SDs (Zappini et al., 2003).

Product	Charpy impact strength (kJ/m^2)	Izod impact strength (1.2-mm notch) (kJ/m^2)	Izod impact strength (3.4-mm notch) (kJ/m^2)	Fracture toughness test K_I, max (MPa-m$^{1/2}$)	Fracture toughness test WOF (kJ/m^2)
GC Luxon	2.85 (0.05)^{c,d}	2.64 (0.15)^{c,d}	2.15(0.15)^{d}	2.63 (0.09)^{d}	1.50 (0.17)^{d,c}
Injectall IPF HI-I	0.92 (0.22)^{a}	1.59 (0.23)^{a}	1.14 (0.33)^{a}	2.08 (0.29)^{c}	0.63 (0.17)^{b}
Ivocap plus	1.47 (0.16)^{b}	2.49 (0.24)^{c}	1.80 (0.25)^{c}	2.41 (0.04)^{d}	1.12 (0.06)^{c}
Luctione 199	2.89 (0.22)^{d}	2.85 (0.26)^{d,c}	2.37 (0.09)^{d}	2.53 (0.08)^{d}	1.41 (0.06)^{d}
Major 2 Base	1.36 (0.03)^{b}	1.99 (0.23)^{b}	1.31(0.28)^{a,b}	1.76 (0.14)^{b}	0.38 (0.03)^{a}
Probase Hot	1.36 (0.09)^{b}	1.79 (0.20)^{a,b}	1.43 (0.20)^{b}	1.44 (0.18)^{a}	0.27 (0.03)^{a}
Trevalon HI	2.71 (0.06)^{c}	3.09 (0.30)^{e}	2.41 (0.11)^{d}	2.56 (0.13)^{d}	1.58 (0.07)^{c}

Note: Within a column, cells having same (lower case) letters are not significantly different from others.

1.9. JUSTIFICATION FOR HIGH IMPACT HEAT-CURED ACRYLIC RESINS

The addition of rubber to conventional heat-cured acrylic resin has been successful in improving the impact strength of denture base resins (Rodford, 1990). The reinforcement of PMMA by the introduction of rubber particles produces a resin that consists of a matrix of PMMA within which is distributed an interpenetrating network of rubber. A crack may accelerate through the PMMA, but when the crack propagates to the rubber interface it will decelerate or even cease; therefore, crack development becomes hard to initiate and progress. One of the main advantages of rubber-reinforced “high impact” resins is that they can absorb greater amounts of energy at higher strain rates before fracture when compared to conventional acrylic resins (Jagger et al., 1999; Stafford et al., 1980a; Stafford et al., 1980b). Figure 1.3 shows fracture toughness and density of commonly used denture materials and HI PMMA shows better fracture toughness than the conventional PMMA.

Studies conducted by Jar et al. reported that conventional heat-cured poly methyl methacrylate has a pure matrix that can fail by crazing. The addition of a small quantity of rubber particles of suitable size can enhance the fracture toughness of PMMA. This fracture toughness is increased because of the potential for the energy absorption of rubber within the matrix is higher than non-rubber containing resins (Jar et al., 1999).

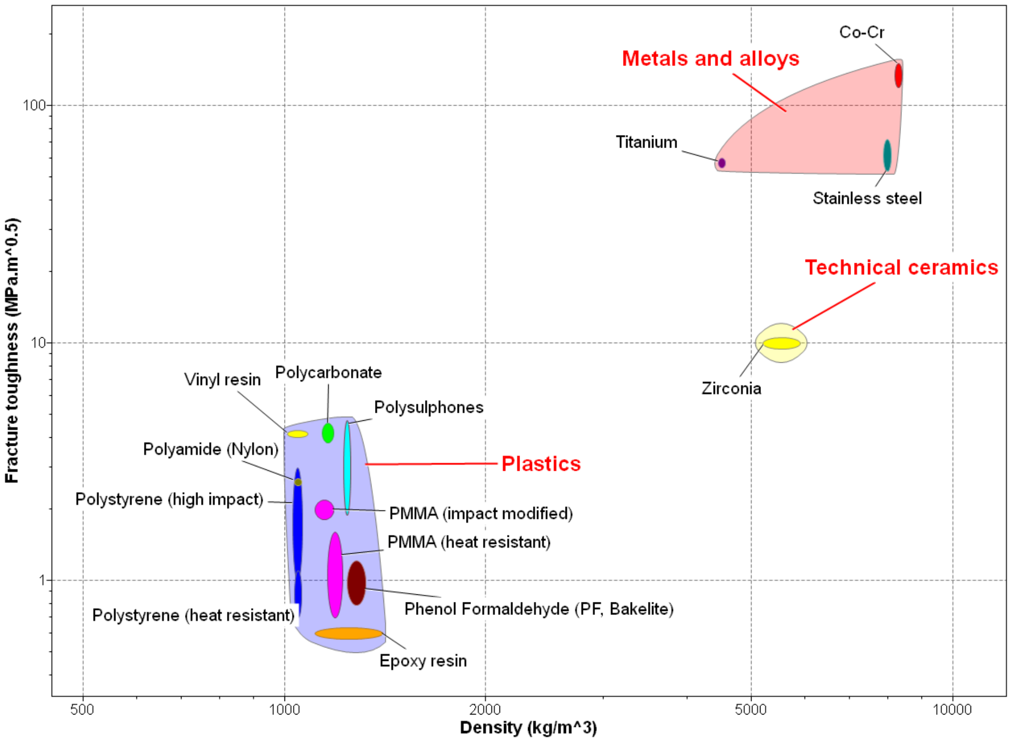

Figure 1.3. Comparison of fracture toughness between HI PMMA and conventional PMMA resins (Graphs drawn by Granta EduPack software).

The incorporation of rubber to conventional heat-cured acrylic denture base resin has not been completely successful in that it still has some problems. These problems include the reduced modulus of elasticity and hence the flexibility of the final denture base. However, the flexural strength for high impact does not increase compared with conventional heat-cured acrylic resins (Jagger et al., 2003; Zheng et al., 2012). In Figure 1.4 and Figure 1.5 conventional PMMA heat cured resin showed higher modulus of elasticity, flexural strength and density in comparation to HI acrylic resin modified with butadiene-styrene rubber. Therefore, the authors have chosen HI acrylic resin for development as a future denture base in this research.

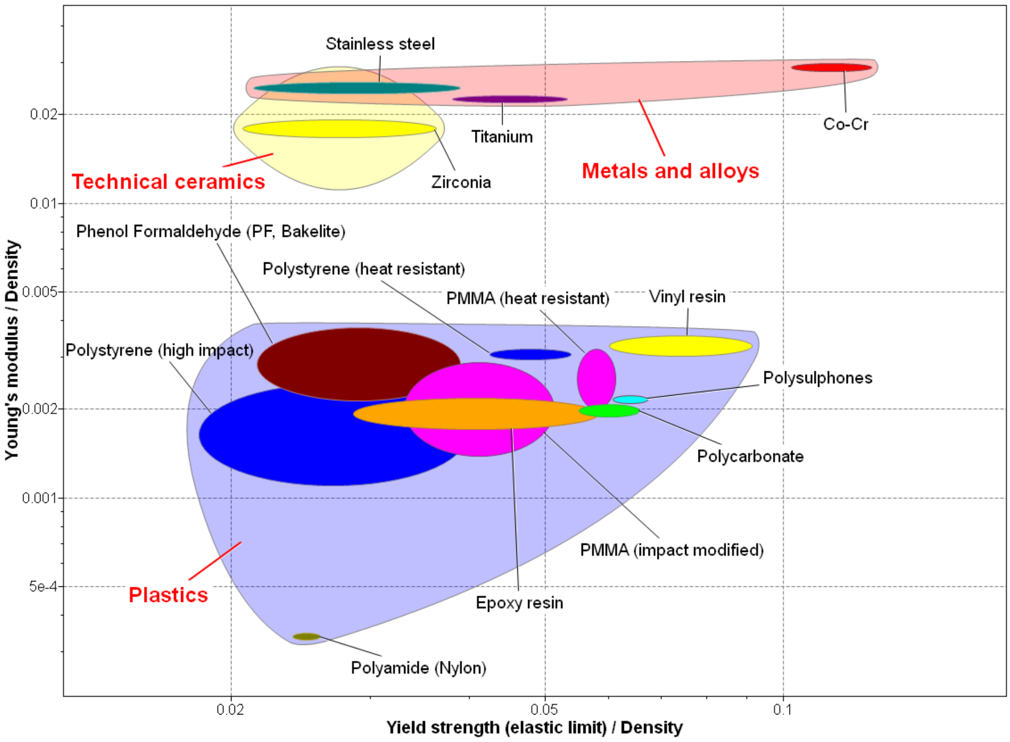

Figure 1.4. Comparison of elastic modulus and strength between HI PMMA and conventional PMMA resins (Graphs drawn by Granta EduPack software).

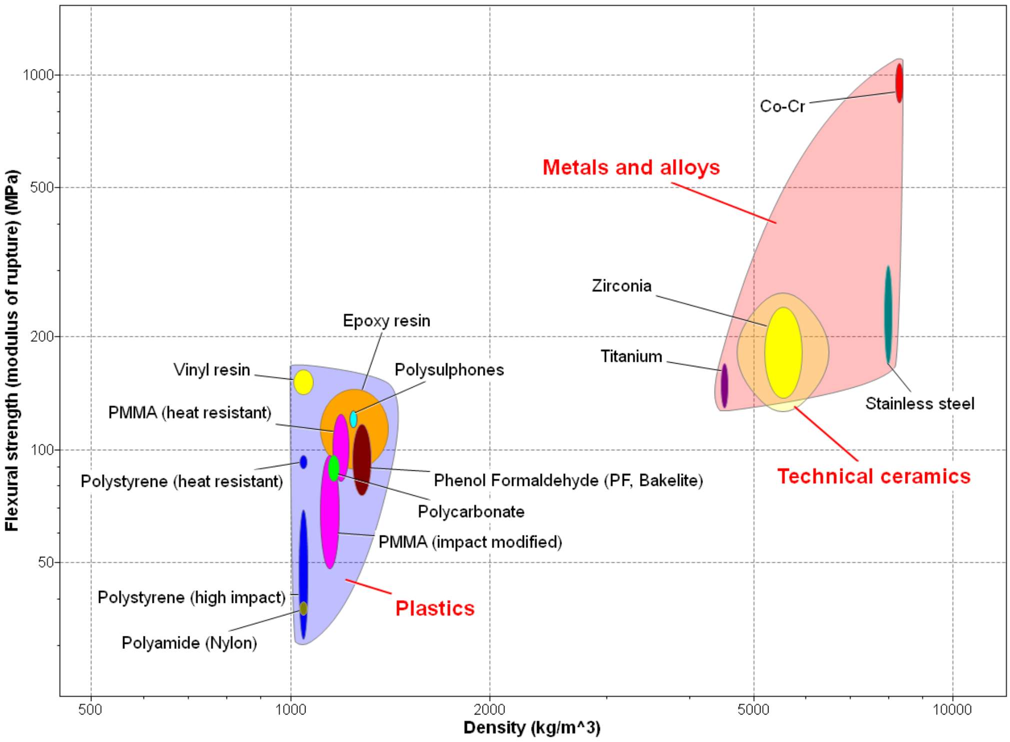

Figure 1.5. Comparison of flexural strength between HI PMMA and conventional PMMA resins (Graphs drawn by Granta EduPack software).

1.10. DEVELOPMENT OF ZIRCONIA IN DENTISTRY

Zirconia is a ceramic material that has mechanical properties similar to some metals as well as being the same colour as mineralised tissues, including enamel, dentine and bone (Manicone et al., 2007). Interestingly, according to Madfa, zircon has been named as a “gem”. “The name zirconium comes from the Arabic “Zargun” (golden in colour) which in turn originates from the two Persian words “Zar” (Gold) and “Gun (Colour).” Additionally, zirconia has been defined as a crystalline dioxide of zirconium oxide (Madfa et al., 2014).

Zirconia was discovered by the German chemist Martin Heinrich Klaproth in 1789. It was prepared by heating gems and then mixing the products with rare earth oxides, and used as a pigment for ceramics (Piconi and Maccauro, 1999).

Volpato reports that zirconia is not naturally available in a pure state. “It can be found in main sources as zirconate with combination of silicon oxide (ZrO_2-SiO_2, $ZrSiO_4$) or Baddeleyite” (ZrO_2). At the time it was noted that it may be difficult to use these minerals in dentistry (or generally) because they are combined with many metallic elements and the material needs to be chemically extracted from these two materials (Volpato et al., 2011). In 1824, Swedish chemist Jons Jakob Berzelius separated zirconia from other elements to obtain pure zirconia (Vagkopoulou et al., 2009).

In 1969, the first use of this material in a medical device was reported. It was used for fabricating a replacement hip head as an alternative material to titanium and alumina (Madfa et al., 2014). In the 1990s, because of superior properties and excellent biocompatibility, it was suggested that zirconia be used in the field of dentistry for restorations, implant abutments or restorative endodontic posts (Pilatthadka et al., 2007). Once established, studies employed the development of dental CAD/CAM processing in order to enhance zirconia production to use as crowns and bridges. This process focused on a type of Yttrium tetragonal zirconia poly crystal (Y-TZP) which could be used for fixed restorations, which had excellent mechanical properties and was wholly biocompatible (Komine et al., 2010; Vagkopoulou et al., 2009).

1.10.1. Phases structure of zirconia

Zirconia has a blue-black colour in its natural state and it can appear as a shiny grey-white metal as shown in Figure 1.6 (Volpato et al., 2011). Zirconia is available in three crystal structures: monoclinic (M), tetragonal (T) and cubic (C) as shown in (Figure 1.7) (Mihai et al., 2014).

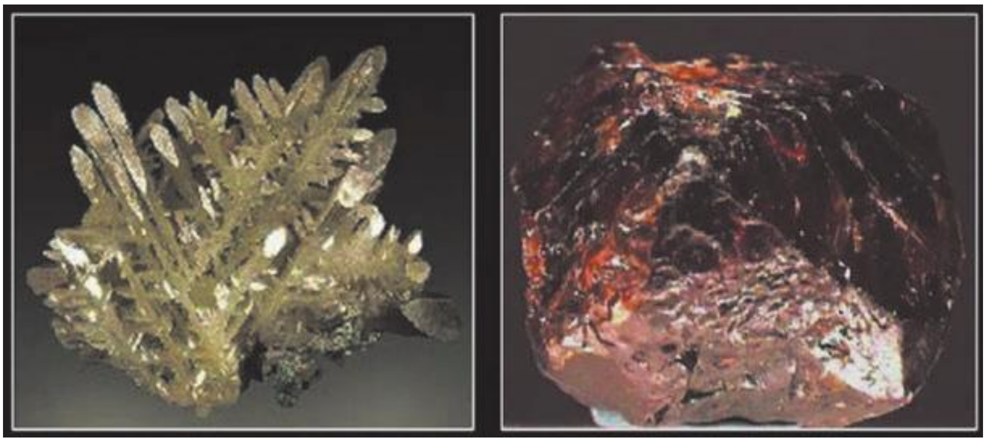

Figure 1.6. Zirconium oxide (ZrO_2) in a natural form (Vagkopoulou et al., 2009).

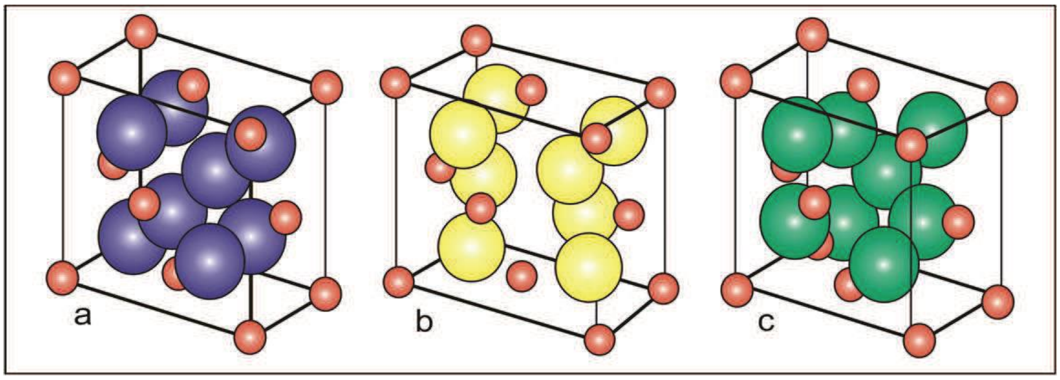

Figure 1.7. Crystal structure of monoclinic (a) tetragonal (b) and cubic zirconia (c) (Volpato et al., 2011).

The first crystal structure is monoclinic which can be pure zirconia at room temperature. The second crystal, tetragonal zirconia, is formed up to 2370°C, and then above this temperature can become cubic zirconia. It has been reported that the tetragonal phase transfers to the monoclinic phase after cooling. Unfortunately, as with all ceramics, this phase can cause cracks and flaws within the crystal structure. Consequently, different oxides have been added to zirconia in order to stabilize the tetragonal phase at room temperature after sintering. The oxides, which are added include yttrium oxide (Y_2O_3), calcium oxide (CaO) and magnesium oxide (MgO) (Volpato et al., 2011).

1.10.2. Types of zirconia used in dentistry

There are various types of zirconia-containing and ceramic systems available within the wider marketplace for use in dentistry. Despite the various forms of zirconia, only three of them are primarily used in dentistry. “These are yttrium cation-doped tetragonal (3%) zirconia poly crystals (3Y-TZP), magnesium cation-doped partially stabilized zirconia (Mg-PSZ) and zirconia-toughened alumina (ZTA)” (Denry and Kelly, 2008).

1.10.2.1. Yttrium tetragonal partially stabilized zirconia poly crystal (Y-TZP)

This group has a small concentration of 2 to 3 mol% yttrium oxide (Y_2O_3) as a stabilizing agent (Vagkopoulou et al., 2009). This gives stability to the zirconia in the tetragonal phase, and consists of the metastable tetragonal phase (up to 98%) after sintering (Volpato et al., 2011). Y-TZP has been widely used in medicine and dentistry since the mid-90’s. Nevertheless, even with its favourable properties some studies have reported that many orthopaedic components have failed but without giving detailed reasons (Silva et al., 2010). Studies have investigated and reported that the Y-TZP zirconia has a high flexural strength ranging from 800 to 1000 MPa which is in contrast to Mg-PSZ, a commonly used dental zirconia, which has values ranging from 450 to 700 MPa (Piconi and Maccauro, 1999; Silva et al., 2010). This confirms the addition of 2-3% of Yttrium (Y_2O_3) to stabilize the zirconia and increases its hardness and resistance to fracture demonstrably (Mihai et al., 2014).

1.10.2.2. Magnesia partially stabilized zirconia (Mg-PSZ)

This structure contains cubic zirconia crystals partially stabilized with magnesium oxide with a percentage from 8 to 10% (Volpato et al., 2011). Denry and Kelly have reported that the Mg-PSZ has some deficiencies such as increased porosity and large grain size that can affect the overall mechanical properties including its fatigue strength. Moreover, during sintering a high temperature is required 1680 to 1800°C, which can be difficult to control both when heating and cooling. For the above reasons, the Mg-PSZ is not an optimal material for dental applications (Denry and Kelly, 2008).

1.10.2.3. Zirconia toughened alumina (ZTA)

The composition of this structure is zirconia with a matrix of alumina (Al_2O_3) that forms ZTA “alumina reinforced with zirconia grains” (Volpato et al., 2011). Studies have determined that the development of ZTA is by addition of “33 vol% of 12 mol% ceriastabilized zirconia to In-Ceram Alumina" (Denry and Kelly, 2008). In-Ceram Zirconia can be manufactured by slip-casting and soft machining techniques, so that its properties may be improved through processing into the final product. The benefit of the slip-casting technique is limited shrinkage. However, the ZTA does have relatively high porosity and this can reduce the mechanical properties of In-Ceram Zirconia. Generally ZTA has lower mechanical properties compared to Y-TZP dental ceramics (Denry and Kelly, 2008).

1.10.3. Application of zirconia in dentistry

Compared to other materials (metals, alloys, resins) zirconia has the advantage of excellent aesthetics for its application in prosthodontics and prosthetics. The most common type of zirconia used in dentistry is the Yttrium tetragonal zirconia poly crystal (Y-TZP). It is used for orthodontic brackets, endodontic posts, crowns and fixed bridges (Komine et al., 2010). In addition, it is also used for implant abutments, implants, veneers and primary telescopic crowns (Vagkopoulou et al., 2009).

1.11. PROPERTIES OF ZIRCONIA

1.11.1. Mechanical and physical properties of yttrium stabilised zirconia (Y-TZP)

Yttrium partially stabilised tetragonal zirconia poly crystal exhibits high flexural strength, compressive strength, hardness and a fracture toughness (Table 1.5). These properties make this type of zirconia an attractive candidate for many dental applications. Young's modulus exhibits a low value (Denry and Kelly, 2008; Trunec and Chlup, 2009). The transformation of zirconia, from monoclinic to the tetragonal phase, allows it to remain stable; however, it can be improved the introduction of Yttrium tetragonal zirconia poly crystal (Y-TZP). The Yttrium tetragonal zirconia reduces compressive stress at a crack's tip and with shear stresses, acting against the stress field generated in the crack area. Therefore, an increase in the toughness of zirconia in this phase (Y-TZP) results in preventing the propagation of cracks and improving the mechanical properties of zirconia (Volpato et al., 2011).

Table 1.5. Mechanical and physical properties of zirconia (Madfa et al., 2014; Mihai et al., 2014).

Materials properties	Values
Porosity	<0.1%
Hardness	1200 HV
Flexural strength	900-1200 MPa
Compressive strength	2000 MPa
Fracture toughness	7-10 MPa.m$^{1/2}$
Young's modulus	210 GPa
Thermal expansion coefficient	11×10^{-6} K^{-1}
Thermal conductivity	2 W m K^{-1}

The surface phase transition and the resulting surface hardness have improved the mechanical and wear properties of Yttrium partially stabilised tetragonal zirconia polycrystal. This type of Yttrium tetragonal zirconia has better mechanical and physical properties than other ceramic biomaterial included, magnesium cation-doped partially stabilized zirconia (Mg-PSZ) and zirconia- toughened alumina (ZTA) (Komine et al., 2010; Piconi and Maccauro, 1999).

1.11.2. Biocompatibility properties of zirconia

A study has reported that zirconia is biocompatible with soft tissues including those in the mouth free mucosa and keratinised mucosa. Although contact irritation can occur due to porosities and surface contamination, zirconia is entirely inert when it is pure and has a highly polished surface (Volpato et al., 2011). In-vitro and in-vivo study assessed two different zirconia implant surfaces prepared by machining (ZrO_2 m) and sandblasting surface (ZrO_2 r) and compared with a titanium surface prepared by sandblasting and acid etching. The findings showed that the highest surface roughness was found in titanium implants, followed by (ZrO_2 r and ZrO_2 m). In addition, roughening changed zirconia implant surface with increased bone apposition and enhanced interfacial shear strength (Gahlert et al., 2007).

1.12. THE CLINICAL PROBLEM

Polymethyl methacrylate (PMMA) acts as main component for fabricating denture bases and has been used widely since 1937 (Kanie et al., 2000). Ideally, denture base materials should have high strength properties including flexural strength, tensile strength, (Zheng et al., 2012) and high impact strength and fatigue resistance (Kim and Watts, 2004). Although PMMA heat-cured acrylic resins are important in the field of dentistry they do have limitations (Gungor et al., 2017). More specifically, denture bases often suffer short term “wear and tear”, and on occasions fracture. These limitations restrict its application in restoring the function and aesthetics of teeth that are lost or damaged (Gungor et al., 2017). Moreover, denture bases absorb water over periods of time, which can then have a detrimental effect on the mechanical properties of the polymer (Polat et al., 2003). Nejatian and Johnson (2006) highlighted this concern, and a survey conducted on the fracture of dentures, revealed that approximately 68% of denture bases broke within 3 years. They also reported that 29% of the fractures were in the midline of the denture and that they occurred more in upper dentures than lower. Furthermore, 33% of the fractures recorded were due to debonded teeth and 38% by other types of fracture (Nejatian et al., 2006). These problems are further compounded when prostheses for implant retained restorations are provided and functional demands are increased.

Zirconia fillers have been commonly used in dental applications for many years because of their advantages which include: high mechanical strength, excellent surface properties with high wear resistance and excellent biocompatibility, when compared to conventional materials such as alloys or polymers (Christel et al., 1989; Gad et al., 2016a). Studies conducted by Asar et al. (2013) investigating the effects of different metal oxides with micro particle size, including TiO_2, ZrO_2 and Al_2O_3, with reinforced heat cured PMMA denture base resins on their mechanical and physical properties demonstrated significant increases of the impact strength, fracture toughness and decreases in water sorption and solubility of the heat-cured acrylic resin reinforced with ZrO_2, when compared to TiO_2 and Al_2O_3 (Asar et al., 2013).

Trunec and Chlup determined that nanocrystalline zirconia, when stabilised with 1.5 mol % Y_2O_3 and with a grain size of 85nm, exhibited high fracture toughness when compared to the submicrometer-grained zirconia stabilised with 3 mol % Y_2O_3. The Yttrium tetragonal zirconia nanocrystalline structure can better accommodate the transformation of strain because of the small grain volume and the large area of grain boundaries (Trunec and Chlup, 2009). Moreover, nano-particles have huge surface free energy that leads to strong bonds with other particles (Mohamed, 2012). Investigators had reported there was a good adhesion bond between the resin matrix reinforced with zirconia nano-fillers which improved the properties of the polymer and zirconia nano-fillers. Thus, surface modification of nanoparticles with a coating of a silane coupling agent (97% 3 trimethoxysily propyl methacrylate monomer) can reduce the amount of aggregation of zirconia nano-fillers thus leading to polymers with enhanced properties (Gad et al., 2016b). A study conducted by Gad et al to evaluate flexural strength of repaired auto-polymerized resin reinforced with glass fiber, zirconia microparticles and zirconia nanoparticles with different concentrations 2 or 5wt%, found that the group containing zirconia nanoparticles with 2 and 5wt% showed the highest flexural strength in comparison to other groups (Gad et al., 2016a).

It has been confirmed that nanoparticles can, and do, play a major role in increasing the physical and mechanical properties of dental materials (Bhardwaj et al., 2014). As detailed above, zirconia nano-fillers have advantages over other metal oxides. In order to develop a superior high impact heat-cured acrylic denture base material, some of the material's mechanical and physical properties, as cited in the literature, need to be improved. When high impact heat-cured acrylic was reinforced with rubber it significantly increased impact strength, however, flexural strength, modulus of elasticity and fatigue resistance were decreased (Jagger et al., 2003). The combination of zirconia nano-fillers with rubber in PMMA might produce a stronger denture base material with an increase in impact strength and wear resistance. That same material may also exhibit a decrease in water sorption and solubility over a longer period of time than the more conventional materials. According to Jagger et al. "the objective of the rubber reinforced 'high impact' acrylic resins is that they absorb greater amounts of energy at a higher strain rate before fracture than the standard resins" (Jagger et al., 1999). The same could be hoped for zirconia impregnated acrylic resins.

1.13. NOVELTY

According to information available in the literature, no work has been dedicated to improve the properties of high-impact PMMA resin reinforced with zirconia nanoparticles at low concentrations (1.5 to 10 wt.%).

Chapter 2: Aims and Objectives

2.1. AIM

The aim of this research project was to formulate and characterise denture base nanocomposites made of high-impact (HI) heat-cured PMMA resin impregnated with different concentrations of zirconia nano fillers and assess the effects of zirconia on enhancing material performance when compared to the pure HI PMMA resin, using both fundamental materials testing and functional testing.

2.2. OBJECTIVES

The objectives and corresponding hypotheses of this research are

1. To characterise the raw materials used in PMMA-ZrO_2 nanocomposite and evaluate the effect of silanisation on the nanocomposite properties

2. To investigate the mechanical properties of the nanocomposites including flexural strength, fracture toughness, impact strength and surface hardness

3. To evaluate the physical properties of the nanocomposites including colour stability, and sorption and solubility in water and saliva

4. To assess the polishability of the nanocomposites

5. To investigate the tensile bond strength between acrylic resin teeth and the nanocomposites

5. To measure the effect of fatigue loading on the equivalent flexural strength of the complete denture nanocomposites with acrylic resin teeth.

The hypothesis of this research is that addition of zirconia nanoparticles to PMMA would affect mechanical, physical and functional properties of the nanocomposite denture base materials compared to the control group (pure PMMA).

2.3. CHAPTER OUTLINE

Figure 2.1. presents details of different other chapters in the thesis with a brief description.

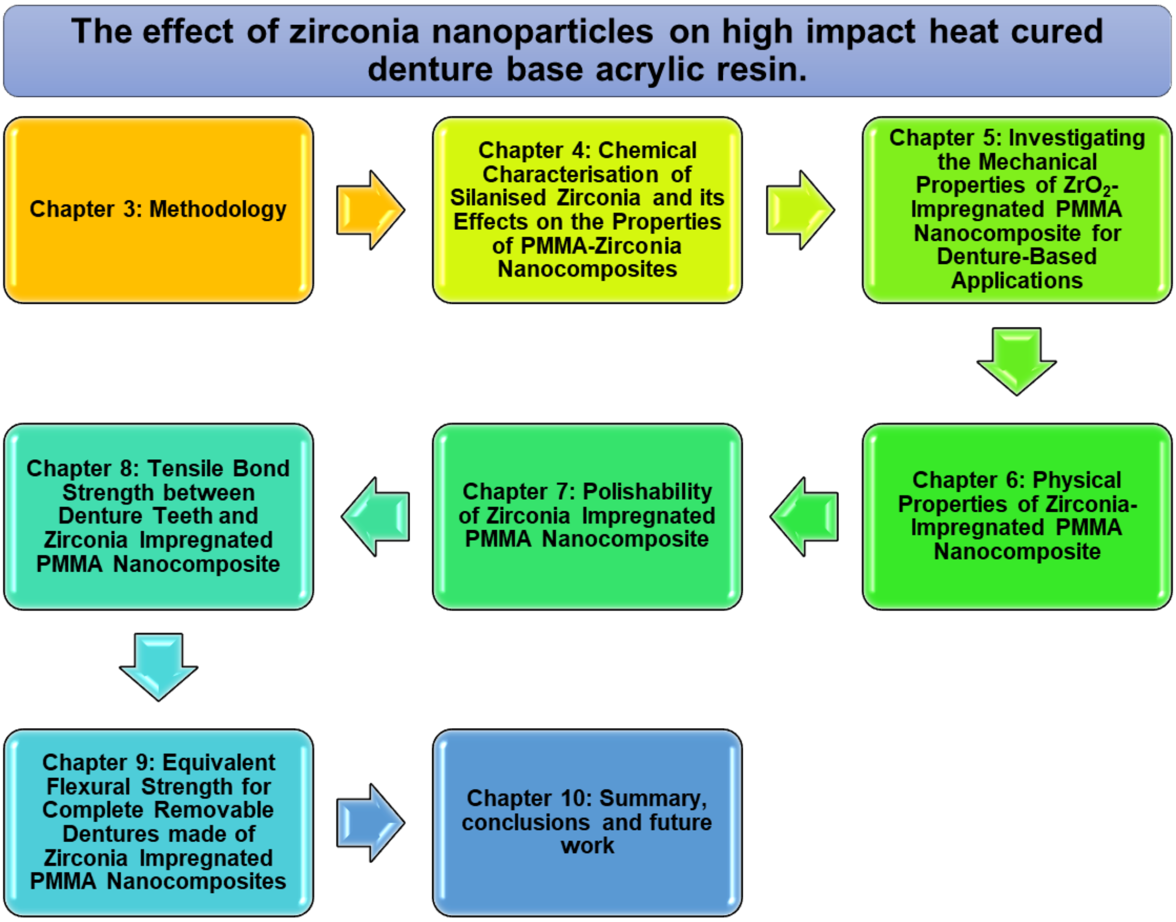

Figure 2.1. Presents details of chapters within the thesis with a brief description.

Chapter 3: Methodology

3.1. INTRODUCTION

Several techniques were used to meet the objectives of this research. Standard techniques were applied to investigate mechanical and physical properties. The methodologies and techniques employed in each study are described in their relevant chapters, however, a more detailed explanation of the processes is included in this chapter. Raw materials used in this study to achieve the research objectives are given in Table 3.1.

Table 3.1. Raw materials used in this research.

Materials	Trade name	Manufacturer	Lot. Number
High-impact heat-cured acrylic denture base resin	HI Metrocryl	Metrodent Limited, Huddersfield, UK	Powder (22828) Liquid (103/4)
Yttria-stabilized zirconium oxide or zirconia	Zirconium oxide	Sky Spring Nano Materials, Inc, Houston, TX, USA	8522-120315
3-trimethoxysilyl propyl methacrylate	Silane coupling agent	Sigma Aldrich, Gillingham, UK	440159

3.2. PREPARATION AND CHARACTERIZATION OF RAW MATERIALS

3.2.1. Characterisation of ZrO_2 and HI PMMA powders

The size and shape distribution of rubber/PMMA (HI heat-cured) powder and zirconia nanoparticles was analysed using a scanning electron microscope (SEM) (Carl Zeiss Ltd, 40 VP, Smart SEM, Cambridge, UK). Specimens were mounted onto aluminium stubs and sputter-coated with gold after which SEM visualization was performed using a secondary electron detector at an acceleration voltage of 2.0 kV. EDX analysis (Energy Dispersive X-ray) was used to evaluate elements within the HI PMMA resin and ZrO_2 nanoparticles. The filler particles were randomly selected and then loaded into the SEM/EDX for imaging using the secondary electron detector at an acceleration voltage of 20.0 kV.

3.2.2. Silanisation of zirconia nanoparticles

Fifteen grams of zirconia nanoparticles and 70 ml of toluene solvent were deposited into a plastic container, which was then placed in a speed mixer (DAC 150.1 FVZK, High Wycombe) and mixed at 1,500 rpm for 20 min. Following the initial mixing, 7 wt.% silane coupling agent (3-trimethoxysilyl propyl methacrylate; product no. 440159, Sigma Aldrich) was added slowly over a period of 20 sec. The mixture was then placed in the speed mixer at 1,500 rpm for 10 min. The mixture was then divided equally into two plastics tubes and spun in a centrifuge at 23 °C at 4,000 rpm for 20 min. The supernatant (separated toluene) was removed, and the remaining silanised nanoparticles were dried in a solvent evaporator (EZ-2 Elite, Genevac Ltd., SP Scientific Company) for 3 hr at 80°C. The silanisation procedure is shown in Figure 3.1.

3.2.3. Assessment of silanised and non-silanised zirconia

Fourier Transform Infrared spectroscopy (FTIR) was conducted to determine the functional groups and bond types within the samples of ZrO_2 nanoparticles powders. Spectra were measured in the wavelength ranging from 4000 to 400 cm^{-1} at a resolution of 4 cm^{-1} and averaging 32 scans using Spotlight 200i FT-IR Microscope System with Spectrum Two (FTIR, Perkin-Elmer, Ohio, USA) at room temperature.

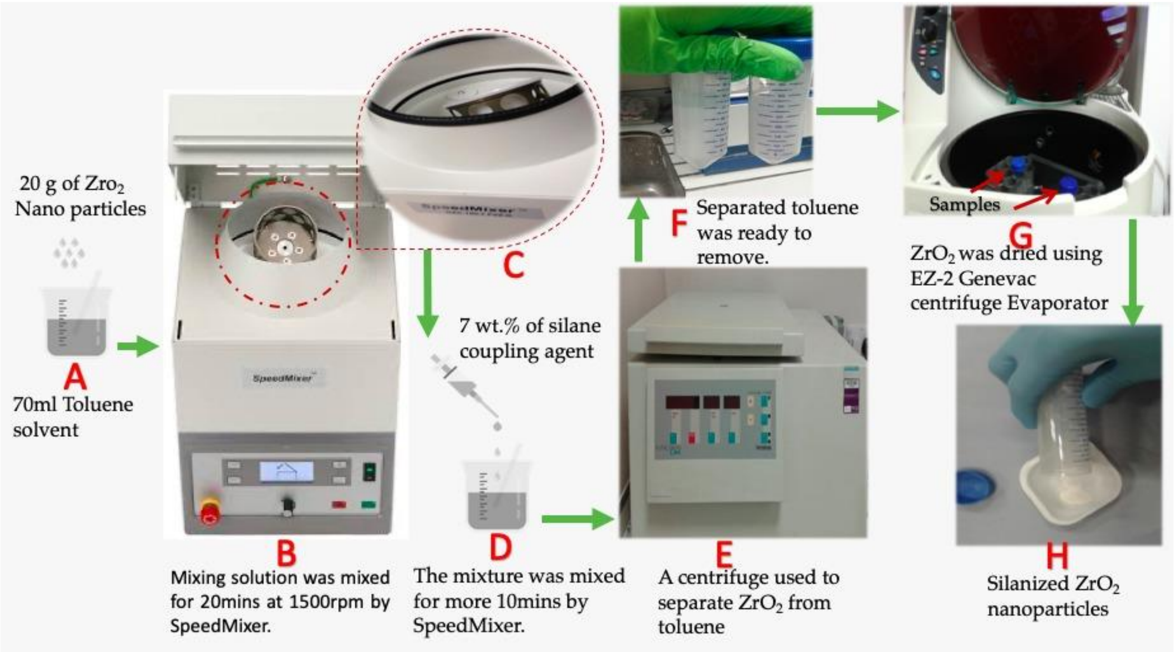

Figure 3.1. Steps of the silanisation procedure of zirconia nanoparticles with silane couple agent.

3.2.4. Selection of concentration of ZrO_2 to HI PMMA resin-Pilot study

To determine the most appropriate weight percentages of silanised zirconia nanoparticles for this research, a pilot study was undertaken using 1.5 wt.%, 10 wt.% and 15 wt.% mixtures. The composition details of the specimen groups used in this pilot study are also described in Table 3.2, with a HI heat-cured acrylic resin powder to monomer ratio of P/L=21 g:10 ml, according to Metrodent Company instructions.

Fifteen specimens of HI PMMA with ZrO_2 nanoparticles with concentrations (1.5%, 10% and 15wt% of ZrO_2), five specimens for each a concentration were fabricated as a pilot study to test by flexural strength. The dimensions of the specimens were produced as a standard size 65 ± 1.0 mm × 10 ± 0.1 mm × 2.50 ± 0.1 mm. The flexural strength and modulus were evaluated using a Zwick universal testing machine (Zwick/Roell Z020 Leominster, UK). The results of the pilot study measuring flexural strength in the samples is presented in Table 3.3.

Table 3.2. Weight percentage of silanised zirconia in combination with acrylic resin powder as well as monomer content of the specimen groups.

Experimental Groups	**Zirconia (wt.%)**	**Zirconia (g)**	**HI PMMA powder (g)**	**HI MMA monomer (ml)**
1.5	1.5	0.315	20.685	10.0
10.0	10.0	2.100	18.900	10.0
15.0	15.0	3.150	17.850	10.0

Table 3.3. Mean (MPa) and Standard deviation (SD) values of flexural strength for specimens of a pilot study on HI PMMA-ZrO_2 nanocomposites with concentrations (1.5%, 10% and 15wt% of ZrO_2).

Weight percent zirconia	**Flexural strength (MPa) & SD**
(1.5 %)	67.6 (17.2)
(10.0 %)	55.4 (2.8)
(15.0 %)	59.1 (9.5)

Based on these results from the pilot study, it was found that addition of 1.5 wt.% of silanised zirconia nanoparticles in HI PMMA showed improved flexural strength. However, both concentrations of 10wt.% and 15 wt.% demonstrated low flexural strength which was less than the recommended British Standard Specification for Denture Base Polymers (no less 65 MPa) (BS 2487: 1989 ISO 1567; 1988) (British Standards, 1989; British Standards, 2008). In addition, the data obtained from relevant literature, a decision was made to use the following weight percentages of silanised zirconia nanoparticles in the denture base formulation: 0.0% (control), 1.5 wt.%, 3.0 wt.%, 5.0 wt.%, 7.0 wt.%, and 10.0 wt.%.

3.3. PREPARATION OF SPECIMENS

3.3.1. Mixing of Zirconia with PMMA

The silane-treated zirconia and acrylic resin powders were weighed according to Table 3.4 using an electronic balance (Ohaus Analytical plus, Ohaus Corporation, USA) with accuracy up to 3 decimal points. The zirconia powder was added to the acrylic resin monomer and mixed by hand using a stainless-steel spatula to make sure all the powder was uniformly distributed within the resin monomer. The HI acrylic resin powder was then added to the monomer, and mixing continued until a consistent mixture was obtained, according to the manufacturer's instruction. The mixing continued for approximately 20 min until the mixture reached a dough-like stage, which was suitable for handling. However, only for the group containing 10 wt.% zirconia, additional 1 min was required to reach the dough-like stage.

3.3.2. Packing and curing

When the mixture reached a consistent dough-like stage (working stage), it was packed into a mould by hand. The moulds were made from aluminium and brass and were used for producing the specimens with different dimensions according to test standards. For flexural strength and surface hardness the mould contained five inserts with dimensions of 65 ± 1.0 mm (l) × 10 ± 0.1 mm (w) × 2.50 ± 0.1 mm (d), for the impact test dimensions of 80 ± 1.0 mm (l) × 10 ± 0.1 mm (w) × 4 ± 0.1 mm (d) and fracture toughness dimensions of 40 ± 1.0 mm (l) × 8 ± 0.1 mm (w) × 4 ± 0.1 mm (d) as seen in Figure 3.2. Before pouring the mixture into the mould, a separating medium, sodium alginate (John Winter, Germany) was applied to the surfaces of the mould for easy removal of the specimens. The mould was then closed and placed in a hydraulic press (Sirio P400/13045) under a pressure of 15 MPa in the first cycle, and then the pressure was released. Excess mixture was removed from the mould periphery, which was then re-pressed at room temperature for 15 min under the same pressure. The mould was then immersed in a temperature-controlled curing water bath for 6 h to allow polymerisation. The curing cycle involved increasing the temperature to 60 °C over 1 h and then maintaining this temperature for 3 h. After this time, the temperature was increased to 95 °C over an additional 2 h to complete the heat polymerisation cycle. The mould was then removed from the curing bath and cooled slowly for 30 min at room temperature. The mould was then opened, and the specimens were removed. The specimens were then trimmed using a tungsten carbide bur, ground with an emery paper and polished with pumice powder in a polishing machine (Tavom, Wigan, UK) in accordance with British International Standard Organization (BS EN ISO 20795-1:2008) and British Standard Specification for Denture Base Polymers (BS 2487: 1989 ISO 1567; 1988) (British Standards, 1989; British Standards, 2008).

Table 3.4. Weight percent zirconia in combination with acrylic resin powder as well as monomer content of the specimen groups

Experimental Groups	Zirconia (wt.%)	Zirconia (g)	HI PMMA powder (g)	HI MMA monomer (ml)
Control	0.0	0.000	21.000	10.0
1.5	1.5	0.315	20.685	10.0
3.0	3.0	0.630	20.370	10.0
5.0	5.0	1.050	19.950	10.0
7.0	7.0	1.470	19.530	10.0
10.0	10.0	2.100	18.900	10.0

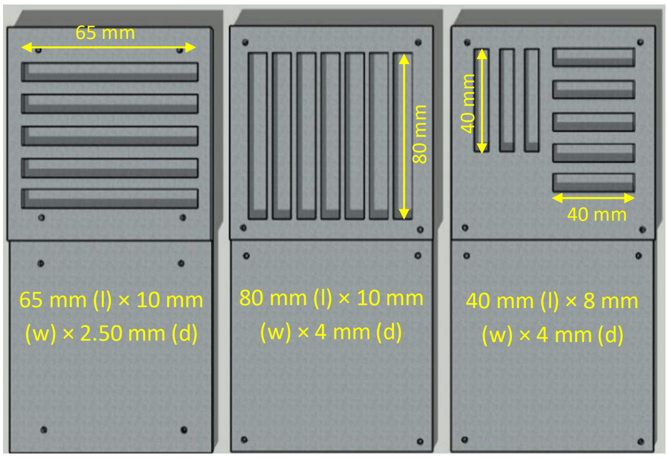

(A) **(B)** **(C)**

Figure 3.2. Design of three different moulds according to the type of tests undertaken, (A) flexural strength and surface hardness (B) impact strength and (C) fracture toughness.

3.4. ASSESSMENT OF MECHANICAL PROPERTIES

3.4.1. Flexural strength, flexural modulus

In order to ensure that dental protheses have an acceptable service life it is important that it meets certain standards in terms of its strength, which can be defined, in general terms, as the ability of the denture to resist stresses caused by mastication without deformation or facture. Accordingly, there are many different categories of strength that are important for dental protheses, including flexural strength, flexural modulus and fracture toughness. Flexural strength is an indicator of the extent to which a prosthesis can avoid plastic deformation under pressure (Anusavice et al., 2012). Flexural strength of the nanocomposite specimens was evaluated using a 3-point bend test in a universal testing machine (Zwick/Roell Z020 Leominster, UK) as shown in Figure 3.3.

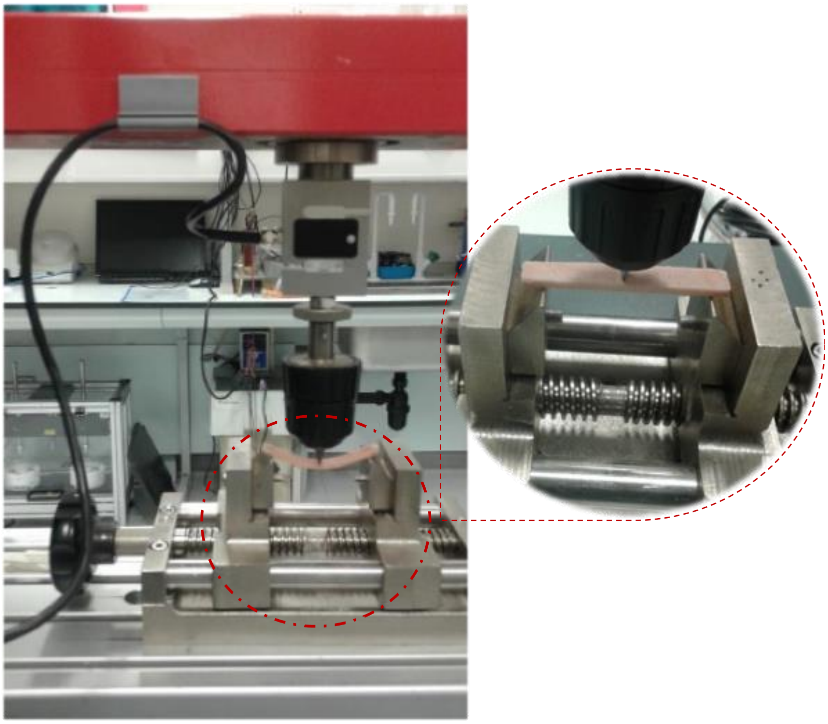

Figure 3.3. Photograph detailing the set-up of the Zwick universal testing machine and specimen (65 mm ×10 mm × 2.5 mm) placed between bending supports with a gap of 50 mm.

In accordance with British International Standard for Denture Base Polymers (2487: 1989) (British Standards, 1989), the specimens were prepared to dimensions of 65 ± 1.0 mm length × 10 ± 0.01 mm width × 2.50 ± 0.01 mm thickness. All specimens were stored in distilled water at a temperature of 37 ± 1 °C for 50 ± 2 h in an incubator before testing. The specimens were then removed from the distilled water and placed on a support jig. The loading plunger (diameter 7.0 mm) was fixed at the centre of the specimen midway between two supports, which were parallel and separated by 50 ± 0.1 mm, and the diameter of the load supports were 3.20 mm. A 500 N load cell was used to record force and the load was applied using a crosshead speed of 5 mm/min. The maximum force (F) was recorded in newtons, and flexural strength was calculated in MPa for all specimens using Equation 3.1 (Anusavice et al., 2012; British Standards, 1989; British Standards, 2001):

$$\sigma = \frac{3\mathrm{Fl}}{2\mathrm{bh}^2} \tag{3.1}$$

where F is the maximum force applied in N, l is the distance between the supports in mm, b is the width of the specimen in mm, and h is the height of the specimen in mm. The flexural modulus was determined as the slope of the linear portion of the stress/strain curve for each test run.

3.4.2. Fracture toughness

Fracture toughness tests were conducted using a single edge span notch bending test on the Zwick universal testing machine in accordance with the British International Standard Organization (BS EN ISO 20795-1:2008) (Al-Haddad et al., 2014; British Standards, 2008). The dimensions of the specimens were 40 ± 1.0 mm (l) × 8 ± 0.1 mm (h) × 4 ± 0.1 mm (w), and a notch was created in the middle of the specimens with a diamond blade and a saw to a depth of 3.0 ± 0.2 mm along a marked centre line. All specimens were then stored in distilled water and placed in an incubator at 37 ± 1 °C for one week before testing. The specimens were removed from the water, dried with a towel and placed edgewise on the supports of the testing rig. The notch in the specimen was placed directly opposite to the load plunger (diameter 7 mm) and in the middle of the span between the two supports (32.0 ± 0.1 mm). The load cell was 500 N, and the cross-head speed was 1.0 mm/min. Fracture toughness was determined by increasing the force from zero to a maximum value in order to propagate a crack from the opposite side of the specimen to the impact point as seen in Figure 3.4. The maximum force (P) in newtons to fracture was recorded in order to calculate the fracture toughness (K_{IC}) in MPa $m^{1/2}$ according Equation 3.2 (Al-Haddad et al., 2014; Kinloch and Young, 1983):

$$K_{IC} = \frac{3PL}{2BW^{3/2}} \times \mathrm{Y} \tag{3.2}$$

where W is the height of the specimen in mm, B is the width of the specimen in mm, L is the distance between the supports in mm, and Y is a geometrical function calculated by Equation 3.3:

$$Y = 1.93 \times \left(\frac{a}{w}\right)^{1/2} - 3.07 \times \left(\frac{a}{w}\right)^{\frac{3}{2}} + 14.53 \times \left(\frac{a}{w}\right)^{\frac{5}{2}} - 25.11 \times \left(\frac{a}{w}\right)^{\frac{7}{2}} + 25.80 \times \left(\frac{a}{w}\right)^{\frac{9}{2}} \tag{3.3}$$

where a is the depth of the notch.

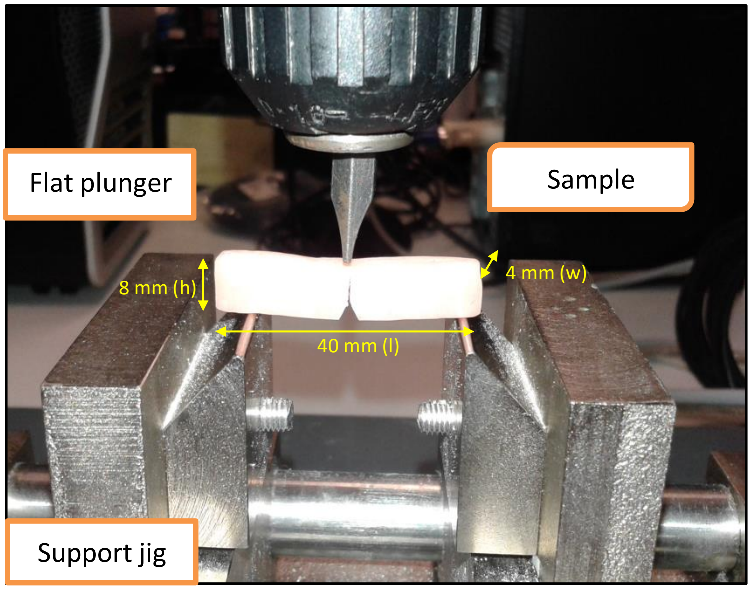

Figure 3.4. Photograph illustrating a sample undergoing fracture toughness testing on the Zwick universal testing machine. Crack propagation through the sample can be observed.

3.4.3. Impact strength

Impact strength is the ability of a material to withstand forces that are applied as a 'shock', for example those sustained during a collision with the floor during a fall, or overclosure onto hard food. In this test the sample was held by a beam that has support on one end only, this is in contrast to the Charpy method in which the beam is support at both ends (Ilie et al., 2017).

The Charpy V-notch impact test (kJ/m^2) utilizes a universal pendulum impact testing machine (Zwick/Roell Z020 Leominster). Specimen were prepared to dimension of 80 ± 1.0 mm (l) × 10 ± 0.01 mm (w) × 4 ± 0.01 mm (h), in accordance with the European International Standard Organization (EN ISO 179-1:2000) (European International Standard; 2000). The specimens were notched in the middle to a depth of 2.0 ± 0.2 mm, with a notch angle of 45 ° and a notch radius of 1.0 ± 0.05 mm. The samples were then stored in distilled water at 37 ± 1 °C for one week in an incubator before testing. The specimens were then removed from the water and dried with a towel. Each specimen was placed in the machine and were supported horizontally at its ends (40 ± 0.2 mm), and the centre of the specimen (the un-notched surface) was hit by a free-swinging pendulum that was released from a fixed height. The pendulum load cell was 0.5 J and directly faced the centre of the specimen. When the test was started, the pendulum was released to strike the specimen, and the impact energy absorbed was recorded in joules (J). The Charpy impact strength ($\boldsymbol{a_{iN}}$) (kJ/m^2) was calculated using Equation 3.4. (Abdulwahhab, 2013; European International Standard , 2000):

$$a_{iN} = \frac{E_c}{h * b_N} \times 10^3 \tag{3.4}$$

where Ec is the breaking energy in joules absorbed by breaking, h is the thickness in mm, and bN is the remaining width in mm after notching.

3.4.4. Surface hardness

The Vickers hardness test involves the use of a pyramid-shaped diamond indenter which forms an indentation on the material to be tested at a specified test force (between 1gf and 100kgf) for a specified time (dwell time).

The Vickers hardness (HV0.05) of the specimens was measured using a micro-hardness testing machine (FM-700, Future Tech Corp, Tokyo, Japan) as seen in Figure 3.5. Specimens were produced with dimensions of 65 ± 1.0 mm length × 10 ± 0.1 mm width × 2.50 ± 0.1 mm thickness, and the test load was fixed at 50 g for 30 sec. During measurement, three indents were taken at different points in a straight line on one side of each specimen. The distances between the indentations were determined by multiplying the average indentation diagonal length by four (4×D) to ensure adequate distance between the indentations. The Vickers hardness was calculated by measuring the diagonals (D1, D2) of the pyramid-shaped indentation impressed on the specimen under the applied load. The hardness values were averaged from five specimens for a particular group. The mean hardness values for all the specimens were determined and were demonstrative of the material in dry conditions at day 0. The specimens were then stored individually in 37 ± 1 °C distilled water for 7 d ± 2 h and were then re-immersed for a total of 45 d ± 2 h. From the raw data, the mean hardness values for each sample group were calculated using Equation 3.5 (Farina et al., 2012; Neppelenbroek et al., 2005; Alamoush et al., 2018).

$$VHN = 1.854 \frac{P}{D^2} \qquad (3.5)$$

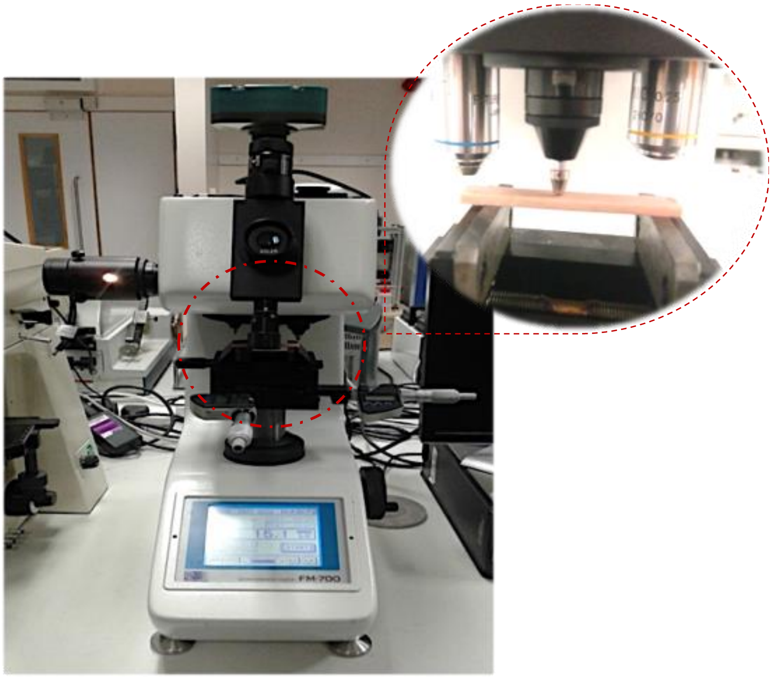

Figure 3.5. A micro-hardness testing instrument with diamond Vickers indenter in action to indent the top surface of specimen (inset).

3.5. ASSESSMENT OF PHYSICAL PROPERTIES

3.5.1. Sorption and solubility

For water sorption and solubility experiments, a brass mould was used to prepare the specimens with dimensions (50 ± 1.0) mm in diameter and a thickness of (0.5 ± 0.1) mm Figure 3.6 (A). Seventy-two acrylic resin specimens were prepared in accordance with EN ISO 20795-1:2008 (British Standards, 2008). Specimens stored in a desiccator containing fresh silica gel were placed in an incubator at 37 ± 1 ℃ for 23 ± 1 h, and then transferred to a second desiccator maintained at room temperature 23 ± 2 ℃ for 1 h. The specimens were then weighed to an accuracy of 0.2 mg (0.0002 g) using a calibrated electronic analytical balance (Ohaus Analytical plus, Ohaus Corporation, USA). The weighing was repeated until the mass loss of each specimen was not more than 0.0002 g in any 24 h period to achieve constant mass in the samples. The final mass in g was recorded as $m1$. Each specimen diameter was measured three times using an electronic digital calliper (Draper, Eastleigh, Hants, UK) in order to calculate the mean values. The mean of five thicknesses measurements at four equally spaced points around the circumference. The volume (V) of each sample was calculated in cm^3 by using the mean dimeter and thickness.

For each group, six specimens were immersed in DW and six specimens were immersed in AS at 37 ± 1 ℃ in an incubator for a period of 180 days. The AS solution was prepared according to a composition shown in Table 3.5 by dissolving in 1000 ml of distilled water with a pH value of 5.52 and mixing using a magnetic stirrer until the components were completely dissolved (Williams et al., 2001). After each time period (1, 2, 3, 4, 5, 6, 7, 14, 21, 30, 60, 90, 120, 150 and 180 days), the specimens were removed from the storage medium, wiped with a clean dry hand-towel until free from visible moisture, and mass in g was recorded as $m2$. After 180 days, specimens were reconditioned in desiccators until a constant mass was reached. This desorption process was carried out over a period of 90 days. The reconditioned mass in g was recorded as $m3$.

The values of water sorption (w_{sp}) in g/cm^3 were calculated by the Equation 3.6 (British Standards, 2008):

$$w_{sp} = \frac{m2 - m3}{v} \tag{3.6}$$

The values of water solubility (w_{sp}) were obtained in g/cm^3 and were calculated by the Equation 3.7:

$$w_{sl} = \frac{m1 - m3}{v} \tag{3.7}$$

Where **v** is the volume of the specimen in cm^3 (British Standards, 2008). After completing the calculations, the values for water sorption and solubility were converted to µg/mm^3.

The percentage mass change in sorption and the percentage solubility that represents the total mass loss of components were calculated by the Equation 3.8 and Equation 3.9 (Alshali et al., 2015).

$$\text{Change in mass SP (\%)} = \frac{m2\,(t) - m1}{m1} \times 100 \tag{3.8}$$

$$Mass\ \text{loss SL(\%)} = \frac{m1\,(t) - m3}{m1} \times 100 \tag{3.9}$$

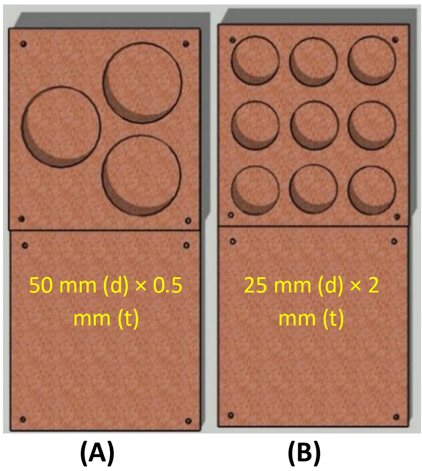

Figure 3.6. Design of two moulds used for preparation of specimens: (A) sorption and solubility and (B) colour stability and surface roughness.

Table 3.5. Composition of artificial saliva (Williams et al., 2001)

Compound	**Amount (g/l)**	**Manufacturer**	**CAS**
Sodium chloride ($NaCl$)	0.400	Acros Organics	7647-14-5
Potassium chloride (KCl)	0.400	Fisher Chemical	7447-40-7
Calcium chloride ($CaCl_2$)	0.795	Acros Organics	10043-52-4
Sodium dihydrogen phosphate (H_2NaO_4P)	0.690	Alfa Aesa	7558-80-7
Sodium sulphide hydrate ($Na_2S \cdot xH_2O$)	0.005	Acros Organics	27610-45-3
Distilled water	1000 mL		

3.5.2. Measurement of colour stability

Specimens were immersed into two cleaning solutions (Steradent (STD) and Milton (MIL) and DW in order to measure the colour stability over time. The cleaning solutions were prepared by immersing one STD tablet (3.184 g) into 250 ml of DW and 20 ml of MIL into 250 ml of DW. Both solutions were stirred for 30 seconds until the solutes were completely dissolved.

A Minolta Chroma Meter CR-221 (Azuchi-Machi, Chuo-Ku, Osaka 541, Japan), a tristimulus colour analyser was used for measuring the colour and colour change (Co, 1988; Liberman et al., 1995). The dimensions of the specimens were 25 ± 1.0 mm diameter × 2 ± 0.1 mm thickness to meet the demands of the measuring instrument Figure 3.6 (B). A total of 90 specimens were fabricated and divided into 6 groups, with fifteen specimens in each group. Every group was divided in to three sub-groups (A, B and C). All specimens were immersed in DW and stored in an incubator at 37±1 °C for 24 h. The specimens were then dried with tissue paper prior to colour measurement. The samples were then placed into the holder of the measuring head (Figure 3.7). During the measurement the light was shone on the specimen at an angle of 45° and reflected light analysed (Liberman et al., 1995). Three measurements were recorded for each specimen as the baseline measurements. Then, five specimens from subgroup A were immersed in 40 ml DW to serve as a control, five specimens from subgroup B were immersed in 40 ml STD solution and the five remaining specimens from subgroup C were immersed into 40 ml MIL solution. The colour values after baseline measurements were then collected at 7, 14, 21, 30, 60, 90, 150 and 180 days.

The Minolta Chroma Meter CR-221 was calibrated before each measurement using the white calibration plates (CR-A45, Channel 00), according to the manufacturer's instructions. The colour differences were assessed by the International Commission on Illumination (C.I.E) L*a*b* scale, where L* is the lightness, a* defines the colour of the sample on red-green and b* on yellow-blue axes. The colour change (ΔE) values were calculated by using Equation 3.10: (Liberman et al., 1995).

$$\Delta E = [\ (\Delta L^*)^2 + (\Delta a^*)^2 + (\Delta b^*)^2]^{½} \tag{3.10}$$

Where, ΔL^*, Δa^* and Δb^* represent the differences between the L*, a* and b* values of the baseline coordinates and those measured after immersion (Hong et al., 2009; Koksal and Dikbas, 2008).

Level of colour change was quantified by the American National Bureau of Standards (NBS). NBS units are calculated using Equation 3.11 (Hong et al., 2009).

$$\mathrm{NBS} = \Delta E \times 0.92 \tag{3.11}$$

If the level of colour change (ΔE) values are less than 1 unit, it will not be appreciable by the human eye. Therefore, the limit of colour change (ΔE) values greater than 1 and less than 3.3 units are considered appreciable and clinically acceptable (Vichi et al., 2011).

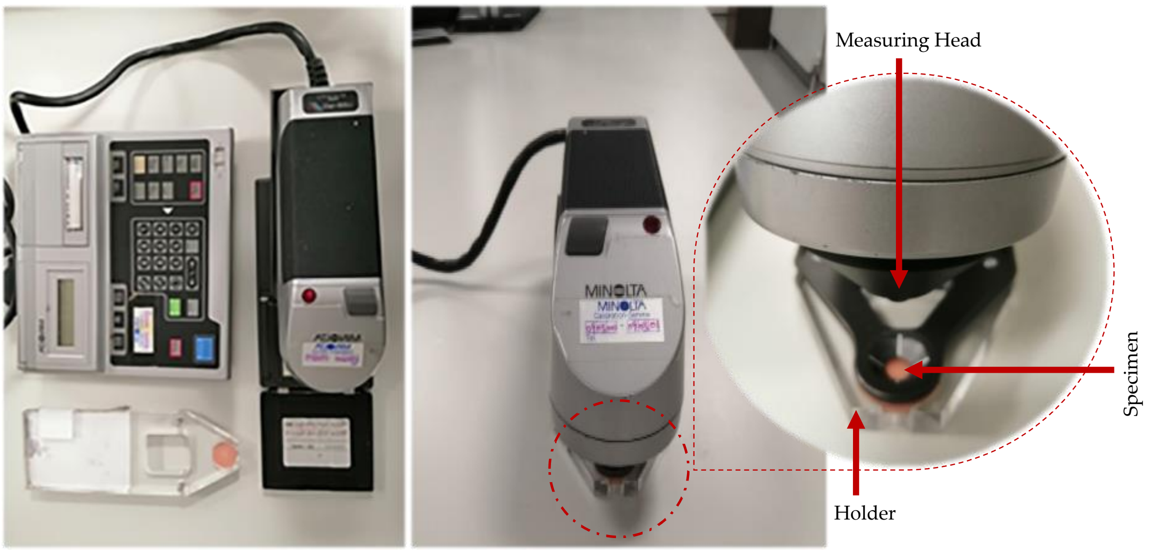

Figure 3.7. Pictures illustrating Minolta Chroma Meter instrument. Measurement of colour change of specimen performed in the holder of Chroma Meter (inset).

3.6. ASSESSMENT OF POLISHABILITY

3.6.1. Roughness measurement machine-Talysurf CLI 1000

A profilometer, Talysurf CLI 1000 (Taylor Hobson Precision, Leicester, UK) was used to provide measurements using of non-contact method, the non-contact method utilised reflectance of light from the sample surface. Furthermore, the machine used offered two types of non-contact measurement, large range and high resolution. The present study used the high-resolution non-contact measurement type (Precision, 2009).

For non-contact high-resolution measurement, a confocal point gauge was employed. This assesses the height of features on the surface of a specimen by focussing on the different elements of white light. A beam of white light was focused though a lens with chromatic aberration, thus causing different focus points for different wavelengths. Once the light was reflected from the surface of the sample it was sent through a pin hole and into the spectrometer. The spectrometer analyses the intensity of different wavelengths of light and creates an intensity curve. The focused wavelength is the one relating to the maximum intensity. A spectrometer deflects the light into a CCD sensor to interpolate spatial position of the data point. Figure 3.8 presents a schematic diagram of the working principle of the surface profilometer (Precision, 2009).

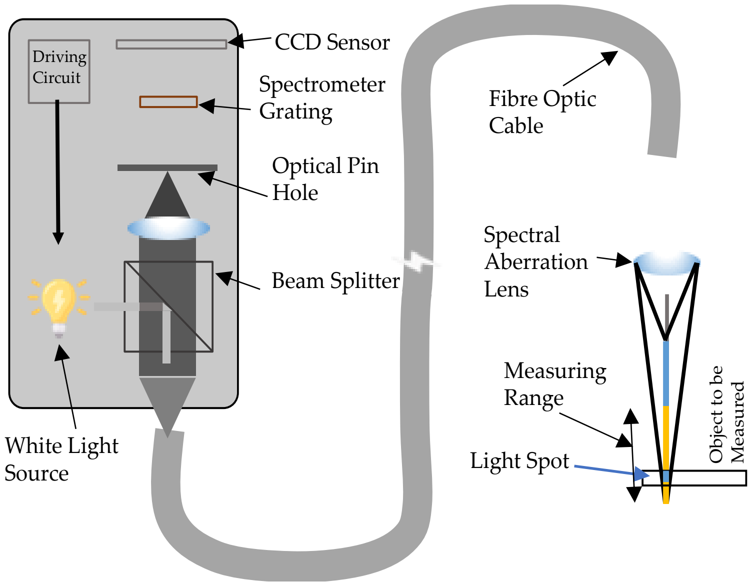

Figure 3.8. Diagram from profilometer of surface roughness instrument Talysurf CLI 1000 representing the working principle of the chromatic length aberration (CLA) confocal point gauge through measurement. (Precision, 2009)

3.6.2. Specimen surface preparation

Surface roughness of the specimens was measured with and without polishing. All polishing was undertaken in conformity to British Standard Specification for denture base polymers (BS EN ISO 1567; 2000)(British Standard, 2000). The dimensions were 25 ± 1.0 mm (Diameter) × 2 ± 0.10 mm (Thickness) as shown in Figure 3.6 (B). The surface preparation started with grinding by a diamond bur and then with a tungsten carbide bur (Dental Sky, UK) at a speed of 1500 rpm to remove any excess acrylic on the surface. Surface roughness was then measured. The first step of all surface polishing was carried out by a lathe bristle brush using slurry of pumice at a speed 1500 rpm for one minute. The specimen surfaces were subjected to a second step polishing by muslin buff wheel using primary polishing compound (Chaperlin & Jacobs Ltd, UK) at the same speed for one minute. The third step of polishing was carried out by a muslin buff wheel using fine polishing compound (secondary) at a slower speed of 500 rpm. After polishing, all the specimens were washed with water and dried in preparation for the surface roughness measurements. After measurement were taken, specimens underwent a second polishing cycle for one minute and a second set of final measurement were then taken. A total of 30 specimens were prepared in this study, five for each concentration of ZrO_2.

3.6.3. Roughness measurement

Surface roughness for all specimen groups were measured using a non-contact high-resolution measurement profilometer technique (Talysurf CLI 1000, Ametek Taylor Hobson Precision, Leicester, UK). The surface roughness (Ra) was measured by placing the specimen in position on a precision X/Y stage of the instrument and scanning was then undertaken by applying a beam of white light through a lens with a chromatic length aberration (CLA 300 µm gauge) focussing on the area of surface to be measured (1 mm × 1 mm) with 0.25 mm cut-off length (Figure 3.9). The mode of measurement was bi-directional with a sampling rate of 500 Hz and a maximum spacing of 1 µm. Three measurements of surface roughness were completed for each specimen. The surface roughness results were analysed using TalyMap software (Ametek Taylor Hobson Precision, Leicester, UK) to create 2D and 3D surface profiles. Average roughness (Ra) values for each specimen group were calculated and used for statistical analysis (Precision, 2009).

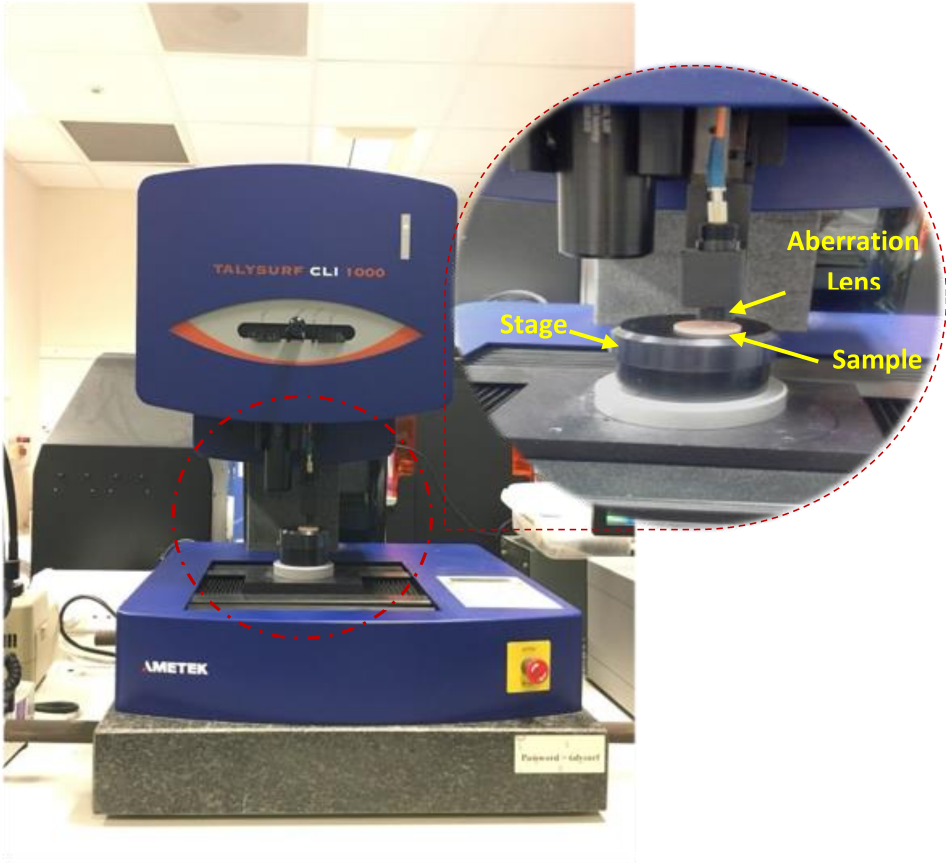

Figure 3.9. The surface roughness profilometer instrument set up. Specimen was placed on a precision X/Y stage for measuring using of non-contact method (inset).

The main limitation of Ra is that it cannot give complete information about the surface roughness (Whitehead et al., 1995), as the measurement process only traces one line (Elbishari, 2012).

3.7. EVALUATION OF TENSILE BOND STRENGTH

3.7.1. Preparation of acrylic resin teeth

Thirty sets of teeth each containing six maxillary anterior teeth (each set consisting of two central and lateral incisor teeth, and canine teeth) manufactured with acrylic resin were used (Artic 6M S40 shade A2, Metrodent Limited, Huddersfield, UK) for the preparation of 30 specimens for TBS tests. The glossy layer was removed from the ridge-lap surfaces of the teeth and a groove was made in each tooth using a tungsten carbide bur (D B Orthodontics, West Yorkshire, UK) as shown in Figure 3.10. The groove dimensions for central incisor and canine teeth were approximately same (2.50 ± 0.10 mm long and 2.50 ± 0.20 mm wide) however, the lateral incisor tooth dimensions were smaller by approximately 1.0 mm. These mechanical tooth preparations were placed to enhance the bond at the interface between the teeth and denture acrylic resin according to previous studies and recommendations for best clinical practice (Cunningham and Benington, 1999). After the treatments, each tooth was thoroughly cleaned with pressurised air to remove any residues on the tooth surfaces that may affect bonding.

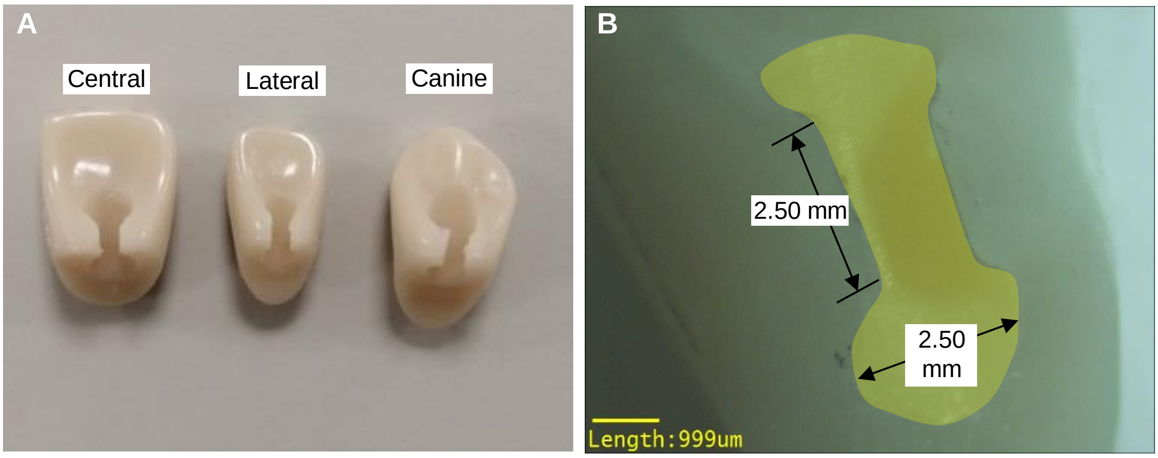

Figure 3.10. Photographs illustrating the tooth preparation for TBS tests (a) Different types of grooved anterior teeth and (b) a sample groove dimensions of a canine tooth

3.7.2. Preparation of the moulds and specimens

Bond strength test specimens were fabricated in a metal grip former, which was also used as the bottom specimen gripper during TBS test as shown in Figure 3.11 The grip former cavity can be adjusted to the correct dimension required for the specimen preparation according to the British standard (BS EN ISO 22112: 2017) (British Standards, 2017). This specimen was used to hold the teeth for the duration of the TBS.

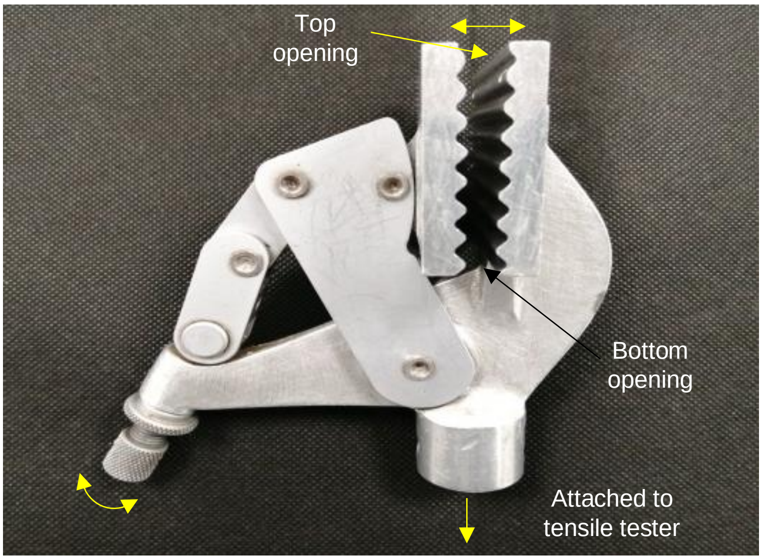

Figure 3.11. Photograph of the metal grip former used in fabricating TBS test specimen.

The top and two side openings of the metal grip former were closed with a strip of base plate wax (Metro wax, Metrodent Limited, Huddersfield, UK) to prevent liquid wax exuding out during pouring. A small amount of the same wax was heated in a spouted container and poured into the grip former cavity to form a wax base the same as the shape of the specimen with dimensions of 75± 0.03 mm in length × 55 ± 0.03 mm in width × 7 ± 0.03 mm (hight). On the top surface of the of wax base, a rectangular groove 5 mm wide and 1.5 mm deep was prepared for each specimen. Six maxillary teeth were mounted onto the grooved wax base using a heated base plate wax as shown in Figure 3.12 (A). Excess wax material attached to the teeth neck and lingual surfaces at the incisal portion of the teeth were carefully removed in order to provide a consistent and realistic method of attachment.

To create the specimen mould, the first half of a denture flask (Bracon limited, UK) was filled with dental plaster and Type 4 Diestone was then poured over the plaster. Subsequently, the wax base with teeth attached was placed onto the Diestone in the flask and left to dry and set for approximately 20 min as shown in Figure 3.12 (B). A separating medium (sodium alginate, John Winter, Germany) was then applied over the set plaster, Dyestone and prepared teeth so that the second half of the flask, filled with plaster, could be processed and facilitate easy removal of the two halves when processing had been completed.

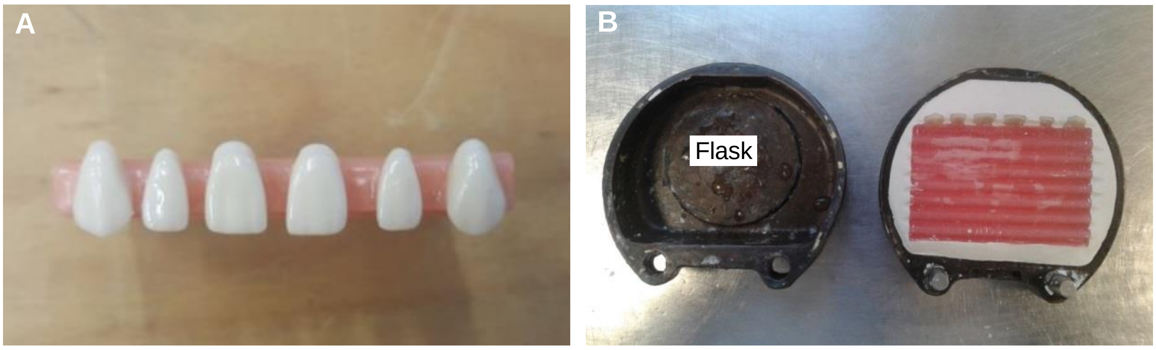

Figure 3.12. Photograph of (A) Wax base with teeth and (B) wax base specimen in the flask

Once the dental plaster was set within the mould, the wax was flushed away with boiling water in a dewaxing machine (Labormat SD, Dreve Dentamid GmbH, Germany) and the flask cleaned with steam (Cape Watch, UK) to remove any remaining wax in the plaster mould cavity. After the flask had reached room temperature, separating medium was again applied in the mould cavity surface with the exception of the teeth in order to facilitate easy removal of the prepared specimen. Nanocomposite denture base resins were prepared by mixing liquid MMA, zirconia nanoparticles and powder PMMA according to Table 3.6. When the mixture reached a consistent “dough”-like stage (working stage), it was packed into the mould. After closing the flask, it was placed in a hydraulic press (Sirio P400/13045, Meldola, Italy) under a pressure of 15 MPa at room temperature (23 ^{o}C) in the first cycle and then the pressure was released. Excess denture base resin was removed from the flask periphery and then re-pressurised under the same pressure at room temperature for 15 min. The flask was then immersed in a temperature-controlled curing water bath for 6 h, to allow polymerisation. The curing cycle involved increasing the temperature to 60°C over 1 h and maintained this temperature for 3 h. After this, the temperature was increased to 95°C over an additional 2 h to complete the heat polymerisation cycle. The flask was removed from the curing bath, cooled slowly for 30 min at room temperature and opened to remove the specimen. The specimen was placed in an ultrasonic cleaning machine with water (Elma, Birmingham, UK) to clean the die stone from the specimen. Any remaining die stone was trimmed away using a tungsten carbide bur (D B Orthodontics, West Yorkshire, UK), and finally polished with pumice powder in a polishing machine (Tavom, Wigan, UK) to fabricate the TBS test specimen.

Table 3.6. Weight percent zirconia in combination with acrylic resin powder as well as monomer content of the specimen groups.

Experimental Groups	Zirconia (wt.%)	Zirconia (g)	HI PMMA powder (g)	HI MMA monomer (ml)
G1 (Control)	0.0	0.000	25.000	12.0
G2	1.5	0.375	24.625	12.0
G2	3.0	0.750	24.250	12.0
G	5.0	1.250	23.750	12.0
G5	7.0	1.750	23.250	12.0
G6	10.0	2.500	22.500	12.0

The specimen was duplicated using addition cured 2-part silicone putty in a 1:1 ratio to produce a copy of the wax specimen. Figure 3.13 presents the duplication steps. The duplicated wax specimens were then used to fabricate the remaining thirty specimens, following the same procedure mentioned earlier for bond strength test. The specimens were stored in distilled water at 37°C for 7 days before conducting TBS test.

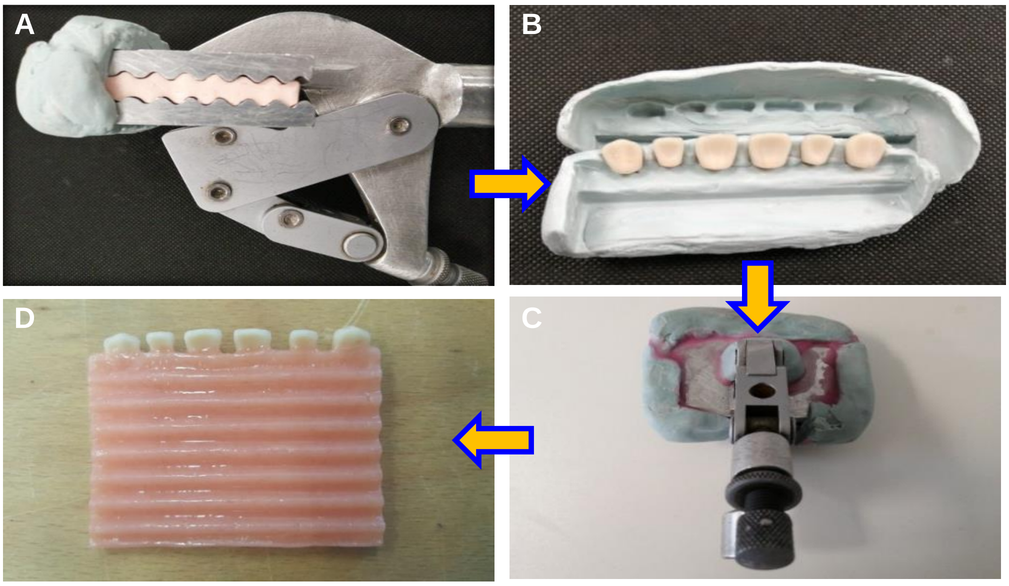

Figure 3.13. Photographs illustrating the steps involved in duplicating the wax specimen in the grip former by Addition cured 2-part silicone putty: (A) creating silicone putty duplication mould (B) placing maxillary anterior teeth in the duplication mould, (C) placing duplication mould containing teeth in the grip former

and pouring denture wax and (D) removing final wax specimen from the silicone putty mould.

3.7.3. Evaluation of tensile bond strength (TBS)

Thirty specimens of teeth on denture base materials were prepared for TBS tests using a universal testing machine (Hounsfield Tensometer, H10KS, Germany), according to the British standard (BS EN ISO 22112: 2017) (British Standards, 2017).The specimens were removed from distilled water and placed in the same metal grip former, which was fixed to the bottom of the testing machine. A jig was designed to pull individual teeth out from the specimens and this was fixed at the upper cross-head of the universal testing machine. The jig was designed in the shape of a tuning fork with two adjustable screws in the two legs as shown in Figure 3.14.

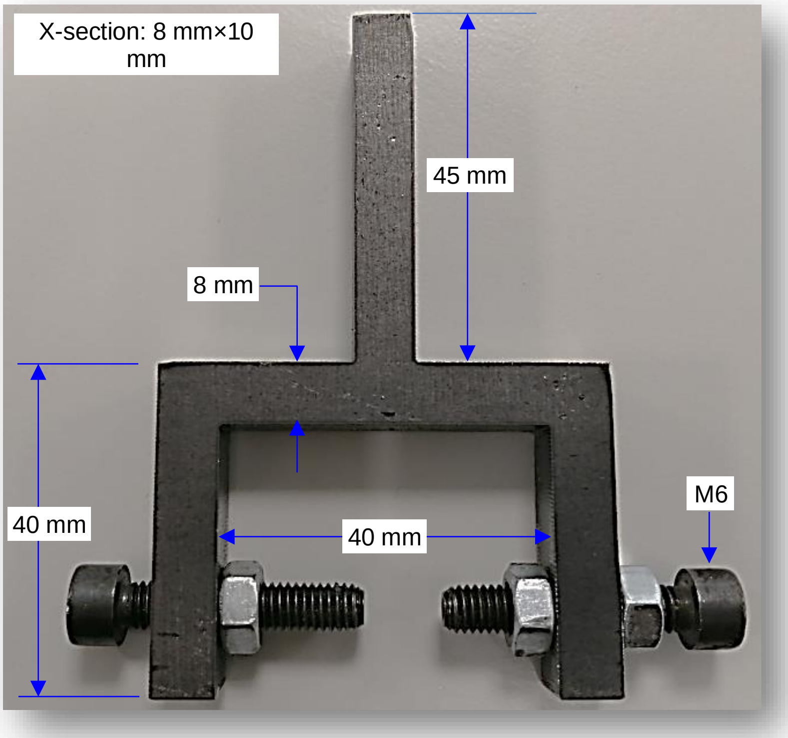

Figure 3.14. Photograph of the jig used to displace teeth from the test specimens

The screws were adjusted to fix against the specimen base from both sides in order to secure the specimen. One screw was pushed underneath the lingual area of a tooth and the other screw positioned under the neck portion of the tooth to allow a direct pull on the ridge lap area of the tooth attached on the base in a labial direction during tensile testing. Figure 3.15 demonstrates the experimental set-up when TBS of the teeth was assessed.

TBS tests were conducted at a crosshead speed of 5 mm/min (British Standards, 2017; Cardash et al., 1990; Kurt et al., 2012), pre-load 0.3 N and the load cell capacity was 1000 N. The load was applied to individual teeth until failure occurred and the maximum breaking forces were recorded in Newtons. The broken specimens were checked visually and under a microscope to determine whether the failure modes were adhesive, cohesive or a combination both.

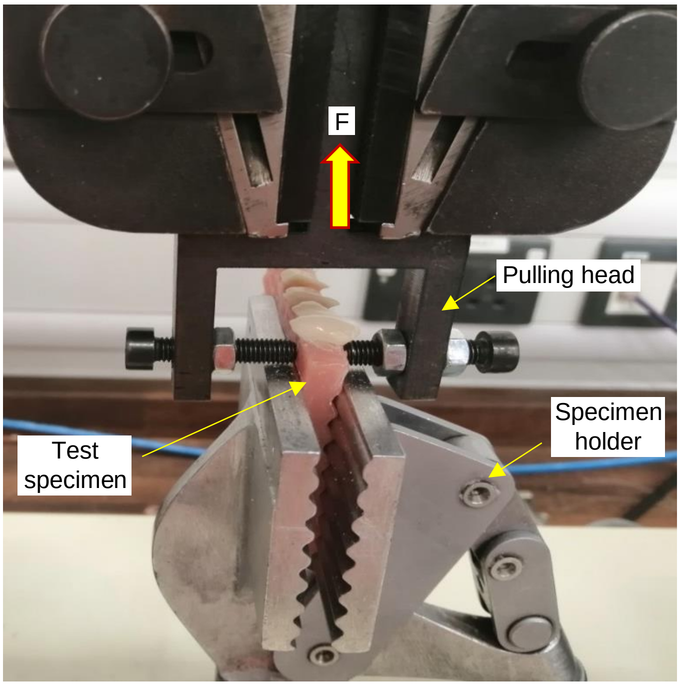

Figure 3.15. Bonding strength test set-up under tensile loading condition using Hounsfield universal testing machine

3.8. EVALUATION OF EQUIVALENT FLEXURAL STRENGTH

3.8.1. Preparation of wax denture

Maxillary edentulous master casts were duplicated using an addition-cure silicone putty to obtain a mould, which was then used to produce thirty identical edentulous casts by pouring high-strength plaster stone into the silicone mould as shown in Figure 3.16. The casts were then trimmed using a standard plaster trimming machine (Gambrini, Cambridgeshire, UK) to remove any rough surfaces around the periphery.

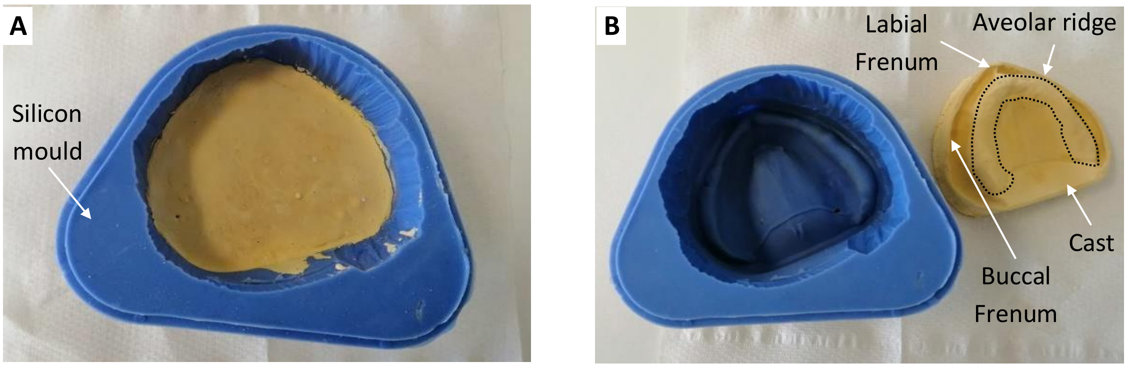

Figure 3.16. Photograhs illustrating (A) Silicone mould poured with high-strength plaster stone, (B) Silicone mould and maxillary edentulous master cast.

Two sheets of baseplate wax (Metro wax) (Metrodent Limited, Huddersfield, UK) with a thickness of 3.50 mm were heated over a flame until soft, and then adapted onto the palatal surface to cover the entire area on the edentulous cast. Any excess wax was removed, and relief areas were made for the labial and buccal frenums. A wax bite block (Metrodent Limited, Huddersfield, UK) in the shape of a horseshoe was placed and adapted onto the base over the alveolar ridge area to form an occlusal rim. The maxillary master cast with occlusal rim was then fixed onto an articulator (John Winter, Halifax, UK) using dental plaster, in preparation for setting the teeth as shown in Figure 3.17 (A).

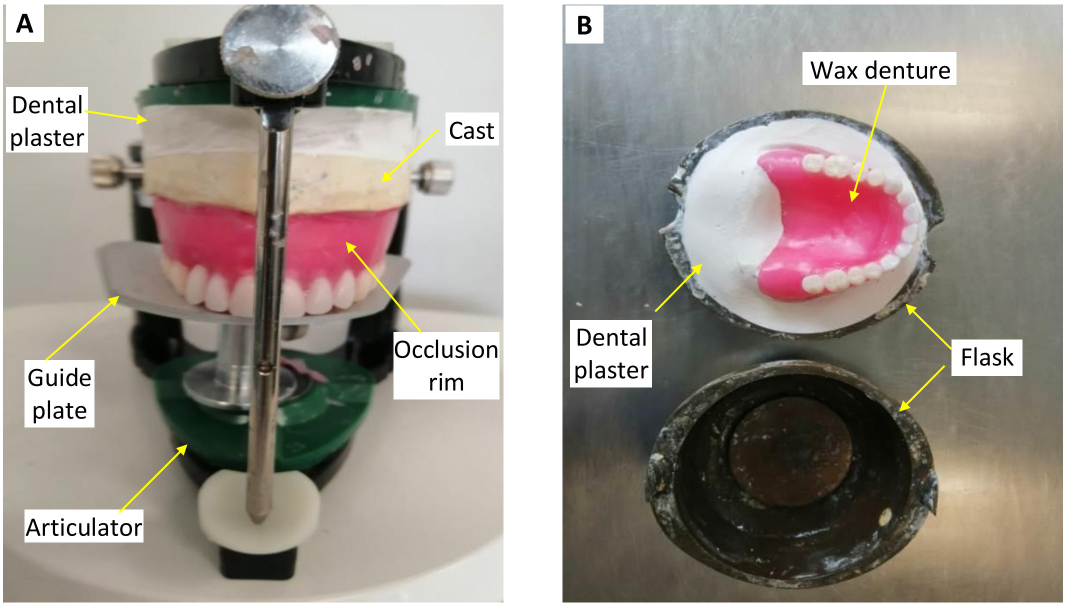

Figure 3.17. Photographs detailing (A) Maxillary master cast with teeth set on occlusion rim fixed on articulator and (B) Wax denture on a cast placed into dental plaster contained within a flask.

Instead of using a mandibular master cast as a guide for setting the maxillary teeth, a metal guide plate was placed on the base of the articulator. Then upper anterior teeth (Artic 6M S10 shade BL3, Metrodent Limited, Huddersfield, UK) and upper posterior teeth (Artic 8M 10 30U shade A2, Metrodent Limited, Huddersfield, UK) were fixed onto the occlusion rim. After waxing of the denture base and teeth, the wax denture and plaster cast was removed from the articulator and prepared for flasking. A sodium alginate separating medium (John Winter, Germany) was then applied to the cast and flasks. After the separating medium had dried, one half of the flask was filled with dental plaster and the cast with wax denture was placed on the dental plaster within the flask as shown in Figure 3.17 (B). Dental stone was then placed on to the teeth to cover the biting surface of the denture avoid any breakages. The other half of the flask was also filled with dental plaster and the two halves closed taking care not to apply excessive force. After one hour, the flask was put in dewaxing machine (Labormat SD, Dreve Dentamid GmbH, Germany) to remove the denture wax in order to allow for the addition of the acrylic to make the final dentures.

3.8.2. Preparation of denture base specimens

The silane treated zirconia and acrylic resin powders were weighed according to Table 3.6. using an electronic balance with an accuracy to three decimal points (A & D Company, Limited, Toshima-ku, Tokyo). Where indicated zirconia powder was added at the appropriate concentration to the acrylic resin monomer and mixed in a speed mixer (DAC 150.1 FVZK, High Wycombe, UK) at 2,500 rpm for 5 min. Once mixed the acrylic resin powder was then added to the solution, and further mixing in accordance with the manufacturer’s instruction was undertaken until a smooth uniform mixture was obtained. After approximately 20 min when the mixture reached a “dough” like consistency, it was packed into the flask by hand. The flask was then securely closed and placed in a hydraulic press (Sirio P400/13045, Meldola, Italy) under a pressure of 15 MPa at room temperature for approximately 15 minutes, and then the pressure was released. Excess acrylic mixture was then removed from the flask periphery and re-pressed at room temperature for a further 15 min under the same pressure. The flask was then immersed in a temperature-controlled curing water bath for 6 hr, to allow polymerisation. The curing cycle involved increasing the temperature to 60 °C over 1 h and maintaining this temperature for 3 h. Subsequently, the temperature was increased to 95 °C over an additional 2 h to complete the heat polymerisation cycle. The flask was then removed from the curing bath and cooled slowly for 30 min at room temperature. The flask was then opened, and the denture removed. The denture was placed in an ultrasonic cleaning machine containing water

(Elma, Birmingham, UK) to remove any attached stone, trimmed using a tungsten carbide bur (D B Orthodontics, West Yorkshire, UK), ground with an emery paper grit 40 (Norton, Saint-Gobain, London, UK), and finally, polished with pumice powder in a polishing machine (Tavom, Wigan, UK). All thirty denture specimens were fabricated individually using the method described above. The specimens were manufactured into three groups of 10 dentures, with the respective quantities of nano-filler incorporated into each group (0wt%, 3 wt.% and 5 wt.% of zirconia). Furthermore, each group was again divided into 2 subgroups of 5 specimens for bending tests with and without fatigue loading.

3.8.3. Measurement of fatigue loading using a chewing simulator

A CS-4.2 chewing simulator was used to measure fatigue loading. The CS-4.2 allows simulation of masticatory forces on dental materials with high levels of standardisation according to chewing frequency, shape of antagonist materials, contact load, number of cycles and sliding speed. Each chamber has an upper specimen holder held in place with a screw and a plastic lower specimen holder fixed by an aluminium rod (Ho et al., 2018).

Fatigue loading was performed according to a previous study by Im et al. (Im et al., 2017) using a chewing simulator (CS-44.2 SD Mechatronik GmbH, Feldkirchen-Westerham, Germany). Fifteen denture specimens, five from each group, were employed for fatigue tests. The specimens were stored in distilled water in an incubator at a temperature of 37±1°C for 7d before applying the fatigue loading. To simulate the mastication motion, a stainless steel "T" shaped jig (50 mm length × 9.75 mm width) was fixed onto an antagonist holder. The upper bar faced the midline of the denture and the T shaped jig was placed against the second premolar (full) and first molar (partial) teeth on each side at 1.6 Hz (Figure 3.18). The initial loading applied on the denture was 8 kg (78.48 N). The vertical movement of the upper bar was set at 2 mm and the lateral movement at 0.2 mm, at a vertical speed of 30 mm/s. A total number of 250,000 mastication cycles were performed in 37°C distilled water to simulate approximately one year of clinical service. All denture specimens were examined after fatigue tests to identify any cracks or failures.

Figure 3.18. Chewing simulator instrument with denture base specimen fixed to the chamber base on the cast for mastication simulation under fatigue cyclic loading (inset).

3.8.4. Evaluation of equivalent flexural strength

Thirty denture specimens with and without fatigue loading were subjected to three-point bending tests in a Hounsfield universal testing machine (Hounsfield Tensometer, H10KS, Germany) as seen in Figure 3.19 (B). The specimens were stored in distilled water at a temperature of 37±1 °C for 7 days in an incubator before conducting the tests. The occlusal surface of the denture was placed within a specially designed specimen holder to prevent any movement of the dentures during the bending tests. The distance between the second molar teeth (last teeth on each sides) acted as a supporting span with a length of 42.33 ± 0.2 mm. The loading head, made from stainless steel, with a length of 70 mm and a tip diameter of 10 mm was attached to the Hounsfield testing machine. The load was applied to the palatal fitting surface at a cross-over point between the palatal midline and the line connecting the centre of first molars on each side of the denture Figure 3.19 (B). After several pilot tests, it was found that this loading position provided a relatively flat surface with minimal chance of slipping. Furthermore, to avoid any slipping between the loading head and palatal surface, a small piece of emery paper with a thickness of 0.60 mm with a small hole at its centre was secured at the contact point with double-sided sticky tape. The hole was aligned with the point of loading as seen in Figure 3.19 (A).

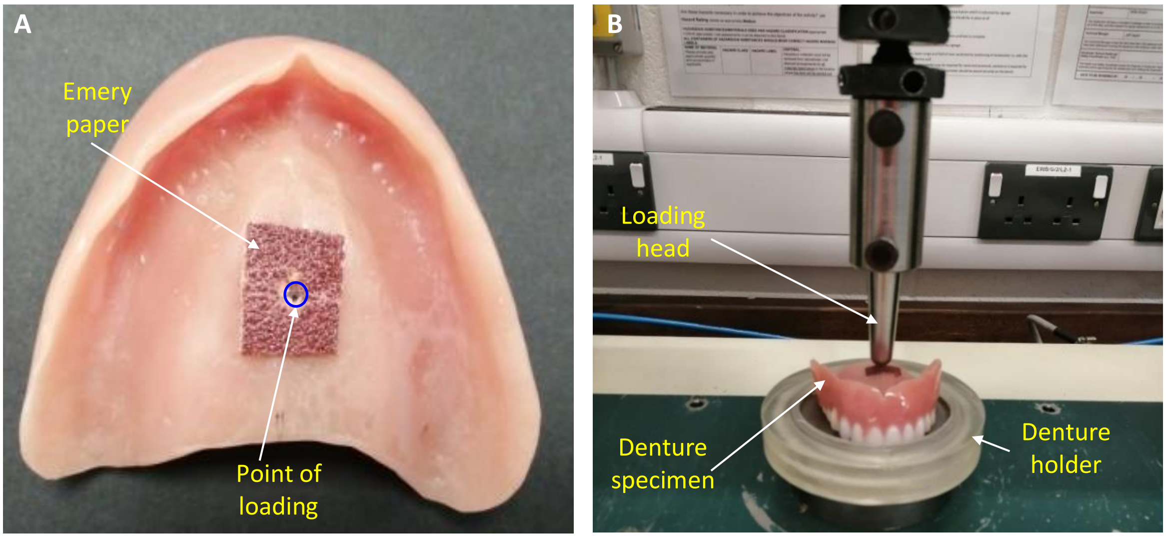

Figure 3.19. Photograph demonstrating (A) Sticking emery paper on the palatal surface with a hole at the point of loading, (B) applying bending load on palatal surface of denture specimen in Hounsfield universal testing machine

The thickness of the dentures was measured using a digital micrometer (Mitutoyo, Hampshire, UK) at the point of loading around the central palatal area (Figure 3.20) with an average dimension of 3 ± 0.2 mm. The width of the load bearing area of the dentures were measured as 42 ± 0.2 mm, and the weight of all denture specimens were measured using an electronic digital scale (Machine Mart Limited, UK). A 10 kN load cell, a cross head speed of 5 mm/min and preload 10 N were used to record maximum fracture force (F) in Newton during the bending tests, and equivalent flexural strength was calculated in MPa for all dentures specimens using Equation 3.12 (British Standards, 1989).

$$\sigma = \frac{3\mathrm{Fl}}{2\mathrm{bh}^2} \tag{3.12}$$

Where F is the maximum force applied in N, l is the distance between the supports in mm, b is the width of load bearing area of the denture specimen in mm, and h is the thickness of the denture specimen in mm at the point of loading.

Figure 3.20. Photograph showing the denture thickness measurement using a micrometer at the point of loading during bending test

Chapter 4: Chemical Characterisation of Silanised Zirconia and its Effects on the Properties of PMMA-Zirconia Nanocomposites

4.1. ABSTRACT

Purpose: The aim of this study was to investigate the flexural strength, flexural modulus and surface hardness of high-impact (HI) heat-cured acrylic denture resin (PMMA) reinforced with silanised and non-silanised zirconia (ZrO_2) nanoparticles.

Materials and Methods: Forty-five high impact heat-cured acrylic resin specimens reinforced with zirconia were fabricated. All the specimens were divided into three groups: Group 1: control group with no zirconia in PMMA, Group 2: PMMA reinforced with 3wt% of non-silanised zirconia nanoparticles and Group 3: PMMA reinforced with 3wt% of salinised zirconia nanoparticles. Ten specimens from each group were used to measure flexural strength and flexural modulus and then another five specimens from each group were used for measuring surface hardness. The dimensions of the specimens were 65 ± 1.0 mm × 10 ± 0.1 mm × 2.50 ± 0.1 mm. For measuring the flexural strength and modulus, a Zwick universal testing machine (Zwick/Roell Z020 Leominster, UK) and for surface hardness, Vickers hardness testing machine (FM-700, Future Tech Corp., Japan) were used. Silanised and non-silanised zirconia nanoparticles were analysed with Fourier Transform Infrared (FTIR) Spectroscopy. Furthermore, raw materials and fractured surfaces of the specimens were examined by a Scanning Electron Microscope (SEM). A one-way ANOVA statistical test followed by a post-hoc Bonferroni test was employed to analyse the results.

Results: The results showed that the mean values for flexural strength and surface hardness of the group containing 3wt% treated ZrO_2 (83.5 ± 6.2 MPa), (20.1 ± 2.3 kg/mm^2) were significantly increased ($P<0.05$) when compared to the specimens in the group containing non-treated zirconia (59.9 ± 7.1 MPa) (15.0 ± 0.2 $HV_{0.05}$) and the control group (72.4 ± 8.6 MPa) (17.1 ± 0.9 $HV_{0.05}$). However, the group with silanised zirconia showed an increase in flexural modulus (2313 ± 161 MPa), but not significantly different ($P>0.05$) from the group without silanisation (2207 ± 252 MPa) and the control group (1971 ± 235 MPa).

Conclusion: Silane treatment of zirconia nano-filler can improve the flexural strength and surface hardness properties of HI PMMA-ZrO_2 nanocomposite, thus leading to a potentially longer service life for the denture base.

4.2. INTRODUCTION

Acrylic resin remains the material of choice for complete dentures as it processes satisfactory properties (da Silva et al., 2012) and provides a satisfaction outcome for patient (Ayaz and Durkan, 2013). The most common prosthetic acrylic resins is polymethyl methacrylate (PMMA) (Diaz-Arnold et al., 2008) or a modified version with butadiene styrene rubber compound to form high-impact denture bases with improved strength (Abdulwahhab, 2013; Sasaki et al., 2016). This modification has been successful in terms of improving the impact strength (Zheng et al., 2012), however, other studies have reported a decrease in the flexural strength (Ayaz and Durkan, 2013) and stiffness (Zheng et al., 2012). Still, in clinical practice, denture bases have been shown to flex under masticatory forces, subjecting the acrylic polymer to internal stresses that may result in crack formation and eventually, fracture of the denture (Machado et al., 2012b).

The incorporation of inorganic nanoparticle fillers into HI PMMA acrylic resin has been suggested as a potential solution to this problem. Mixing of nanoparticles with organic polymers represents a new class of materials that exhibit improved performance when compared with the micro-particle filled polymers (Elshereksi et al., 2017). The effect of nanoparticles on the mechanical properties of PMMA depends on several factors including the polymer-particle interface, particle size, fabrication method and particle dispersion within the PMMA matrix (Ergun et al., 2018; Reyes-Acosta et al., 2015). Nanomaterials have a high specific surface area and show excellent performance and unique features that are often radically different from conventional materials (Elshereksi et al., 2017).

Researchers have attempted to improve the mechanical properties of denture base acrylic resins with the addition of various metal oxide nanoparticles, such as titanium oxide (Asar et al., 2013; Elshereksi et al., 2017), alumina (Alhareb et al., 2018; Kundie et al., 2018; Vojdani et al., 2012; Zhang et al., 2014) and silica (da Silva et al., 2012). Zirconium oxide (zirconia, ZrO_2) is another metal oxide that is widely used and has attracted interest as an inorganic filler material for developing polymer nanocomposites (Alhavaz et al., 2017). The incorporation of zirconia nanoparticles has been investigated and found to improve the mechanical properties of conventional PMMA denture base resins (Alhareb et al., 2018; Alhavaz et al., 2017; Fan et al., 2013; Gad et al., 2016a; Zhang et al., 2014). Zirconia has beneficial mechanical properties such as high flexural strength (900 to 1200 MPa), hardness (1200 HV) and fracture toughness (9–10 MPa $m^{1/2}$), abrasion and corrosion resistance and biocompatibility, which make it a good choice for polymer reinforcement in denture base applications (de Souza Leão et al., 2019).

As nanoparticles exhibit high surface energy, high polarity and hydrophilic surfaces, uniform distribution throughout the polymer matrix can be challenging, causing some phase separation and aggregation (Mallakpour et al., 2015; Mallakpour and Ezhieh, 2017; Sabzi et al., 2009). The surface of the nanoparticles must be modified with coupling agents such as silane (Mallakpour and Ezhieh, 2017), which can create a strong interfacial bond with the resin matrix (Mohsen and Craig, 1995). Silane coupling agent is required to retain fillers in the resin matrix. Silane has two (or more) functional groups that can form a chemical bond to connect to different substrates (inorganic fillers and organic resin matrix) (Lung et al., 2016). Modification of nanoparticles can be achieved in two ways. The first method refers to a chemical treatment, where a small molecule of coupling agent, is absorbed on the surface of the nanoparticles (Mallakpour et al., 2015; Zhao et al., 2012). The second method of modification can be performed by grafting polymeric molecules, such as poly-methyl methacrylate, onto the hydroxyl groups present on the surface of the nanoparticles through covalent bonds leading to an, improved adhesion (Mallakpour et al., 2015; Wang et al., 2007).

According to previous research which evaluated conventional PMMA acrylic resin reinforced with metal oxides silanisation improved the properties (Asar et al., 2013; Gad et al., 2016b). Therefore, it could be useful to investigate the advantages of silanisation in this study. To the authors best knowledge, there are no data available in the literature regarding the effect of zirconia nanoparticle silanisation on the mechanical properties of zirconia impregnated HI PMMA nanocomposites. The purpose of this study was to investigate how silanisation of zirconia nanoparticles affect flexural strength, flexural modulus and surface hardness of HI PMMA reinforced with 3 wt.% zirconia.

The hypothesis was that there would be no significant difference between silanised and non-silanised PMMA-ZrO_2 nanocomposites with respect to flexural strength, flexural modulus and surface hardness.

4.3. MATERIALS AND METHODS

4.3.1. Materials

High impact heat-cured acrylic resin polymethyl methacrylate (PMMA) powder and methyl methacrylate liquid monomer (Metrodent MMA; product no. 202-327-6) were selected as the denture base material. Yttria-stabilised zirconia (ZrO_2) nanoparticles

(Product no. 8522QI, Sky Spring Nano Materials) were chosen as the filler material for manufacturing the nanocomposite specimens.

4.3.2. Specimen preparation

Zirconia nanoparticle surfaces was treated with 7 wt.% silane coupling agent (3-trimethoxysilyl propyl methacrylate; product no. 440159, Sigma Aldrich) as explained in section 3.2.2 Preparation of silanisation in Chapter 3.

According to previous studies, a small percentage addition (1% to 7.5wt%) of different metal oxide nanoparticles can improve the properties of PMMA denture base resin (Asar et al., 2013; Gad et al., 2016b; Vojdani et al., 2012; Zhang et al., 2014).Therefore, a low concentrations of zirconia nanoparticles (3 wt.%) was used to prepare nanocomposite specimens for this study.

The composition details of the silane-treated and non-silane zirconia and acrylic resin powders were weighed according to Table 4.1 using an electronic balance (Ohaus Analytical). The zirconia powder was added to the acrylic resin monomer and mixed by hand using a stainless-steel spatula to ensure all the powder was uniformly distributed within the resin monomer and to avoid any aggregation. The HI acrylic resin powder was then added to the liquid, and mixing continued until a consistent mixture was obtained, according to the manufacturer’s instructions. When the mixture reached a dough-like stage that was suitable for handling, it was packed into a mould by hand. The mould was then closed and placed in a hydraulic press (Sirio P400/13045) under a pressure of 15 MPa and then excess mixture was removed from the periphery of the mould. The mould was immersed in curing bath for 6 hours polymerisation at temperature 95°C, and then the mould was removed from the curing bath and cooled slowly for 30 min at room temperature. The mould was then opened, and the specimens were removed. The specimens were then trimmed using a tungsten carbide bur, ground with an emery paper and polished with pumice powder in a polishing machine (Tavom, UK).

Table 4.1. Weight percent zirconia in combination with acrylic resin powder as well as monomer content of the specimen groups

Experimental Groups	Zirconia (wt.%)	Zirconia (g)	HI PMMA powder (g)	HI MMA monomer (ml)
Control	0.0	0.000	21.000	10.0
3.0	3.0	0.630	20.370	10.0

In order to understand their behaviour the comparison between silanised and non-silanised zirconia nanoparticles was assessed in methyl methacrylate monomer (MMA) and water Figure 4.1. In both liquid (MMA and water) silanised particles were homogeneously distributed and remained suspended and this was in contrast to the non-silanised particles which appeared to settle at the bottom of the containers. Therefore, it is expected that silane functionalisation would encourage the homogeneous distribution of particles in the nanocomposites.

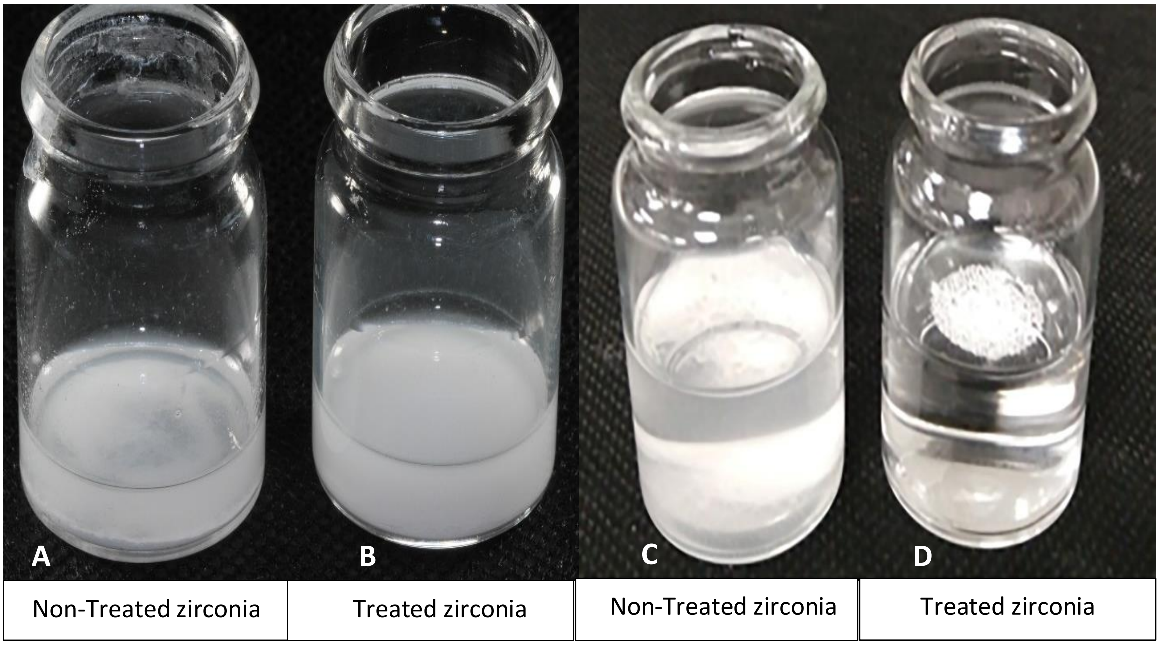

Figure 4.1. Photographs illustrating non-treated and silane treated zirconia nanoparticles mixed in (A, B) monomer (MMA) and (C, D) water.

4.3.3. Materials Characterization

4.3.3.1. Particle chemical analysis procedure

An Energy Dispersive X-ray Spectroscopy (EDX) was used to analyse the elemental compositions of PMMA and zirconia particles. The particles were randomly selected and then loaded into the SEM/EDX (Carl Zeiss Ltd, 40 VP, Smart SEM) for imaging using the secondary electron detector at an acceleration voltage of 20.0 kV.

4.3.3.2. Analysis procedure silane bonding on zirconia

Fourier Transform Infrared spectroscopic (FTIR) (Perkin-Elmer Spectrum Two, Spotlight 200i) were used to determine the functional groups and bonding types in the silanised zirconia nanoparticles powders and non-silanised zirconia. Spectra were obtained with the wavenumber range from 4000 to 400 cm^{-1} at a resolution of 4 cm^{-1} at room temperature.

4.3.4. Mechanical tests

4.3.4.1. Flexural test

Flexural strength of the specimens was evaluated using a 3-point bending test in a universal testing machine (Zwick/Roell Z020 Leominster) in accordance with British International Standard for Denture Base Polymers (2487:1989) (British Standards, 1989). The dimensions of the specimens were 65 ± 1.0 mm length × 10 ± 0.1 mm width × 2.50 ± 0.1 mm thickness, and the specimens were stored in water at a temperature of 37 ± 1°C for 50 ± 2 hours in an incubator before testing. The specimens were then removed from the water and placed on a support jig. The loading plunger (diameter 7.0 mm) was fixed at the centre of the specimen midway between two supports, which were parallel and separated by 50 ± 0.1 mm. A load cell of 500 N with a cross-head speed of 5 mm/min was applied until fracture occurred. The maximum force (F) was recorded in Newtons, and then flexural strength was calculated in MPa for all specimens using the following Equation 4.1 (British Standards, 1989).

$$\sigma = \frac{3\mathrm{Fl}}{2\mathrm{bh}^2} \qquad (4.1)$$

Where F is the maximum force applied in N, l is the distance between the supports in mm, b is the width of the specimen in mm, and h is the height of the specimen. For flexural modulus determination, the machine was calibrated to record the results of individual specimens.

4.3.4.2. Hardness test

The Vickers hardness ($HV_{0.05}$) of the specimens was measured using a micro-hardness testing machine (FM-700, Future Tech Corp). The dimensions of the specimens were 65 ± 1.0 mm length × 10 ± 0.1 mm width × 2.50 ± 0.1mm thickness, and the test load fixed at 50 g was applied for 30 sec. The Vickers hardness was calculated by measuring the diagonals of the pyramid-shaped indentation impressed on the specimen. A total of three indentations were taken at different points in each specimen, and then a mean value was calculated. The average values for all the specimens were determined to provide an overall mean value demonstrative of the materials in the dry condition at day 0. The specimens were stored individually in distilled water at a temperature of 37 ± 1°C for 7 d ± 2 hours and 45 d ± 2 hours in an incubator before testing to evaluate the effect of distilled water on all the specimens. From the raw data, the mean hardness values for each specimen group were calculated (Farina et al., 2012; Neppelenbroek et al., 2005).

4.3.5. Imaging of particles and fractured surface

The distribution of the particulate size and structure of the HI PMMA powder and zirconia nanoparticles in raw form was analysed with a scanning electron microscope (SEM). The fractured surfaces of the nanocomposite specimens from the flexural test were also studied using the SEM. The particles from the raw materials and the fractured nanocomposite specimens were mounted onto aluminium stubs and coated with a thin layer of gold using a sputter-coater. The specimens were then loaded into the SEM for imaging using the secondary electron detector at an acceleration voltage of 2.0 kV.

4.3.6. Statistical analysis of test results

The mechanical tests results were recorded and statistically analysed using a statistical software (SPSS) (IBM SPSS statistics version 23, USA). Descriptive statistics were conducted for each of the tests to determine if the data were normally distributed. According to tests on normality with Kolmogorov-Smirnov and Shapiro-Wilk, the data were normally distributed for all tests. The flexural strength, flexural modulus and hardness tests data were analysed by using a one-way analysis of variance (ANOVA) with post-hoc Tukey significant difference test ($P<0.05$).

4.4. RESULTS

4.4.1. Surface morphology analysis of particles

SEM analysis showed that the average particle size of the PMMA powder was approximately 50 µm with a range between 10 µm and 100 µm as shown in Figure 4.2 (A).

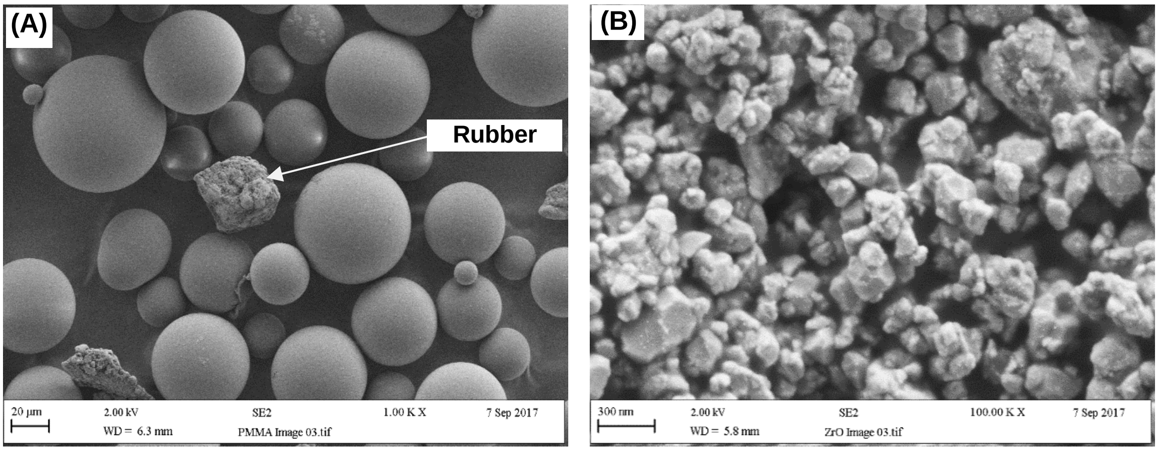

Figure 4.2. SEM illustrating the surface morphology and size distribution of (a) HI PMMA with rubber and (b) Zirconia particles

The butadiene styrene rubber particles were also visible within the powder, with an average size of approximately 30-50 µm. The yttria-stabilized zirconia nanoparticles had an average size ranging between 30 nm and 60 nm for individual particles and 200 nm to 300 nm when clustered, as shown in Figure 4.2 (B).

4.4.2. Chemical analysis of particles

Figure 4.3 presents SEM images and EDX spectra of butadiene styrene rubber within PMMA, PMMA particles and zirconia particles. The elemental compositions obtained are also presented in terms of weight and atomic percentages. EDX confirmed rubber particle represented by high percentages of carbon and oxygen with traces of other elements such as Al and Si in contrast to only carbon and oxygen in the PMMA particles. Other than zirconium and oxygen, a noticeable amount of carbon was present in the zirconia particles.

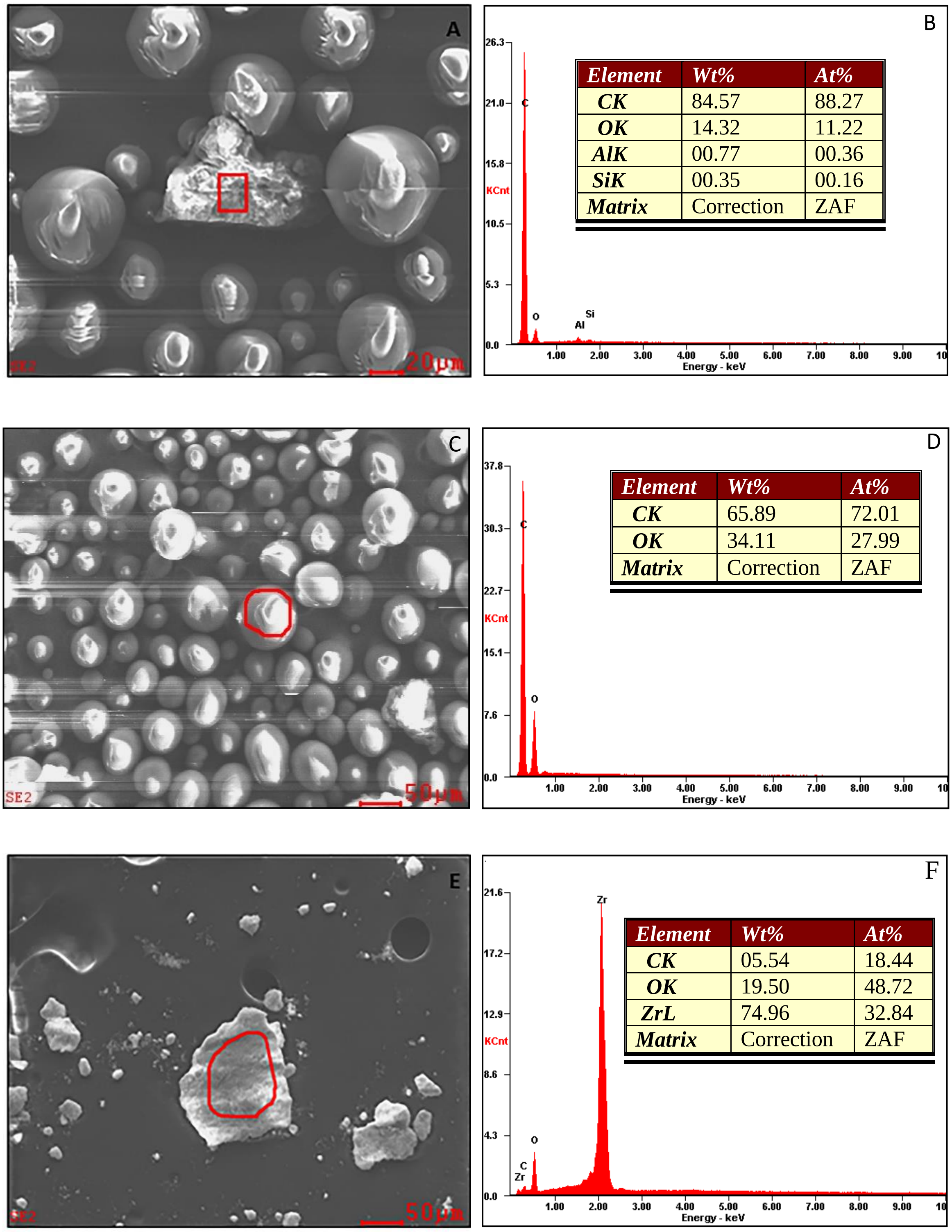

Element	Wt%	At%
CK	84.57	88.27
OK	14.32	11.22
AlK	00.77	00.36
SiK	00.35	00.16
Matrix	Correction	ZAF

Element	Wt%	At%
CK	65.89	72.01
OK	34.11	27.99
Matrix	Correction	ZAF

Element	Wt%	At%
CK	05.54	18.44
OK	19.50	48.72
ZrL	74.96	32.84
Matrix	Correction	ZAF

Figure 4.3. SEM images and EDX spectra representing (A & B) rubber particles into PMMA powder, (C & D) PMMA particles and (E & F) zirconia nanoparticles.

4.4.3. Analysis of zirconia functionalising by silane

Figure 4.4 illustrates the FTIR spectrum structure of silane coupling agents (γ-MPS) and presents the spectra curves of pure zirconia (without silane) and silanised zirconia. Both the zirconia spectra curves displayed the absorption peak between 3650 and 3200 cm^{-1}

associated with stretching vibrations of OH (hydroxy group) on the surface of the zirconia nanoparticles, (Fan et al., 2013; Kundie et al., 2018), with broader absorption peak in silanised zirconia.

In the spectral curve of γ-MPS, the peaks between 2944 and 2841cm^{-1} exhibited the asymmetric and symmetric vibrations of CH_3 and CH_2 groups. In contrast, the curve relating to silanised zirconia demonstrated absorption peaks around 2966 and 2844 cm^{-1}. The absorption peak in γ-MPS curve at approximately 1717 cm^{-1} was attached to the C=O group (carbonyl) vibrations of the (γ-MPS) molecules (Elshereksi et al., 2017). An absorption peak observed on the surface of silanised zirconia at 1717 cm^{-1}, indicated the formation of a C=O group vibrations. The absorption peak at 1638 cm^{-1} was attributed to C=C group in the γ-MPS on the silanised zirconia surface. The characteristic peaks between 1160 and 1078 cm^{-1} in γ-MPS spectrum represented vibration absorption bands of the Si-O-C and Si-O-Si, respectively. The strong peak at 813 cm^{-1} was assigned to the vibration of Si-C (Elshereksi et al., 2017). In silanized zirconia, the peaks at 1174 and 1054 cm^{-1} corresponded to Zr-O, while the peaks at 1330 and 1054 cm^{-1} indicated Zr-O-Si. The silanol groups produced by silane hydrolysis condensing with surface hydroxyl groups on the inorganic particles (ZrO_2) form a covalent bond (Sideridou and Karabela, 2009). The FTIR analysis confirmed that the coating of silane (γ-MPS) was successfully grafted onto the surface of zirconia nanoparticles. Table 4.2 lists all bond types and wavelengths.

Table 4.2. Bond type and wavelength of Silane coupling agent, 3-trimethoxysilyl propyl methacrylate (γ-MPS) and silanized zirconia nanoparticles.

Bond type	**Wavelength (cm^{-1})**	**Reference of** γ-MPS
O–H	3650-3200	3425
CH_3--CH_2	2966-2844	2944-2841
C=O	1717	1717
C=C	1638	1638
Zr-O	1174 - 1054	1160 - 1078
Zr-O-Si	1330 -1054	1160 - 1078

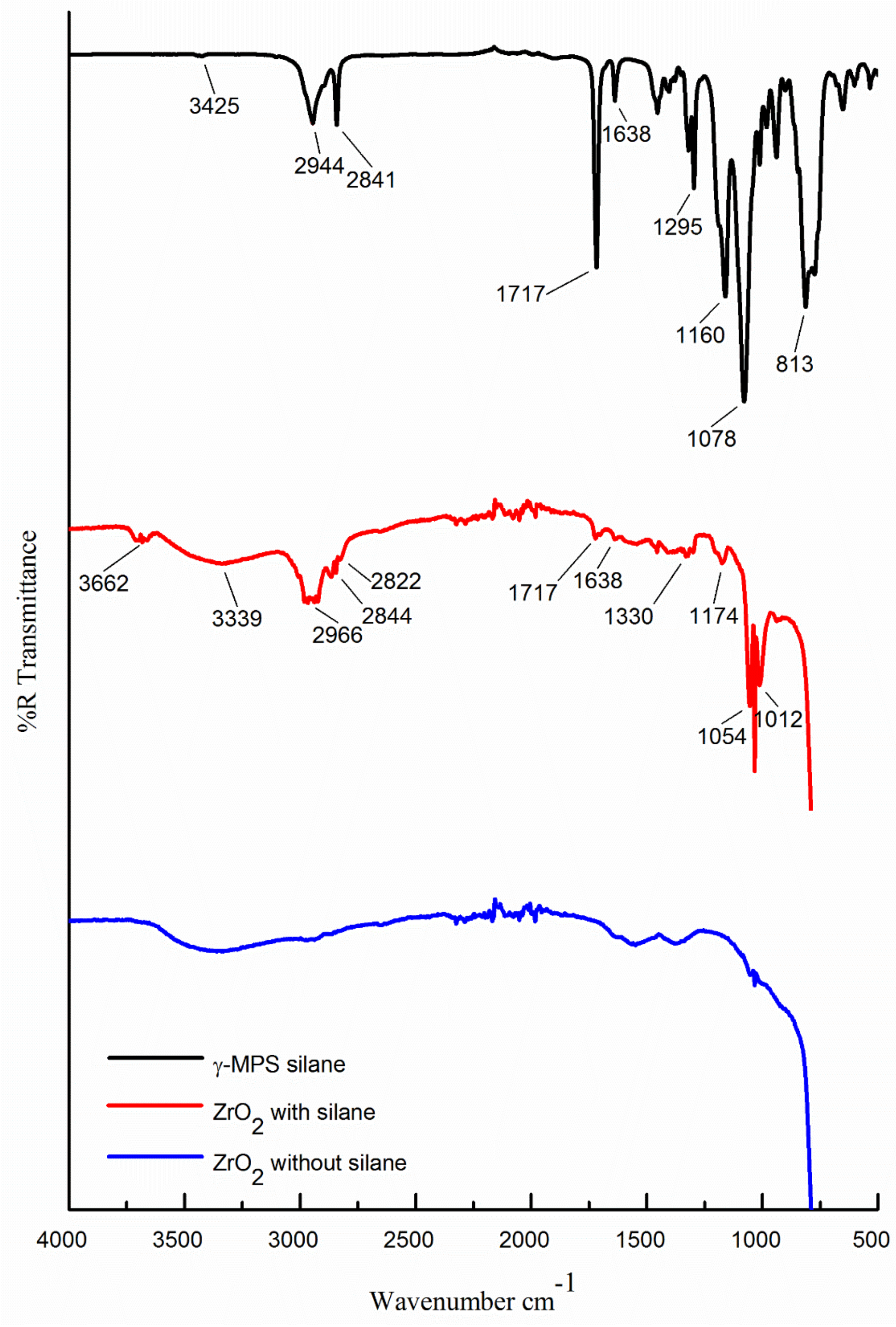

Figure 4.4. FTIR spectra showing (black curve, top) silane coupling agent (γ-MPS), (red curve, middle) zirconia nanoparticles after treatment with silane (γ-MPS) and (blue curve, bottom) zirconia nanoparticles without silane

The mechanism by which 3-trimethoxysilyl propyl methacrylate silane coupling agent reacts with zirconia nanoparticles surface and the bonding with PMMA is shown in Figure 4.5 (Hu et al., 2009).

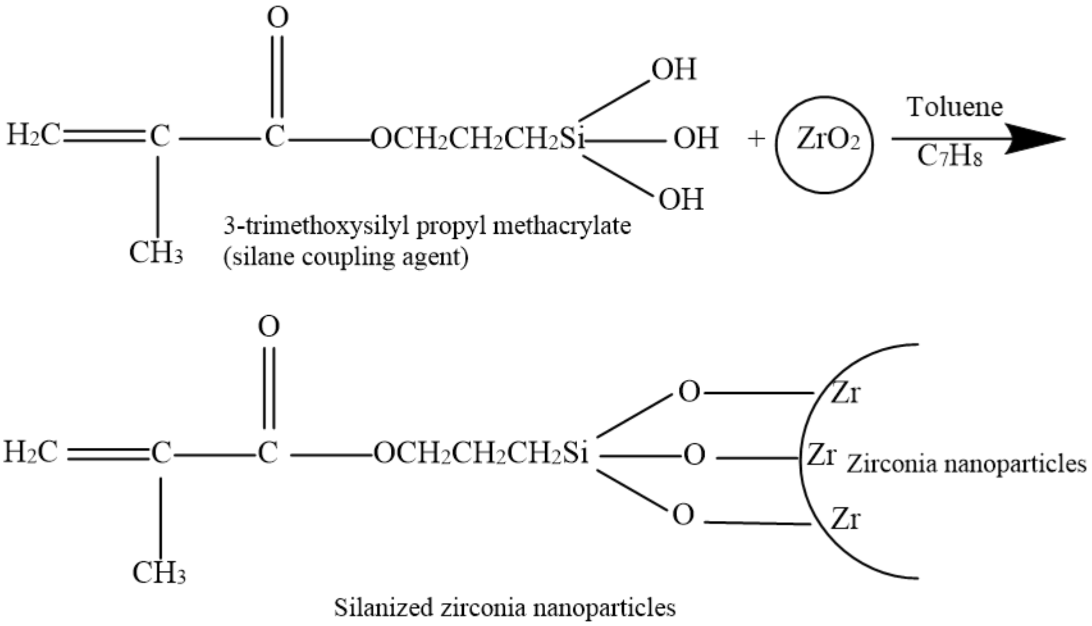

Figure 4.5. Illustration showing the chemical bonding of silane (MPS) with zirconia (ZrO_2) nanoparticles

4.4.4. Flexural strength and modulus

The mean and standard deviation values of flexural strength and modulus for each experimental group are presented in Table 4.3, Figure 4.6 and Figure 4.7. One-way ANOVA indicated a statistically significant difference between the mean values ($p<0.001$) and the Tukey test showed that there was a significant difference ($p<0.05$) between test groups of silanised and non-silanised nanocomposites and the control group. However, flexural modulus values showed no significant difference ($p>0.05$) between silanised and non- silanised groups.

The highest mean value of flexural strength was (83.5 ± 6.2 MPa) for the silanised group compared to the non-silanised group (59.9 ± 7.1 MPa). The reinforcement (3 wt.%) of HI PMMA with silanised zirconia nanoparticles increased flexural strengths by 40% and 15% compared to the non-silanised group and control group respectively. The highest mean value of flexural modulus was found (2313.00 ± 161.3 MPa) for the group containing 3 wt% of silanised zirconia representing a 5% increase in the modulus compared to the non-silanised group (2207.0 ± 252.7 MPa), but not significantly different ($p<0.05$). In comparison to the control group, this represented an increase in the flexural modulus of 17%.

4.4.5. Vickers Hardness

The mean and standard deviation values of surface hardness for each experimental group are listed in Table 4.3 and Figure 4.8. The Tukey test showed that there was a significant difference ($p<0.05$) between the test groups of silanised and non-silanised nanocomposites and control group. The highest value of Vickers hardness was obtained (20.1 ± 2.3 kg/mm^2) for the group containing 3 wt.% silanised zirconia, and significantly different ($p< 0.05$) compared to the non-silanised (15.0 ± 0.2 $HV_{0.05}$) and control (17.1 ± 0.9 $HV_{0.05}$) groups, representing a 33% and 17% increase in the surface hardness respectively.

Table 4.3. Mean and standard deviation (SD) values of flexural strength, flexural modulus and Vickers hardness for the test groups.

Specimen groups	**Flexural strength (MPa)**	**Flexural Modulus (MPa)**	**Hardness (kg/mm^2)**
	Mean & SD	Mean & SD	Mean & SD
Control (0.0wt %)	72.4 (8.6)^A	1971.0 (235.0)^A	17.1 (0.9)^A
Non-silanised (3.0wt %)	59.9 (7.1)^B	2207.0 (252.7)^{AB}	15.0 (0.2)^A
Silanised (3.0wt %)	83.5 (6.2)^C	2313.0 (161.3)^B	20.1 (2.3)^B

Note: Within a column, cells having similar (upper case) letters are not significantly different.

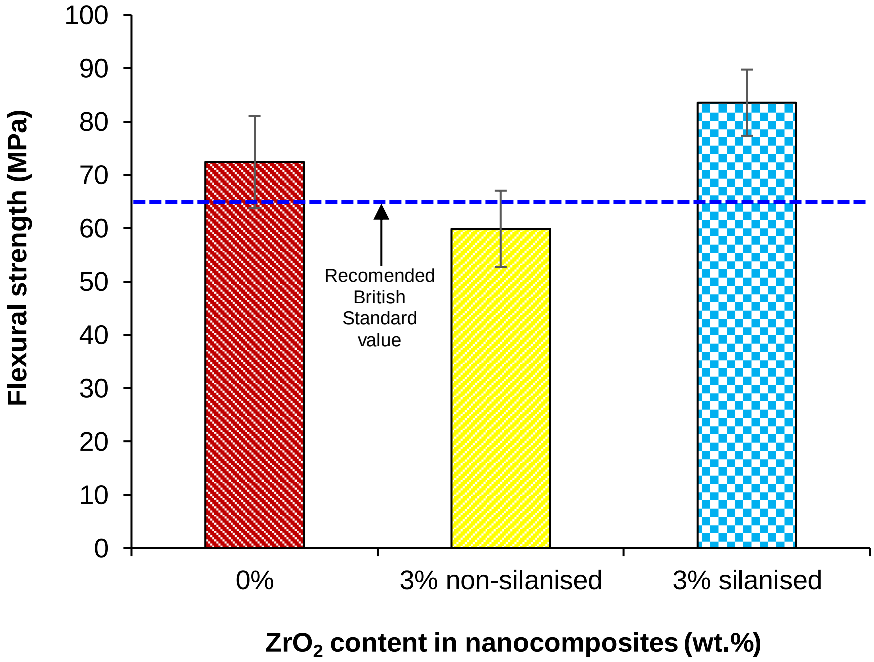

Figure 4.6. Bar charts showing the effect of treating zirconia nanoparticles on the flexural strength of PMMA+ zirconia nanocomposites.

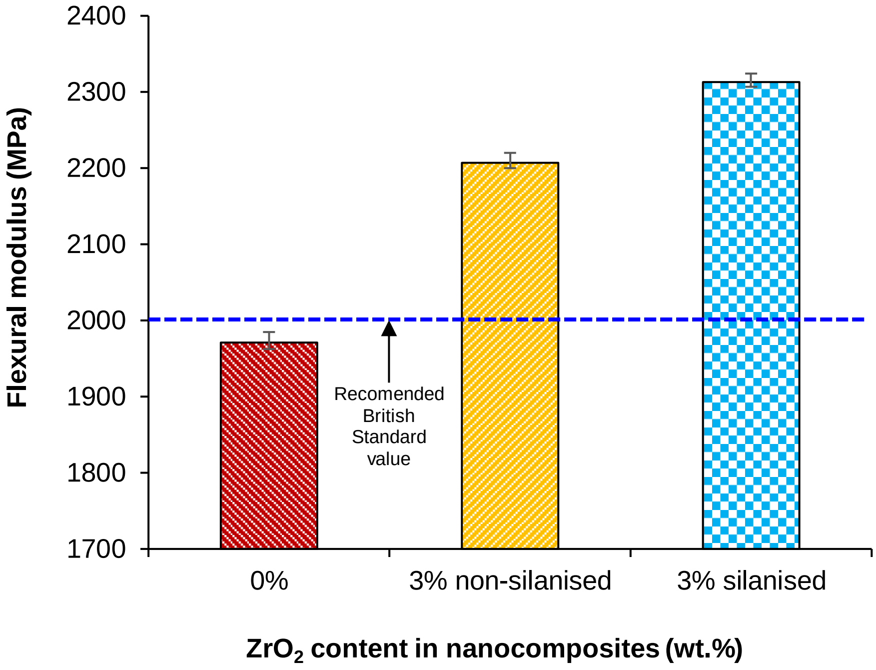

Figure 4.7. Bar chart showing the effect of treating zirconia nanoparticles on the flexural modulus of the PMMA+ zirconia nanocomposites.

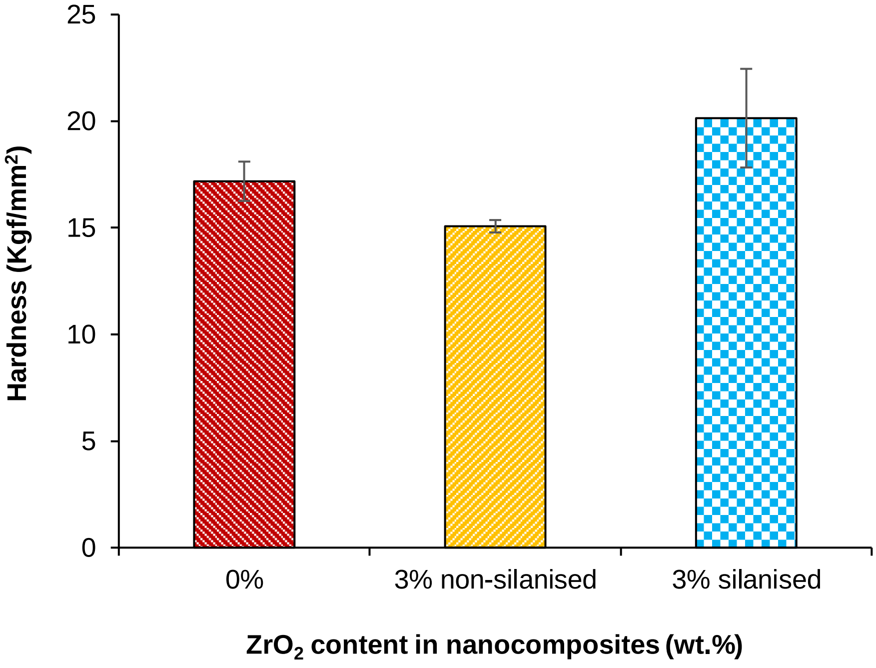

Figure 4.8. Bar chart showing the effect of treating zirconia nanoparticles on the hardness of the PMMA+ zirconia nanocomposites.

4.4.6. Fractured surface analysis

The SEM micrographs in Figure 4.9 show the fractured surfaces of PMMA and nanocomposites with silanised and non-silanised zirconia. Zirconia particles were visible in the PMMA matrix but specimens with silane treated zirconia showed less cluster formation compared the specimen with non-treated zirconia. Similar behaviour was also observed by Elshereksi et al. (2017) in composites with PMMA and nanobarium titanate.

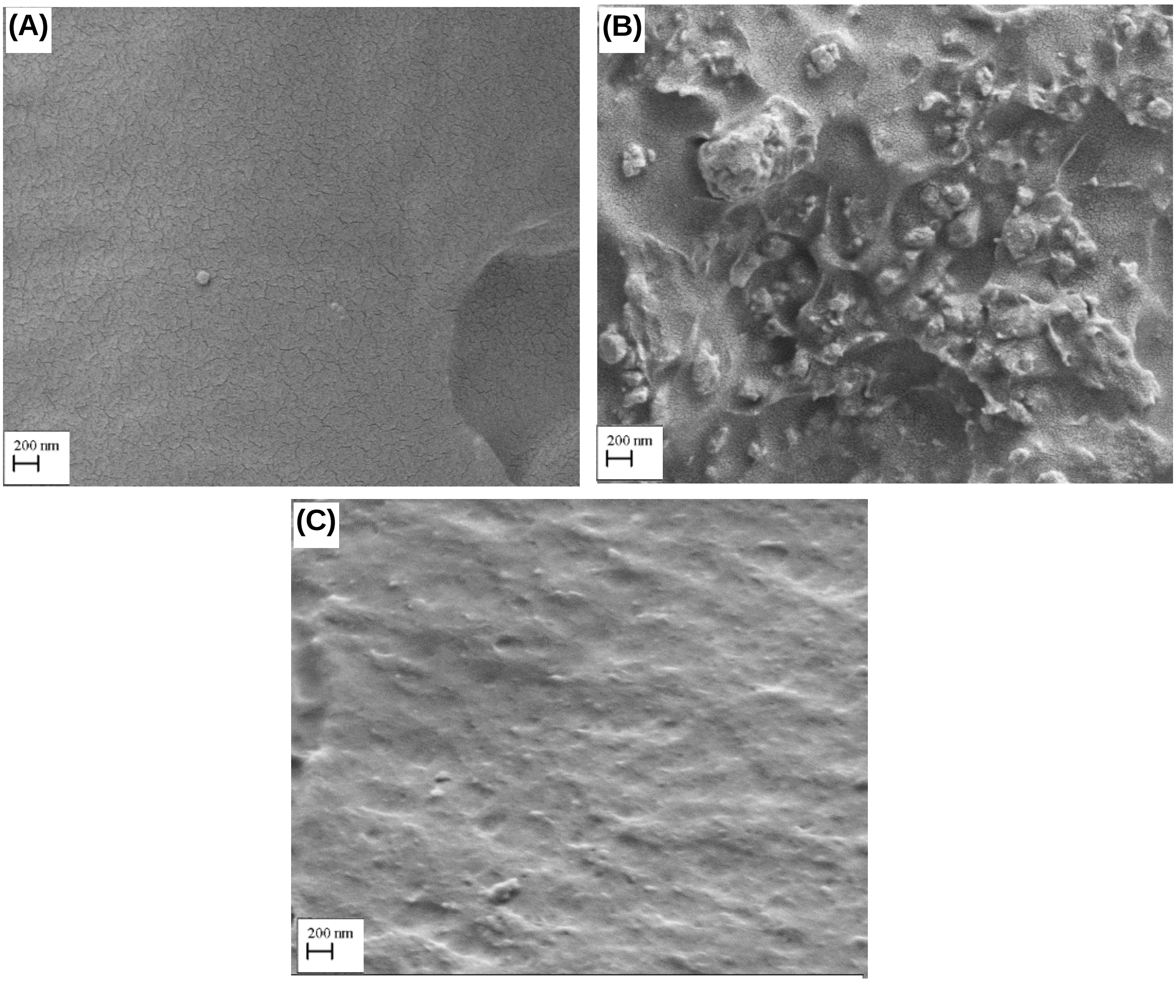

Figure 4.9. SEM micrographs detailing the fractured surfaces of (A) pure HI PMMA (B) PMMA-Zirconia nanocomposite with non-treated zirconia and (C) PMMA-zirconia nanocomposite with silane-treated zirconia

4.5. DISCUSSION

Silanisation of zirconia nanoparticles can improve the mechanical properties of HI PMMA-ZrO_2 nanocomposites. The hypothesis was therefore rejected as significant differences in the flexural strength and surface hardness of the nanocomposites with salinized zirconia were found compared to both the nanocomposite with non-salinized zirconia and the control group. However, the hypothesis was partially accepted as there was no significant difference in flexural modulus between the silanised and non- silanised groups.

According to British International Standard for Denture Base Polymers (2487: 1989) (British Standards, 1989) flexural strength and modulus should not be less than 65 MPa and 2000 MPa. In the current study, the flexural strength values obtained for the silanised group (83.5 MPa) and control group (72.4 MPa) were acceptable. However, the flexural strength of the non-silanised group (59.9 MPa) was not acceptable according to the aforementioned British Standard. In the current study, silane treatment of zirconia nanoparticles in HI PMMA composites had improved the flexural strength by 40% and 15% when compared to the non silanised and control groups. The findings agreed with a previous study demonstrating that inclusion of silanised zirconia nanoparticles into a repaired denture base resin enhanced flexural strength (Gad et al., 2016b). It was pointed out that the reason for the increase in flexural strength could be related to the nanoparticle sizes, their distribution within the matrix resin and the silanisation process used (Gad et al., 2016b).

A similar study by Zhang et al. investigated reinforcement of PMMA denture bases with silanised zirconia nanoparticles and aluminium borate at different concentrations and their effects on flexural strength. They found that 2 wt.% and 3 wt.% of silanised zirconia significantly increased the flexural strength of PMMA (Zhang et al., 2014). Vojdani et al showed a significant increase in flexural strength with addition of 2.5 wt.% aluminium oxide into a conventional PMMA denture base resin (Vojdani et al., 2012). da Silva et al. reported significantly higher flexural strength for microwave-heat-cured (PMMA) denture base resin reinforced with 0.5 wt.% and 1.0 wt.% silanised silica compared to pure PMMA and suggested the underpinning mechanism in increase of the flexural strength could be due to use of a microwave curing process instead of a water bath (da Silva et al., 2012). A different study by Ergun et al., who evaluated zirconia nanoparticles at different concentrations (5%, 10%, 20 wt.%) impregnated into conventional PMMA acrylic resin, showed that the flexural strength decreased with an increase in zirconia percentages in contrast to pure PMMA. Heterogeneous dispersion of the nanoparticle filler within the resin matrix and filler clustering were reported as the reasons for the decrease in strength (Ergun et al., 2018).

The increase in flexural strength observed in the presented study may be explained by the fact that reinforcement of the HI PMMA acrylic resin matrix with silanised zirconia nanoparticles resulted in better adhesion between the particles and the matrix facilitated by favourable chemical bonding by the silane coupling agent. This silane (γ-MPS) has a bifunctional molecule that can react by its alkoxysilane groups with the filler and itself, and with the resin due to its methacrylate functional group (Antonucci et al., 2005). According to Karabela et al., who evaluated the effect of silane molecules on dental resin-nanocomposites, during silanisation of silica nanoparticles, the $–OCH_3$ functional groups in silane molecules are hydrolysed to silanol groups by moisture containing solvent and the silanol groups condense with surface hydroxyl groups on the silica to form covalent bonds (Karabela and Sideridou, 2008). During the silanisation process, multiple layers of silane molecules form a film around the filler particles, which is either chemically or physically attached to the filler particles (Tham et al., 2010a). Furthermore, hydrogen bonds are formed between the carbonyl groups of silane, the hydroxyl groups of silica surface (Karabela and Sideridou, 2008).

According to Lung et al., the rate of silane hydrolysis depends on several factors including temperature and type of solvent used for hydrolysis activation. The study also states that the silane concentration should between 1-10 vol.% and the pH adjusted between 2-6 (Lung et al., 2016). In the current study, during the silanisation procedure, silane (γ-MPS) was dissolved in toluene solvent before incorporation into the monomer. After the silane hydrolysis and condensation had taken place on the surface of zirconia nanoparticles, an EZ-2 Elite personal solvent evaporator machine was used for drying the samples at 80°C for 3 hours, which increased stability of silane coating layer on the surface of zirconia as indicated by the FTIR analysis in Figure 4.4, compared to the non-treated zirconia.

The flexural modulus values varying between 2207 MPa to 2313 MPa for both silanised and non-silanised nanocomposites was acceptable according to the British Standard. However, flexural modulus value of 1971 MPa for the control group and was not acceptable. The modulus value is slightly lower than the recommended values and the reason for the lower value could be explained by the fact that PMMA reinforced with rubber particles increases impact strength but reduces flexural modulus (Zheng et al., 2012). A study by Alhareb et al. evaluated the effect of incorporating 7.5 wt.% nitrile butadiene rubber as impact modifier together with Al_2O_3/YSZ particles with different concentrations (1, 3, 5, 7, 10 w.t%) into PMMA denture base. The finding demonstrated that an increase in fillers improved the flexural modulus (Alhareb et al., 2018). In addition, some previous studies assessed the effect of silane surface treatment of hydroxyapatite particles used to reinforce PMMA denture base resin and found an increase in flexural modulus of the denture base resin. The reason for improvement was attributed to silane which enhanced the interfacial interaction between the PMMA and hydroxyapatite particles (Chow et al., 2012; Tham et al., 2010a; Tham et al., 2011). The results of the current study match those observed in the earlier studies: the flexural modulus of silanised nanocomposites increased by 5% compared to the non-silanised group in contrast to a significant increase (17%) compared to the control group.

A high hardness commonly corresponds to a high abrasive wear resistance (Reyes-Acosta et al., 2015). It interesting to note that the surface hardness of silanised nanocomposites significantly increased with the silane treatment compared to the non-silanised and control groups. Zhang et al. revealed that the surface hardness of modified PMMA with 3 wt.% of zirconia and aluminum significantly improved compared to the nanocomposite group containing 3 wt.% of silanised zirconia in this study (Zhang et al., 2014). Lung et al. evaluated the effect of adding non-treated and silane treated hydroxyapatite fillers to dental resin and found that silanisation of hydroxyapatite particles increased surface hardness of the composite. The reason for this increase was attributed to the higher stiffness of the filler particles than the resin matrix along with strong chemical bond formed between the matrix and nanoparticles, which required more energy to break these linkages (Lung et al., 2016). This explanation is in agreement with the current study that confirmed that adhesive silane coating was formed on the surface of zirconia nanoparticles as observed in FTIR analysis (Figure 4.4). Moreover, surface hardness of conventional PMMA resin increased with the increase of zirconia nanoparticle concentration (da Silva et al., 2012; Ergun et al., 2018; Reyes-Acosta et al., 2015).

In relation to the microscopic structure, in the present study, SEM image analysis in (Figure 4.9) showed non-homogenous dispersion and cluster formations of nanoparticles on fractured surface in the non-silanised HI PMMA-ZrO_2 nanocomposites, which could be one of the reasons for the decrease in flexural strength, flexural modulus and surface hardness. In comparison, the specimen group with silanised zirconia displayed no significant clustering and good distribution of silanised nanoparticles within the HI PMMA matrix. Additionally, improved adhesion between nanoparticles and resin matrix could significantly improve the mechanical properties. Consequently, a combination of good particle distribution and adhesion with the matrix can prevent a crack propagating through the PMMA. This process is identified to as dispersion strengthening (Alhavaz et al., 2017).

4.6. CLINICAL IMPLICATIONS

Silanisation of zirconia nanoparticles is important in the clinical practice for denture base application to improve the mechanical properties of the HI PMMA-zirconia nanocomposite through strong filler bonding with the resin matrix.

4.7. CONCLUSION

Within the limitations of this study, the following conclusions can be drawn:

Flexural strength and surface hardness of denture base nanocomposite based on PMMA and silane treated 3wt% zirconia (ZrO_2) were improved significantly ($p<0.05$) compared to the nanocomposite reinforced with non-treated zirconia and pure PMMA (control group).

Flexural modulus of the nanocomposite with treated zirconia was significantly increased compared to the control group. However, no significant difference was found when compared to the nanocomposite with non-treated zirconia.

Therefore, in order to improve the clinical service life of complete denture, PMMA resin should be reinforced silane treated zirconia nanoparticles.

Chapter 5: Investigating the Mechanical Properties of ZrO_2-Impregnated PMMA Nanocomposite for Denture-Based Applications

Saleh Zidan, Nikolaos Silikas, Abdulaziz Alhotan, Julfikar Haider and Julian Yates

Published in Materials MPDI. 2019; 12(8), 1344

https://doi.org/10.3390/ma12081344

(Appendix: Published copy of the paper)

5.1. ABSTRACT

Acrylic resin PMMA (poly-methyl methacrylate) is used in the manufacture of denture bases but its mechanical properties can be deficient in this role. This study investigated the mechanical properties (flexural strength, fracture toughness, impact strength, and hardness) and fracture behaviour of a commercial, high impact (HI), heat-cured denture base acrylic resin impregnated with different concentrations of yttria-stabilized zirconia (ZrO_2) nanoparticles. Six groups were prepared having different wt.% concentrations of ZrO_2 nanoparticles: 0% (control), 1.5%, 3%, 5%, 7%, and 10%, respectively. Flexural strength and flexural modulus were measured using a three-point bending test and surface hardness was evaluated using the Vickers hardness test. Fracture toughness and impact strength were evaluated using a single edge bending test and Charpy impact instrument. The fractured surfaces of impact test specimens were also observed using a scanning electron microscope (SEM). Statistical analyses were conducted on the data obtained from the experiments. The mean flexural strength of ZrO_2-PMMA nanocomposites (84 ± 6 MPa) at 3 wt.% zirconia was significantly greater than that of the control group (72 ± 9 MPa) ($p<0.05$). The mean flexural modulus was also significantly improved with different concentrations of zirconia when compared to the control group, with 5 wt.% zirconia demonstrating the largest (23%) improvement. The mean fracture toughness increased in the group containing 5 wt.% zirconia compared to the control group, but it was not significant. However, the median impact strength for all groups containing zirconia generally decreased when compared to the control group. Vickers hardness (HV) values significantly increased with an increase in ZrO_2 content, with the highest values obtained at 10 wt.%, at 0 day (22.9 $HV_{0.05}$) in dry conditions when compared to the values obtained after immersing the specimens for seven days (18.4 $HV_{0.05}$) and 45 days (16.3 $HV_{0.05}$) in distilled water. Incorporation of ZrO_2 nanoparticles into high impact PMMA resin significantly improved flexural strength, flexural modulus, fracture toughness and surface hardness, with an optimum concentration of 3–5 wt.% zirconia. However, the impact strength of the nanocomposites decreased, apart from the 5 wt.% zirconia group.

5.2. INTRODUCTION

In practical applications, denture base materials experiences different types of stresses, such as compressive, tensile and shear, which can lead to premature failure. Intra-orally, repeated mastication over a period of time can lead to denture base fatigue failure. Extra-orally, denture bases can also experience high impact forces when dropped by accident (Kanie et al., 2000; Zappini et al., 2003). Impact fractures occur extra-orally as a result of inadvertent denture damage (Vojdani et al., 2012; Zappini et al., 2003). The incidence of denture fracture is relatively high: 68% of dentures fail within three years of fabrication and the incidence in partial denture is greater than that of complete dentures(Jagger et al., 1999; Sasaki et al., 2016). Studies have also reported that 33% of the repairs in dental laboratories are as a result of de-bonded teeth, and 29% percent of fractures occur in the midline of the denture base, being seen more frequently in the upper than in the lower prosthesis (Agha et al., 2016; Nejatian et al., 2006). The remaining 38% of fractures are caused by other types of failure (Agha et al., 2016; Nejatian et al., 2006).

High impact (HI) denture base resins are widely used in prosthetic dentistry. These materials are provided in either powder or liquid forms and are processed in the same manner as other heat-cured, poly-methyl methacrylate (PMMA) resins. HI resins are reinforced with butadiene-styrene rubber, with the rubber particles grafted to the poly-methyl methacrylate so that the particles are covalently bonded into the polymerized acrylic matrix in order to better absorb mechanical loads (Abdulwahhab, 2013; Jagger et al., 2003; Sasaki et al., 2016; Stafford et al., 1980a). Incorporation of butadiene-styrene rubber into PMMA resins improves impact strength and dimensional stability (Jagger et al., 2003; Jagger et al., 2002; Zheng et al., 2012). However, such reinforcement can result in the reduction of mechanical properties, including flexural strength, fatigue strength and stiffness (Jagger et al., 2003; Jagger et al., 2002; Kim and Watts, 2004).

Many attempts have been made to improve the strength of denture base resins, including the addition of metal wires and plates made of either Co-Cr alloy or stainless steel. However, these materials present limitations contrary to the standard requirements, including poor adhesion between the acrylic resin and reinforcing metal. This separation can result in a reduction in overall mechanical strength within the prosthesis, as well as poor aesthetics. Additionally, metal-reinforced denture bases can become noticeably heavier (Kim and Watts, 2004; Yu et al., 2015). Other attempts to improve denture base mechanical properties include fibre reinforcement to enhance fracture toughness, flexural and impact strength, and fatigue properties (Gad et al., 2017; Kim and Watts, 2004).

Different fibre types, such as ultra-high modulus polyethylene fibre (UHMPE), aramid fibre, nylon fibre, carbon fibre and glass fibre, have all been investigated (Gad et al., 2017; Kim and Watts, 2004; Uzun et al., 1999). UHMPE fibre does not demonstrate good adhesion to PMMA, and therefore, no significant increase in flexural properties has been demonstrated (Koroglu et al., 2009). Carbon and aramid fibres are not practical materials because of difficulties in polishing the final prostheses, and resultant poor aesthetics (Kim et al., 2012). However, nylon reinforcement enhances fracture resistance and structural elasticity of acrylic resins (Gad et al., 2017). A study undertaken by Vallittu et.al, on the transverse strength of heat-cured PMMA denture bases reinforced with a high concentration of continuous glass fibre demonstrated an improvement in these properties (Vallittu et al., 1994b). Additionally, silane coupling agents have been added to enhance adhesion between the polymer resin and glass fibres to improve mechanical strength, resulting in enhanced flexural and fatigue strength (Vallittu et al., 1994b; Vallittu et al., 1994a). However, fibre orientation in the resin matrix is technically difficult to control and a random distribution could result in defects within the finished product (Pan et al., 2013).

In recent years, several investigations have focused on improving the mechanical properties of PMMA acrylic resins by adding nanomaterials, such as bio-ceramic nanoparticles, due to their special characteristics (Zhang et al., 2014). Zirconia (ZrO_2) is a bio-ceramic material that has been widely used for various dental applications, such as crowns and bridges, implant fixture “screws” and abutments, and orthodontic brackets (Wang et al., 2016). Zirconia has a high flexural strength (900 to 1200 MPa), hardness (1200 HV), and fracture toughness (9–10 MPa $m^{1/2}$) (Kawai et al., 2012). Furthermore, zirconia shows excellent biocompatibility compared to other ceramic materials, such as alumina (Kawai et al., 2012; Zhang et al., 2014). A number of studies found that reinforcement of conventional, heat-cured denture base resins with zirconia nanoparticles significantly improved mechanical properties such as flexural and impact strength, as well as surface hardness (Gad et al., 2016b; Zhang et al., 2014). However, no systematic study on the effect of zirconia addition in the high impact (HI) heat-cured PMMA denture base material has been reported in the literature. Therefore, research is needed to identify an optimum amount of zirconia suitable for improving performance and life of HI PMMA denture bases.

The purpose of this study is to evaluate the effects of zirconia nanoparticle addition at low concentrations (up to 10%) to a commercially available, high-impact, PMMA denture base resin on selected mechanical properties such as flexural strength, impact strength, fracture toughness, hardness and fracture behaviour.

5.3. MATERIAL AND METHODS

5.3.1. Materials

A commercially available, Metrocryl HI denture base powder, (PMMA, poly-methyl methacrylate) and Metrocryl HI (X-linked) denture base liquid (MMA, methyl methacrylate) (Metrodent Limited, Huddersfield, UK) were selected as the denture base material. Yttria-stabilized zirconia (ZrO_2) nanoparticles (Sky Spring Nano materials, Inc., Houston, TX, USA) were chosen as the inorganic filler agent for fabricating the nanocomposite denture base specimens.

5.3.2. Specimen Preparation

5.3.2.1. Silane Functionalization of Zirconia Nanoparticle Surfaces

Fifteen grams of zirconia nanoparticles and 70 mL of toluene solvent were deposited into a plastic container, which was then placed in a speed mixer (DAC 150.1 FVZK, High Wycombe, UK), and mixed at 1500 rpm for 20 min. Following the initial mixing, 7 wt.% silane coupling agent (3-trimethoxysilyl propyl methacrylate; product no. 440159, Sigma Aldrich, Gillingham, UK) was added slowly over a period of 20 sec. The mixture was then placed in the speed mixer at 1500 rpm for 10 min and divided equally into two tubes and spun in a centrifuge at 23 °C at 4000 rpm for 20 min. The supernatant (separated toluene) was removed, and the remaining silanised nanoparticles were transferred into a personal solvent evaporator (EZ-2 Elite, Genevac Ltd., SP Scientific Company, Ipswich, UK) for 3 h of drying at 60 °C.

5.3.2.2. Selection of Appropriate Percentages of Zirconia Nanoparticles

To determine the most appropriate weight percentages of zirconia nanoparticles for the current study, preliminary investigations were undertaken using 1.5 wt.%, 10 wt.% and 15 wt.% mixtures. Based on these results and knowledge from relevant literature, a decision was made to utilize the following weight percentages of silanised zirconia nanoparticles in the denture base formulation: 0.0% (control), 1.5 wt.%, 3.0 wt.%, 5.0 wt.%, 7.0 wt.%, and 10.0 wt.%. The composition details of the specimen groups used in this study are described in Table 5.1 (all used an acrylic resin powder: monomer ratio of 21 g:10 mL, in accordance with manufacturer’s instructions).

Table 5.1 Weight percent zirconia in combination with acrylic resin powder as well as monomer content of the specimen groups. HI: High impact; PMMA: Poly-methyl methacrylate; MMA: methyl methacrylate.

Experimental Groups	Zirconia (wt.%)	Zirconia (g)	HI PMMA Powder (g)	HI MMA Monomer (mL)
Control	0.0	0.000	21.000	10.0
1.5	1.5	0.315	20.685	10.0
3.0	3.0	0.630	20.370	10.0
5.0	5.0	1.050	19.950	10.0
7.0	7.0	1.470	19.530	10.0
10.0	10.0	2.100	18.900	10.0

5.3.2.3. Mixing of Zirconia with PMMA

The silane-treated zirconia and acrylic resin powders were weighed according to Table 5.1 using an electronic balance (Ohaus Analytical with accuracy up to 3 decimal points). The zirconia powder was added to the acrylic resin monomer and mixed by hand using a stainless-steel spatula to make sure all the powder was uniformly distributed within the resin monomer. The HI acrylic resin powder was then added to the liquid, and mixing continued until a consistent mixture was obtained, according to the manufacturer's instruction. The mixing continued for approximately 20 min until the mixture reached a dough-like stage, which was suitable for handling. When the mixture reached a consistent dough-like stage (working stage), it was packed into a mould by hand. The moulds were made from aluminium alloy, which contained five cavities with a dimension of 65 mm (l) × 10 mm (w) × 2.50 mm (d) for producing flexural strength and hardness test samples. However, the cavity dimensions for the impact test was as follows: 80 mm (l) × 10 mm (w) × 4 mm (d) and fracture toughness was 40 mm (l) × 8 mm (w) × 4 mm (d). Before pouring the mixture into the mould, sodium alginate as a separating medium (John Winter, Germany) was applied to the surfaces of the mould for easy removal of the specimens. The mould was then closed and placed in a hydraulic press (Sirio P400/13045) under a pressure of 15 MPa in the first cycle, and then the pressure was released. Excess mixture was removed from the mould periphery, which was then re-pressed at room temperature for 15 min under the same pressure. The mould was then immersed in a temperature-controlled curing water bath for 6 h to allow polymerisation. The curing cycle involved increasing the temperature to 60 °C over 1 h and maintained this temperature for 3 h. After this time, the temperature was increased to 95 °C over an additional 2 h to complete the heat polymerisation cycle. The mould was removed from the curing bath and cooled slowly for 30 min at room temperature. The mould was then opened, and the specimens were removed. The specimens were then trimmed using a tungsten carbide bur, ground with an emery paper and polished with pumice powder in a polishing machine (Tavom, Wigan, UK) in accordance with British International Standard Organization (BS EN ISO 20795-1:2008) and British Standard Specification for Denture Base Polymers (BS 2487: 1989 ISO 1567; 1988) (British Standards, 1989; British Standards, 2008).

5.3.3. Mechanical Characterization of the Nanocomposite

5.3.3.1. Flexural Strength Test

Flexural strength of the nanocomposite specimens was evaluated using a 3-point bend test in a universal testing machine (Zwick/Roell Z020 Leominster, UK) in accordance with British International Standard for Denture Base Polymers (2487: 1989) (British Standards, 1989). The dimensions of the specimens were 65 ± 1.0 mm length × 10 ± 0.01 mm width × 2.50 ± 0.01 mm thickness. All specimens were stored in distilled water at a temperature of 37 ± 1 °C for 50 ± 2 h in an incubator before testing. The specimens were then removed from the distilled water and placed on a support jig. The loading plunger (diameter 7.0 mm) was fixed at the centre of the specimen midway between two supports, which were parallel and separated by 50 ± 0.1 mm, and the diameter of the load supports were 3.20 mm. A 500 N load cell was used to record force and the load was applied using a cross-head speed of 5 mm/min. The maximum force (F) was recorded in newtons, and flexural strength was calculated in MPa for all specimens using Equation 5.1 (Jerolimov et al., 1989):

$$\sigma = \frac{3\mathrm{Fl}}{2\mathrm{bh}^2} \tag{5.1}$$

where F is the maximum force applied in N, l is the distance between the supports in mm, b is the width of the specimen in mm, and h is the height of the specimen in mm. The flexural modulus was determined as the slope of the linear portion of the stress/strain curve for each test run.

5.3.3.2. Fracture Toughness Test

Fracture toughness tests were conducted using a single edge span notch bending test on the Zwick universal testing machine in accordance with the British International Standard Organization (BS EN ISO 20795-1:2008) (Al-Haddad et al., 2014; British Standards, 2008). The dimensions of the specimens were 40 ± 1.0 mm (l) × 8 ± 0.01 mm (h) × 4 ± 0.01 mm (w), and a notch was created in the middle of the specimens with a diamond blade and a saw to a depth of 3.0 ± 0.2 mm along a marked centre line. All specimens were then stored in distilled water and placed in an incubator at 37 ± 1 °C for 168 ± 2 h before testing. The specimens were removed from the water, dried by a towel and placed edgewise on the supports of the testing rig. The notch of the specimen was placed directly opposite to the load plunger (diameter 7 mm) and in the middle of the span between the two supports (32.0 ± 0.1 mm). The load cell was 500 N, and the cross-head speed was 1.0 mm/min. Fracture toughness was determined by increasing the force from zero to a maximum value in order to propagate a crack from the opposite side of the specimen to the impact point. The maximum force (P) in newtons to fracture was recorded in order to calculate the fracture toughness (K_{IC}) in MPa $m^{1/2}$ according to Equation 5.2 (Al-Haddad et al., 2014):

$$K_{IC} = \frac{3PL}{2BW^{3/2}} \times Y \tag{5.2}$$

where W is the height of the specimen in mm, B is the width of the specimen in mm, L is the distance between the supports in mm, and Y is a geometrical function calculated by Equation 5.3:

$$\begin{aligned} Y = 1.93 \times \left(\frac{a}{w}\right)^{1/2} - 3.07 \times \left(\frac{a}{w}\right)^{\frac{3}{2}} + 14.53 \times \left(\frac{a}{w}\right)^{\frac{5}{2}} - 25.11 \times \left(\frac{a}{w}\right)^{\frac{7}{2}} \\ + 25.80 \times \left(\frac{a}{w}\right)^{\frac{9}{2}} \end{aligned} \tag{5.3}$$

where a is the depth of the notch.

5.3.3.3. Impact Test

The Charpy V-notch impact test (kJ/m^2) utilized a universal pendulum impact testing machine (Zwick/Roell Z020 Leominster). Specimen dimensions were 80 ± 1.0 mm (l) × 10 ± 0.01 mm (w) × 4 ± 0.01 mm (h), in accordance with the European International Standard Organization (EN ISO 179-1:2000)(European International Standard, 2000). The specimens were notched in the middle to a depth of 2.0 ± 0.2 mm, a notch angle of 45° and a notch radius of 1.0 ± 0.05 mm and were then stored in distilled water at 37 ± 1 °C for 168 ± 2 h in an incubator before testing. The specimens were then removed from the water and dried with a towel. Each specimen was placed in the machine and were supported horizontally at its ends (40 ± 0.2 mm), and the centre of the specimen (the un-notched surface) was hit by a free-swinging pendulum that was released from a fixed height. The pendulum load cell was 0.5 J and directly faced the centre of the specimen, as shown in Figure 5.1. When the test was started, the pendulum was released to strike the specimen, and the impact energy absorbed was recorded in joules (J). The Charpy impact strength (a_{iN}) (kJ/m^2) was calculated using Equation 5.4 (Abdulwahhab, 2013; European International Standard Organization, 2000):

$$a_{iN} = \frac{E_c}{h * b_N} \times 10^3 \tag{5.4}$$

where E_c is the breaking energy in joules absorbed by breaking, h is the thickness in mm, and b_N is the remaining width in mm after notching.

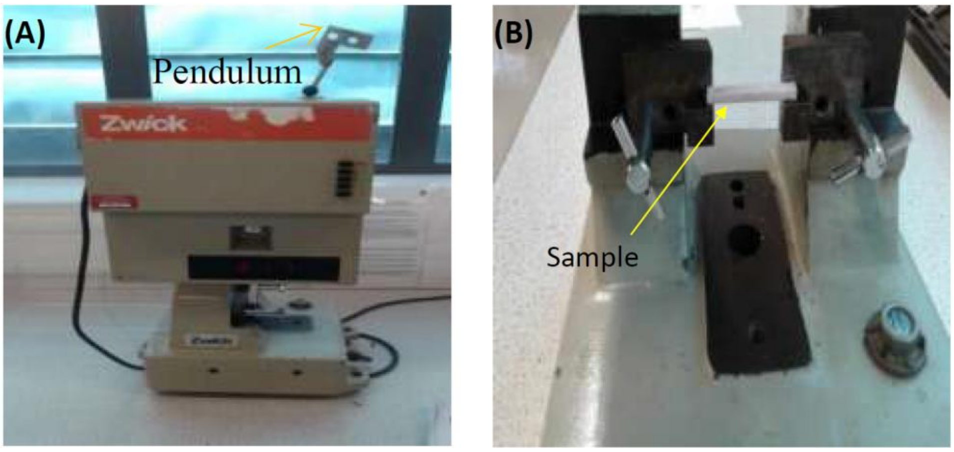

Figure 5.1. (A) Photograph illustrating the impact test machine and (B) position of sample in the machine before the test.

5.3.3.4. Hardness Test

The Vickers hardness ($HV_{0.05}$) of the specimens was measured using a micro-hardness testing machine (FM-700, Future Tech Corp, Tokyo, Japan). Specimens were 65± 1.0 mm length × 10 ± 0.01 mm width × 2.50 ± 0.01 mm thickness, and the test load was fixed at 50 g for 30 sec. The Vickers hardness was calculated by measuring the diagonals of the pyramid-shaped indentation impressed on the specimen. A total of three indentations were taken at different points in each specimen one side, and then a mean value was calculated. The mean hardness values for all the specimens were determined demonstrative of the materials in the dry condition at day 0. The specimens were then stored individually in 37 ± 1 °C distilled water for 7 d ± 2 h and were then re-immersed for a total of 45 d ± 2 h. From the raw data, the mean hardness values for each sample group were calculated (Farina et al., 2012; Neppelenbroek et al., 2005).

5.3.4. Scanning Electron Microscopy (SEM) Examination

The size and shape distribution of the PMMA powder and zirconia nanoparticles was analysed using a scanning electron microscope (SEM) (Carl Zeiss Ltd, 40 VP, Smart SEM, Cambridge, UK). The fractured surface was also studied to identify failure mechanism. Specimens were mounted onto aluminium stubs and sputter-coated with gold after which SEM visualization was performed using a secondary electron detector at an acceleration voltage of 2.0 kV.

5.3.5. Statistical Analyses

Flexural strength, modulus, impact strength, fracture toughness and Vickers hardness data were analysed using a statistical software (SPSS statistics version 23, IBM, New York, NY, USA). Non-significant Shapiro–Wilk and Levene tests showed that the data of flexural and fracture toughness were normally distributed and there was homogeneity of variance. The flexural and fracture toughness data were analysed using a one-way analysis of variance (ANOVA) with the Tukey honestly significant difference post-hoc test at a pre-set alpha of 0.05. Impact strength and hardness data demonstrated nonparametric distributions as evidenced by significant Shapiro–Wilk test results for two groups, and therefore the Kruskal–Wallis test was used to analyse the results as well as to compare the differences among the test groups at a pre-set alpha of 0.05. In addition, the Friedman's two-way analysis test was applied to identify any significant difference between the three immersion time groups ($p<0.05$).

5.4. RESULTS

5.4.1. Visual Analysis

SEM analysis revealed that the average particle size of the PMMA powder was approximately 50 µm with a range from 10 µm to 100 µm, as shown in Figure 5.2 A. The rubber particles were also visible within the powder, with an average size of approximately 50 µm. The as-received, yttria-stabilized zirconia nanoparticles demonstrated an average size ranging between 30 nm and 60 nm for individual particles and 200 nm to 300 nm for clusters, as shown in Figure 5.2 B.

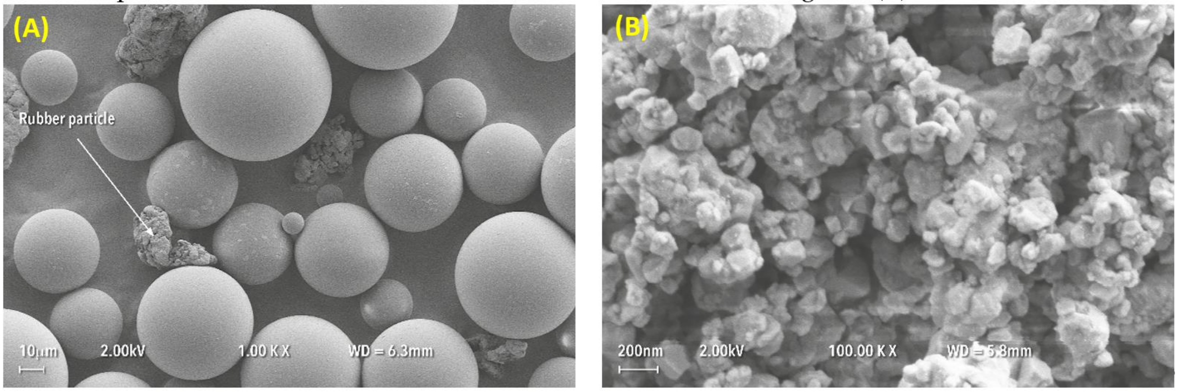

Figure 5.2. SEM images showing particle size and shape distributions of (A) PMMA powder and (B) zirconia nanoparticles.

5.4.2. Mechanical Tests

5.4.2.1. Flexural Strength and Flexural Modulus

One-way analysis of variance (ANOVA) of flexural strength values presented in Table 5.2 show a significant difference ($p<0.05$) for the specimen group containing 3 wt.% zirconia. However, the mean values of flexural modulus showed a significant increase ($p<0.05$) for all specimens, except that containing 7 wt.% zirconia, which was not significantly different ($p>0.05$) from the control group. The flexural strength data in the table demonstrates that an addition of zirconia nanoparticles to the HI PMMA gradually increased the strength up to 3 wt.% and then gradually decreased for other compositions when compared to the control group (0 wt.%). The highest value of flexural strength was recorded for the group containing 3 wt.% zirconia (83.5 MPa) in comparison with the control group (72.4 MPa), representing a 15% increase in the flexural strength. However, a higher percentage of zirconia nanoparticles (7 wt.% to 10 wt.%) in the specimens reduced the strength, which was comparable to the control group. A similar behaviour was also found for the flexural modulus of the nanocomposites with increasing zirconia content (Table 5.2). However, a maximum value of the flexural modulus was reached at a zirconia content of 5 wt.% (2419 MPa) when compared to the control group (1971 MPa), meaning an increase of 22.7%. Furthermore, even though at high zirconia content the modulus values decreased, they were still higher than those of the control group.

Table 5.2. Mean (MPa) Standard deviation (SD) values of flexural strength, flexural modulus and fracture toughness as well as median of impact strength (kJ/m^2) Interquartile range (IQR) for the test groups

Zirconia Content (wt.%)	**Flexural Strength and SD (MPa)**	**Flexural Modulus and SD (MPa)**	**Impact Strength and (IQR) (kJ/m^2)**	**Fracture Toughness and (SD) (MPa m$^{1/2}$)**
Control (0%)	72.4 (8.6) ^{A}	1971 (235) ^{A}	10.0 (2.69) ^{A}	2.12 (0.1) ^{A}
1.5	78.7 (6.9) ^{A}	2237 (117) ^{B}	7.03 (4.45) ^{A}	1.91 (0.2) ^{A}
3.0	83.5 (6.2) ^{B}	2313 (161) ^{B}	7.38 (4.50) ^{A}	1.97 (0.2) ^{A}
5.0	78.7 (7.2) ^{A}	2419 (147) ^{B}	9.05 (3.50) ^{A}	2.14 (0.1) ^{A}
7.0	72.2 (7.0) ^{A}	2144 (85) ^{A}	7.12 (1.50) ^{A}	1.86 (0.1) ^{A}
10.0	71.5 (5.7) ^{A}	2204 (91) ^{B}	5.89 (2.33) ^{B}	1.76 (0.8) ^{B}

Note: Within a column, cells having similar (upper case) letters are not significantly different from the control (0% zirconia content) value. N = 10 specimens per group.

5.4.2.2. Fracture Toughness and Impact Strength

The mean values of the fracture toughness (Table 5.2) of the nanocomposites decreased significantly compared to that of the control group at the zirconia concentrations of 7% and 10% ($p<0.05$). Furthermore, after the initial decrease of fracture toughness at 1.5 wt.% zirconia, the values slightly increased in the groups containing 3 wt.% and 5 wt.% zirconia, but they were not statistically significant increases ($p>0.05$). Table 5.2 shows that the best fracture toughness could be achieved at 5 wt.% zirconia.

The values of the impact strength for all nanocomposite groups were not statistically significant (p>0.05), as shown in Table 5.2. The median impact strength gradually decreased with the increase in zirconia content, except in the group containing 5 wt.% zirconia, which showed the best impact strength (only 10% reduction compared to the control group). However, all measured impact strength values for the nanocomposites were lower than that for the control group.

5.4.2.3. Hardness

The median values of Vickers hardness in Table 5.3 show significant differences ($p<0.05$) for the specimen groups containing 7 wt.% and 10 wt.% zirconia in both dry (0 day) and wet (7 days) conditions. From the graphical presentation of the hardness results (Figure 5.3), it is interesting to note that at lower zirconia contents (1.5–5.0%), the difference in hardness between dry and wet conditions was much lower than that at higher zirconia contents (7.0–10.0 wt.%). Furthermore, no significant difference was found between the hardness of the specimens stored in water for seven days and 45 days at all zirconia contents. This finding indicates that the hardness of the nanocomposites does not degrade over time in the wet condition at lower zirconia contents, particularly up to 3 wt.% zirconia.

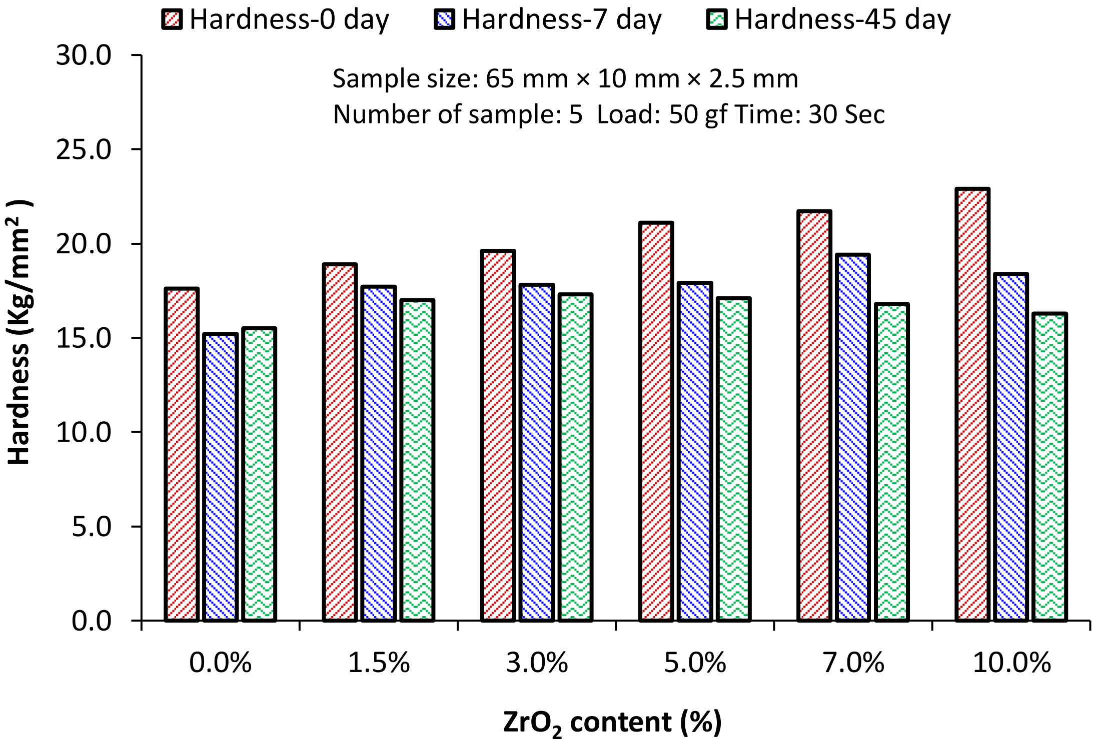

Figure 5.3. Vickers hardness median (kg/mm^2) after 0, 7, and 45 days of water immersion.

Table 5.3. Vickers hardness (kg/mm^2) (median and interquartile range) after 0, 7 and 45 days of water immersion.

Title	**Day Zero (Dry)**	**7-Days Water-Immersion**	**45 Days Water-Immersion**
Weight Percent Zirconia	Vickers Hardness (kg/mm^2) Median (IQR)	Vickers Hardness (kg/mm^2) Median (IQR)	Vickers Hardness (kg/mm^2) Median (IQR)
Control (0.0%)	17.6 (1.7) ^{Aa}	15.2 (2.0) ^{Ab}	15.5 (3.3) ^{Ab*}
1.5%	18.9 (3.2) ^{Ab}	17.7 (1.1) ^{Ab}	17.0 (1.8) ^{Ab*}
3.0%	19.6 (4.0) ^{Ac}	17.8 (1.2) ^{Ac}	17.3 (2.8) ^{Ac}
5.0%	21.1 (3.1) ^{Ad}	17.9 (2.9) ^{Ad}	17.1 (2.2) ^{Ad*}
7.0%	21.7 (3.0) ^{Be}	19.4 (0.9) ^{Be}	16.8 (2.3) ^{Ae*}
10.0%	22.9 (2.9) ^{Bf}	18.4 (3.3) ^{Bf}	16.3 (1.2) ^{Af*}

Note: Within a column, values identified using similar upper-case letters are not significantly different from the control group value; within rows values identified using the same lower-case letters are not significantly different; asterisks indicate significant differences between day 0 and 45 days; N = 5 specimens per experimental group.

5.4.3. Microstructural Characteristics

The fractured surface of pure PMMA specimens displayed a smooth surface in small areas and revealed a ductile type failure behaviour exhibiting irregular and rough surface as is shown in Figure 5.4(A). The composite fractured surface showed signs of cracks and particle clustering with small voids (Figure 5.4(B)). Figure 5.4(C) presents more clear fracture features and shows that the distribution of the nanoparticles was not uniform. The image highlights particle clustering in several places and voids on the fractured surface.

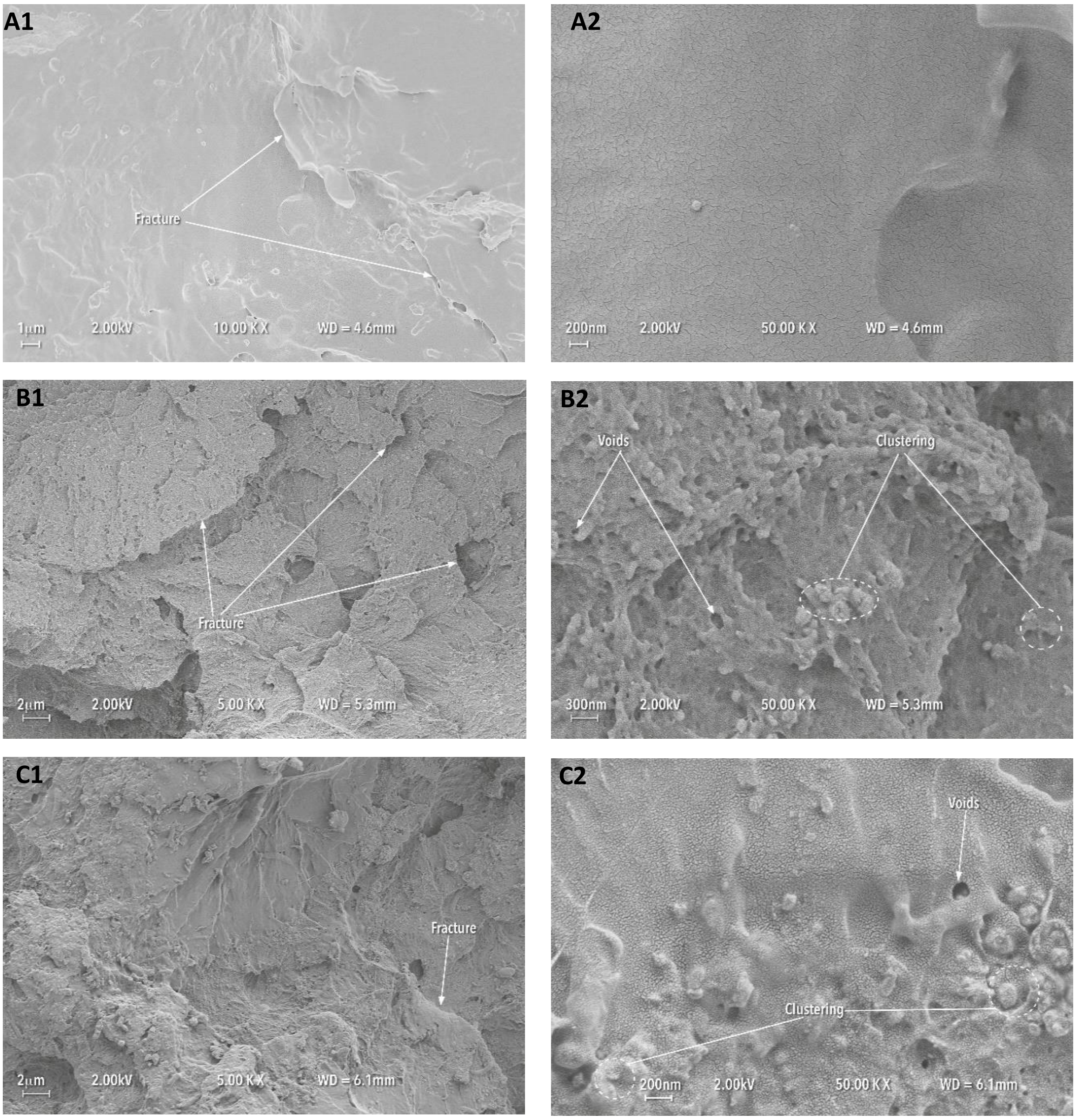

Figure 5.4. Representative SEM images of the fractured surfaces of impact strength test specimens at two different magnifications (1 at 10K and 2 at 50K for the control group (A) 0 wt.%, (B) 5 wt.% and (C) 10 wt.% added zirconia, respectively).

5.5. DISCUSSION

In this study, it was shown that combining zirconia nanoparticles to HI acrylic resin improved flexural strength and flexural modulus, which can lead to a reduction in different types of stresses encountered during the mastication process, including compressive, tensile and shear stresses (Li et al., 2016). However, the reinforced HI acrylic resin with lower concentration of zirconia (5%) did not show any significant difference from the control group on fracture toughness and impact strength.

The inorganic reinforcing nano-fillers have a large surface area that provides high surface energy, and this produces nanoparticles with a strong tendency to aggregate. This characteristic may decrease the chemical interaction between the nanoparticles and the base PMMA (Zhang et al., 2014). In this study, to enhance the chemical adhesion between the ZrO_2 nanoparticles and ZrO_2-PMMA, the surface of the ZrO_2 particles was treated with 7 wt.% silane coupling agents (γ-MPS) to create reactive functional groups. This could be responsible for improving the flexural properties of the nanocomposites at lower concentrations of zirconia nanoparticles. Moreover, the improvement in flexural strength and flexural modulus could be a result of the improved dispersion of the ZrO_2 nanoparticles when mixing with the speed mixer machine during the preparation stage. This improvement would decrease the agglomeration tendency in the composites. Additionally, the large interfacial area of the nanoparticles contributes to more contact points between the ZrO_2 and PMMA, thus enhancing mechanical interlocking and offers additional flexibility in the nanocomposites (Gad et al., 2018a).

Only a few studies on the effect of adding ZrO_2 nanoparticles in HI heat-cured denture base acrylic resin are available in the literature. In contrast, investigators have worked on improving the mechanical properties of conventional heat-cured denture base acrylic resin by incorporating different types of fillers (Asar et al., 2013). Alhareb et al. showed a 16% increase in flexural strength value compared to control samples when PMMA was reinforced with Al_2O_3 and ZrO_2 with a filler concentration of 5 wt.%. Moreover, the flexural modulus increased with an increase in Al_2O_3/ZrO_2 nanoparticle concentration (Alhareb and Ahmad, 2011). The greater value of the modulus indicates a stiffer material (Uzun et al., 1999), and this improvement can be explained by a homogenous distribution of the fillers within the polymer matrix. Vojdani et al. (Vojdani et al., 2012) evaluated the effect of adding Al_2O_3 particles to PMMA denture bases on flexural strength. They found that a 6% increase in flexural strength value with 2.5 wt.% Al_2O_3 compared to a control group could be obtained. Zhang et al. (Zhang et al., 2014) investigated the effect of hybrid ZrO_2 nanoparticles and micro-particles of aluminium borate whiskers (ABWS) at concentrations of 1 wt.%, 2 wt.%, 3 wt.%, and 4 wt.% on the flexural strength of PMMA denture base resin. They found that 2 wt.% nano-ZrO_2 with a ZrO_2/ABWS ratio of 1:2 improved flexural strength by 32% when compared to a control group. These previous studies in the literature were in agreement with the results obtained in this study, which revealed that zirconia positively influenced the flexural properties of HI PMMA with an optimum zirconia concentration between 3 wt.% and 5 wt.%.

Fracture toughness (K_{IC}) is a critical stress intensity factor that provides information on crack formation (Al-Haddad et al., 2014) and the ability of a material to resist crack propagation (Hamza et al., 2004). The reduction of fracture toughness in the PMMA-ZrO_2 nanocomposites with increasing filler content could be due to a number of reasons, such as particle distribution in the polymer matrix, the type and size of the particles, the concentration of the added particles, and chemical reactions between the particles and polymer (Asar et al., 2013; Gad et al., 2017; Kundie et al., 2018). A high filler concentration leads to more filler-to-filler interactions than filler-to-matrix interactions; therefore, agglomeration may act as a point of stress concentration that could lead to non-uniform stress distribution. When applying the load, the agglomeration restrains the movement of molecular deformation and reduces the fracture toughness (Kundie et al., 2018). Sodagar et al. (Sodagar et al., 2013) determined that the incorporation of TiO_2 nanoparticles to the PMMA matrix causes agglomeration, which acts as a stress raiser in the centre of the matrix and reduces the mechanical properties of the polymer material with increasing concentrations of the TiO_2 nanoparticles. Fangqiang et al. (Fan et al., 2013) investigated the distribution of ZrO_2 particles in PMMA matrix using two strategies during mixing: Physical method and chemical method. The physical method was conducted by melt blending, high-energy ball milling or ultrasonic vibration. In the chemical method, when mixing nanoparticles with an MMA monomer, the inorganic ZrO_2 nanoparticles acted as a core, and the monomer as a shell structure by in situ polymerisation of the monomers, known as grafting. The chemically modified nanoparticle surfaces with MMA enhanced the dispersion stability of the nanoparticles in the polymer matrix. Owing to a combined physical and chemical preparation, it was observed that the dispersion of ZrO_2 nanoparticles in the polymer matrix was enhanced and particle aggregation and phase separation decreased to a demonstrable extent. The results of the present study on fracture toughness are consistent with those reported in the study of Alhareb et al.*(*Alhareb and Ahmad, 2011), where a PMMA denture base reinforced with 5 wt.% fillers (80/20 Al_2O_3/ZrO_2) showed an improvement in fracture toughness but an increase in zirconia concentration decreased toughness.

The incorporation of hard ZrO_2 ceramic into PMMA can increase brittleness in the specimens, which would reduce the impact strength. Additionally, the lack of adhesion due to poor chemical reaction at the interface between the particles and PMMA or the inhomogeneous distribution of the nanoparticles with frequent clustering could affect the impact strength negatively (Alhareb and Ahmad 2011; Gad et al., 2016b). A study conducted by Gad et al. (Gad et al., 2016b) evaluated the effect of the incorporation of ZrO_2 nanoparticles with varying concentrations (2.5 wt.%, 5 wt.% and 7 wt.%) to PMMA denture bases on impact strength. The results showed that the impact strength decreased with an increase in ZrO_2 nanoparticle concentration. The finding of the impact strength in the present study is in agreement with that of the previous study, with the exception of the 5 wt.% ZrO_2-PMMA nanocomposite results. This result can be explained by the fact that a concentration of 5 wt.% might be the optimum quantity to improve particle distribution and reduce amalgamation. Asar et al. (Asar et al., 2013) investigated the influence of metal oxides, ZrO_2, TiO_3, and Al_2O_3, with 1% and 2% by volume on the impact strength of the PMMA acrylic resin. In contrast to the current study, the findings showed a slight increase in the values of impact strength with 2% ZrO_2 addition.

Denture base materials should also have adequate abrasion resistance to prevent high wear of the material by abrasive denture cleansers, food or general functional forces (Ali et al., 2008). Greater hardness in the denture base will reduce abrasive wear. The improvement of hardness in the nanocomposites might be related to the using of tetragonal-stabilized zirconia poly-crystals (TZP) nanoparticles phase. During preparation this phase in the manufacture company, it was prepared by addition a small amount of yttrium oxide (Y_2O_3) that gives stability at temperatures below the tetragonal to monoclinic transformation temperature, which leads to improve mechanical and wear properties of type of zirconia (Vagkopoulou et al., 2009). The reason for hardness decrease after water immersion was described in a previous study conducted on acrylic resin denture base materials, where residual monomers release and water absorption occurring simultaneously caused the surface to become softened (Hu et al., 2009). In addition, weakness of the bonding between HI PMMA matrix and zirconia nanoparticles at the interface could cause the decrease in hardness after immersing for 45 days in water. Tham et al., investigated flexural strength properties of PMMA denture base resin reinforced with silanised hydroxyapatite (HA) after immersing in Simulated Body Fluid (SBF) and water for a period of two months (Tham et al., 2010b). A decrease in flexural strength and an increase in absorption in both SBF and water were recorded. They explained the reason as hydrolytic degradation where the water molecules could lead to plasticizing effect in the matrix and caused degradation at the filler-matrix interface.

The finding of the present study is in agreement with a study by Hu et al. (Hu et al., 2009), who evaluated the hardness of PMMA-ZrO_2 nanocomposites with different ZrO_2 concentrations (0.5 wt.%, 1 wt.%, 2 wt.%, 3 wt.%, 4 wt.%, 5 wt.%, 7 wt.% and 15 wt.%) using indentation and pendulum hardness tests. They found that the hardness values were increased with an increase in the ratio of ZrO_2 to PMMA, with the highest value being 15 wt.%. Zhang et al.(Zhang et al., 2014) investigated the effect of zirconia nanoparticles and aluminium borate whiskers (ABW) in PMMA denture bases on the surface hardness at concentrations of 1 wt.%, 2 wt.%, 3 wt.% and 4 wt.%. The results showed an increase in surface hardness with an increase in ZrO_2/ABW content, and the optimum hardness was achieved at 3 wt.% ZrO_2 nanoparticles. They suggested that the decrease in surface hardness with higher filler loading was caused by poor adhesion of the particles to the resin matrix and filler clustering within the matrix. In another study, the incorporation of aluminium oxide (Al_2O_3) with percentages of 0.5 wt.%, 1 wt.%, 2.5 wt.% and 5 wt.% to PMMA acrylic resin exhibited an improvement in Vickers hardness with an increase of Al_2O_3 filler concentrations (Vojdani et al., 2012).

The lower impact strength in the nanocomposites can be related to the presence of voids and clustering of the nanoparticles (Alhareb and Ahmad, 2011; Zhang et al., 2014). At high magnification, the SEM images showed voids on the fractured surface, and these voids could lead to the generation of stress concentration under loading and initiate crack propagation by crossing the HI PMMA-ZrO_2 nanocomposite matrix. At low magnification, the fractured surfaces of the nanocomposite specimens exhibited less ductile fracture compared to the control group with a large amount of fragment crack deformation, which formed an irregular surface. Furthermore, the distribution of ZrO_2 nanoparticles in the polymer matrix was not homogeneous with evidence of agglomerations, which could reduce the impact strength, particularly at high ZrO_2 concentrations (10 wt.%).

5.6. CONCLUSION

With consideration to the limitations of this study, the following conclusions can be drawn:

The flexural strength of the high impact (HI) heat-cured PMMA denture base was significantly enhanced by the addition of zirconia nanoparticles with 3 wt.% when compared to the pure acrylic material (control group).

The flexural modulus of the high impact (HI) heat-cured PMMA denture base was significantly enhanced compared to the control group by addition of zirconia nanoparticles with 1.5 wt.%, 3 wt.%, 5 wt.% and 10 wt.%. The 7 wt.% of zirconia showed a non-significant enhancement compared to the control group.

The fracture toughness of the zirconia reinforced PMMA was significantly decreased, particularly at 10 wt.% ZrO_2 concentration. The fracture toughness was slightly increased at 5 wt.%, but this was not significantly different compared to the control group.

For all zirconia contents, the impact strength of the nanocomposites was significantly lower than that of the control group. However, at 5 wt.% and 3 wt.% zirconia content, the proportion of reduction in impact strength was not significantly different from that of the control group.

Surface hardness continuously increased with increase of zirconia content, in the dry condition at day 0. However, in the wet condition after seven days, and 45 days surface hardness was decreased with all groups.

Addition of zirconia in PMMA between 3 wt.% and 5 wt.% zirconia would provide the optimum mechanical properties suitable for denture base applications.

Chapter 6: Physical Properties of Zirconia-Impregnated PMMA Nanocomposite

6.1. ABSTRACT

Statement of problem. Exposure of denture base acrylic resins to the oral environment and storage media for extended periods of time, results in sorption of saliva or water leading to a reduction in physical properties and thus clinical service life. Additionally, discoloration of the denture base following cleaning can occur due to changes in the properties of the material.

Purpose. The purpose of this *in vitro* study was to assess the sorption and solubility of high-impact heat-polymerized denture base acrylic resin (PMMA) impregnated with zirconia nanoparticles after storing for six months (180 days) in distilled water (DW) and artificial saliva (AS). Colour stability was also assessed after exposure of the bases to different denture cleaners (DW, Steradent (STD) and Milton (MIL)) for six months.

Materials and Methods. Seventy-two specimens with a nominal dimeter of 50 ± l.0 mm and a thickness of 0.5 ± 0.1 mm were used for sorption and solubility studies. Half of the specimens were immersed in DW and the other half in AS. The specimens were divided into six groups for each storage medium, according to the concentration of zirconia nanoparticles (0, 1.5, 3.0, 5.0, 7.0, and 10.0 wt. %). For the colour stability study, ninety specimens were prepared with a diameter and thickness of 25 ± 1.0 mm x 2 ± 0.1 mm and divided in to six groups while each group was further divided in to three subgroups: storage in water (control), STD and MIL. Colour changes were measured with a Minolta Chroma Meter and assessed using the CIE L*a*b* colorimetric system. Data were statistically analysed for sorption and solubility using one-way and 2-way ANOVA statistical tests. Colour change data were analysed with Friedman's Two-way test and Kruskal-Wallis test at a pre-set alpha value level of 0.05.

Results. Sorption in DW and AS for all groups reached a stable mass within 90 days though a further slow increase was noticed until 150 days. All groups containing ZrO_2 showed sorption values lower than the control group at 90 days, though not significantly different ($p>0.05$). For both the DW and AS groups the lowest solubility value was measured in the group containing 3 wt.% ZrO_2, however, there was no significant difference except when observing 10 wt.% ZrO_2 in AS, which showed a significantly higher solubility ($p<0.05$). Sorption and solubility values in DW ranged from 24.80 $\mu g/mm^3$ and 3.74 $\mu g/mm^3$ respectively for group 3wt% of ZrO_2 to 27.05 $\mu g/mm^3$ and 8.01 $\mu g/mm^3$ for the control group. The colour change (ΔE) exhibiting significant differences were found among all groups immersed in denture cleaners, and all values increased with

time. According to the National Bureau of Standards, the control group had the lowest colour change $\Delta E = 1.22$, and the highest value was for 10 wt.% ZrO_2 stored in MIL ($\Delta E = 6.07$). The values of colour change for storage in water ranged from ΔE 0.49 (control) to ΔE 1.82 (10 wt.% ZrO_2).

Conclusion. High Impact PMMA and 3wt % of ZrO_2 nanocomposite showed the lowest sorption and solubility in both media. In addition, the colour change for the composite group containing 3 wt.% zirconia was clinically acceptable. However, high concentrations of denture cleaners should be avoided, and the shortest cleaning time is recommended to improve the clinical life of the nanocomposite denture base.

6.2. INTRODUCTION

Since the beginning of the twentieth century, poly-methyl methacrylate (PMMA) acrylic resin has been the material of choice for constructing denture bases (Figueroa et al., 2018). PMMA resin has been reinforced with butadiene-styrene to develop high-impact PMMA in an attempt to improve its physical and mechanical properties. These materials are provided in a powder-liquid form and are processed in the same way as other conventional heat-polymerized methyl methacrylate resins (Sasaki et al., 2016). Within the oral environment, the physical properties of PMMA undergo rapid changes with time and this influences the mechanical properties (Rad et al., 2017). Water sorption and solubility are major problems that can affect the durability of the denture bases (Tuna et al., 2008). In relation to general aesthetics, in the long term, staining affects the gloss surface and the shine of the denture, which are of concern to both patient and dentist (Rad et al., 2017).

Poly-methyl methacrylate (PMMA) absorbs water slowly over a period time in the oral environment (Miettinen and Vallittu, 1997; Polat et al., 2003; Rad et al., 2017), because of the polarity of the resin molecules. By forcing the polymer chains apart, the absorbed water spreads between the macromolecules of the material by diffusion (Tuna et al., 2008), causing an expansion that may compensate for the polymerisation shrinkage that occurs during fabrication of the heat-cured denture bases (Asar et al., 2013). The amount of water sorption into a polymeric structure is influenced by the degree of conversion, the cross-link density and hydrophilicity of the polymeric network (Alshali et al., 2015). Additionally, water absorbed into the PMMA material can act as a plasticizer, causing it to become soft, which can result in a physical change of the polymer networks. This change can lead to a decrease in mechanical properties such as transverse strength, hardness and fatigue limit, and thus possibly increasing the potential for fractures (Asar et al., 2013; Machado Cucci et al., 1998; Polat et al., 2003; Zuo et al., 2016). High water sorption rates tend to affect the material properties and reduce the clinical lifespan of a denture within the oral cavity. Therefore, it is important to use materials with the lowest possible water sorption rates (Jang et al., 2015). According to British Standard (EN ISO) specification NO. 20795, water sorption should not exceed 32 $\mu g/mm^3$ for heat-cured acrylic resin materials (British Standards, 2008).

Solubility represents the fraction of material dissolved from a polymer (Arikan et al., 2005). In general, denture base acrylic resins have low solubility, and the little that occurs is a result of the leaching out of traces of unreacted monomer and water-soluble additives, plasticizers and initiators into the oral fluids (Asar et al., 2013). However, these monomers sometimes produce a soft tissue reactions (Tuna et al., 2008). According to the British Standard (EN ISO) specification No. 20795, the solubility of denture bases should not exceed 1.6 µg/mm^3 for heat-cured acrylic resin materials (British Standards, 2008).

Acrylic resin denture bases should also be colour-stable, matching the natural appearance of the intraoral soft tissues (Altıncı and Durkaya, 2016; Zoidis et al., 2019). However, denture base resin may be discoloured due to a number of different factors (Zuo et al., 2016), including water sorption, dissolution of the components and surface roughness (Zoidis et al., 2019). Dentures absorb liquid over time and undergo staining through the intake of fluids and foods. In addition, external pigments, such as tea, coffee, wine, and some artificial food dyes may attach and penetrate the base resin causing discoloration (Zoidis et al., 2019; Zuo et al., 2016).

Denture cleaners are commonly employed to remove stains and debris from denture surfaces and to prevent the formation of plaque or colonisation of bacteria. However, their daily use may impact the physical properties of the denture base resin, affecting its surface roughness, hardness, gloss or colour (Zoidis et al., 2019). In addition, lack of information on using cleaning solutions correctly may affect the denture properties (Peracini et al., 2010).

Several studies (Davi et al., 2010; Goiato et al., 2013a; Hong et al., 2009; Polyzois et al., 2013), have investigated the short and long-term effects of denture cleaners such as efferdent, chlorhexidine, sodium hypochlorite, peroxide and other commercial cleaning agents on the colour stability of different denture base resins. They found that the colour change (defined by ΔE) of the denture bases was influenced by the type of denture cleaners used, and ΔE values increased with an increase in duration in exposure to cleaning solutions. McNeme et al., found that denture cleaners (sodium hypochlorite) could cause bleaching of a denture base acrylic resin (McNeme et al., 1991). Polychronakis et al., also reported a significantly decrease of the gloss and higher surface roughness with different denture base resin materials immersed in dental cleaning agents (Corega Extradent) (Polychronakis et al., 2015).

Pfeiffer et al., conducted a study to evaluate water sorption and solubility of denture base resins (Sinomer: heat-polymerized, modified methacrylate; Polyan: thermoplastic, modified methacrylate; Promysan: thermoplastic, enterephthalate-based; Microbase: microwave polymerized, polyurethane-based, and Paladon 65: heat-polymerized, methacrylate, control group). The findings showed that thermoplastic polymerisation

(Polyan) resulted in lower water sorption than conventional heat-cured acrylic resin and other groups. However, water solubility was not significantly different among the groups (Pfeiffer and Rosenbauer, 2004). Zuo et al., evaluated organic-inorganic hybrid coated denture base surfaces for water sorption, solubility and colour stability. They reported that water uptake and solubility were reduced, and colour stability improved due to the application of the coating (Zuo et al., 2016). Asar et al., also demonstrated that reinforcing conventional heat-polymerised acrylic resin with different metal oxide fillers (Al_2O_3, TiO_2 and ZrO_2) significantly decreased water sorption and solubility, particularly with the use of ZrO_2 (Asar et al., 2013).

Recent literature shows that the addition of nanoscale reinforcing agents with polymer materials produce new mechanical and physical properties, creating a new class of nanocomposite. In dentistry, many attempts have been made to create and improved PMMA with the addition of different nanosized fillers (Gad and Abualsaud, 2019a) and their physical and mechanical properties evaluated. However, there is no study in the literature investigating the physical properties (e.g., water sorption, solubility and colour stability) of HI heat-cured denture base resins reinforced with zirconia nanoparticles.

The aim of this study was to evaluate the effect of adding zirconia nanoparticles at different concentrations to High-impact PMMA on sorption, solubility and colour change when stored in different media for up to 180 days. Sorption and solubility were measured following storage in in distilled water (DW) and artificial saliva (AS), and colour changes were assessed following storage in DW and two different denture cleaners (Steradent (STD) and Milton (MIL)) cleaners.

The hypotheses to be tested were that there would be no significant change in (i) sorption, (ii) solubility, and (iii) colour stability for HI PMMA nanocomposite experimental groups compared to the pure HI PMMA (control group).

6.3. MATERIALS AND EXPERIMENTAL METHOD

6.3.1. Materials

A commercially available Metrocryl HI denture base powder, (PMMA, poly-methyl methacrylate) and Metrocryl HI (X-Linked) denture base liquid (MMA, methyl methacrylate) were selected as the denture base material. Yttria-stabilized zirconia (ZrO_2) nanoparticles were chosen as the inorganic filler agent for fabricating nanocomposite denture specimens. The details of the denture base materials and cleaning solutions used to conduct the sorption, solubility and colour change experiments are shown in Table 6.1.

Table 6.1. Materials and denture cleaners used in this study

Materials	Trade name	Manufacturer	Lot. Number
High impact heat-curing acrylic denture base resin	HI Metrocryl	Metrodent Limited, Huddersfield, UK	Powder (22828) Liquid (103/4)
Yttria-stabilized zirconium oxide	Zirconium oxide	Sky Spring Nano Materials, Inc, Houston, TX, USA	8522-120315
Sodium bicarbonate, potassium carbonate peroxide, sodium sulfate, citric acid	Steradent	Reckitt Benckiser Healthcare, Dansom Lane, Limited, UK	0378493
Sodium hypochlorite	Milton	Laboratoire, Rivadis, Louzy, France	7227-430939

6.3.2. Preparation of Specimens

6.3.2.1. Silane functionalization of zirconia nanoparticle surfaces

Zirconia nanoparticle surfaces was treated with 7 wt.% silane coupling agent (3-trimethoxysilyl propyl methacrylate; product no. 440159, Sigma Aldrich) as detailed in Section 3.2.2 Chapter 3: Methodology.

6.3.2.2. Selection of appropriate percentages of zirconia nanoparticles

According to a previous study (Zidan et al., 2019), the most appropriate weight percentages of zirconia nanoparticles were used in this study: 0% (control), 1.5 wt.%, 3.0 wt.%, 5.0 wt.%, 7.0 wt.%, and 10.0 wt.%.

6.3.2.3. Mixing of zirconia with PMMA

The silane-treated zirconia and acrylic resin powders were weighed according to Table 6.2., using an electronic balance (Ohaus Analytical plus, Ohaus Corporation, USA) with accuracy up to 3 decimal points. The zirconia powder was added to the acrylic resin monomer and mixed by hand using a stainless-steel spatula to ensure all the powder was uniformly distributed within the resin monomer and to avoid any aggregation. The HI acrylic resin powder was then added to the liquid, and mixing continued until a consistent mixture was obtained, according to the manufacturer’s instructions. When the mixture reached a dough-like stage that was suitable for handling, it was packed into a mould by hand. The mould was then closed and placed in a hydraulic press (Sirio P400/13045) under a pressure of 15 MPa and then excess mixture was removed from the periphery of the mould. The mould was immersed in curing bath for 6 hours polymerisation at temperature 95°C, and then the mould was removed from the curing bath and cooled slowly for 30 min at room temperature. The mould was then opened, and the specimens were removed. The specimens were then trimmed using a tungsten carbide bur, ground with an emery paper and polished with pumice powder in a polishing machine (Tavom, UK).

Table 6.2. Weight percent zirconia in combination with acrylic resin powder as well as monomer content of the specimen groups

Experimental Groups	**Zirconia (wt.%)**	**Zirconia (g)**	**HI PMMA powder (g)**	**HI MMA monomer (ml)**
Control	0.0	0.000	21.000	10.0
1.5	1.5	0.315	20.685	10.0
3.0	3.0	0.630	20.370	10.0
5.0	5.0	1.050	19.950	10.0
7.0	7.0	1.470	19.530	10.0
10.0	10.0	2.100	18.900	10.0

6.3.3. Sorption and solubility test procedures

For water sorption and solubility experiments, a brass mould was used to prepare specimens with dimensions (50 ± 1.0) mm in diameter and a thickness of (0.5 ± 0.1) mm. Seventy-two acrylic resin specimens were prepared according to EN ISO 20795-1:2008 (British Standards, 2008). Specimens stored in a desiccator containing fresh silica gel were placed in an incubator at (37 ± 1)℃ for (23 ± 1) h and transferred to a second desiccator maintained at room temperature (23 ± 2) ℃ for 1 h. The specimens were then weighed to an accuracy of 0.0002 g using a calibrated electronic analytical balance (Ohaus Analytical plus, Ohaus Corporation, USA). The weighing was repeated until the mass loss of each specimen was not more than 0.2 mg in any 24 h period to achieve constant mass in the samples. The final mass in g was recorded as $m1$. Each specimen diameter was measured thrice using an electronic digital calliper (Draper, Eastleigh, Hants, UK) to calculate the mean values. The mean of five thicknesses measurements at four equally spaced points around the circumference. The volume (V) of each sample was calculated in cm^3 by using the mean dimeter and thickness.

For each group, six specimens were immersed in DW and six specimens were immersed in AS at (37 ± 1)°C in stored an incubator for a period of 180 days. The AS solution was prepared according to a composition shown in Table 6.3 by dissolving in 1000 ml of distilled water with a pH value of 5.52 and mixing using a magnetic stirrer until the components were completely dissolved (Williams et al., 2001). After each period (1, 2, 3, 4, 5, 6, 7, 14, 21, 30, 60, 90, 120, 150 and 180 days), the specimens were removed from the storage medium, wiped with a clean dry hand-towel until free from visible moisture, and mass in g was recorded as $m2$. After 180 days, specimens were reconditioned in desiccators until a constant mass was reached. This desorption process was carried out over a period of 90 days. The reconditioned mass in g was recorded as $m3$.

The values of water sorption (w_{sp}) in g/cm^3 were calculated by the Equation 6.1 (British Standards, 2008).

$$w_{sp} = \frac{m2 - m3}{v} \tag{6.1}$$

The values of water solubility (w_{sp}) were obtained in g/cm^3 and were calculated by the Equation 6.2:

$$w_{sl} = \frac{m1 - m3}{v} \tag{6.2}$$

where **v** is the volume of the specimen in cm^3 (British Standards, 2008). After completing the calculations, the values for water sorption and solubility were converted to $\mu g/mm^3$.

The percentage mass change and the percentage solubility that represents the total mass loss of components were calculated by the Equation 6.3 and Equation 6.4 (Alshali et al., 2015).

$$\text{Change in mass SP (\%)} = \frac{m2\,(t) - m1}{m1} \times 100 \tag{6.3}$$

$$Mass\ \text{loss SL(\%)} = \frac{m1\,(t) - m3}{m1} \times 100 \tag{6.4}$$

Table 6.3. Composition of artificial saliva (Williams et al., 2001)

Compound	**Amount (g/l)**	**Manufacturer**	**CAS**
Sodium chloride (NaCl)	0.400	Acros Organics	7647-14-5
Potassium chloride (KCl)	0.400	Fisher Chemical	7447-40-7
Calcium chloride ($CaCl_2$)	0.795	Acros Organics	10043-52-4
Sodium dihydrogen phosphate (H_2NaO_4P)	0.690	Alfa Aesa	7558-80-7
Sodium sulphide hydrate ($Na_2S \cdot xH_2O$)	0.005	Acros Organics	27610-45-3

6.3.4. Colour measurement procedure

Specimens were immersed into two cleaning solutions (Steradent (STD) and Milton (MIL)) and DW to measure the colour change. The cleaning solutions were prepared by immersing one STD tablet (3.184 g) into 250 ml of DW and 20 ml of MIL into 250 ml of DW. Both solutions were stirred for 30 seconds until the solutes were completely dissolved.

Minolta Chroma Meter CR-221 (Azuchi-Machi, Chuo-Ku, Osaka 541, Japan), a tristimulus colour analyser was used for measuring the colour and colour change (Co, 1988; Liberman et al., 1995). The dimensions of the specimens were 25 mm diameter × 2 mm thickness to meet the demands of the measuring instrument. A total of 90 specimens were fabricated with fifteen specimens for each group (6 groups). Every group was divided in to three sub-groups (A, B and C). All specimens were immersed in DW and stored in an incubator at 37±1 °C for 24 h. The specimens were dried with tissue paper before colour measurement and placed into the holder of the measuring head. During the measurement the light was shone on the specimen at an angle of 45° and reflected light was analysed (Liberman et al., 1995). Three measurements were recorded for each specimen as the baseline measurements. Then, five specimens from subgroup A were immersed in 40 ml DW to serve as control, five specimens from subgroup B were immersed in 40 ml STD solution and the remaining five specimens from subgroup C were immersed into 40 ml MIL solution. The colour values after baseline measurements were collected at 7, 14, 21, 30, 60, 90, 150 and 180 days.

Minolta Chroma Meter CR-221 was calibrated before each measurement using the white calibration plates, according to the manufacturer’s instructions. The colour differences were assessed by the International Commission on Illumination (C.I.E) L*a*b* scale, where L* is the lightness, a* defines the colour of the sample on red-green and b* on yellow-blue axes. The colour change (ΔE) values were calculated by using Equation 6.5: (Liberman et al., 1995):

$$\Delta E = [\ (\Delta L^*)^2 + (\Delta a^*)^2 + (\Delta b^*)^2]^{½} \qquad (6.5)$$

where, ΔL^*, Δa^* and Δb^* represent the differences between the L*, a* and b* values of the baseline coordinates and those measured after immersion (Hong et al., 2009; Koksal and Dikbas, 2008).

Level of colour change was quantified by the American National Bureau of Standards (NBS) (Table 6.4). NBS units are calculated using Equation 6.6 (Hong et al., 2009).

$$\mathrm{NBS} = \Delta E \times 0.92 \qquad (6.6)$$

Table 6.4. Critical marks of colour difference according to the National Bureau of Standards (Hong et al., 2009)

Critical Marks of Colour Difference	Textile Terms (NBS Unit)
Trace	0.0 - 0.5
Slight	0.5 - 1.5
Noticeable	1.5 - 3.0
Appreciable	3.0 - 6.0
Much	6.0 - 12.0
Very much	>12.0

6.3.5. Statistical analyses

The recorded data of sorption, solubility and colour change were calculated and statistically analysed using SPSS statistics version 23 (IBM, New York, NY, USA). Non-significant Shapiro-Wilk test showed that the data of sorption and solubility tests were normally distributed and there was homogeneity of variances. The percentage of mass change for sorption and solubility data were analysed with repeated measurements (One-way ANOVA) to evaluate the effect of storage time. The mean values of sorption to solubility among different groups were compared using Two-way ANOVA followed by

Tukey post-hoc analysis for multiple comparisons at a pre-set alpha value level of 0.05. The Shapiro-Wilk test showed that the data for the colour change (ΔE) were not normally distributed. Therefore, nonparametric tests were used to analyse the results on three factors (time, solutions and groups). The Friedman's Two-way test with related samples was analysed for the effect of time followed by the Kruskal-Wallis test with independent samples analysed variances on the solutions and groups. The data were checked to see whether there were significant differences between of three factors at a pre-set alpha of 0.05.

6.4. RESULTS

6.4.1. Solubility and sorption analysis

All experimental groups showed mass changed with time upon storage in DW and AS. For DW, the mass steadily increased in the first 21 days of immersion for all groups. This was then followed by a reduction in the rate of increase until 60 days, and then a slow or even decrease in mass until equilibrium was reached after 90 days. This was then followed by a slow (except for the control group) increase for the next 60 days, and finally mass was decreased at 180 days (Figure 6.1). The highest rate of mass increase was with the group containing 3 wt.% of zirconia, but it was not significantly different to other groups.

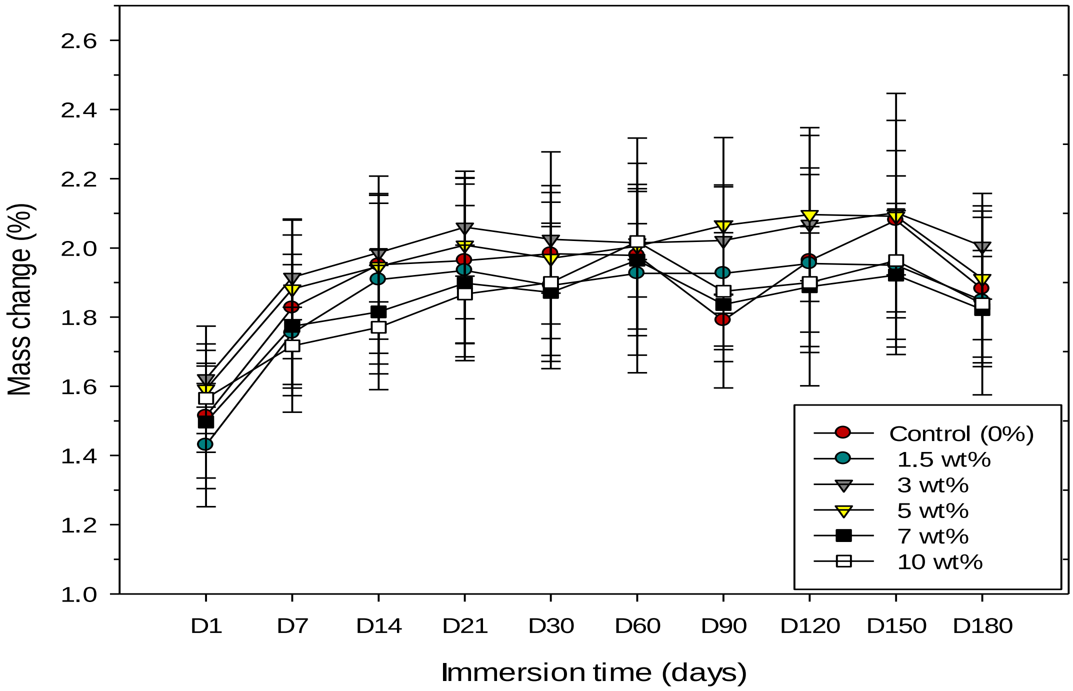

Figure 6.1. Line graph illustrating the mass change of specimens from six groups immersed in distilled water over 180 days

In AS, all the groups demonstrated a gradual mass increase within the first 7 days except the group containing 10 wt.% of zirconia whose mass was not significantly increased until 14 days, as well as showing a significant difference compared to the control group. Mass change for all the groups decreased 21 days and then started to increase until 90 days. After that, there was no significant mass change until 180 days, which was an indication of reaching equilibrium state (Figure 6.2). The percentage increase of mass change after 180 days for all the experimental groups in AS was significantly higher than that in DW. However, it should be noted that after 90 days there was no significant change in mass until 180 days for both solutions. Therefore, sorption values were only presented here for 90 days.

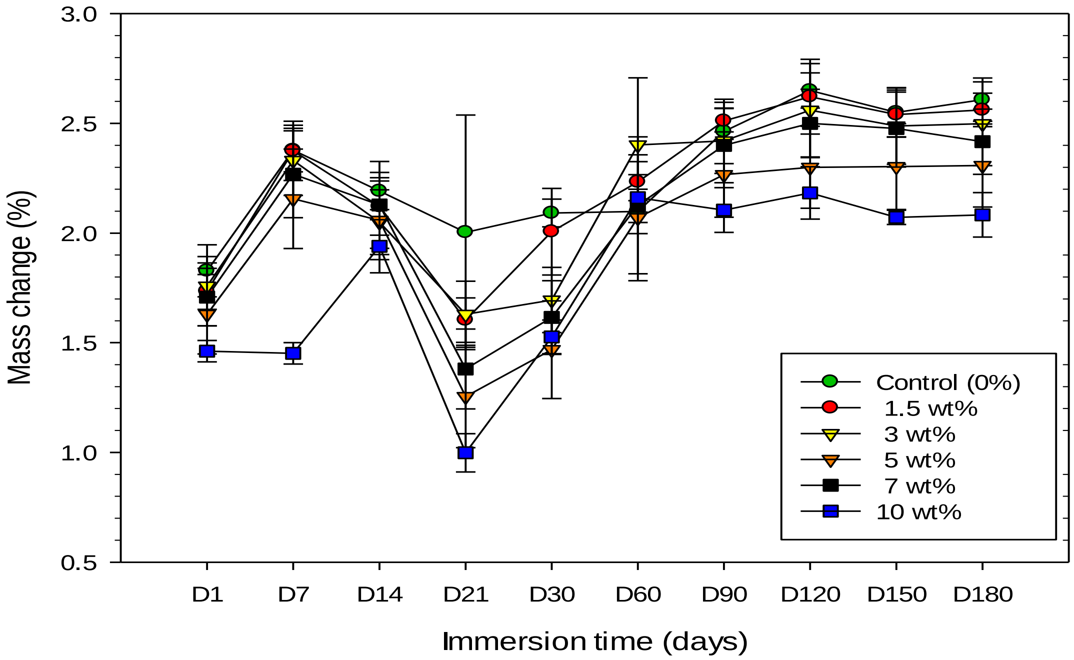

Figure 6.2. Line graph illustrating the mass change of specimens from six groups immersed in artificial saliva over 180 days

The mean and standard deviation values for sorption and solubility in DW and sorption and solubility in AS are presented in Table 6.5 and Table 6.6 respectively. The results showed that at 90 days, sorption by the experimental groups containing zirconia was lower than that by the control group for both solutions, but not significant (P>0.05) (Figure 6.3).

At 180 days in DW, all groups of nanocomposites showed lower solubility compared to the control group, however, the difference was not significant. The lowest solubility was recorded for the group with 3 wt.% of ZrO_2 in both solutions. In general, the specimens stored in AS showed significantly lower solubility than specimens stored in DW Figure

6.4. Specimens immersed in DW exhibited more colour change compared to the specimens immersed in AS after 180 days and specimens in the dry condition as shown in Figure 6.5.

Table 6.5. Mean and standard deviation values of sorption (µg/mm^3) and percentage of sorption (%) after 90 days of storage in distilled water; solubility (µg/mm^3) and its percentage (%) values after 180 days.

Experimental Group	**Water Sorption (%)**	**Water Sorption (µg/mm^3)**	**Water Solubility (%)**	**Water Solubility (µg/mm^3)**
Control 0%	1.79 (0.07)^a	27.05 (4.55)^a	0.75 (0.52)^a	8.01 (5.48)^a
1.5 %	1.92 (0.25)^a	25.16 (2.00)^a	0.45 (0.43)^a	4.78 (4.57)^a
3%	2.02 (0.15)^a	24.80 (1.29)^a	0.36 (0.25)^a	3.78 (2.64)^a
5%	2.06 (0.25)^a	26.18 (2.68)^a	0.42 (0.18)^a	5.06 (0.60)^a
7%	1.83 (0.24)^a	25.83 (2.51)^a	0.59 (0.04)^a	6.28 (0.46)^a
10%	1.87 (0.16)^a	25.90 (2.69)^a	0.71 (0.25)^a	7.55 (2.71)^a

Note: Same lower-case letters within column indicate no significant difference (P>.05) from control.

Table 6.6. Mean and standard deviation values of sorption (µg/mm3) and percentage of sorption (%) after 90 days of storage in artificial saliva; solubility (µg/mm^3) and its percentage (%) values after 180 days

Experimental Group	**Saliva Sorption (%)**	**Saliva Sorption (µg/mm^3)**	**Saliva Solubility (%)**	**Saliva Solubility (µg/mm^3)**
Control 0%	2.46 (0.14)^a	25.17 (2.12)^a	-0.20 (0.07)^a	-2.32 (0.89)^a
1.5 %	2.51 (0.08)^a	24.99 (1.13)^a	-0.22 (0.02)^a	-2.40 (0.28)^a
3%	2.42 (0.14)^a	24.22 (1.72)^a	-0.26 (0.07)^a	-3.03 (0.95)^a
5%	2.26 (0.19)^a	23.77 (1.68)^a	-0.14 (0.04)^{a,b}	-1.56 (0.46)^{a,b}
7%	2.40 (0.16)^a	25.16 (1.76)^a	-0.14 (0.03)^{a,b}	-1.68 (0.36)^{a,b}
10%	2.10 (0.10)^a	23.61 (1.20)^a	-0.05 (0.03)^b	-0.58 (0.46)^b

Note: Same lower letters within column indicated no significant difference (P>.05) with control.

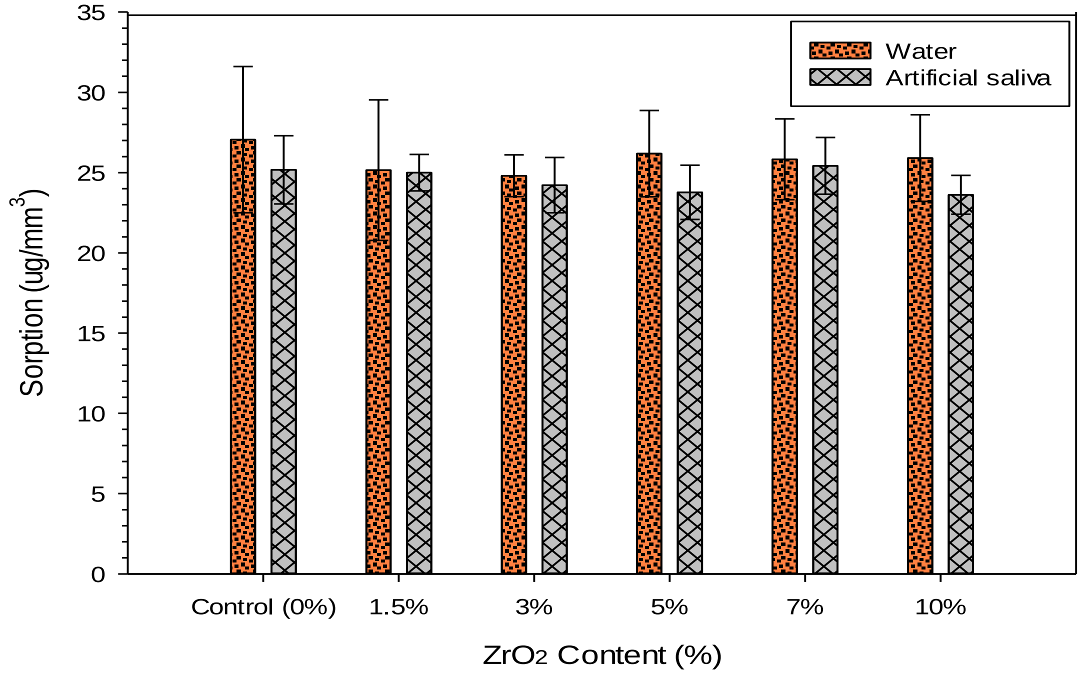

Figure 6.3. Bar chart demonstrating the mean sorption values of specimens after immersing for 90 days in distilled water and artificial saliva

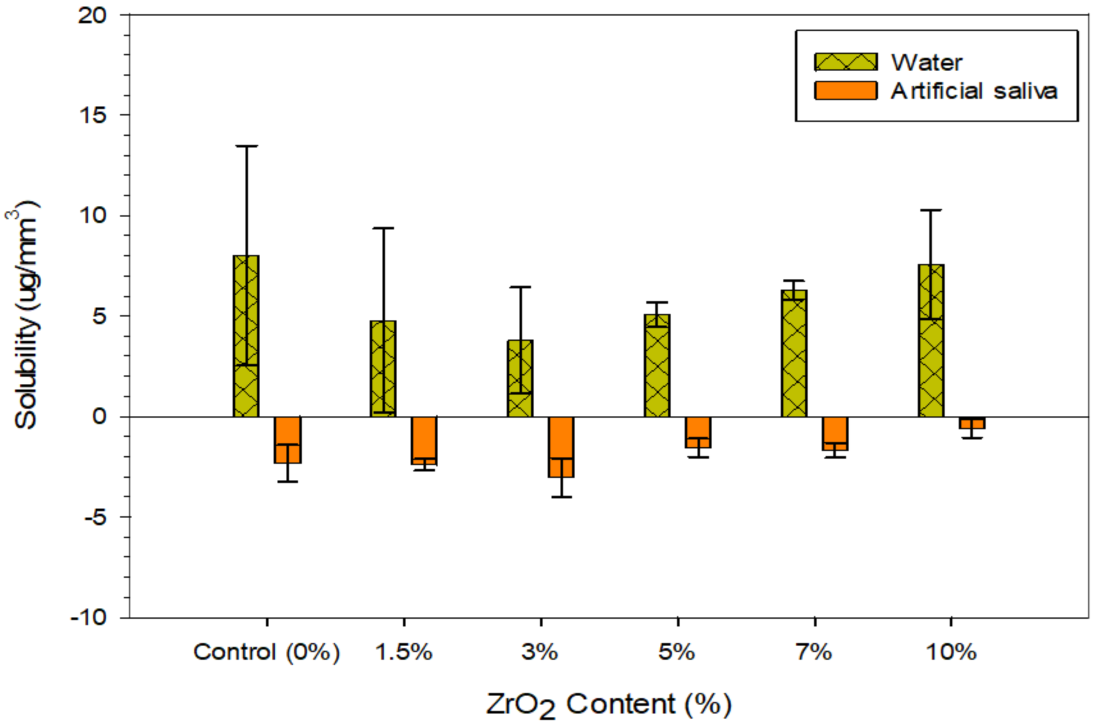

Figure 6.4. Bar chart demonstrating the mean solubility values of specimens after immersing for 180 days in distilled water and artificial saliva

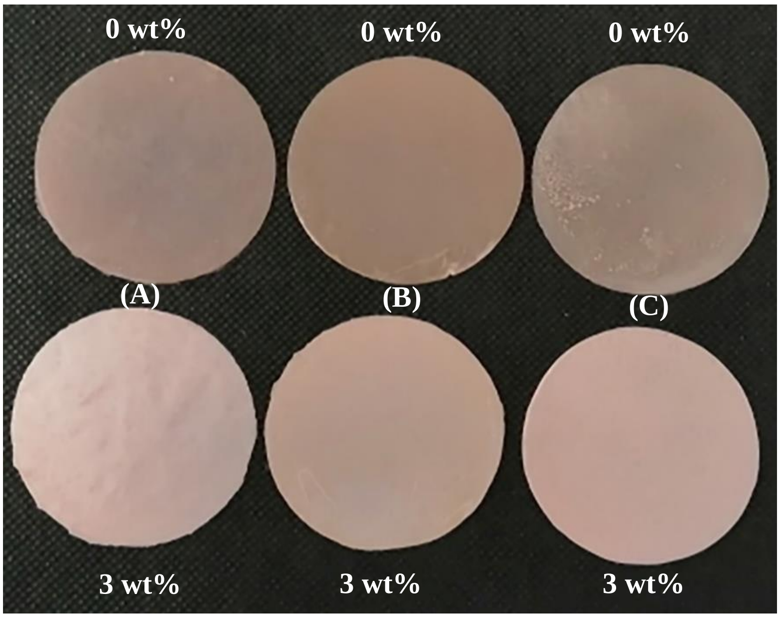

Figure 6.5. Photograph showing the colour changes in the control group (0 wt.%) and group containing 3 wt.% of ZrO_2 (A) before immersion in DW or AS, (B) after immersing for 180 days in DW and (C) after immersing for 180 days in AS.

6.4.2. Colour change

The colour changes of HI PMMA nanocomposite denture specimens after 180 days of immersion in two different cleansers and DW are presented in Figure 6.6. Baseline of (C.I.E) L*a*b* colour measurement values (mean and standard deviations) of the six experimental groups after 24 hours immersion in DW are listed in Table 6.7. The median values, Interquartile Range (IQR) and colour expressed in NBS unit, for the colour change (ΔE) measurements after 7, 30, 60, 90, 150 and 180 days are shown in Table 6.8.

In general, for all groups and after all immersion durations, there was a difference in colour change between the samples immersed in DW and the other solutions (Table 6.9). In majority of the cases the difference is not significant. However, significant differences were found for only three groups. Firstly, for the group containing 1.5 wt.% ZrO_2, after 180 days there was a significant increase of colour change when compared between DW and STD. Secondly, for the group containing 3.0 wt.% ZrO_2, after 150 days there was a significant increase of colour change when compared between DW and MIL. Thirdly, for the group containing 7.0 wt.% ZrO_2, after all immersion intervals, there was a significant increase of colour change when compared between DW and STD, and DW and MIL.

Again, an increasing trend of colour change between 7 days and 180 days for any specimen group immersed in any individual cleaner, but no significantly different (P>0.05).

Significant differences ($p<0.05$) were found in colour change (ΔE) between all groups containing zirconia and the control group after immersing in STD cleaner at 90 and 150 days. However, for any particular immersion duration in DW and MIL solution, there was no significant colour difference among the groups.

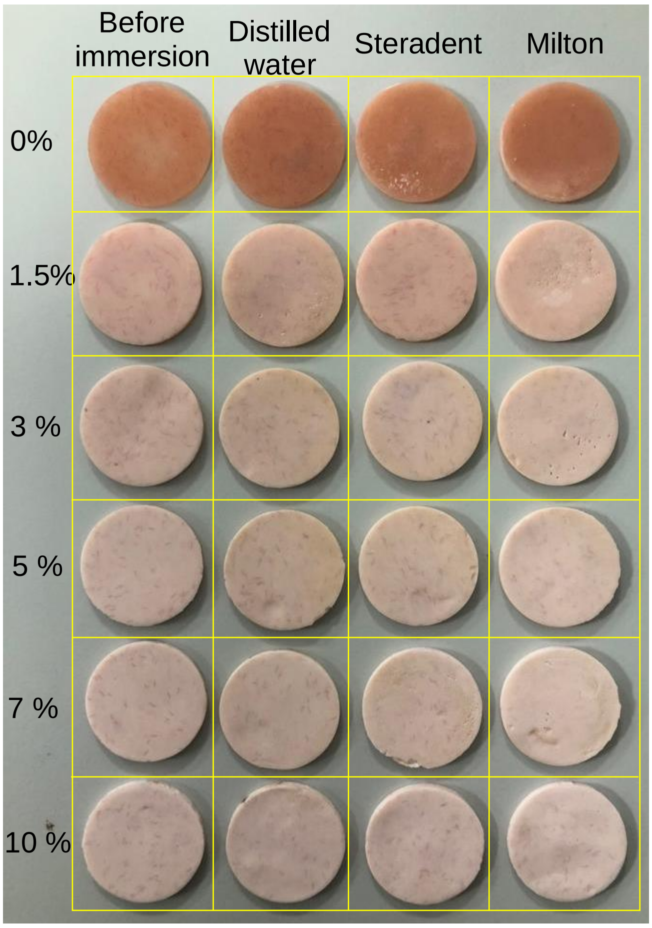

Figure 6.6. Photographs showing the colour changes in the samples before and after 180 days' immersion in different solutions.

Table 6.7. Mean & SD baseline colour measurements after 24 hours' immersion in distilled water.

Experimental Groups	L* Mean (SD)	a* Mean (SD)	b* Mean (SD)
Control	8.98 (0.64)	0.342 (0.00)	0.331 (0.00)
1.5	33.96 (2.90)	0.346 (0.00)	0.342 (0.00)
3.0	44.67 (3.59)	0.344 (0.00)	0.343 (0.00)
5.0	54.05 (2.38)	0.345 (0.00)	0.343 (0.00)
7.0	56.53 (2.42)	0.342 (0.00)	0.342 (0.00)
10.0	60.19 (3.70)	0.339 (0.00)	0.340 (0.00)

Table 6.8. Median values and Interquartile Range (IQR) of colour change and National Bureau of Standards (NBS) unit for specimens (control 0%, 1.5%, 3%, 5%, 7% and 10 wt.% of zirconia) immersed in distilled water, Steradent and Milton over time.

Experimental Group	Cleaners	Day 7	Day 30	Day 60	Day 90	Day 150	Day 180
		ΔE IQR NBS	ΔE IQR NBS	ΔE IQR NBS	ΔE IQR NBS	ΔE IQR NBS	ΔE IQR NBS
Control 0%	Distilled water	0.20 (0.80) 0.18	0.33 (0.95) 0.30	0.51 (0.76) 0.46	0.49 (0.54) 0.45	0.52 (0.84) 0.47	0.54 (1.06) 0.49
	Steradent	0.31 (0.85) 0.28	0.49 (0.85) 0.45	0.52 (0.87) 0.47	0.49 (0.97) 0.45	0.75 (0.47) 0.69	1.10 (0.82) 1.01
	Milton	0.91 (0.53) 0.83	0.91 (0.92) 0.83	0.91 (0.99) 0.83	0.97 (0.74) 0.89	1.41 (0.45) 1.29	1.33 (1.43) 1.22
1.5 %	Distilled water	0.43 (0.88) 0.39	0.44 (1.21) 0.40	0.50 (1.21) 0.46	0.54 (1.37) 0.49	0.63 (2.85) 0.57	1.15 (3.63) 1.05
	Steradent	1.62 (7.38) 1.49	1.62 (7.63) 1.49	1.62 (7.65) 1.49	2.17 (3.57) 1.99	2.76 (6.57) 2.53	3.01 (5.79) 2.76
	Milton	1.78 (7.67) 1.63	1.78 (7.45) 1.63	1.78 (7.54) 1.63	1.55 (8.25) 1.42	1.46 (7.55) 1.34	1.89 (9.30) 1.73
3%	Distilled water	0.54 (2.26) 0.50	0.56 (2.26) 0.51	0.56 (2.15) 0.51	0.57 (1.83) 0.52	0.64 (1.76) 0.58	1.05 (1.98) 0.96
	Steradent	2.39 (4.12) 2.19	2.39 (3.87) 2.19	2.45 (3.89) 2.25	2.81 (3.33) 2.58	2.89 (3.10) 2.65	3.09 (3.56) 2.84
	Milton	1.15 (5.97) 1.05	1.24 (5.98) 1.14	1.46 (5.90) 1.34	2.84 (3.50) 2.61	3.05 (3.27) 2.80	3.25 (3.70) 2.99
5%	Distilled water	0.64 (2.72) 0.59	0.69 (2.57) 0.63	0.69 (2.57) 0.63	1.88 (3.72) 1.72	1.87 (3.29) 1.72	1.92 (2.55) 1.76
	Steradent	2.26 (4.40) 2.07	2.43 (4.35) 2.23	2.43 (4.55) 2.23	2.83 (2.77) 2.60	2.95 (3.64) 2.71	3.82 (3.53) 3.51
	Milton	3.51 (4.54) 3.22	3.51 (4.44) 3.22	3.51 (4.39) 3.22	3.96 (2.11) 3.64	3.98 (2.89) 3.66	3.37 (3.90) 3.14
7%	Distilled water	0.68 (1.60) 0.63	0.97 (1.51) 0.89	1.26 (1.59) 1.15	1.33 (0.62) 1.22	1.54 (2.46) 1.41	1.94 (1.71) 1.78
	Steradent	3.85 (2.82) 3.54	3.85 (2.57) 3.54	3.85 (2.55) 3.54	3.93 (3.32) 3.61	4.46 (3.23) 4.10	4.26 (2.95) 3.91
	Milton	4.21 (5.48) 3.87	4.25 (5.38) 3.91	4.25 (5.08) 3.91	4.19 (3.25) 3.85	4.70 (4.67) 4.32	5.10 (4.41) 4.69
10%	Distilled water	0.70 (3.32) 0.64	0.74 (3.31) 0.68	0.78 (3.41) 0.71	1.23 (2.39) 1.13	1.92 (2.19) 1.76	1.98 (3.84) 1.82
	Steradent	2.46 (7.31) 2.26	2.46 (7.50) 2.26	2.46 (7.57) 2.26	2.36 (6.09) 2.17	4.83 (6.62) 4.44	4.81 (7.62) 4.42
	Milton	3.66 (7.23) 3.36	3.66 (7.48) 3.36	3.66 (7.58) 3.36	3.20 (6.07) 2.94	5.36 (6.01) 4.93	6.60 (6.71) 6.07

Table 6.9. The median colour change values and statistical differences of specimens following immersion in STD and MIL compared to DW over time

Experimental Group	**Solutions**			
	Period	Distilled water	Steradent	Militon
Control 0%	7 D	$0.20^{A,a}$	$0.31^{A, a}$	$0.91^{A, a}$
	30 D	$0.33^{A, a}$	$0.49^{A, a}$	$0.91^{A, a}$
	60 D	$0.51^{A, a}$	$0.52^{A, a}$	$0.91^{A, a}$
	90 D	$0.49^{A, a}$	$0.49^{A, \phi, a}$	$0.97^{A, a}$
	150 D	$0.52^{A, a}$	$0.75^{A, \phi, a\,b}$	$1.41^{A, b}$
	180 D	$0.54^{A, a}$	$1.10^{A, a}$	$1.33^{A, a}$
1.5 %	7 D	$0.43^{A, a}$	$1.62^{A, a}$	$1.78^{A, a}$
	30 D	$0.44^{A, a}$	$1.62^{A, a}$	$1.78^{A, a}$
	60 D	$0.50^{A, a}$	$1.62^{A, a}$	$1.78^{A, a}$
	90 D	$0.54^{A, a}$	$2.17^{A, \Omega, a}$	$1.55^{A, a}$
	150 D	$0.63^{A, a}$	$2.76^{A, \Omega, a}$	$1.46^{A, a}$
	180 D	$1.15^{A, a}$	$3.01^{A, b}$	$1.89^{A, a, b}$
3%	7 D	$0.54^{A, a}$	$2.39^{A, a}$	$1.15^{A, a}$
	30 D	$0.56^{A, a}$	$2.39^{A, a}$	$1.24^{A, a}$
	60 D	$0.56^{A, a}$	$2.45^{A, a}$	$1.46^{A, a}$
	90 D	$0.57^{A, a}$	$2.81^{A, \Omega, a}$	$2.84^{A, a}$
	150 D	$0.64^{A\,a}$	$2.89^{A, \Omega, a\,b}$	$3.05^{A, b}$
	180 D	$1.05^{A, a}$	$3.09^{A, a}$	$3.25^{A, a}$
5 %	7 D	$0.64^{A, a}$	$2.26^{A, a}$	$3.51^{A, a}$
	30 D	$0.69^{A\,a}$	$2.43^{A, a}$	$3.51^{A, a}$
	60 D	$0.69^{A, a}$	$2.43^{A, a}$	$3.51^{A, a}$
	90 D	$1.88^{A, a}$	$2.83^{A, \Omega, a}$	$3.96^{A, a}$
	150 D	$1.87^{A, a}$	$2.95^{A, \Omega, a}$	$3.98^{A, a}$
	180 D	$1.92^{A, a}$	$3.02^{A, a}$	$3.37^{A, a}$
7%	7 D	$0.68^{A, a}$	$3.85^{A, b}$	$4.21^{A, b}$
	30 D	$0.97^{A, a}$	$3.85^{A, b}$	$4.25^{A, b}$
	60 D	$1.26^{A, a}$	$3.85^{A, b}$	$4.25^{A, b}$
	90 D	$1.33^{A, a}$	$3.93^{A,\Omega, b}$	$4.19^{A, b}$
	150 D	$1.54^{A\,a}$	$4.46^{A, \Omega, b}$	$4.70^{A, b}$
	180 D	$1.94^{A\,a}$	$4.26^{A, b}$	$5.10^{A, b}$
10 %	7 D	$0.70^{A, a}$	$2.46^{A, a}$	$3.66^{A, a}$
	30 D	$0.74^{A, a}$	$2.46^{A, a}$	$3.66^{A, a}$
	60 D	$0.78^{A, a}$	$2.46^{A, a}$	$3.66^{A, a}$
	90 D	$1.23^{A, a}$	$2.36^{A ,\Omega, a}$	$3.20^{A, a}$
	150 D	$1.92^{A, a}$	$4.83^{A, \Omega, a}$	$5.36^{A, a}$
	180 D	$1.98^{A, a}$	$4.81^{A, a}$	$6.60^{A, a}$

Note: Same uppercase letter within column represents no significant difference (p>0.05) for within group and between groups, while same lowercase letter within same row represents no significant difference (p>0.05), different symbols within column of Steradent represents significant difference (p<0.05) between groups.

The Friedman's Two-way test with related samples and the Kruskal-Wallis test with independent samples showed that within each experimental group, there was significant differences ($p<0.05$) between distilled water and the two cleaners (STD, MIL) over time.

In the control group (0% ZrO_2) significant differences in colour change (ΔE) between specimens stored in DW and MIL cleaner were observed at 150 days. Specimens containing 1.5 wt.% of ZrO_2 immersed in STD showed significant differences in colour change (ΔE) at 180 days compared to DW. The group containing 3 wt.% ZrO_2 immersed in MIL also showed significant increases in colour change (ΔE) compared to DW at 150 days. Significant differences in the colour change (ΔE) were also found in specimens containing 7 wt.% ZrO_2 immersed in MIL compared to DW at all intervals. However, in groups containing 5 wt.% and 10 wt.% ZrO_2 there were no significant differences in colour change (ΔE) between two the cleaners and distilled water (Table 6.9).

The values of colour change (ΔE) at 180 days were expressed in NBS values as listed in Table 6.10 and presented in Figure 6.7. Specimens in groups containing 1.5 wt.% and 3 wt. % of ZrO_2 immersed in DW demonstrated “slight change” compared to the control group, while the other groups (5 wt.%, 7wt% and 10 wt.%) showed “noticeable change”. However, the control group also demonstrated “slight change” following immersion in STD and MIL cleaners. All ZrO_2 containing specimens in both MIL and STD solution showed at least noticeable change or higher.

It is interesting to notice that colour change was strongly associated with whitening (L^*) between control group and other groups containing of zirconia in contrast to redness/greenness (a^*) and yellowness/blueness (b^*) values as shown in Table 6.7. In addition, as the concentration of zirconia was increased. the whitening effect was also increased and this can be visually evident in Figure 6.6.

Table 6.10. Colour change values after 180 days according to NBS unit system

Experimental Group	**Solutions**		
	Distilled Water (DW)	Steradent (STD)	Milton (MIL)
Control 0%	0.49	1.01^{*}	1.22^{*}
1.5 %	1.05^{*}	$2.76^{\wedge}$	$1.73^{\wedge}$
3%	0.96^{*}	$2.84^{\wedge}$	$2.99^{\wedge}$
5%	$1.76^{\wedge}$	3.51^{+}	3.10^{+}
7%	$1.78^{\wedge}$	3.91^{+}	4.69^{+}
10%	$1.82^{\wedge}$	4.42^{+}	6.07^{++}

Note: Critical marks of colour difference: Trace (0.0-0.5); Slight* (0.5-1.5); Noticeable^ (1.5-3.0), Appreciable+ (3.0-6.0) and Much++ (6.0-12)

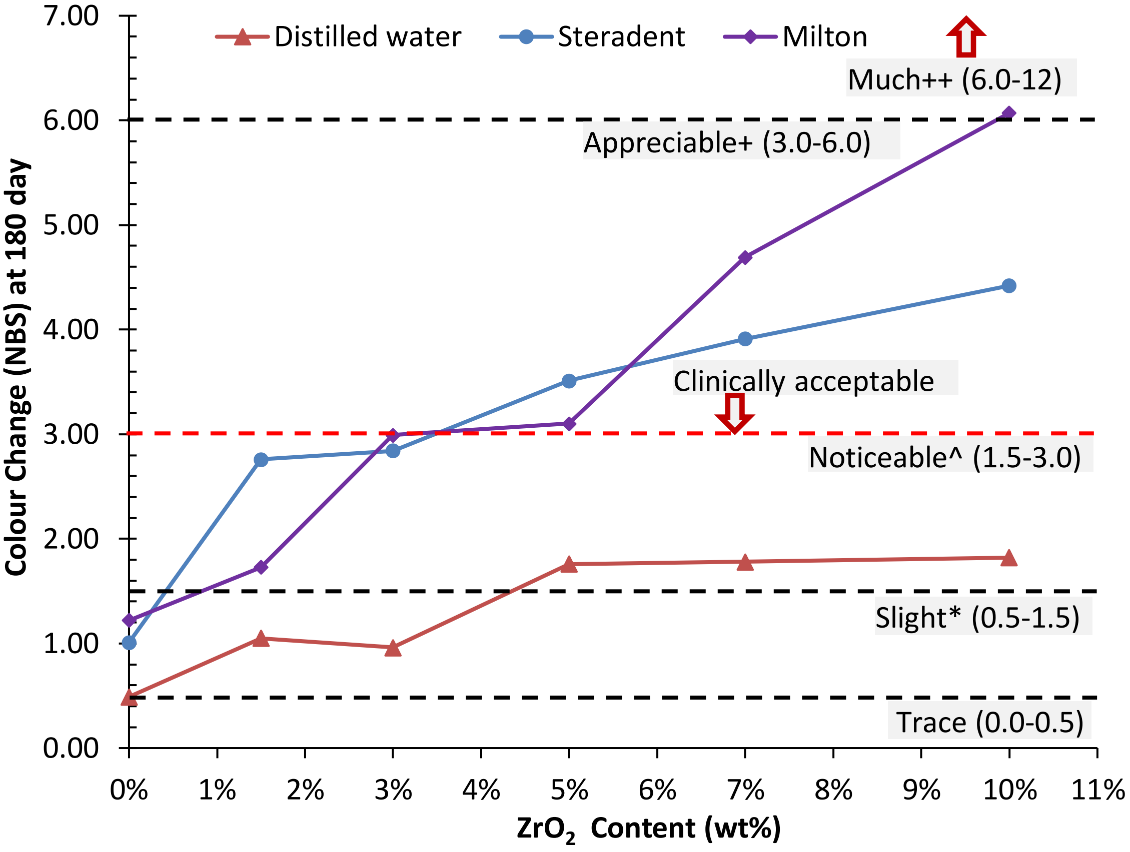

Figure 6.7. Line graph showing the colour change according to NBS unit system in specimens immersed in DW, Steradent (STD) and Milton (MIL) for 180 days.

6.5. DISCUSSION

In this study, water sorption and solubility characteristics of HI PMMA nanocomposites with different concentrations of ZrO_2 were measured after storing for up to 180 days in DW and AS. DW and AS were used as storage media in this study because they simulate oral fluids and react with the denture base inside and outside (stored overnight in water) the mouth. No significant difference was observed in mass change between the groups stored in DW. However, the group with 10 wt.% of zirconia showed a significant decrease ($p<0.05$) in mass compared to the control group during storage in AS. The experimental groups containing zirconia showed decreased sorption in both media compared to the control group, especially with the group containing 3 wt.% zirconia. As the decrease was not statistically significant ($p>0.05$), the first hypothesis was accepted. The lowest solubility was found for the group containing 3 wt.% of ZrO_2 in both storage media, after storing for 180 days but not significantly different from the control group. However, the group containing 10 wt.% of ZrO_2 was significantly different from the control group, and the groups containing 1.5% wt.% and 3 wt.% of zirconia upon storage in AS and thus the second hypothesis was rejected.

Previous studies reported values of water sorption ranging from 11.64 µg/mm^3 to 38.31 µg/mm^3 for different types of denture base acrylic resins after 7 days of immersion in water (Machado Cucci et al., 1998; Miettinen and Vallittu, 1997; Pfeiffer and Rosenbauer, 2004; Polyzois et al., 2013; Zuo et al., 2016). The results of this study indicated that HI PMMA nanocomposite experimental groups complied with the British Standard (EN ISO) specification NO. 20795 (not exceed 32 µg/mm^3 for heat-cured acrylic resin) as mean values ranged from 24.80 µg/mm^3 to 25.90 µg/mm^3 compared to the control group (27.05 µg/mm^3) in DW storage. The mean values of specimen sorption stored in AS ranged from 23.61 µg/mm^3 to 25.41 µg/mm^3 after 90 days, compared to the control group (25.17 µg/mm^3).

The findings of this study on water sorption are in agreement with those of Asar et al., who evaluated the effect of reinforcing conventional heat-cured acrylic resin with various metal oxide microparticles (TiO_2, ZrO_2 and Al_2O_3 using 1% and 2% by volume) on mechanical and physical properties such as, water sorption and solubility. The results showed that incorporation of metal oxides significantly decreased water sorption and solubility, particularly with 2% of ZrO_2 which showed the lowest solubility compared to the conventional acrylic resins (Asar et al., 2013).

In the present study, the lower water sorption could be related to the use of long curing polymerisation (cycling for 6 hours in a water bath) to avoid any voids and obtain full polymerisation. Garcia et al., reported that high-temperature curing of acrylic resin increased the degree of conversion that led to an increase in crosslinking, resulting in reduced water sorption values (Garcia et al., 2010). Dogan et al., studied the effect of curing time of heat-cured resins on water sorption and concluded that longer curing times led to a reduction in residual monomer content and water sorption (Dogan et al., 1995). Wong et al., reported that the initial water content in the specimens of denture acrylic resin that were wet heat–cured was slightly lower than that of dry heat–cured (without water bath) (Wong et al., 1999) due to an increased degree of conversion or a reduced residual monomer content.

When the control group was compared with the groups containing ZrO_2, it was noted that reinforcement with zirconia nanoparticles led to a decrease in sorption values in DW and AS. The group containing 3wt% ZrO_2 showed the lowest value of sorption after storage in DW compared to the control group, even though the effect was not significantly different. However, the group with 10 wt.% of ZrO_2 stored in AS demonstrated significantly lower sorption values, followed by the groups with 5wt% and 3%wt of ZrO_2 when compared to the control group. Inorganic metal oxide fillers usually demonstrate high surface energy because of their hydrophilic nature. However, due to the difference in surface energies, the hydrophobic polymer does not wet or interact with the filler. It is therefore necessary to alter the surface of the fillers to improve wetting and adhesion at the filler-matrix interface (Asar et al., 2013), as well as to ensure even dispersion of the fillers throughout the polymer matrix (Santos et al., 2002). The decrease in sorption by the nanocomposites in this study may be related to the silane couple agent used for treating the zirconia surface to enhance the interfacial bonding between the zirconia and PMMA matrix. Polat et al., mentioned that denture base polymers reinforced with short glass fibres exhibited decreased water sorption and solubility. The reason for this decrease could be attributed to good bonding between glass fibres conditioned by silane coupling agent and the polymer matrix (Polat et al., 2003).

Other factors that could potentially influence the sorption and solubility of resin composites include storage media (Alshali et al., 2015), immersion period (Alshali et al., 2015), or filler loading (Lung et al., 2016). Water sorption into a polymer is a process when the water is being absorbed and at the same time the polymer material is diffused out (Al-Mulla et al., 1989). Water molecules can spread across polymer matrix due to of small size of the water molecule, the diameter of water molecule is less than 0.28nm, which is smaller than the polymer chain distance in polymer matrix (Polat et al., 2003).

In this study according to mass change as shown in Figure 6.1 and Figure 6.2, a general trend of gradual increase in mass change over the time was found and reached equilibrium state after 90 days. However, it is interesting to note that all for specimens stored in AS, the mean mass values dropped during 7 days and 14 days, whereas for DW no such trend was observed. The reason for a decrease in mass change values in AS during the first two weeks in our study could be related to AS, a stronger solvent, contains a mix of various salts and other additives compare to the DW and reacts with the specimen (Parker et al. 1997). Therefore, more monomers can come out from the specimens which leads to a decrease in mass and decrease in sorption in AS. Jagger et al., found a linear relationship between residual monomer and water sorption, which means as the residual monomer content in the specimens increased the water sorption also increased (Jagger, 1978). Dogan et al., have hypothesised that the residual monomer near the surface of the resin leaches into water, causing a decrease in polymer mass. If the residual monomer is not close to the surface of the specimen, rather entrapped in the inner layers of resin specimen, it cannot diffuse out into water after a short time (Dogan et al., 1995).

The highest mass change was observed for the control group and lowest for the group containing 10wt% zirconia for all of the test durations. This could be related to the fact that addition of zirconia fills the empty spaces in the PMMA resin and reduced sorption of saliva or mass change compared to the control group. Alsharif et al., who studied the effect of different ratios of filler loading on saliva sorption and solubility in resin composite, found that samples with higher filler loadings showed the lowest change in mass when compared to the unfilled resin. The explained this as a result of filler loading (Alsharif et al., 2013). In the current study, the changing of mass during long-term storage may be related to the release of residual monomer which is, at the same time, replaced with storage solution, leading to an increased sorption, particularly with the control group. However, the inclusion of ZrO_2 might reduce the amount of residual monomer in the nanocomposite composition, evidenced by less sorption in comparison to the control group.

The current study found that sorption in DW was higher than that in AS. When the water diffuses into the material it is pulled to the hydrophilic/water dissolvable sites and solution droplets are formed. The contrast in osmotic pressure between the inside solution droplet and the outside solution will result in an osmotic force to increase the sorption (Parker et al. 1997).

Ergun et al., investigated the effect of reinforcing conventional heat-cured PMMA with concentration of (5%, 10% and 20 wt%) zirconia nanoparticles on water sorption and solubility after 28 days. The findings showed that an increase in ZrO_2 concentration increased water sorption. This was explained by the weak polymer chains allowing water to permeate into the matrix and the increase in the nanoparticle filler concentration causing more nanoparticles filler-matrix particle interface (Ergun et al., 2018). Kundie et al., evaluated the effect of different ratios of nano and micro-alumina fillers on water sorption and solubility in denture base acrylic resin after 7 days. The reinforced samples showed slightly higher water sorption than the control group. The reason was attributed to the filler particle size and distribution and interfacial bond between the filler and the resin matrix (Kundie et al., 2018). Al-mulla et al., investigated the effect of HI acrylic resin, conventional heat-cured acrylic resin and other type of resin on sorption over 28 days storage in two types of artificial saliva and distilled water. They found that the HI resin had slightly less sorption in distilled water than that in artificial saliva, but not significantly. Whereas in conventional resin, sorption in distilled water was higher than that in the artificial saliva (Al-Mulla et al., 1989). The findings of these previous studies contradict with the results obtained in the present study, in which all groups containing (1.5%, 3%, 5%, 7%, 10 wt %) zirconia exhibited lower sorption values compared to the control group in both storage media.

Solubility represents the mass of the materials dissolved from the polymer. The only soluble materials present in denture base resins are residual or unreacted monomers, plasticizers and initiators that are most likely leached over the immersion time (Arikan et al., 2005). This study showed that the lowest mean value of solubility was found for the group containing 3 wt% of ZrO_2 stored in AS (-3.03 ± 0.95 µg/mm^3), whereas the mean value of the control group was -2.32 ± 0.89 µg/mm^3, both of which were lower than the British Standard (EN ISO) specification No. 20795 (solubility value should not exceed 1.6 µg/mm^3 for heat-cured acrylic resin). However, the groups stored in DW had higher solubility compared to the groups stored in AS and the recommended value by the British Standard. The highest mean value of solubility was 8.01 ± 5.48 µg/mm^3 in the control group and lowest mean value of 3.78 ± 2.64 µg/mm^3 was for the group containing 3 wt% ZrO_2.

The solubility values obtained in this study for specimens stored in DW were higher than those reported in previous studies (Range from 0.03 to 2.68 µg/mm^3) (Arikan et al., 2005; Asar et al., 2013; Machado Cucci et al., 1998; Miettinen and Vallittu, 1997; Pfeiffer and Rosenbauer, 2004). However, specimens stored in AS showed lower solubility values compared to the earlier mentioned studies that evaluated the solubility of different types of acrylic resin (Arikan et al., 2005; Asar et al., 2013; Machado Cucci et al., 1998; Miettinen and Vallittu, 1997; Pfeiffer and Rosenbauer, 2004). This difference in values could be attributed to the amount of water sorption over a long time being high enough to offset the mass lost by the diffusion of residual monomer (Dogan et al., 1995). In addition, Silva et al., highlighted that an increase in the amount of water absorbed could lead to an increase in the capacity for dissolution (Silva et al., 2008). Pfeiffer et al., reported that water sorption and solubility of polymers depended on the homogeneity of the material. The more homogeneous a material is, the less water it absorbs and the less soluble it is (Pfeiffer and Rosenbauer, 2004). In the present study, this might be the reason for higher solubility in DW compared to that in the artificial saliva.

In this study, there was a significant difference in colour stability of HI PMMA nanocomposites with different concentrations of ZrO_2 when stored in different storage media, therefore the third hypothesis was rejected. The colour changes of all experimental groups increased as the storage time increased. In addition, specimens stored in STD and MIL cleaners showed more colour change than those stored in DW (Figure 6.6). The control group exhibited less colour change (ΔE) after 180 days storage in cleaners, whereas groups containing 1.5 wt% and 3wt % of ZrO_2 demonstrated clinically acceptable colour change, the group containing 5wt% of ZrO_2 showed colour change slightly above the clinically acceptable value, and the groups containing 7wt% and 10wt% of ZrO_2 showed colour change above the clinically accepted values (Figure 6.7).

It was interesting to investigate the difference in colour change (ΔE) as result of the addition zirconia nanoparticles to HI heat-polymerized denture base acrylic resin. When specimens stored in distilled water at 7 days were compared with baseline data, the finding showed that there were slight changes in colour values between the groups containing zirconia and the control group (without ZrO_2) (Table 6.8). As the concentration of ZrO_2 increased colour change increased, however, these changes were clinically acceptable according to NBS. Therefore, the combined effect of the cleaning solutions and concentration of ZrO_2 nanoparticles could be accounted for the colour change in the nanocomposite specimens.

No identical studies are available in the literature for direct comparison with the present study. However, a similar study was reported by Davi et al., who evaluated the colour stability of microwave polymerised acrylic resin immersion in different percentages of sodium hypochlorite (0.5% and 1%), Clorox/Calgon and water after 180 days. They reported significant colour change with 1% of sodium hypochlorite cleaner, whereas Clorox/Calgon and 0.5% of sodium hypochlorite produced no whitening effect. It was explained that the concentration of sodium hypochlorite and length of immersion could have affected the colour change (Davi et al., 2010). Hong et al., found that colour change in acrylic resins increased with immersion time and was caused by monomer leaching out and water being absorbed (Hong et al., 2009). Another study by Peracini et al., investigated the colour stability of heat-cured denture base acrylic resins following immersion in effervescent denture cleaners (Corega tabs and Bony Plus), over 180 days. Although, a higher colour change (ΔE) was measured for the both cleaners, the differences were clinically insignificant (Peracini et al., 2010). In addition, Goiato et al., reported significant colour change (ΔE) of denture base acrylic resins after immersing for 60 days in Efferdent, 4% chlorhexidine and 1% hypochlorite; however, all values were within clinically acceptable parameters (Goiato et al., 2013a). The findings of the current study are in agreement with the aforementioned studies as the colour change values obtained from the control group storage in MIL (sodium hypochlorite 2%) and STD after 180 days provided similar results. However, groups containing ZrO_2 showed higher colour change (ΔE) values for both cleaners.

Polyzois et al., evaluated the effect of water, peroxide and hypochlorite (5.25 %) cleaners on gloss, colour and sorption of pink acetal and thermoplastic acrylic resins after 100 days immersion. They found the highest colour change (ΔE) for the resin after storage in water was 7.64, whereas in in hypochlorite it was 26.54, which was clinically unacceptable (Polyzois et al., 2013). This is in disagreement with the present study where the highest value of colour change was measured as 1.82 (storage in water) for the group containing 10 wt% ZrO_2 and was clinically acceptable. However, storage in MIL for 180 days resulted a colour change value (ΔE) of 6.07, which was clinically unacceptable and in agreement with Polyzois study.

Colour and gloss are important determiners of the aesthetics of dentures, whereby changes in colour and gloss are indicators of the degradation of the denture base material (Polychronakis et al., 2015). The increase of the colour change (ΔE) values suggested loss of surface gloss (Altıncı and Durkaya, 2016). It has been reported that a smooth surface prevents the formation of discolouring films, affects plaque formation and facilitates its removal (Polyzois et al., 2013). The composition of the acrylic resin and built-up substances can also influence the colour stability, especially if the surface roughness is higher (Goiato et al., 2017). Polychronakis et al., (2015) evaluated the influence of denture cleaners on colour, surface roughness and gloss of nylon and heat polymerized acrylic denture base resins before and after 30 days of immersion. The finding showed that the surface roughness, gloss and colour were affected in both types of dentures (Polychronakis et al., 2015). This is in agreement with our finding that groups containing 5 wt%, 7 wt% and 10 wt% of ZrO_2 (Figure 6.7) showed higher colour change (ΔE) after 180 days storage in cleaners compared to the control group. Even though gloss was not measured in this study, it could be assumed that this change in colour could affect the gloss layer on the specimen surfaces.

Goiato et al., found that the release of monomer during storage could interact with the glaze layer and cause increased colour change (Goiato et al., 2017). In addition, residual monomer can react with pigments inside the polymer, causing further colour changes (Rad et al., 2017). Goiato et al., evaluated the effect of the addition of nanoparticle pigmentation (3% and 7%) on the colour stability of acrylic resin immersed in water. They reported that the addition of pigments reduced colour change (ΔE) and that the lowest colour change value was found with samples of 7% pigmentation (Goiato et al., 2013b). In our study, the control group showed lowest colour change (ΔE) in all three-storage media in contrast to the groups containing ZrO_2. This could be related to change of pigment in the control group as an increase of ZrO_2 concentration could gradually replace the pigment and increase the colour change.

The effect of high colour change appeared as whitening or bleaching in some areas on specimen surfaces (Figure 6.6). In the current study, a possible explanation for these results, especially when stored in denture cleaners over time, may be related to sodium hypochlorite in the composition of MIL, which has been reported to cause bleaching of acrylic resin in Goiate study (Goiato et al., 2013a). Moreover, Me Neme et al., assessed the effect of sodium hypochlorite 1% and other cleaners over time from 15 minutes to 72 hours on the colour stability of denture base acrylic resins. They reported colour change (ΔE) after 2 hours and bleaching was noticed after immersing for 72 hours (McNeme et al., 1991). Several authors reported that peroxide-type denture cleaners include an effervescent component such as sodium perborate or sodium bicarbonate. When effervescent tablets dissolve in water, the sodium perborate readily decomposes to form an alkaline peroxide solution (Hong et al., 2009; Peracini et al., 2010). The alkaline peroxide solution reduces surface tension and agents such as sodium perborate release oxygen from the solution (Ozyilmaz and Akin, 2019). Through reduction, these free radicals convert larger molecules into smaller ones (Durkan et al., 2013), which influences both mechanical and chemical cleaning (Ozyilmaz and Akin, 2019). Other researchers mentioned that denture cleaners could affect denture acrylic resins after a period of storage and caused whitening or bleaching, loss of soluble components and monomer leaching out (Hong et al., 2009; Purnaveja et al., 1982; Saraç et al., 2007), while water absorption affected their physical properties (Jang et al., 2015). This could be an explanation for the results found in this investigation where the bleaching action was caused by peroxide content in STD and sodium hypochlorite in MIL. MIL showed higher colour change (ΔE) values than STD. It can also be noticed by visual inspection (Figure 6.6) that the most striking colour change was caused by addition ZrO_2 rather than the immersion in denture cleaners. With higher zirconia content a very pale pink/white colour was observed.

In the present study, micro porosity could be generated possibly due to overheating or inadequate pressure during polymerisation (Keyf and Etikan, 2004). A high amount of porosity will facilitate fluid transport in and out of the polymeric network, leading to increased water uptake and elution (Tuna et al., 2008), which over time could led to the colour change (ΔE) in the specimen groups.

To overcome the limitations of the current in-vitro study, further investigation should be designed to evaluate residual monomer, thermal expansion and gloss for HI PMMA nanocomposite denture base using artificial saliva to provide additional simulation of the oral environment more accurately. The specimen size should be increased to 10 specimens per group in order to obtain a better statistical distribution. To overcome the colour change of HI PMMA denture base materials (pale pink/white) due to the addition zirconia, natural biocompatible colour pigments can be added to improve the aesthetic.

6.6. CLINICAL IMPLICATIONS

The HI PMMA nanocomposite denture base impregnated with 3 wt% of zirconia had improved physical properties through reducing sorption and solubility and maintaining acceptable colour stability for a long period of time (180 days). This nanocomposite will have the potential to replace traditional PMMA with increased clinical life of artificial denture.

6.7. CONCLUSION

Within the limitations of this *in vitro* study, the following conclusions can be drawn:

HI PMMA resin reinforced with zirconia nanoparticles with a range of concentrations (1.5wt%, 3wt%, 5wt%, 7 wt% and 10wt%) showed lower sorption compared to the control group (0wt% zirconia) in both distilled water (DW) and artificial saliva (AS) for up to 90 days but not statistically significant. With 3 wt% of ZrO_2 exhibited the lowest water sorption compared to the control group. On the other hand, in saliva sorption, the nanocomposite with 10wt% of ZrO_2 showed lowest sorption.

All nanocomposite groups in DW and the groups with 1.5 wt% and 3.0 wt% zirconia in AS showed lower solubility than the control group after 180 days of storage but not statistically significant. However, the group with 3 wt% of ZrO_2 demonstrated lowest solubility in water and saliva storage. However, the nanocomposite with 10 wt% of ZrO_2 showed significantly higher solubility in AS compared to the control group.

Colour changes were affected by denture cleaners (Steradent (STD) and Milton (MIL) over time for all experimental groups, the highest colour changes observed in the groups with 7 wt% and 10 wt% of ZrO_2 immersed in MIL, followed by STD after 180 days. Based on NBS unit, all groups in DW, and the groups including control and 1.5 wt% and 3 wt% of ZrO_2 in denture cleaners were clinically acceptable. However, the groups with 5 wt%, 7 wt% and 10 wt% ZrO_2 were unacceptable for cleaning with STD and MIL.

Chapter 7: Polishability of Zirconia Impregnated PMMA Nanocomposite

7.1. ABSTRACT

Statement of problem. The surface of denture base materials may lead to the accumulation of microorganisms and plaque formation. Therefore, the nature of the surface of these base materials may be important in improving the aesthetics and cleansabilty of these devices.

Purpose. The purpose of this study was to evaluate the effect of polishing times on the surface roughness of high-impact heat-polymerized denture base acrylic resin (HI PMMA) impregnated with zirconia nanoparticles (nanocomposite).

Materials and Methods. Thirty specimens (25 ± 0.50 mm in diameter and 2 ± 0.10 mm thickness) were fabricated from high-impact heat-polymerized acrylic resin (HI PMMA) impregnated with different concentrations of zirconia nanoparticles (0 wt.%, 1.5 wt.%, 3 wt.%, 5 wt.%, 7 wt.%, and 10 wt.%). Specimens were divided into six groups ($n = 5$) and surface roughness (Ra) was measured with a profilometer before polishing and after polishing for one minute and two minutes. Data were analysed with Kruskal–Wallis and Friedman’s two-way analysis of variance tests to identify any statistical significance.

Results. Median surface roughness (Ra) values showed no significant difference between the groups before polishing. However, after polishing for one minute, the first four nanocomposite groups (1.5 wt.% to 7 wt.%) (0.12 ± 0.05, 0.11 ± 0.01, 0.13 ± 0.04, 0.16 ± 0.04 µm) did not show any significant difference in surface finish compared to the control group (0.11 ± 0.01 µm) except the group with 10 wt.% zirconia (0.17 ± 0.03 µm) which showed a significant increase. The group containing 3 wt. % (0.10 ± 0.01 µm) of zirconia showed the lowest Ra value among all the groups. Increase in polishing time slightly reduced Ra for the nanocomposite groups with high zirconia concentrations (7 wt.% to 10 wt.%) but not significantly.

Conclusion. Addition of zirconia in PMMA at low concentrations (1.5 wt.%, 3 wt.% and 5 wt.%) did not affect the surface finish negatively after conventional polishing of the denture base material and remained below the clinically acceptable limit (0.2 µm).

7.2. INTRODUCTION

Poly methyl methacrylate (PMMA) acrylic resin has been accepted as the most common denture base material (Al-Dwairi et al., 2019; Cierech et al., 2016; Consani et al., 2016; Moussa et al., 2016; Onwubu et al., 2018; Santos et al., 2013; Sofya et al., 2017). In recent years, acrylics such as PMMA modified by adding rubber compound to improve have shown improved strength (Abdulwahhab, 2013). They have been successfully used for denture bases, for removable partial or complete dentures (Kuhar and Funduk, 2005), implant overdentures, and maxillofacial prosthesis (Kim et al., 2009) because of the ease of processing (Vojdani et al., 2012). Dentures are used to protect lost tissues or residual alveolar ridges and transfer masticatory forces from dentures to residual ridges (Kim et al., 2009; Kuhar and Funduk, 2005).

A well-polished and smooth surface is a fundamental requirement for successful dental prostheses in order to achieve ideal aesthetics and oral hygiene (Gungor et al., 2014). Surface roughness (Ra) measures waviness and/or irregularity present on the surface on an object (Sofya et al., 2017). The surface roughness (Ra) of denture base resins affects staining, patient comfort and aesthetics (Al-Harbi et al., 2019; Alp et al., 2019). Several studies have demonstrated that a rough denture base surface promotes adhesion of bacteria and plaque formation compared to a smooth surface (Ayaz et al., 2014; Izumida et al., 2011; Kuhar and Funduk, 2005; Ozyilmaz and Akin, 2019). These microorganisms can only survive in the oral environment if they can attach to the surfaces (Hiramatsu et al., 2011), which may cause fungal infections (Ozyegin et al., 2012) as well as caries and periodontal infections (Ergun et al., 2018). In addition, the presence of microorganisms in the oral cavity presents a significant risk of respiratory tract infections particularly for elderly people (Machado et al., 2009).

The surface roughness of denture base materials depends on material structures, polishing techniques, reinforcement, polymerisation time and dental hygiene habits of users (Al-Harbi et al., 2019; Alp et al., 2019). Therefore, a smooth and highly polished denture resin surface is vital for maintenance of oral health (Onwubu et al., 2018). Improper finishing and polishing can result in increased wear rates and plaque formation on the denture surface (Reis et al., 2003). Dental technicians should use effective techniques for polishing acrylic resin denture bases (Kuhar and Funduk, 2005). The initial finishing procedure should include pre-polishing with water and a pumice slurry, followed by high-shine polishing compound or silicone polishers, and finally with fine polishing using polishing paste or liquid polish that contains fine aluminum oxide particles (Berger et al., 2006;

Kuhar and Funduk, 2005). Various in vivo studies have recommended that the surface roughness of denture prostheses should not exceed 0.2 µm in order to decrease plaque accumulation and colonisation of microorganisms (Al-Dwairi et al., 2019; Al-Harbi et al., 2019; Alp et al., 2019; Kuhar and Funduk, 2005).

Oliveira et al. reported that the mechanical polishing was more effective than chemical polishing in reducing surface roughness of PMMA denture bases. However, surface roughness was also influenced by dental brushing procedures (Oliveira et al., 2008). Gungor et al. (Gungor et al., 2014) and Kuhar et al. (Kuhar and Funduk, 2005) found that conventional laboratory polishing resulted in smoother denture surface, and thereby achieving higher clinical quality of dental prostheses, than polishing with chairside kits. Abuzar et al. (Abuzar et al., 2010) demonstrated that the surface of PMMA resin for denture base were 20 times smoother than polyamide after polishing. It has been observed that some disinfectant solutions increase the roughness of acrylic resin surface after immersion for 7 days (Machado et al., 2009). Gad et al. (Gad et al., 2018b) evaluated surface roughness (Ra) of glass-fibre-reinforced PMMA denture base resins using autoclave polymerisation and they found that the addition of glass fibres increased roughness.

The development of nanomaterials has led to significant improvements in dental composites. This technology produces a smoother surface with higher translucency and polishability (Rahim et al., 2011). A study conducted by Fouda et al. (Fouda et al., 2019) found that the addition of nanodiamonds to PMMA acrylic denture base resin significantly decreased surface roughness, with the lowest values observed at a nanodiamond concentration between 0.5% and 1.0 wt. %. However, the incorporation of silica and prepolymer nanoparticles (1% and 5 wt. %) to PMMA denture base resin increased surface roughness (Cevik and Yildirim-Bicer, 2018).

In recent years, studies have investigated mechanical and physical properties of nanocomposite made of conventional heat-cured denture base acrylic resin reinforced by zirconia nanoparticles. The properties of the nanocomposite depend on the type of nanoparticles incorporated; their size and shape; as well as the concentration and interaction with the polymer matrix (Ergun et al., 2018). There are no data available in the literature regarding the effect on surface roughness of the addition of zirconia nanoparticles to HI PMMA denture base acrylic resin. The present *in vitro* study evaluated the effect of polishing times on HI PMMA reinforced with zirconia nanoparticles (0%, 1.5%, 3%, 5%, 7%, and 10 wt. %) by measuring their surface roughness. The research hypothesis assumed that there would be no significant difference in surface roughness between HI PMMA specimens (control) and HI PMMA zirconia nanocomposites after polishing. Also, it was assumed that increase in polishing time (one-minute and two minute) makes no difference in reducing surface roughness.

7.3. MATERIALS AND EXPERIMENTAL METHOD

7.3.1. Materials

A commercially available denture base powder, Metrocryl HI (PMMA, poly-methyl methacrylate), and Metrocryl HI (X-Linked) denture base liquid (MMA, methyl methacrylate) (Metrodent Limited, Huddersfield, UK) were selected as the denture base material. Yttria-stabilized zirconia (ZrO_2) nanoparticles (Sky Spring Nano Materials Inc., Houston, TX, USA) was chosen as the inorganic filler agent for fabricating nanocomposite specimens for denture base as shown in Table 7.1.

Table 7.1. Materials used in making PMMA-zirconia nanocomposites

Materials	Trade name	Manufacturer	Lot. Number
High impact heat-curing acrylic denture base resin	HI Metrocryl	Metrodent Limited, Huddersfield, UK	Powder (22828) Liquid (103/4)
Yttria-stabilized zirconium oxide	Zirconium oxide	Sky Spring Nano Materials, Inc, Houston, TX, USA	8522-120315

7.3.2. Preparation of Specimens

7.3.2.1. Silanisation process and proportioning of zirconia nanoparticles

Silane functionalization of zirconia nanoparticle surfaces was carried out according to a procedure described earlier (Zidan et al., 2019). According to a previous study (Zidan et al., 2019), the most appropriate weight percentages of zirconia nanoparticles used in this study were 0.0% (control), 1.5 wt.%, 3.0 wt.%, 5.0 wt.%, 7.0 wt.% and 10.0 wt.%.

7.3.2.2. Mixing HI PMMA and zirconia nanoparticles

The composition details of the silane-treated and non-silane zirconia and acrylic resin powders were weighed according to Table 7.2 using an electronic balance (Ohaus

Analytical plus, Ohaus Corporation, USA). The zirconia powder was added to the acrylic resin monomer and mixed by hand using a stainless-steel spatula to ensure all the powder was uniformly distributed within the resin monomer and to avoid any aggregation. The HI acrylic resin powder was then added to the liquid, and mixing continued until a consistent mixture was obtained, according to the manufacturer's instructions. When the mixture reached a dough-like stage that was suitable for handling, it was packed into a mould by hand. The mould was then closed and placed in a hydraulic press (Sirio P400/13045) under a pressure of 15 MPa and then excess mixture was removed from the periphery of the mould. The mould was immersed in curing bath for 6 hours polymerisation at temperature 95°C, and then the mould was removed from the curing bath and cooled slowly for 30 min at room temperature. The mould was then opened, and the specimens were removed. The specimens were then trimmed using a tungsten carbide bur, ground with an emery paper and polished with pumice powder in a polishing machine (Tavom, UK).

Table 7.2. Weight percent of zirconia in combination with acrylic resin powder as well as monomer content in the specimen groups

Experimental Groups	**Zirconia (wt. %)**	**Zirconia (g)**	**HI PMMA powder (g)**	**HI MMA monomer (ml)**
Control	0.0	0.000	21.000	10.0
1.5	1.5	0.315	20.685	10.0
3.0	3.0	0.630	20.370	10.0
5.0	5.0	1.050	19.950	10.0
7.0	7.0	1.470	19.530	10.0
10.0	10.0	2.100	18.900	10.0

7.3.2.3. Specimens surface polishing

Surface roughness of the specimens was measured with and without polishing. All polishing was carried out in conformance with the British Standard Specification for denture base polymers (BS EN ISO 1567; 2000) (Standard, 2000). The dimensions were 25 ± 1.0 mm (Diameter) × 2 ± 0.10 mm (Thickness). Specimens were polished for one minute; the surface roughness was measured and then polished further for another minute (two minutes in total) to achieve a highly smooth surface. The roughness was then measured again. A total of 30 specimens were prepared in this study, five for each experiment group as per Table 7.2.

The surface preparation started with grinding by a diamond bur and then with a tungsten carbide bur (Dental Sky, UK) at a speed of 1500 rpm to remove any excess acrylic on the surface. Surface roughness was then measured. The first step of all surface polishing was carried out by a lathe bristle brush using slurry of pumice at the same speed for one minute. The specimen surfaces were subjected to a second stage polishing with a muslin buff wheel using primary polishing compound (Chaperlin & Jacobs Ltd, UK) at the same speed for one minute. The third stage of polishing was carried out with a muslin buff wheel using fine polishing compound (secondary) at a slower speed of 500 rpm. After polishing, all the specimens were washed by water and dried to make them ready for surface roughness measurement. After measurement was taken, specimens underwent the polishing cycle a second time and the final measurement was taken. Figure 7.1 shows the specimens from different groups after polishing for two-minutes.

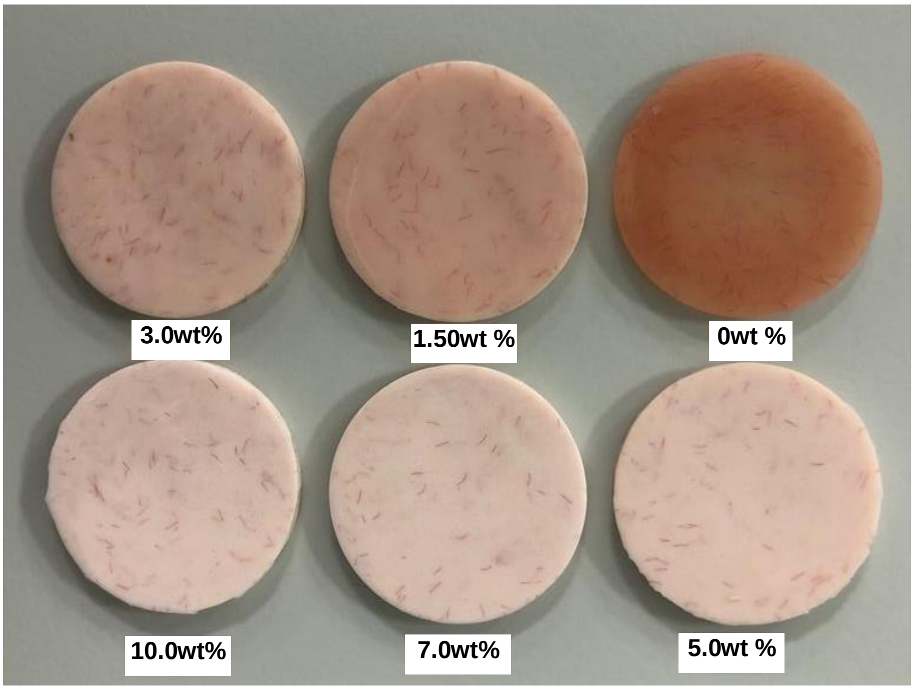

Figure 7.1. Photograph demonstrating specimens with different wt.% of zirconia in HI PMMA acrylic resin after polishing for two minutes.

7.3.3. Surface roughness measurements

Surface roughness for all specimen groups was measured by using a non-contact high-resolution measurement profilometer (Talysurf CLI 1000, Ametek Taylor Hobson Precision, Leicester, UK) (Figure 7.2. Photograph demonstrating the surface profile measurement of the denture base specimens with Talysurf CLI 1000 surface profiling system.). The surface roughness (Ra) was measured by placing the specimen over a flat surface above the cross-slides of the instrument and scanning by applying a beam of white light through a lens with a chromatic length aberration (CLA 300 µm gauge) focussing on the area of surface measured (1 mm × 1 mm) with 0.25 mm cut-off length. The mode of measurement was bi-directional with a sampling rate of 500 Hz and a maximum spacing of 1 µm. Three measurements of surface roughness were completed for each specimen. The surface roughness results were analysed by TalyMap software (Ametek Taylor Hobson Precision, Leicester, UK) to create 2D and 3D surface profiles. Average roughness values of specimens for each group were calculated and used for statistical analysis (Precision, 2009).

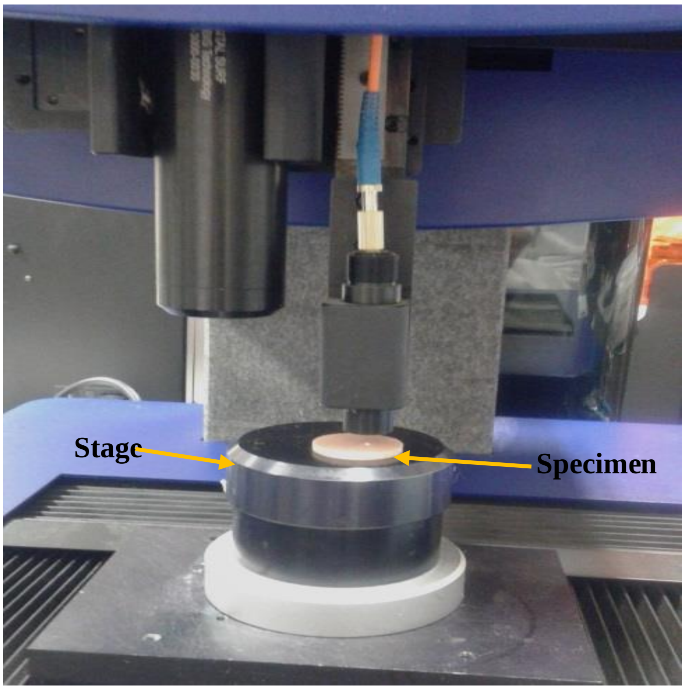

Figure 7.2. Photograph demonstrating the surface profile measurement of the denture base specimens with Talysurf CLI 1000 surface profiling system.

7.3.4. Imaging of particle surface morphology

The size and shape distribution of the PMMA powder and zirconia nanoparticles was analysed using a scanning electron microscope (SEM) (Carl Zeiss Ltd, 40 VP, Smart SEM, Cambridge, UK). In addition, the surfaces of the unpolished and polished specimens were characterised using a scanning electron microscope (SEM). Specimens from each group were mounted onto slotted aluminium stubs that were placed into a numbered specimen holder and loaded into the SEM for imaging using a secondary electron detector at an acceleration voltage of 2.0 kV and a magnification of ×25k.

7.3.5. Statistical analyses

The recorded results of the surface roughness values for different specimens were statistically analysed using a statistical software (SPSS 23, IBM, New York, NY, USA). Shapiro-Wilk test showed that the data of surface roughness test was not normally distributed. Therefore, Kruskal–Wallis test was used to analyse the results from the test groups at a pre-set alpha value of 0.05. In addition, Friedman’s two-way analysis of variance test was conducted to identify any significant difference between the polished and unpolished surface roughness ($p < 0.05$).

7.4. RESULTS

7.4.1. Analysis of surface roughness

There was no significant difference ($P > 0.05$) in surface roughness (Ra) between the nanocomposite specimen groups and the control group without polishing. Again, without polishing, the groups containing 3 wt.% (0.29 ± 0.08 µm) and 5 wt. % (0.27 ± 0.21 µm) of zirconia showed lowest roughness compared to the control group (0.40 ± 0.14). In addition, mean values of surface roughness presented in (Sa) were shown the groups containing 3% and 5 wt.% lowest roughness after both polishing times. All surface roughness measurements are presented in Table 7.3 (2D), Table 7.4 (3D) and Figure 7.3 (2D).

Table 7.3. 2D Surface roughness values for different denture base materials before and after polishing at different polishing times

Experimental Groups	**Surface roughness Ra (µm)**		
	Without polishing	Polishing for 1 min	Polishing for 2 min
	Median (IQR)	Median (IQR)	Median (IQR)
0.0 wt.% (Control)	0.40 (0.14) ^{A,a}	0.11 (0.01) ^{A,b}	0.12 (0.03)$^{A, B,a,b}$
1.5 wt.%	0.31 (0.10) ^{A,a}	0.12 (0.05) ^{A,B,a}	0.12 (0.02) $^{A, a}$
3.0 wt.%	0.29 (0.08) ^{A,a}	0.11 (0.01) ^{A,b}	0.10 (0.02) ^{A,b}
5.0 wt.%	0.27 (0.21) ^{A,a}	0.13 (0.04) ^{A,B,b}	0.13 (0.02) ^{A,B,b}
7.0 wt.%	0.33 (0.21) ^{A,a}	0.16 (0.04) ^{A,B,a,b}	0.12 (0.04) ^{A,B,b}
10.0 wt.%	0.39 (0.14) ^{A,a}	0.17 (0.03) ^{B,a,b}	0.15 (0.01) ^{B,b}

Note: For each group, same uppercase letter within column represents no significant difference (P>0.05), while same lowercase letter within same row represents no significant difference (P> 0.05).

Table 7.4. 3D Surface roughness values for different denture base materials after polishing at different polishing times

Experimental Groups	**Surface roughness Sa (µm)**	
	Polishing for 1 min	Polishing for 2 min
	Mean (SD)	Mean (SD)
0.0 wt.% (Control)	5.27 (1.55)	7.25 (2.35)
1.5 wt.%	7.32 (1.51)	5.48 (2.55)
3.0 wt.%	3.92 (1.45)	4.78 (1.90)
5.0 wt.%	3.34 (1.69)	4.74 (2.18)
7.0 wt.%	7.23 (3.07)	5.50 (1.54)
10.0 wt.%	7.43 (3.03)	6.50 (1.19)

There was no significant difference in Ra values after one-minute polishing between the control group and the groups containing up to 7 wt. % of zirconia, but the control group showed significantly lower Ra value than the 10 wt.% group. However, among the nanocomposites, only 3 wt.% group showed significantly lower Ra value than the 10 wt.% group and equal Ra value of the control group with polishing for one-minute.

There was no significant difference in Ra values after two-minute polishing between the control group and the nanocomposite groups. The lowest surface roughness was recorded for the group containing 3 wt. % of zirconia (0.10 ± 0.02) after polishing for two-minute. This was significantly different ($P< 0.05$) from the 10 wt. % group (0.15 ± 0.01).

No significant difference was found between the polishing times for all groups. Overall, the nanocomposite groups showed a constant value or a decrease in surface roughness with an increase of polishing time. However, for the groups with 7 wt.% and 10 wt.% displayed slightly higher deceasing trend in the Ra values.

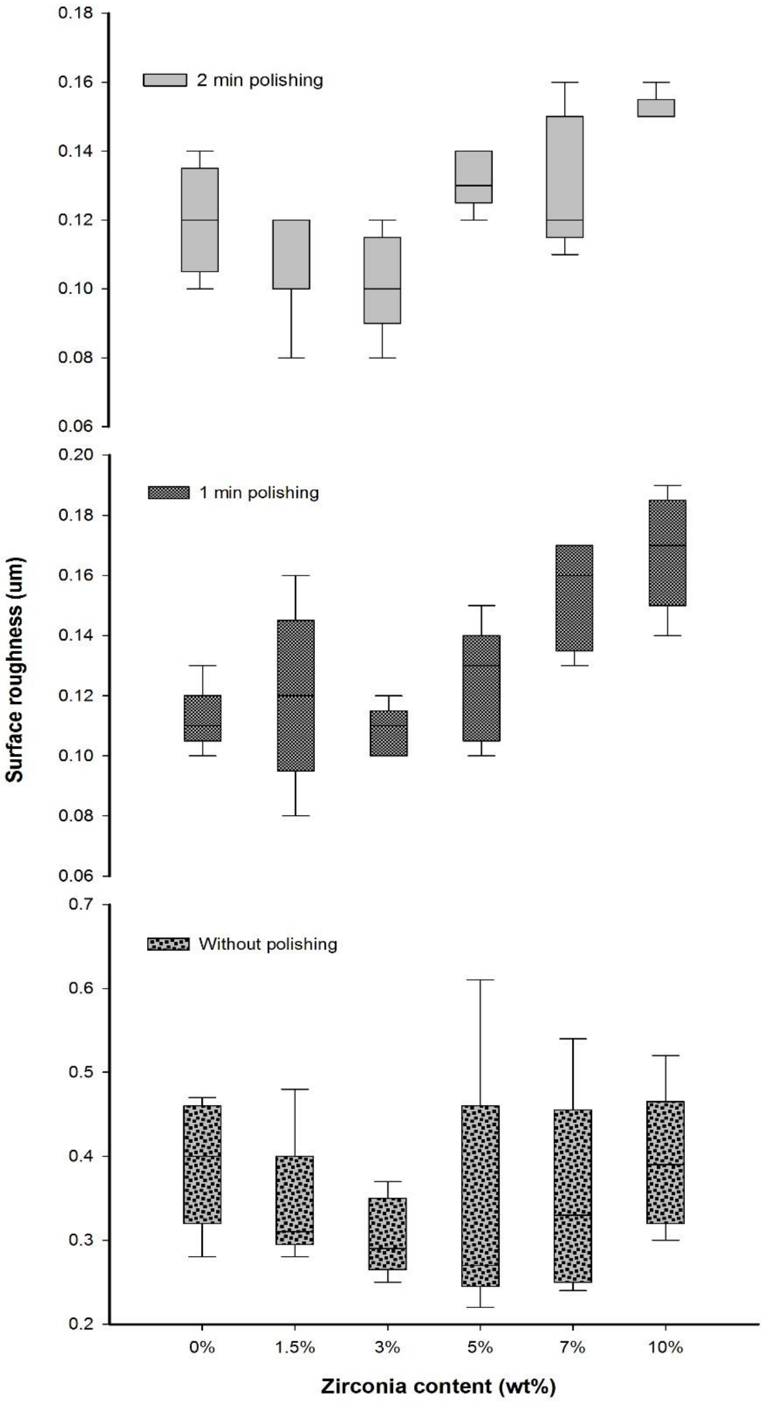

Figure 7.3. Box plot graph showing surface roughness of denture base materials before and after polishing (one and two minutes).

7.4.2. Particle surfaces analysis

SEM analysis revealed that the average particle size of the PMMA powder was approximately 50 µm with a range from 10 µm to 100 µm, as shown in Figure 7.4 A. The rubber particles were also visible within the powder, with an average size of approximately 50 µm. The as-received, yttria-stabilized zirconia nanoparticles demonstrated an average size ranging between 30 nm and 60 nm for individual particles and 200 nm to 300 nm for clusters, as shown in Figure 7.4 B.

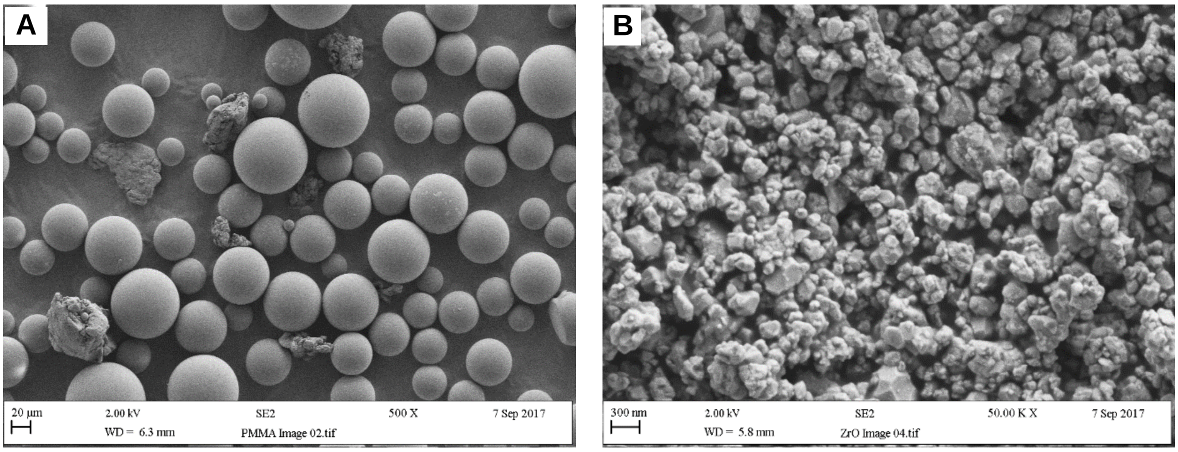

Figure 7.4. Particle surface morphologies of (A) PMMA and (B) Zirconia

Figure 7.5 and Figure 7.6 present 2D and 3D surface images for selected groups (0%, 3%, 5% and 10 wt. % of Zirconia) before and after polishing. The images show the colour bar representing the average surface roughness (Ra) values. The colour bar ranged from bottom with blue colour (darker shade) to top with red colour (lighter shade). The red colour demonstrated the high peaks of the rough surface, while the blue represented the valley depth and the interlinked colours in between showed areas between the peaks and valleys.

	0wt. %zirconia	3.0 wt. % zirconia
Before polishing	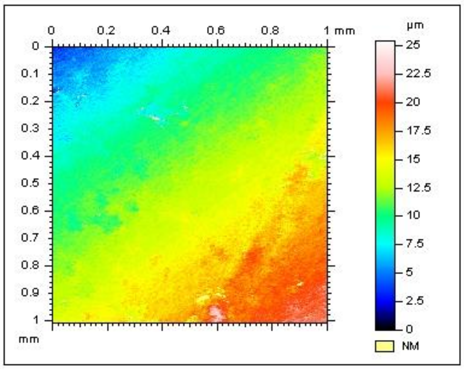	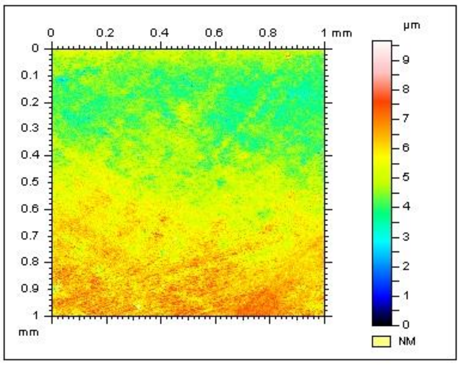
	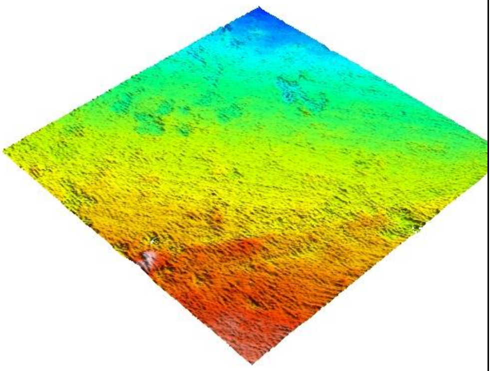	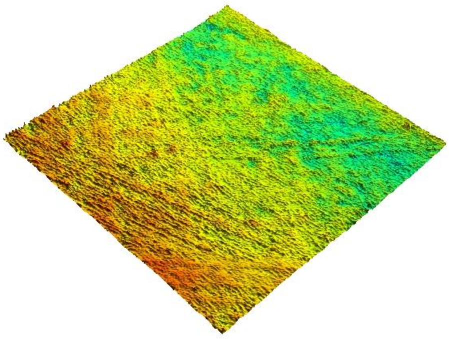
After Polishing	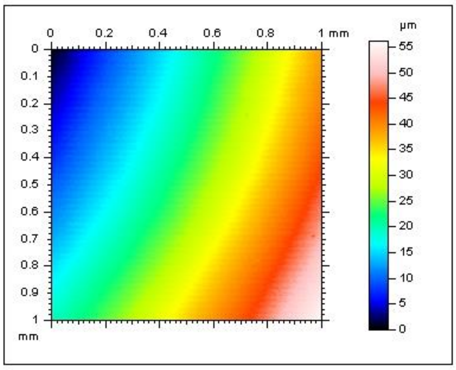	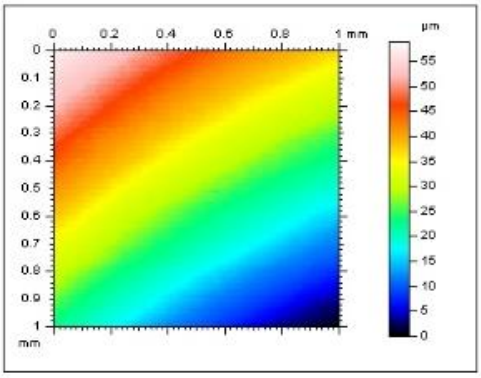
	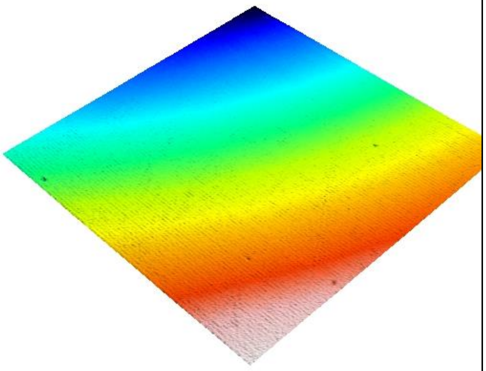	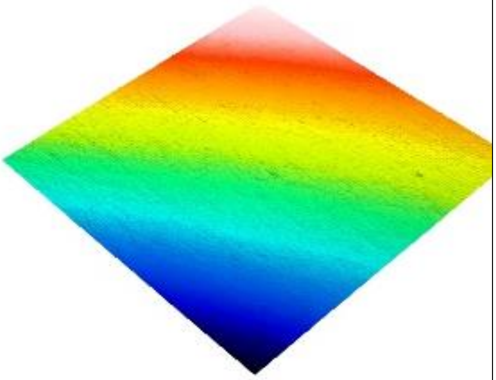

Figure 7.5. Representative 2D and 3D surface images for the tested specimens in groups containing 0 wt.% and 3 wt. % of zirconia before and after polishing

	5.0 wt. % zirconia	10.0 wt. % zirconia
Before polishing	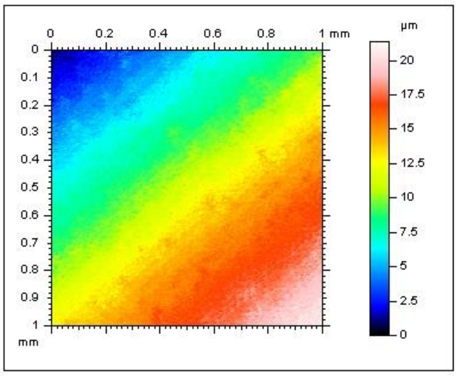	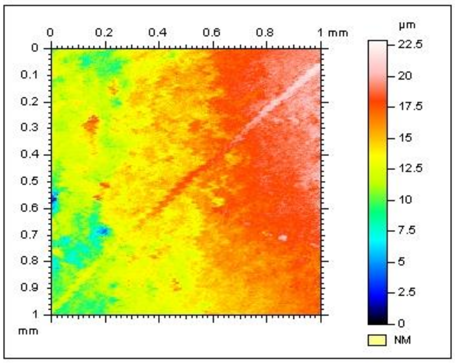
	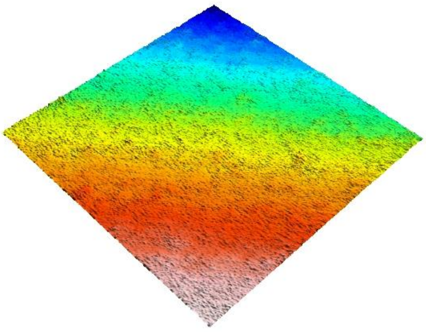	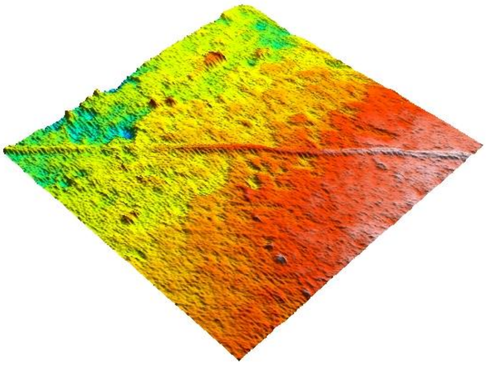
After Polishing	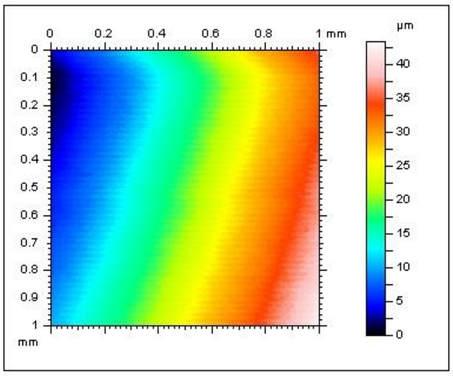	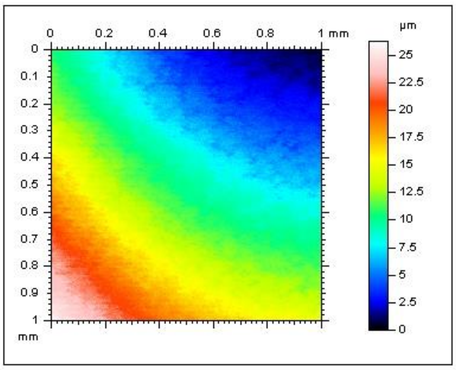
	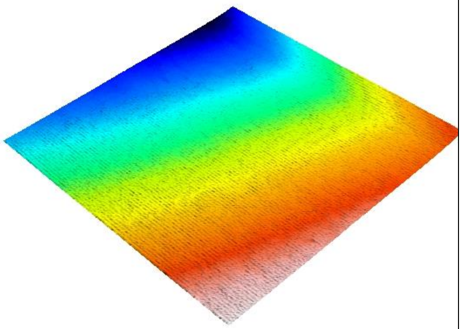	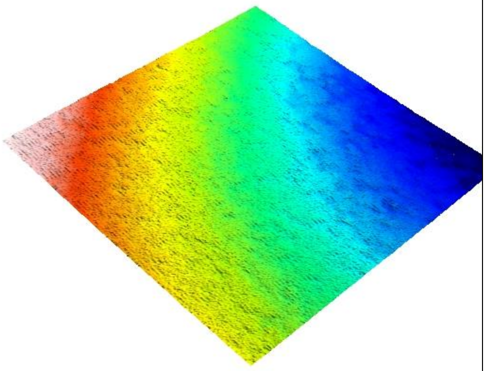

Figure 7.6. Representative 2D and 3D surface images for the tested specimens in groups containing 5 wt.% and 10 wt. % of zirconia before and after polishing

7.4.3. Specimen surfaces analysis

Figure 7.7 and Figure 7.8 present SEM micrographs of the specimen surfaces before and after polishing. Before polishing the particles of PMMA are visible on specimen surface in the control group with evidences of some micropores and a rougher surface while after polishing for one minute, surface roughness decreased with a few particles remaining on the surface. The 1.5 wt.% group showed tiny zirconia nanoparticles on the surface even after polishing. The groups containing 3 wt.% and 5 wt. % of zirconia showed a smooth surface with uniform distribution of particles after polishing. At higher zirconia concentrations (7 wt.% and 10 wt.%), rougher surface was noticed before polishing. However, after polishing the surface clearly showed indication of nanoparticle clustering particularly for the group with 10 wt. % of zirconia.

Specimen Groups	**Before polishing**	**After polishing**
0wt. % zirconia (Control group)	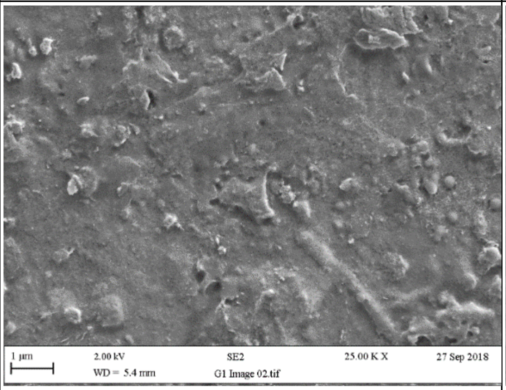	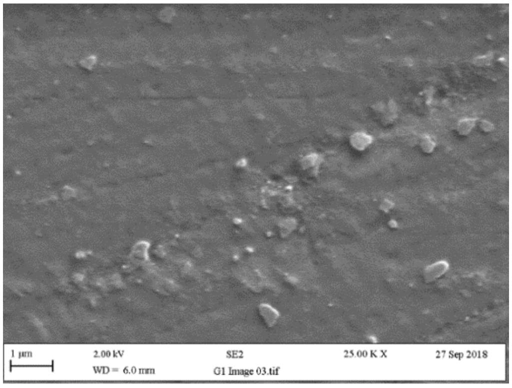
1.5 wt. % zirconia	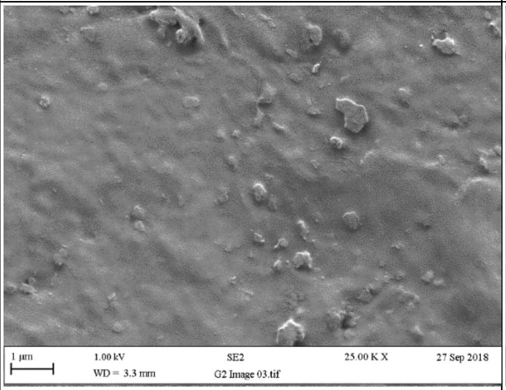	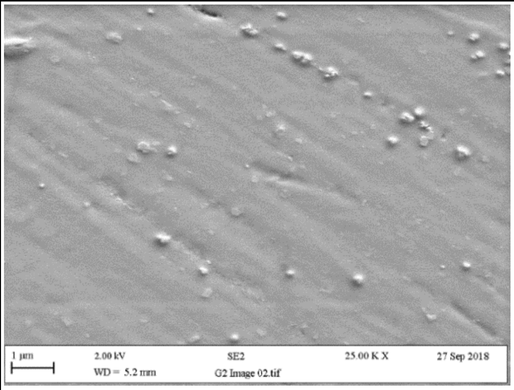
3.0 wt. % zirconia	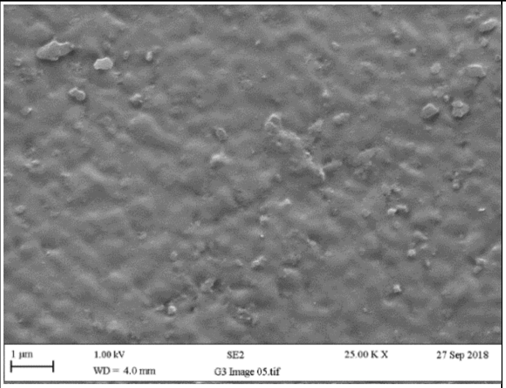	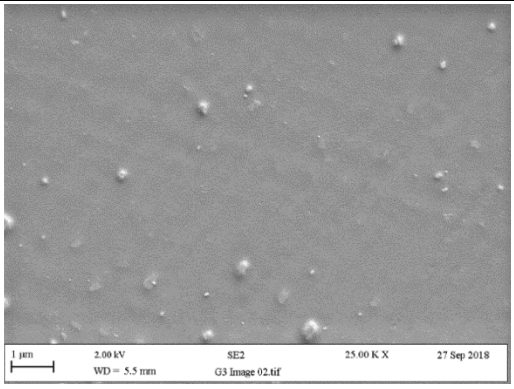

Figure 7.7. Representative SEM micrographs of the tested specimens in the groups containing (0 wt.%, 1.5 wt.% and 3 wt.% of zirconia) before and after polishing (two-minute).

Specimen Groups	Before polishing	After polishing
5.0 wt. % zirconia	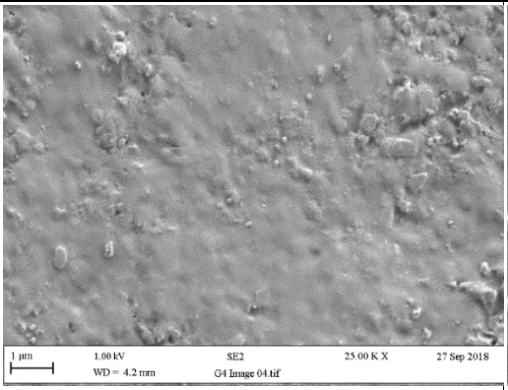	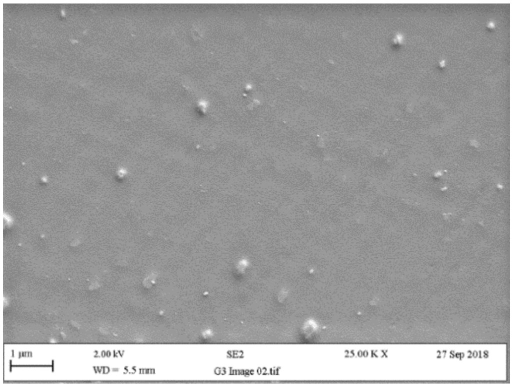
7.0 wt. % zirconia	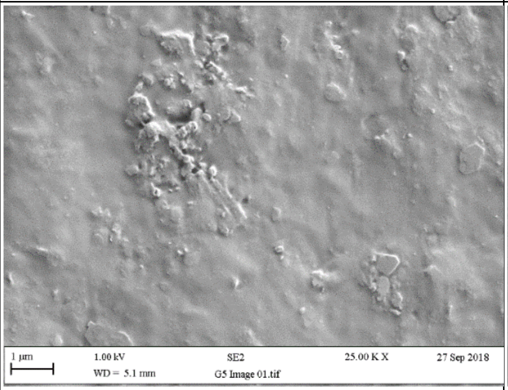	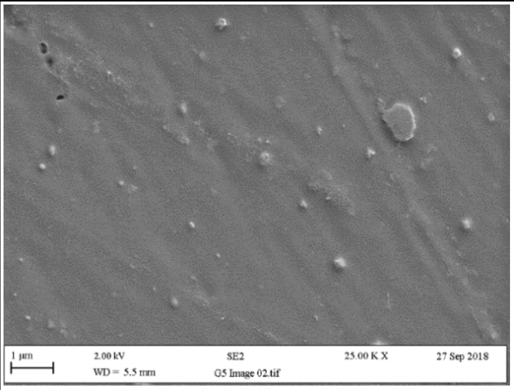
10.0 wt. % zirconia	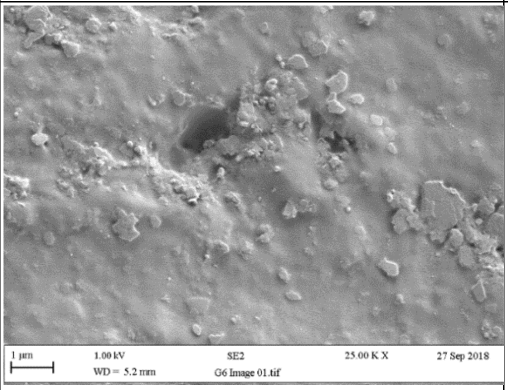	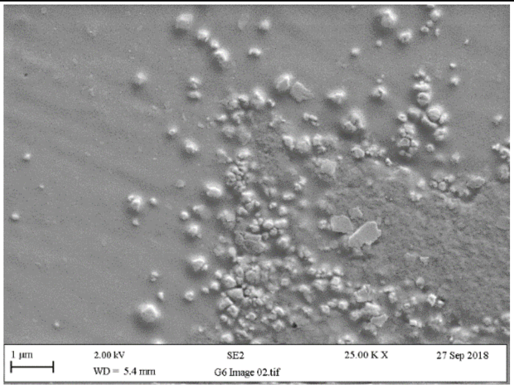

Figure 7.8. Representative SEM micrographs of the tested specimens in the groups containing (5 wt.%, 7 wt.% and 10 wt.% of zirconia) before and after polishing (two-minutes).

7.5. DISCUSSION

The first research hypothesis that there would be no significant difference in surface roughness (Ra) between HI PMMA (control) and HI PMMA zirconia nanocomposites was rejected as 10 wt.% group showed significant difference from the control group for both one-minute and two-minute polishing times. The second hypothesis was accepted, as the two different polishing times did not significantly affect Ra for all groups.

The nanocomposites specimens in all groups showed Ra higher than the clinically accepted value (0.2 µm) before polishing as evidenced by the measured values, surface profiles and SEM images. Without polishing, the highest Ra value was found in the control group whereas the group containing 5 wt.% zirconia showed the lowest value. These values could have been affected by the mould surface under the pressure of the hydraulic press machine during compression. Additionally, some degree of disintegration of the mould surface might have occurred when heated to a higher temperature during the curing process, (Abuzar et al., 2010).

It is highly doubtful that we can reasonably make direct comparisons of Ra values with other studies owing to the differences in experimental procedures, methodology used for polishing and surface roughness measuring techniques (Abuzar et al., 2010). The surface roughness values of acrylic resin from previous studies ranged from 0.03 µm to 1.06 µm, depending on the finishing and polishing techniques employed (Al-Harbi et al., 2019; Cevik and Yildirim-Bicer, 2018; Ergun et al., 2018; Fouda et al., 2019; Gungor et al., 2014; Kuhar and Funduk, 2005; Onwubu et al., 2018).

In the present study, all groups showed roughness values less than the clinically accepted level of 0.2 µm (Alp et al., 2019) with conventional polishing for both one minute and two minutes. After one-minute polishing, the median Ra values of the nanocomposites ranged from 0.11 µm (control group) to 0.11 µm (3 wt.% group) and then to 0.17 µm (10 wt.% group) which were all clinically acceptable (Al-Dwairi et al., 2019; Al-Harbi et al., 2019; Alp et al., 2019). At this level, the chances of various micro-organisms adhering on the surface of a denture would be minimised. An increase in polishing time up to 2 min, further decreased the Ra values for the groups containing 7 wt.% and 10 wt.% of zirconia, though not statistically significant. This indicated that at lower zirconia concentration (1.5 wt.% to 5 wt.%) increasing polishing time did not make any difference. At both polishing times, 3 wt.% group produced the best surface with lowest Ra value among all groups. Therefore, one-minute polishing would be sufficient to produce clinically acceptable level of Ra in the nanocomposites.

In a similar study by Ergun et al. (Ergun et al., 2018), the addition of nano-fillers (5 wt.%, 10 wt. % and 20 wt.% of zirconia) to conventional PMMA denture base acrylic resin demonstrated higher surface roughness (R_a) than that in the present study. The authors reported a significant increase with 20 wt. % of zirconia compared to the control group and the group with low concentration 5 wt. % of zirconia. Other studies showed results consistent with the present study such as those by Al-Harbi et al. (Al-Harbi et al., 2019) and Fouda et al. (Fouda et al., 2019) who evaluated the effect of adding nanodiamonds (NDs) on surface roughness at different concentrations (0.5 wt.%, 1.0 wt.% and 1.5 wt.%) to the conventional PMMA denture base acrylic resin. The finding showed that the use of nanodiamonds reduced Ra with the lowest value found in the 0.5 wt. % NDs and were also clinically acceptable. They reported that the reason for this reduction in surface roughness could be due to the use of small-size particles with a low concentration and a good distribution of nanoparticles within the resin matrix. In addition, the nanoparticles filled interspaces and pores in the polymeric chains leading to a smooth surface (Al-Harbi et al., 2019; Ergun et al., 2018; Fouda et al., 2019). In the current study, groups containing 1.5 wt.%, 3 wt.% and 5 wt.% of zirconia presented uniform distribution with a few nanoparticles appearing on the surface as seen in Figure 7.7 and Figure 7.8.

A possible explanation for the increase surface roughness (R_a) of the nanocomposite specimens with the group containing 10 wt.% of zirconia in our study could be related to the higher concentration of the nanoparticles added to the PMMA matrix causing a non-homogenous distribution. The nanoparticles had a strong tendency to aggregate due to the high specific surface area, surface energy and chemical activity (Ergun et al., 2018). In this study, the clustering of nanoparticles was evident particularly on the surface of 10 wt.% when compared to the groups containing lower zirconia concentrations as seen in SEM micrographs in Figure 7.8. The clustered particles on surface can be easily detached during finishing and polishing, leaving voids that could increase the surface roughness. (Al-Harbi et al., 2019). and (Gad et al., 2018b) also reported that the addition of glass fibre to PMMA acrylic resin increased Ra values as the glass fibre concentration was increased (2.5 wt.% and 5 wt.%) in all tested groups in comparison to the control group. The increase of surface roughness was explained by the random arrangement of the glass fibres at the surface and the possibility of glass fibre protruding from surface (Gad et al., 2018b).

In this study, the reduction in Ra values after polishing could be related to a combination of conventional polishing technique applied by using pumice followed by different high shine polishing compounds. Kuhar et al. (Kuhar and Funduk, 2005) reported the smoothest surface of denture base acrylic resin (Ra below 0.2 µm) was produced by conventional laboratory polishing methods. (Berger et al., 2006) and (Gungor et al., 2014) compared conventional polishing to three types of chairside polishing kits and recommended that conventional polishing method using pumice was the most effective method.

In all nanocomposites, either a reduction or no alteration in Ra values was observed for all the nanocomposite groups when polishing time increased from one to two minutes.

However, interestingly for the control group a slightly increased Ra value (by 0.01 µm) was found when the polishing time was increased. At longer polishing time, surface at slightly higher depth would appear with voids or unreacted bigger polymer particles that might slightly increase the Ra value. Furthermore, longer polishing time could generate more waviness on the surface, which could be responsible for the increased roughness.

The limitations of this study included number of specimens in each group (n = 5), which could be increased to ten specimens for obtaining better statistical distribution. Further research needs to be conducted to investigate the effect of oral environment such as artificial saliva and denture cleaners on the surface roughness, gloss and colour properties. Antimicrobial studies can also be conducted on optimisation of zirconia concentration to minimise the microbial activities on the surface.

7.6. CLINICAL IMPLICATIONS

Impregnation of HI PMMA denture base acrylic resin with low concentrations (1.5 wt.% to 5 wt.%) of zirconia nanoparticles does not negatively affect the surface finish. Addition of 3 wt.% zirconia in combination with conventional dental laboratory polishing techniques could produce the best surface finish within the limit of clinical acceptability among all the groups.

7.7. CONCLUSION

The polishability of the zirconia (ZrO_2) impregnated PMMA nanocomposites at five different concentrations (between 1.5 wt.% to 10 wt.%) were evaluated by measuring surface roughness (Ra) of the specimens at different polishing times (one-minute and two-minute). Within the limitations of this *in vitro* study, the following conclusions can be drawn:

Without polishing, pure PMMA (control) and the nanocomposites specimen groups showed surface roughness higher than the level of clinically acceptability and thus needs polishing. However, all the nanocomposites showed lower Ra than the control group.

All experimental groups demonstrated smooth surface (Ra<0.2µm) of clinical acceptability after one-minute and two-minute polishing.

Lower concentrations of zirconia (1.5, 3 and 5 wt. %) in PMMA providing the lowest roughness values similar to that of the control group are recommended to prevent significant propagation of microorganisms in the denture base nanocomposites.

A higher concentration of zirconia (10 wt.%) in PMMA could significantly increase the surface roughness compared to the control group and thus should be avoided.

For all experimental groups an increase in polishing time did not significantly reduce the surface roughness. However, for both polishing times, the nanocomposite with 3 wt. % of zirconia produced the best surface finish, which was same as or slightly better than that of the control group.

Chapter 8: Tensile Bond Strength between Denture Teeth and Zirconia Impregnated PMMA Nanocomposite

8.1. ABSTRACT

Statement of problem. Teeth debonding from acrylic dentures is a common problem in partial and complete removable prosthetics.

Purpose. This study evaluated tensile bond strength (TBS) between anterior acrylic teeth and denture bases made of high-impact heat-cured denture base acrylic resin (HI PMMA) impregnated with zirconia nanoparticles.

Materials and Methods: A total of 30 specimens (each specimen containing a set of six upper anterior teeth) were fabricated from HI PMMA denture base acrylic resin reinforced with different weight concentrations of zirconia nanoparticles: 0% (control), 1.5%, 3%, 5%, 7% and 10%. Specimens were divided into six groups according to the nanoparticle concentrations with each group containing five identical specimens. The specimens were immersed in distilled water for 7 days before tested with a universal testing machine (Hounsfield Tensometer, H10KS, Germany) according to a British standard (BS EN ISO 22112: 2017). Failure modes and mechanisms of the fractured specimens were observed visually under an optical microscope and scanning electron microscope. A One-Way analysis of variance (ANOVA) was employed with the Tukey significant difference post-hoc test at a pre-set alpha value of 0.05.

Results. TBS values between the anterior teeth (central and lateral incisor and canine) and HI-PMMA denture base groups containing 7 wt.% (261.5 N ± 66.0 SD, 172.5 N ± 57.4 SD and 271.9 N ± 86.3 SD) and 10 wt.% (332.1 N ± 122.9 SD, 165.4 N ± 48.7 SD and 301.6 N ± 73.2 SD) zirconia were significantly lower compared to the control group (645.4 N ± 84.8 SD, 306.1 N ± 81.6 SD and 496.7 N ± 179.1 SD). However, TBS values for HI PMMA with 1.5wt% (534.4 N ± 115.3 SD, 304.7 N ± 86.4 SD, 514.0 N ± 143.2 SD), 3wt% (685.7 N ± 159.6 SD, 281.1 N ± 78.3 SD, 462.6 N ± 122.1 SD) and 5wt% (514.5 N ± 134.3 SD, 229.8 N ± 67.3 SD, 387.2 N ± 99.4 SD) zirconia showed slightly lower values than that of PMMA with no zirconia. However, group containing 10wt.% of zirconia showed significantly difference ($p>0.05$) reduced the bonding strength compared to control group and no significant difference observed compared to other groups containing zirconia. Failure modes between the teeth and denture base nanocomposites were predominantly found as cohesive fractures, which was clinically acceptable according to the Standard.

Conclusion. The addition of zirconia nanoparticles to HI PMMA denture base at high concentration (7 wt.% and 10 wt. %) significantly ($p>0.05$) reduced the bonding strength

for all types of anterior teeth compared to the control group with no zirconia although no indication of pure adhesive failure was observed.

8.2. INTRODUCTION

Acrylic resin teeth have been widely used in the fabrication of partial and complete removable dentures and more recently in implant-supported prostheses (Saavedra et al., 2007). These prostheses, especially implant retained overdentures help prevent bone loss and provide more stability and retention during functioning. They have also been shown to improve patients quality of life when compared to the conventional dentures (Chaves et al., 2009). When setting acrylic teeth into an acrylic resin denture base such as poly-methyl methacrylate (PMMA), a strong bond is formed with the denture base through copolymerisation with a cross-bonding element due to their chemical compatibility (Clements et al., 2018; Moffitt et al., 2008). Other advantages of acrylic teeth are ease of adjustment, low cost (Chaves et al., 2009; Moffitt et al., 2008) and improved patient satisfaction and quality of life (Matos et al., 2018).

The adhesion between acrylic teeth and denture base resin is one of the most important factors for desirable performance and durability of a denture (Kurt et al., 2012; Palitsch et al., 2012). However, tooth debonding or fracture remains a major problem in clinical applications (Patil et al., 2006). It has been reported that the failure of dentures due to tooth debonding usually occurred in the anterior region of the denture and ranged between 22% and 30%, (Chaves et al., 2009; Colebeck et al., 2015; Cunningham, 1993; Kurt et al., 2012; Patil et al., 2006; Perea et al., 2014; Stoia et al., 2010). More recently, the use of implant-supported dentures has demonstrated improved masticatory function, and this has led to higher biting forces on the teeth. This further increases the likelihood of tooth debonding from the denture base (Barpal et al., 1998; Chaves et al., 2009). A number of factors could affect the adherence of the teeth to the denture base such as poor chemical incompatibility between different types of tooth and denture base materials or a smaller ridge lap surface area on the tooth available for bonding (Cunningham, 1993; Kurt et al., 2012; Patil et al., 2006; Stoia et al., 2010). Other factors include excessive occlusal force or fatigue loading on the teeth during mastication, surface contamination due to residual wax left at the interface between tooth and base material during denture fabrication, inappropriate use of separating medium layer during acrylic resin processing, insufficient monomer availability during polymerisation and ineffective or sub-optimal curing methods (Cunningham, 1993; Matos et al., 2018; Patil et al., 2006; Taczała and Sawicki, 2018). Evidence has also been reported that regular use of cleansing and disinfection chemicals could cause a change in the mechanical and physical properties of denture base and tooth materials leading to bond weakening and subsequent tooth failure (Tukmachi et al., 2018). These factors can cause tooth failure either adhesively or cohesively or a combination of both (Moffitt et al., 2008).

Adhesive failure occurs along the junction of contact between the acrylic tooth and denture base and is characterised by the absence of tooth or denture base fragments on the opposing surface. When the fracture occurs completely within the denture tooth or denture base acrylic resin, it is called cohesive failure. However, if there remains any fragment of denture base material on the tooth surface or any part of the tooth material on the denture base, it is called mixed mode of failure (Moffitt et al., 2008).

Previous studies have investigated different methods to enhance the bond strength, which included mechanical and chemical preparation of the ridge-lap surface of the tooth (Barpal et al., 1998; Colebeck et al., 2015). The mechanical preparations reported are pins, diatoric undercuts, grooving, grinding of the glossy surface and high-energy abrasion of teeth (Cardash et al., 1986; Perea et al., 2014; Saavedra et al., 2007) to improve the mechanical interlocking. A number of review studies also reported that the mechanical modification of the ridge-lap surfaces of acrylic teeth and showed an increase in bond strength (Cardash et al., 1986; Cunningham and Benington, 1999; Patil et al., 2006; Perea et al., 2014), although other studies did not find any improvement (Barpal et al., 1998; Patil et al., 2006; Perea et al., 2014). In contrast, chemical modification usually employed a monomer (MMA), solvents or adhesive bonding agent to the teeth (Perea et al., 2014; Taczała and Sawicki, 2018) in order to increase the chemical bonding. Several investigators also documented enhancement in bond strength with chemical surface treatments, but others also found no significant changes (Colebeck et al., 2015; Patil et al., 2006; Perea et al., 2014; Thongrakard and Wiwatwarrapan, 2016). Perea et al. (Perea et al., 2014) evaluated the effect of various chemical surface-conditioning monomers on ridge-lap surfaces of acrylic resin denture teeth, and the results demonstrated an improvement in the shear bond strength as the monomer systems caused dissolution of denture teeth.

Furthermore, the denture base materials and their polymerisation technique can have a measurable influence on the bond strength. Higher bond strength was obtained with the conventional heat-polymerized acrylic resin compared to the microwave-polymerized acrylic resin (Schneider et al., 2002). In another investigation, light- and microwave-cured resins showed reduced bond strength in comparison to the conventional heat-cured acrylic resins (Palitsch et al., 2012). However, in contrast, a more recent study found that microwave assisted polymerisation of denture base resin could improve the bond strength when compared to standard techniques (Andrade de Freitas et al., 2018). Cardash et al. found that the high-impact heat-cured denture base acrylic resin increased bond strength more than conventional resin without any impact modifier (Cardash et al., 1990). However, further research is needed to evaluate the bond strength of high-impact heat-cured PMMA resin to denture teeth.

A number of national and international standards are available to determine bond strength but there exists a wide variation in the materials used, shape, size and fabrication techniques of test samples and the methodology employed for testing samples (Patil et al., 2006). In clinical condition, the direction of load applied on the denture teeth during mastication can lead to separation of teeth by a combination of tensile, compressive and shear failure (Palitsch et al., 2012). Various methods have been used to estimate the adhesion bond between the teeth and denture base, and include tensile or (micro) tensile, shear, compression, flexural strength tests and finite element stress analysis (Chaves et al., 2009; Palitsch et al., 2012).

Zirconia nanoparticles have been used as a reinforcement in denture base acrylic resin to help improve its mechanical strength and to avoid premature fatigue or fracture failures (Gad et al., 2018a). According to a previous study it was determined that denture base nanocomposites developed with 3-5wt% of zirconia PMMA matrix can result in improved mechanical properties (Zidan et al., 2019). However, it is acknowledged that improvements in the mechanical properties of denture base alone cannot fully avoid denture failures in clinical practice. A combination of high strength in the denture base, and a strong bond between the teeth and base is vital to ensure sound performance and durability of the prosthesis. Therefore, it is essential to evaluate the bond strength of emerging denture base materials such as zirconia-PMMA nanocomposites. At present, no studies are available in the literature relating to the evaluation of tensile bond strength (TBS) between the teeth and denture base materials composed of zirconia based PMMA nanocomposites.

Hence, the aim of this study was to investigate the influence of adding different ZrO_2-nanoparticles concentrations (0%, 1.5%, 3%, 5%, 7%, and 10 wt. %) to HI-PMMA, on the TBS between denture teeth and base. The first hypothesis was based on the assumption that there would be no significant difference in the TBS of denture bases made of zirconia impregnated PMMA nanocomposites and pure acrylic denture teeth. The second hypothesis was based on the assumption that the British standard provides clear guidance on TBS sample preparation and jig design for pulling teeth.

8.3. MATERIALS AND EXPERIMENTAL METHOD

8.3.1. Tooth and denture base materials

A commercially available, denture base powder, (PMMA, poly-methyl methacrylate) and Metrocryl HI (X-Linked) denture base liquid (MMA, methyl methacrylate) (Metrodent Limited, Huddersfield, UK) were selected as the denture base material. Yttria-stabilized zirconia (ZrO_2) nanoparticles (Sky Spring Nano materials, Inc., Houston, TX, USA) were chosen as the inorganic filler agent for fabricating the nanocomposite denture base specimens. The specifications for other materials including the artificial tooth (cross-linked polymethylmethacrylate with colour pigments) used in preparing denture specimens for bond strength tests are presented in Table 8.1.

Table 8.1. Materials used in this study

Materials	**Trade name**	**Manufacturer**	**Lot. Number**
High-impact heat-cured acrylic denture base resin	HI Metrocryl	Metrodent Limited, Huddersfield, UK	Powder (22828) Liquid (103/4)
Yttria-stabilized zirconium oxide or zirconia	Zirconium oxide	Sky Spring Nano Materials, Inc, Houston, TX, USA	8522-120315
Acrylic resin teeth	Artic 6M S40 shade A2	Metrodent Limited, Huddersfield, UK	1813342008
Dental Plaster	Flasking plaster	Saint-Gobain, Formula, Newark, UK	0411217-3
Type 4 Diestone	Metrostone	Metrodent Limited, Huddersfield, UK	032218-1
Addition cured 2-part silicone lab putty 1:1	Matrix Duo Laboratory Putty	Metrodent Limited, Huddersfield, UK	18222-70054

8.3.2. Surface treatment of zirconia nanoparticles

Zirconia nanoparticle surfaces was treated with 7 wt.% silane coupling agent (3-trimethoxysilyl propyl methacrylate; product no. 440159, Sigma Aldrich) as explained in section 3.2.2 Preparation of silanisation in chapter 3 the methodology.

Based on a previous study (Zidan et al., 2019) a decision was made to utilize the different weight percentages of silanised zirconia nanoparticles in the denture base formulation. The composition details of the specimen groups used in this study are described in Table 8.2, all using an acrylic resin powder-to-monomer ratio of 21 g:10 ml, in accordance with the manufacturer’s instructions.

Table 8.2. Weight percent zirconia in combination with acrylic resin powder as well as monomer content of the specimen groups.

Experimental Groups	Zirconia (wt.%)	Zirconia (g)	HI PMMA powder (g)	HI MMA monomer (ml)
G1 (Control)	0.0	0.000	25.000	12.0
G2	1.5	0.375	24.625	12.0
G2	3.0	0.750	24.250	12.0
G	5.0	1.250	23.750	12.0
G5	7.0	1.750	23.250	12.0
G6	10.0	2.500	22.500	12.0

8.3.3. Preparation of denture teeth

Thirty sets of teeth each containing six maxillary anterior teeth (each set consisting of two central, lateral and canine teeth) manufactured with acrylic resin were used for the preparation of 30 denture specimens for TBS tests. The glossy layer was removed from the ridge-lap surfaces of the teeth and a groove was made in each tooth by a tungsten carbide bur (D B Orthodontics, West Yorkshire, UK) as shown in Figure 8.1.

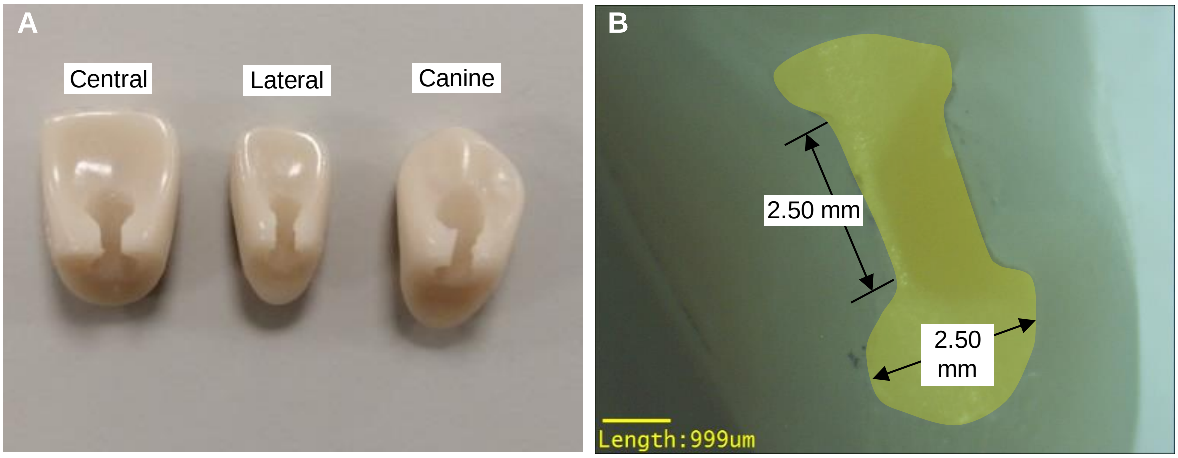

Figure 8.1. Photograph of (a) Different types of grooved anterior teeth and (b) a sample groove dimensions of a canine tooth.

The groove dimensions for central and canine were approximately same (2.50 ± 0.10 mm long and 2.50 ± 0.20 mm wide) but lateral tooth dimensions were smaller by approximately 1.0 mm. These mechanical tooth preparations might enhance the bond at the interface between teeth and denture acrylic resin according to previous studies and recommendations for best clinical practice (Cunningham and Benington, 1999). After the treatments, each tooth was thoroughly cleaned with pressurised air to remove any dust residue on the tooth surfaces that may affect the bonding.

8.3.4. Preparation of specimens

Specimens were prepared by base plate wax with a dimension of 75 mm × 55 mm × 7mm) at room temperature (23 ^{o}C). At the top surface of the of wax base, a rectangular groove of 5 mm wide and 1.5 mm deep was prepared. Six maxillary teeth were mounted onto the groove of wax base using heated base plate wax. Excess wax materials attached with the teeth neck and one-half of the lingual surfaces at the incisal portion of the teeth were carefully removed.

The flask (Bracon limited, UK) was filled with dental plaster and Type 4 Diestone and then a specimen was removed from the mould. Subsequently the wax base with teeth placed onto the Diestone in the flask left for drying for approximately 20 min. Once the dental plaster was set, the wax was flushed away with boiling water in a dewaxing machine (Labormat SD, Dreve Dentamid GmbH, Germany) and the flask was cleaned with steam (Cape Watch, UK) to remove any remaining wax in the plaster mould cavity. Nanocomposite denture base resins were prepared by mixing liquid MMA, zirconia nanoparticles and powder PMMA according to Table 8.2. When the mixture reached a consistent “dough”-like stage (working stage), it was packed into flask and closed, the flask was then immersed in a temperature-controlled curing water bath for 6 hr, to allow polymerisation to 95°C. The flask was removed from the curing bath, cooled slowly for 30 min at room temperature and opened to remove the specimen. The specimen was placed in an ultrasonic cleaning machine with water (Elma, Birmingham, UK) to clean the die stone from the specimen. Any remaining die stone was trimmed away using a tungsten carbide bur (D B Orthodontics, West Yorkshire, UK), and finally polished with pumice powder in a polishing machine (Tavom, Wigan, UK) to fabricate the TBS test specimen.

The specimen was duplicated by using Addition cured 2-part silicone putty with 1:1 ratio to produce a copy of the wax specimen. Figure 8.2 presents the duplication steps. The duplication wax specimens were used to fabricate all the thirty specimens following the same procedure mentioned earlier for bond strength test. The specimens were stored in distilled water at 37°C for 7 days before conducting TBS test.

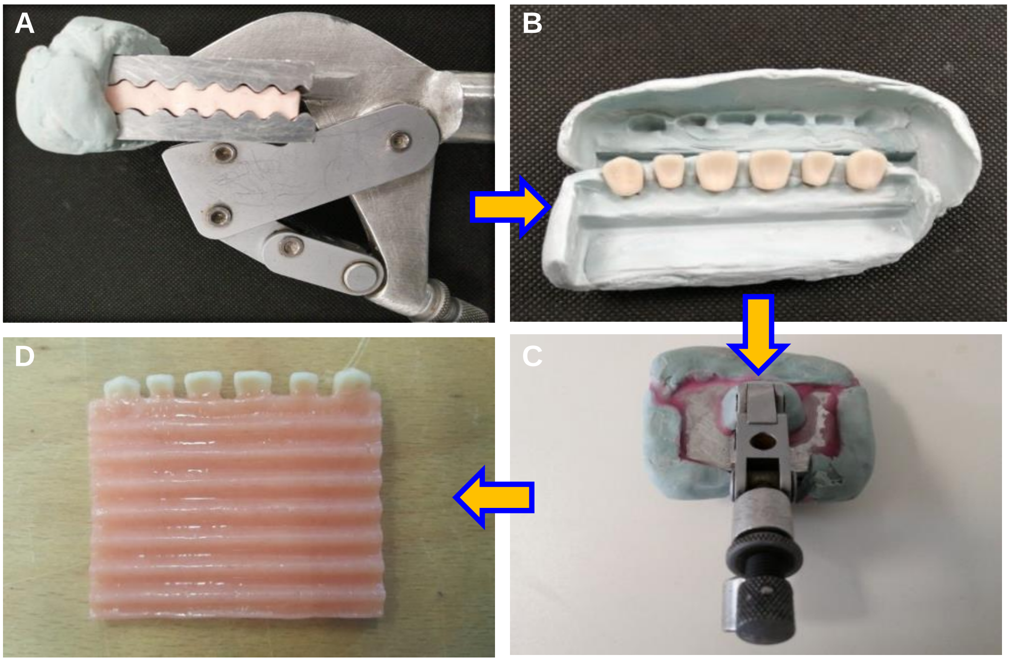

Figure 8.2. Photographs illustrating the steps of duplication of wax specimen in the grip former by Addition cured 2-part silicone putty: (A) creating silicone putty duplication mould (B) placing maxillary anterior teeth in the duplication mould, (C) placing duplication mould containing teeth in the grip former and pouring denture wax and (D) removing final wax specimen from the silicone putty mould.

8.3.5. Tensile bond strength (TBS) test

Thirty specimens of teeth on denture base materials were prepared for TBS tests using a universal testing machine (Hounsfield Tensometer, H10KS, Germany), according to the British standard (BS EN ISO 22112: 2017) (British Standards, 2017). A schematic diagram of the specimen with the teeth mounted on the denture base nanocomposites with dimensions of 75± 0.03 mm in length × 55 ± 0.03 mm in width × 7 ± 0.03 mm (H) is shown in Figure 8.3.

The specimens were removed from distilled water and placed in the same metal grip former, which was fixed at the bottom of the testing machine. A jig was designed to pull individual teeth out from the specimens by fixing at the upper cross-head of the universal testing machine. The jig was designed in the shape of a tuning fork with two adjustable screws in the two legs as shown in Figure 8.4.

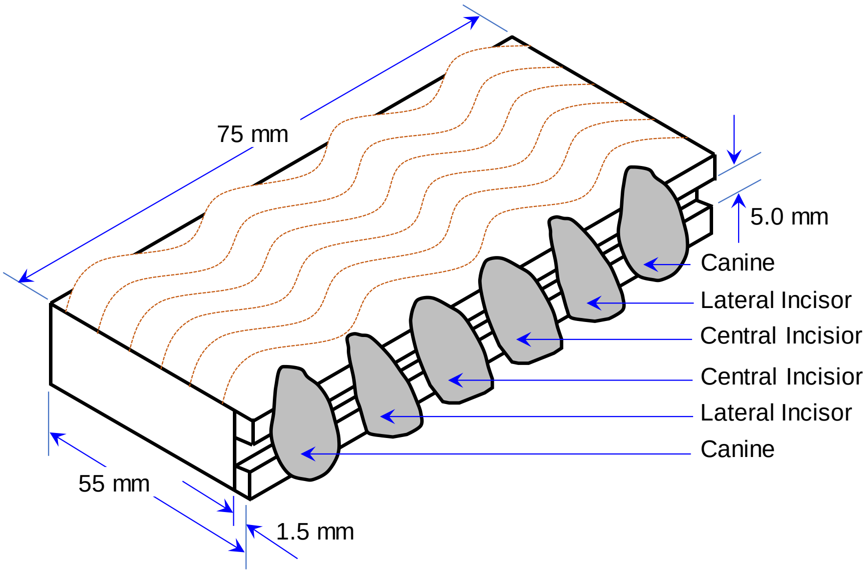

Figure 8.3. Schematic diagram of prepared specimen with different dimensions (adapted from (Kurt et al., 2012)).

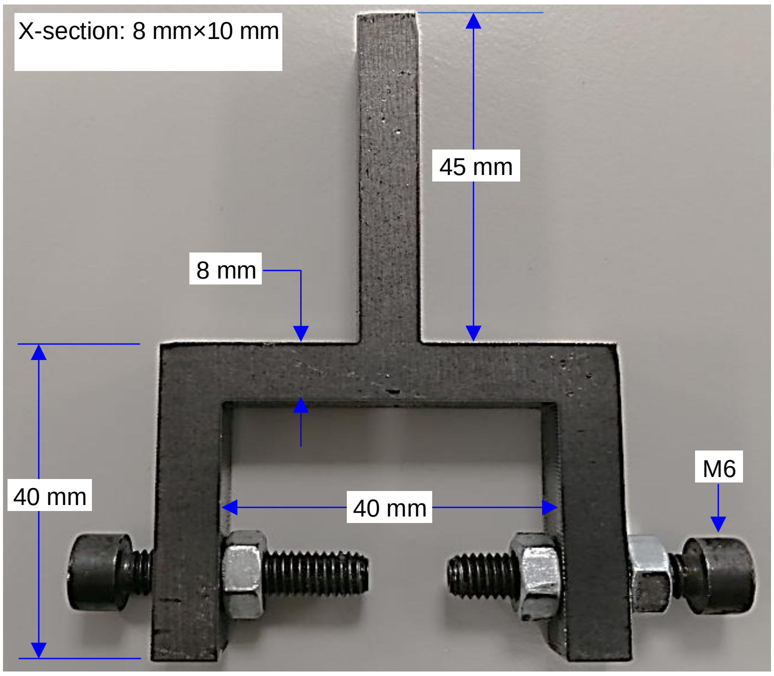

Figure 8.4.Photogrpah of the jig used for pulling teeth from the test specimen.

The screws were adjusted to fix against the base from both sides to tighten the specimen. One screw was pushed underneath the lingual area of a tooth and the other screw under the neck portion of the tooth to allow direct pull on the ridge lap area of the tooth attached on the base in a labial direction during tensile testing. Figure 8.5 presents image of the experimental set-up when a tooth was pulled up. TBS test was conducted at a crosshead speed of 5 mm/min (British Standards , 2017; Cardash et al., 1990; Kurt et al., 2012), pre-load 0.3 N and the load cell capacity was 1000 N. The load was applied to individual tooth until failure occurred and the maximum breaking forces were recorded in Newtons. The broken specimens were checked visually and under a microscope to determine whether the failure modes were adhesive, cohesive or a combination both.

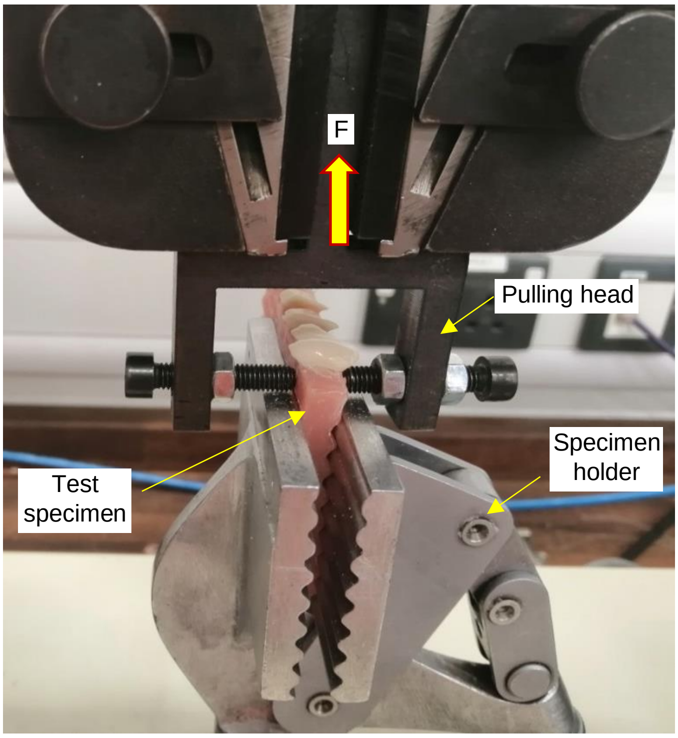

Figure 8.5. Photograph illustrating the bonding strength test set-up under tensile loading condition using Hounsfield universal testing machine

8.3.6. Examination of fractured specimens

The failure modes and mechanisms between the denture base and tooth were analysed visually and using an optical microscope and a scanning electron microscope (SEM) (Carl Zeiss Ltd, 40 VP, Smart SEM). The failed specimens were sectioned to correct size, mounted onto aluminium stubs using adhesive and coated with a thin layer of Gold/Palladium (Au/Pd) using a sputter coater to enhance conductivity. The stubs were then placed into a numbered sample holder and loaded into the SEM for imaging using a secondary electron detector at an acceleration voltage of 2.0 kV.

8.3.7. Statistical analyses

The TBS were recorded in terms of breaking forces and statistically analysed using a statistical software (SPSS statistics version 23, IBM, New York, NY, USA). Non-significant Shapiro-Wilk test showed that the data of tensile bonding strength was normally distributed and there was homogeneity of variance. A one-way analysis of variance (ANOVA) was used and means were compared with Tukey-post-hoc test at 0.05 significant level.

8.4. RESULTS

8.4.1. Tensile bonding strength

Thirty specimens each containing six maxillary anterior teeth and a total of 180 teeth for six specimen groups were subjected to TBS tests. Typical force vs elongation graphs for different denture base materials are presented in Figure 8.6. The mean of maximum breaking forces with standard deviations are listed in Table 8.3 for each type of tooth and presented as a bar chart in Figure 8.7. The mean TBS values of the groups containing 7 wt.% and 10 wt. % of zirconia were significantly lower ($P<0.05$) than that of the control group for all three types of teeth: central, lateral and canine. Again, in general, the groups containing 1.5 wt.%, 3 wt.% and 5 wt.% of zirconia showed lower TBS values compared to the control group but statistically not significant ($P> 0.05$). However, TBS between the central teeth and denture base group containing 3wt% zirconia showed the highest mean TBS value (685.7 N), though the highest TBS values for the lateral teeth were recorded with the denture base made of PMMA with no zirconia particles (control group).

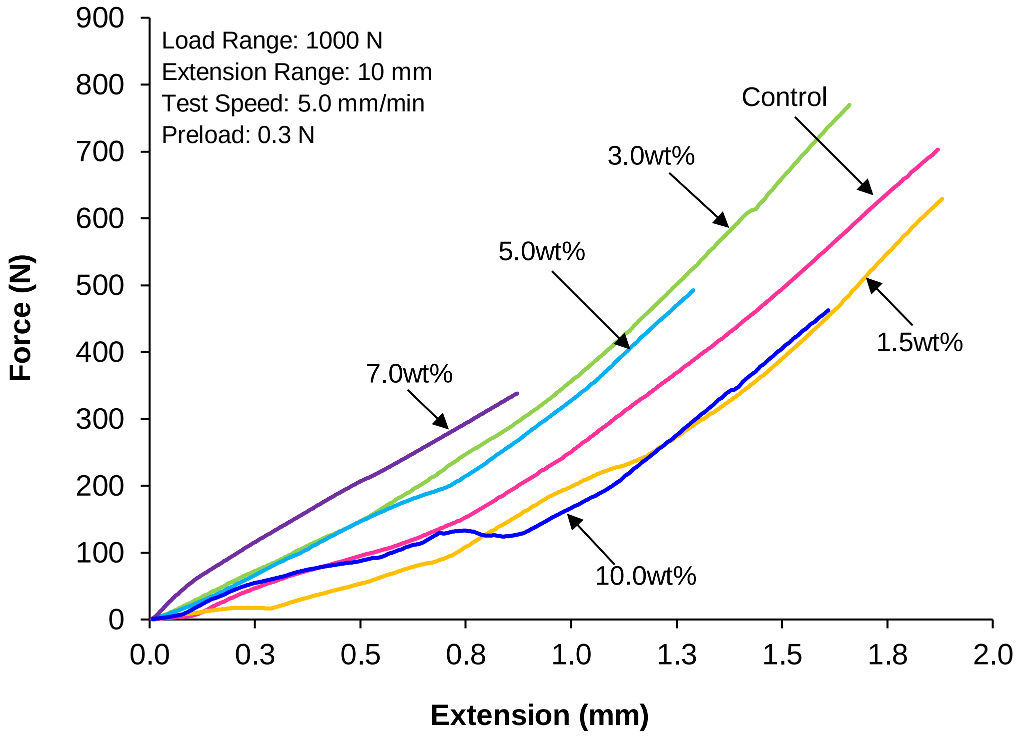

Figure 8.6. Line graph showing the representative force vs extension graphs for different test groups during TBS tests

Table 8.3. Mean and Standard deviation (SD) of tensile bond strength values (N) with a count of teeth failure types.

Zirconia Content (wt.%)	**Tensile bonding strength (N) (± SD)**		
	Central	Lateral	Canine
Control (0.0)	645.4 (84.8)^{A}	306.1 (81.6)^{A}	496.7 (179.1)^{A}
1.5	534.4 (115.3)^{A}	304.7 (86.4)^{A}	514.0 (143.2)^{A}
3.0	685.7 (159.6)^{A}	281.1 (78.3)^{A}	462.6 (122.1)^{A}
5.0	514.5 (134.3)^{A}	229.8 (67.3)^{A}	387.2 (99.4)^{A}
7.0	261.5 (66.0)^{B}	172.5 (57.4)^{B}	271.9 (86.3)^{B}
10.0	332.1 (122.9)^{B}	165.4 (48.7)^{B}	301.6 (73.2)^{B}

Note: Within a column, cells having similar (upper case) letters are not significantly different from the control (0% zirconia content) value; N = 10 specimens per group.

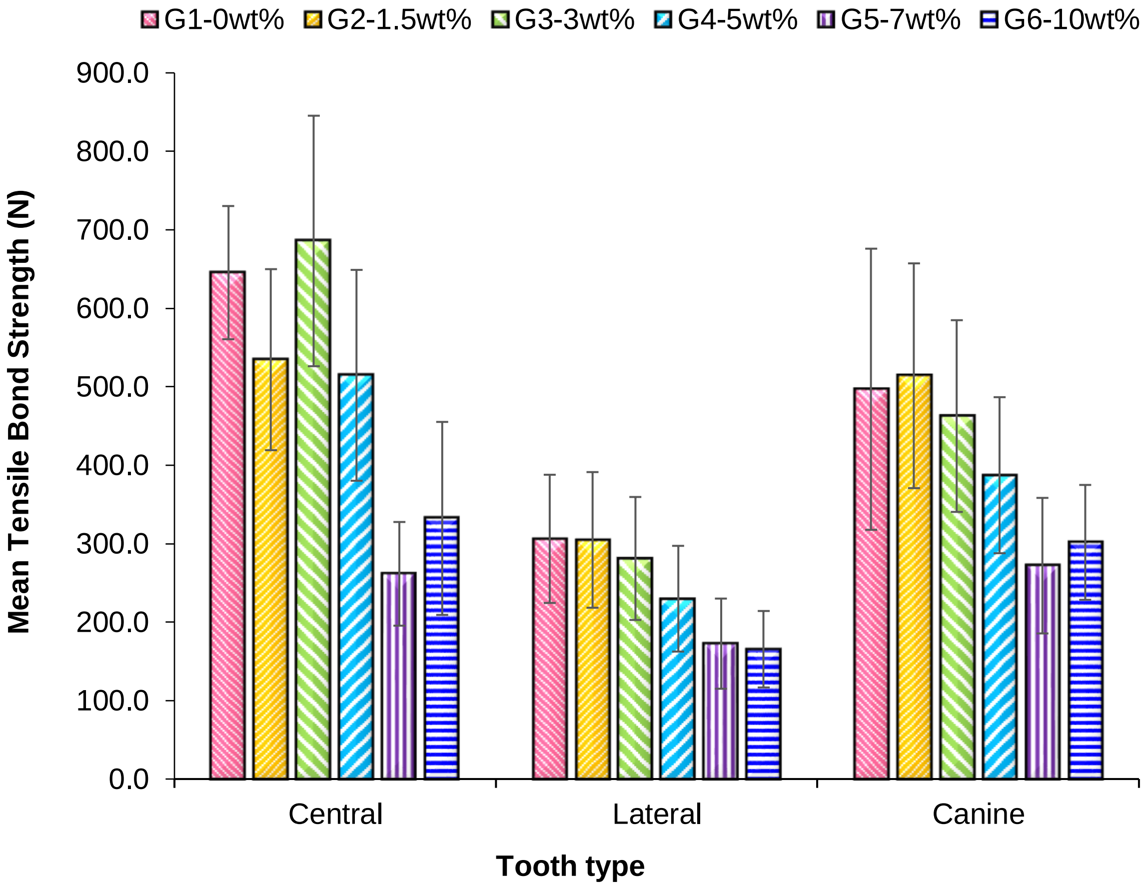

Figure 8.7. Bar chart showing the mean and standard deviation of TBS values between anterior teeth (central, lateral and canine) and denture base nanocomposites.

Figure 8.8 presents the number of teeth that fractured through different types of failure modes for each type of tooth. Complete adhesive failure at the interface between the teeth and denture base materials was not observed for any tooth within the six specimen groups. The most common failure mode was found as cohesive representing approximately 76% of the total failure. In general, the majority of the cohesive failures occurred within the teeth. In addition, few mixed cases, which combined both cohesive and adhesive failures, were noticed representing the rest of the failures.

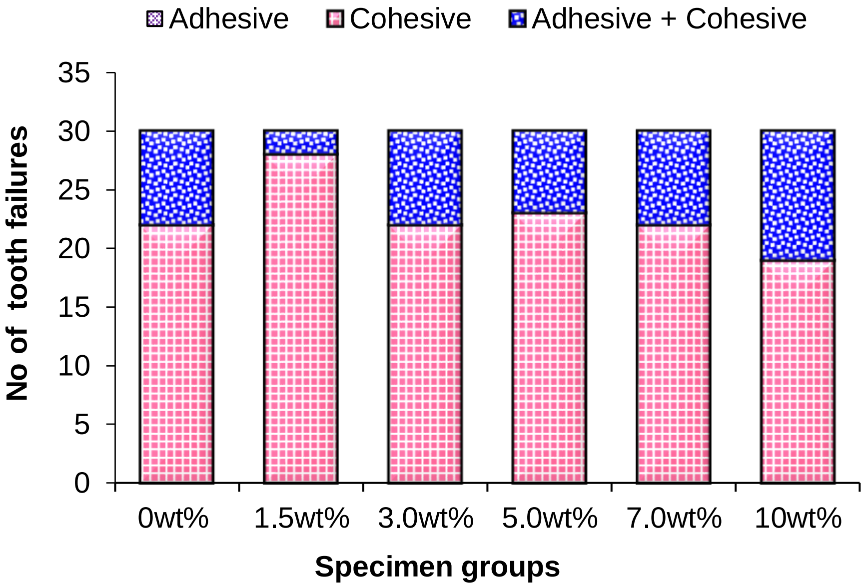

Figure 8.8. Bar chart showing the modes of tooth failures in the studied groups.

A strong negative correlation (r^2 =0.84) was found between the concentration of zirconia and the TBS with canine teeth as shown in Figure 8.9.

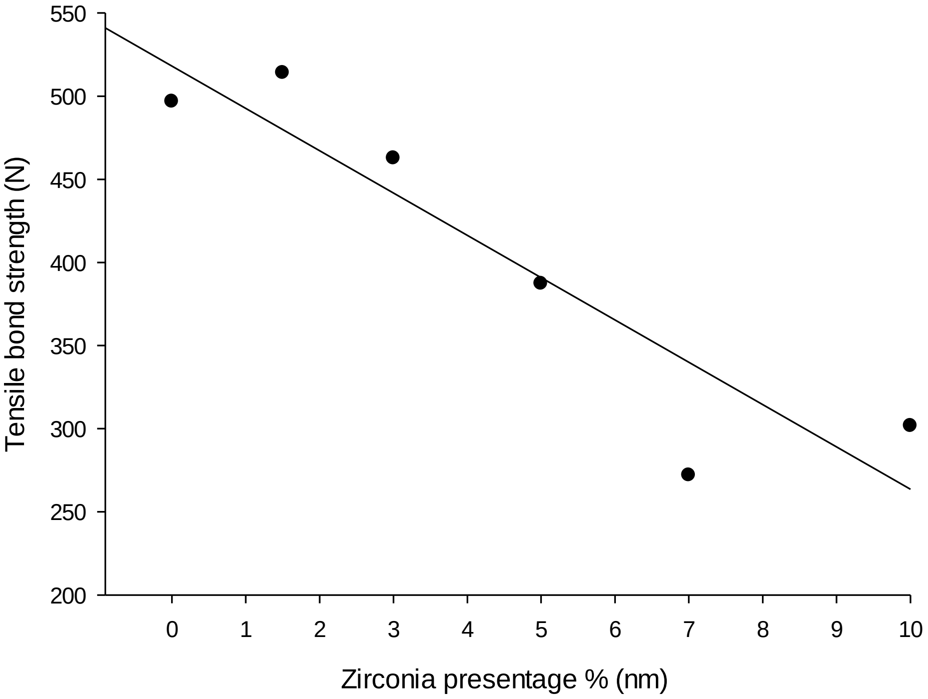

Figure 8.9. Correlation between zirconia nanoparticle concentrations and tensile bond strength for canine teeth.

8.4.2. Fractured sample analysis

In some cases, the crack propagated through the root of the groove at the ridge lap area and fractured parts of the tooth from two sides of the groove remained in the denture base as shown in Figure 8.10.

Micrographs of fractured surfaces presented in Figure 8.11(A) illustrate a mixed cohesive and adhesive failure, where part of the denture base PMMA resin remained on the tooth. At low magnification, generally it appeared that both materials were strongly bonded. At higher magnification, strong bond was further evidenced with no gap at the materials interface at one part, but a small interfacial gap was observed indicating a possible weaker bond. A strong bond was also evidenced by a layer of base material attached on the tooth in Figure 8.11 (B). Figure 8.11 (C) showed cohesive failure fracture within a tooth in a specimen of the group containing 10 wt.% zirconia and cracks were visible on the remained layer of the tooth surface at low magnification (50×). However, at higher magnification the propagation of cracks and their direction were clearly visible.

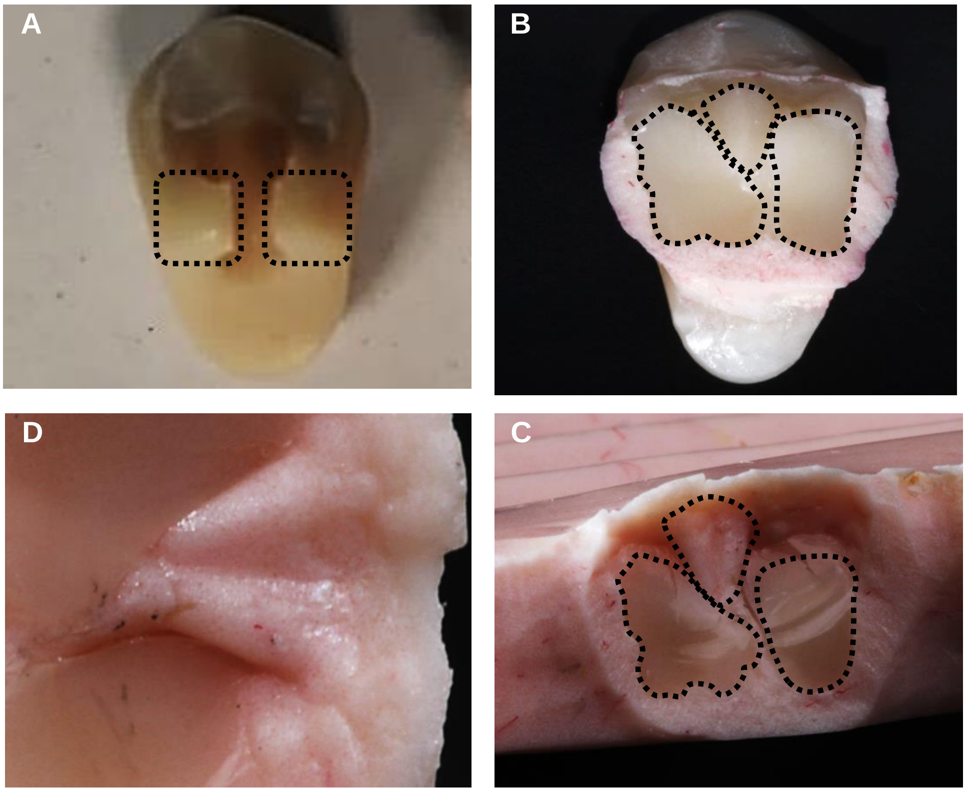

Figure 8.10. Photographs of (A) Canine tooth with groove (dotted boxes highlight the failed area), (B) broken canine tooth from groove root (C) part of the denture base with broken parts of tooth from the groove (dotted areas in B and C highlight matching broken surfaces in tooth and HI PMMA nanocomposite body) and (D) filling of tooth groove by denture base material.

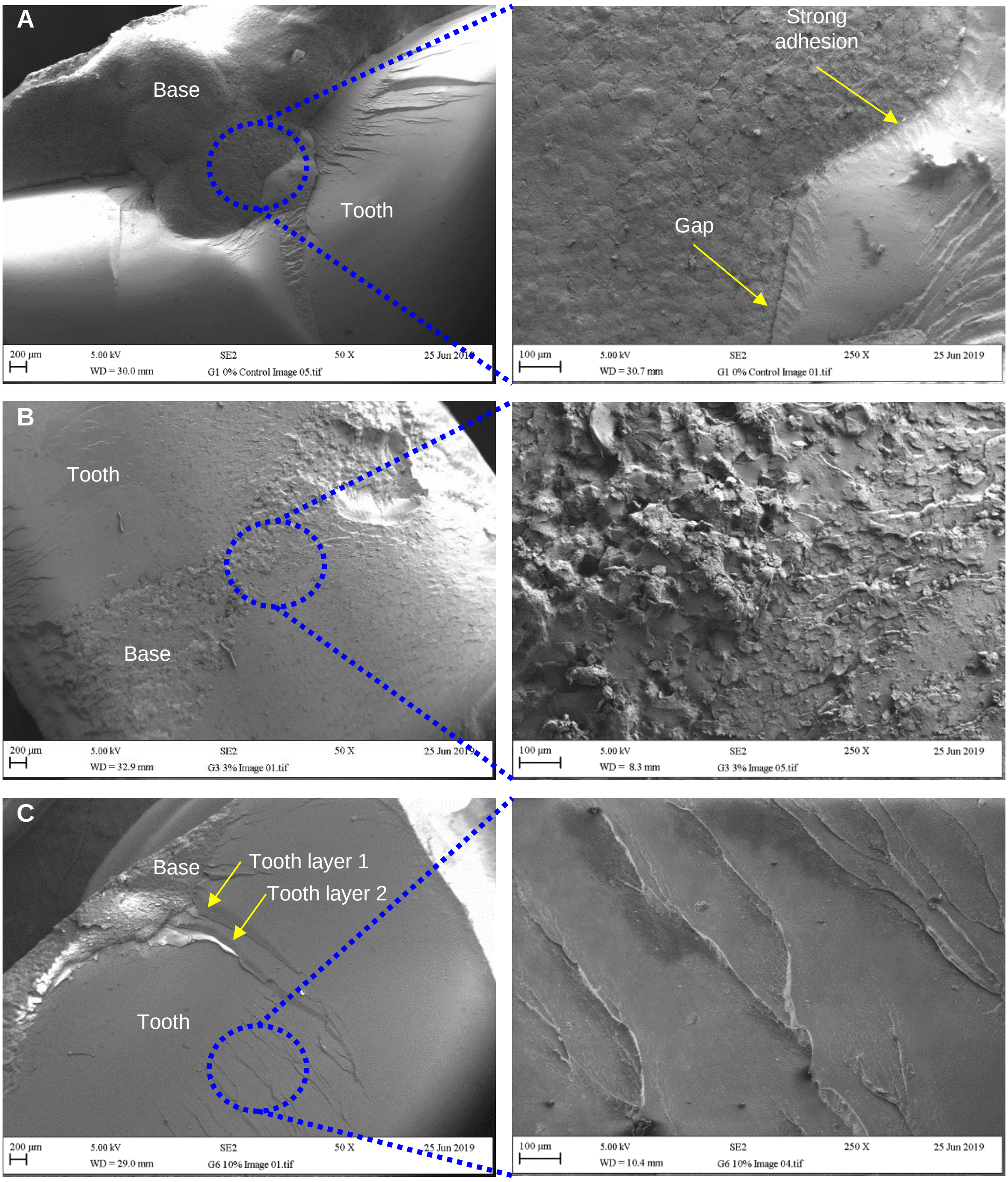

Figure 8.11. SEM images of fracture surfaces: (A) mixed cohesive failure with part of denture base material on tooth surface (B) mixed cohesive failure with layer of denture base material on tooth surface and (C) cohesive failure within tooth showing cracks and their propagation on the fractured tooth surfaces.

8.5. DISCUSSION

Following these investigations, the original research hypothesis was partially. accepted TBS values of acrylic resin teeth bonded to high-impact PMMA resin reinforced with small concentration of zirconia nanoparticles (1.5 wt.%, 3 wt.% and 5 wt. %) showed no significant difference compared to the pure PMMA resin (control group). However, the TBS values for PMMA resin reinforced with high zirconia concentrations (7 wt.% and 10 wt. %) were significantly lower than that for the control group. With few exceptions, a general trend of decreasing bond strength with increasing zirconia concentration was observed for all three tooth types. However, there was a strong correlation (r^2 = 0.85) between zirconia and TBS for canine teeth due to the larger surface area. However, for the central incisor tooth with 3wt% and the canine tooth with 1.5wt% reinforcement the results demonstrated a higher TBS value when compared to the pure PMMA group. A disruption in the trend was also noticed for the central incisor and canine teeth where the bond strength at 10wt% zirconia was slightly higher than that at 7wt%. In this study, it was clear from the failure behaviour that all the denture base nanocomposites passed the TBS test according to the standard, as there was no pure adhesive failure.

The bond strength values available in literature cannot be directly compared with the reported studies due to the difference in materials or mechanical properties of the artificial denture teeth, materials of denture base, methods of polymerisation used and type of evaluation method applied (Chaves et al., 2009; Palitsch et al., 2012). In addition, several countries have their own national specifications standard (Clark and Hsu, 2014). It is also worth detailing that other studies presented the bond quality in terms strength (MPa) calculated by dividing the breaking force with a flat contact area at the interface. Unfortunately, these results cannot be compared as the contact areas were not flat in this study (Kurt et al., 2012). Only two other studies were found in the literature, which followed directly comparable specimen shape and tensile testing procedure. One study did not report the breaking force during testing as the bond quality was defined by the failure modes only, where 26 tooth debonding occurred through adhesive failures (Korkmaz et al., 2010). The other study (Kurt et al., 2012) created a flat surface on the ridge lap area (5 mm × 5 mm) to measure the bond strength (17.65 MPa) between acrylic resin polymer tooth and a conventional heat-polymerised PMMA denture base material. The equivalent breaking force (441.25 N) was smaller than the results in this study for the groups with lower zirconia concentrations. Furthermore, 57 tooth failures determined through adhesive modes against 0 adhesive failures for all groups in this study again demonstrated that HI heat-cured PMMA or zirconia-PMMA nanocomposites could be a better choice to improve the integrity of denture base.

Cardash evaluated TBS comparing no retentive features against horizontal and vertical grooves on the ridge lap with central incisors, lateral incisor and canine teeth bonding to standard and high impact denture base resins. The findings showed that the highest TBS results were obtained with canines bonded with the aid of vertical retention grooves. An increased surface area on the ridge lap for bonding to acrylic resin along with the vertical groove supporting the mechanical retention of the canine were attributed for this (Cardash et al., 1990). This is in agreement with the current study, where the improvement in TBS was greater for central incisor and canine teeth rather than the lateral incisor teeth. The lowest bonding strengths associated with the lateral incisors could be due to the relatively smaller contact area at the ridge lap, smaller retention grooves, and smaller protruding areas left on both sides of the ridge lap area for effective pulling during tensile testing.

The reason for the apparent reduction in bond strength at higher zirconia concentration is not that clear. Sprately suggested that during specimen fabrication a rougher surface might trap more wax residue, which could lead to a lower bond strength. With higher zirconia concentrations, surface roughness in the denture base might increase, thus resulting in a decreased bond strength (Spratley, 1987). In addition, particle clustering found at higher zirconia concentration (Zidan et al., 2019) could reduce the interaction between the tooth and base materials leading to a weak bond. However, absence of any significant adhesive failure in this study does not fully support these possibilities. Studies designed by Suzuki et al (Suzuki et al., 1990), to evaluate the relationship between adhesive bonding and surface hardness showed that the highly cross-linked resin teeth with higher hardness had poorer bonding to denture base resin compared to normal conventional acrylic teeth having less cross-linking characteristics. In this study, with the increase in zirconia concentration, the relative hardness of denture base increased (Zidan et al., 2019), unlike the increase tooth hardness in the previous study, could affect the bond strength. However, this needs further investigation.

According to British standard (BS EN ISO 22112: 2017) (British Standards, 2017), when the mode of tooth failure occurs cohesively, it means that the bond strength was achieved successfully (British Standards Institution (BSI), 2017). In the present study, the majority of specimen failures in all the experimental groups happened in a cohesive manner with the denture teeth leaving a layer of tooth material on the denture base. In contrast, a relatively a small number of teeth (24%) showed a combination of cohesive and adhesive failure occurred on denture base and/or teeth. These findings are also in agreement with the results presented by other studies (Robison et al., 2016).

With a small increase in zirconia concentration the bond strength was reduced. Therefore, the nanocomposite denture base material might play an important role in maintaining the integrity of the denture. Even with optimum zirconia concentration, the denture base nanocomposite did not show any improvement in TBS values over pure PMMA. However, in all cases no adhesive failure or cohesive failure within the denture base was observed. This could indicate that mechanical interlocking and chemical bond at the interface were strong enough to maintain the integrity of the denture.

From the failure modes, failure statistics and fracture surface characteristics, it was clear that good bonding was achieved. Therefore, the bond strength was limited by the strength of the tooth rather than the strength at the interface or denture base (Andrade de Freitas et al., 2018). Robison et al. also reached the same conclusions that after achieving good bonding, the bond strength was determined by the strength of the denture teeth, which could be affected by the processing technique (Robison et al., 2016). The Artic 6 acrylic teeth used in this study contained multilayer structures. Therefore, during tensile testing, the applied load on the lingual surface near the incisal third of the tooth caused high stress not only at the tooth-denture base bond, but within the tooth leading to cohesive failure of teeth (Cunningham, 1993). Figure 8.11(C) shows different layers in a fractured tooth surface.

A study conducted by Clancy et al, assessed the TBS on heat-cured and auto polymerisation resins to two types of denture teeth (regular acrylic and IPN abrasion-resistant). The findings showed that the highest TBS was obtained with heat-cured resin bonded to regular acrylic teeth and they argued that heat-cured resin underwent complete polymerisation when compared to the auto polymerisation resin. Moreover, the degree of cross-liking also affected the TBS. The regular acrylic teeth having less cross-linking than the abrasion resistant IPN teeth showed significantly higher bond strength to heat-cured acrylic resin (Clancy and Boyer, 1989). It is also expected that regular teeth and heat-cured PMMA used in this study formed a better chemical compatibility to create a strong bond.

A number of good practices were followed during the specimen preparation, which included thoroughly cleaning wax at the ridge lap area, creating retention groove in the teeth, using teeth with cross-linking characteristics, adding MMA monomer (liquid) on the ridge lap surface of the tooth and strictly following the manufacturer's instructions during polymer processing (Radford et al., 2014). It is believed that the application of these good practices optimised the processing conditions and made the bond strength as high as possible in order to resist debonding under the application of tensile loading. The absence of single adhesive failure also indicated that specimen preparation was consistent for all teeth. The findings from this study will influence the future clinical practices in preparing denture base materials resulting in reduced tooth failures in denture, reduced no of denture repairing, reduced number of visits to dentists and increased patient satisfaction.

In the mixed mode failure, small areas of adhesive failure appeared on the incisal side of the tooth where the load was applied. However, the fracture propagated into the denture tooth body and failed cohesively. Cohesive tooth failure in the groove area has been observed in other studies (Patil et al., 2006; Vallittu, 1995). Therefore, this fracture behaviour indicated that the teeth were more brittle or less strong than the nanocomposite denture bases. Evidence was found that the grooves were filled by the denture base acrylic leading to an increased mechanical retention and improved bonding strength by effectively locking the teeth to the denture base (Cardash et al., 1990; Patil et al., 2006). Vallitu (Vallittu, 1995) also attributed the stronger bond due to penetration of denture base resins in the grooves and greater contact surface area.

A number of shortcomings were identified in the British standard used in this study to conduct the tests and the second hypothesis has been rejected. Firstly, it does not specify any minimum breaking force or strength for assessing an acceptable bond quality, which was only defined by the type of failure. Secondly, the standard does not specify the unit of the bonding strength in terms of maximum breaking forces in N or stress in MPa and does not provide any guidance in making the ridge lap surface flat for calculating the bond strength by dividing the contact area with the maximum tensile breaking force. Again, displacing teeth from both sides does not represent the real clinical scenario during mastication as a combination of other types of forces such as shear or bending could also be involved. It was found that setting up the pulling head with different tooth types was also very challenging due to its poor inherent design, which could cause inconsistencies in test results. Therefore, a revision of the standard in the light of the above points could be beneficial for reporting test results in a consistent manner.

Variations in TBS values were somewhat higher due to the scattering of results. Previous investigations also reported high variation in the bond strengths (Kurt et al., 2012, Radford et al., 2014). High repeatability of specimen fabrication could be an important factor to obtain consistent bond strength results. Careful attention was given during denture base preparation, tooth preparation and denture specimen fabrication. However, slight inconsistency in tooth grinding or grooving, positioning of teeth on the denture specimen base in terms of contact surface area at the ridge lap, depth of ridge lap into the base and length of a tooth protruding from either side of the base could cause inconsistency in the specimens. Experimental error during tensile testing could also come from minor error in positioning the teeth with respect to the adjusting screw in the pulling head. This could be due to only a small protruding part of a tooth engaged with the screw in the pulling head. In addition, one screw was pulling from one side and the other screw was not fully engaged due to a minor geometrical inconsistency in the denture specimens or differences in tooth geometry on the two sides of the ridge lap area.

In this study only mechanical modifications of the tooth surface were conducted through grinding and grooving. Further investigations need to be carried out to evaluate the effect of other surface treatments of tooth ridge-lap such as monomer and adhesive bonding on the teeth with low and high cross-linking characteristics. Moreover, the influence of types of teeth having different mechanical properties (e.g., surface hardness) could also be studied to select appropriate teeth for achieving maximum bonding with zirconia impregnated denture base nanocomposites. More recently, it was found that, shear bond strength was significantly improved with surface treatments were carried out by laser compared to mechanical and chemical surface treatments (Akin et al., 2014). This option can also be explored in future to further improve the bond strength of zirconia-PMMA nanocomposites.

8.6. CLINICAL IMPLICATIONS

The results obtained from this *in vitro* investigation suggest that the tensile bond strength between high-impact heat-cured PMMA denture base impregnated with small quantities of zirconia nanoparticles and acrylic teeth were equally good when compared to the same with pure PMMA, while also providing improved mechanical properties than the latter. An appropriate concentration of zirconia (between 1.5wt% to 5wt%) should be considered to maximise the bond strength in clinical practice.

8.7. CONCLUSION

Within the experimental limitations of this in-vitro study, the following conclusions can be drawn.

The tensile bond strength (TBS) between tooth and HI PMMA denture base nanocomposites with 1.5 wt.%, 3 wt.% and 5 wt.% of ZrO_2 was not significantly different than the control group (without zirconia). However, the nanocomposites with 7 wt.% and 10 wt.% zirconia displayed relatively poorer strength compared to the control group. Among the denture base nanocomposites, 3 wt.% zirconia impregnated PMMA could be the optimum denture base material for obtaining highest bonding strength, which could be comparable to pure PMMA resin.

The most common mode identified was cohesive failure through fracture within the teeth. A few mixed modes in combination with cohesive and adhesive failures were also observed but no pure adhesive failure at the interface between the teeth and denture base, an indicator of poor bonding, was recorded. The results also suggested that the tooth failure in denture was not limited by the bond strength or strength of denture bases rather the strength of the teeth.

Chapter 9: Equivalent Flexural Strength for Complete Removable Dentures made of Zirconia Impregnated PMMA Nanocomposites

Saleh Zidan, Nikolaos Silikas, Abdulaziz Alhotan, Julfikar Haider and Julian Yates

Published in Materials MPDI. 2020; 13, 2580

https://doi.org/10.3390/ma13112580

(Appendix: Published copy of the paper)

9.1. ABSTRACT

Statement of problem. High-Impact (HI) poly-methyl methacrylate (PMMA), obtained from modification of conventional PMMA, is commonly used in prosthodontics as a denture base material for improved impact resistance. However, it suffers from poor flexural strength properties.

Purpose. The aim of this study was to investigate the flexural strength of complete removable dentures made of HI PMMA heat-polymerized resin, reinforced with zirconia nanoparticles at two different concentrations. The effect of fatigue loading on the flexural strength behaviour of the dentures was also investigated.

Materials and Methods. A total of 30 denture specimens were fabricated from PMMA with different concentrations of zirconia nanoparticles: 0 wt.% (control), 3 wt.% and 5 wt.%. Each specimen group was divided into two subgroups, with five specimens in each, to conduct both flexural strength and fatigue loading test of each of the sub-groups. Fatigue loading was applied on the dentures using a mastication simulator and equivalent flexural strength was calculated with data from bending tests with and without fatigue cyclic loading. One-way analysis of variance (ANOVA) of the test data was conducted with the Bonferroni significant difference post-hoc test at a pre-set alpha value of 0.05. Paired t-test was employed to identify any difference between the specimens with and without the application of fatigue loading. The fractured surface of the denture specimens was examined with a Scanning Electron Microscope (SEM).

Results. The bending tests demonstrated that the mean equivalent flexural strength of reinforced HI PMMA denture specimens with 5 wt.% zirconia nanoparticles increased significantly (134.9 MPa ± 13.9 SD) compared to the control group (0 wt.%) (106.3 MPa ± 21.3 SD) without any fatigue loading. The mean strength of the dentures with PMMA+3 wt.% zirconia also increased, but not significantly. Although the mean strength of all specimen groups subjected to fatigue loading slightly decreased compared to that of the specimen groups without any fatigue cyclic loading, it was not statistically significant.

Conclusion. Denture specimens made of HI PMMA heat-polymerized reinforced with 5 wt. % zirconia nanoparticles significantly improved equivalent flexural strength compared to that made of pure PMMA when the specimens were not subjected to any prior fatigue cyclic loading. In addition, the application of fatigue cyclic loading did not significantly influence the equivalent flexural strengths of all denture specimen groups.

9.2. INTRODUCTION

The acrylic resin poly-methyl methacrylate (PMMA) is widely used for the manufacture of dental prostheses including conventional removable complete or partial dentures and implant supported prostheses (Diaz-Arnold et al., 2008). Acrylic resins have many advantages including acceptable aesthetic appearance (Gad et al., 2018a), lightness, biocompatibility and ease of processing in the laboratory for clinical use (Yu et al., 2015). However, this material is still some way from possessing the ideal mechanical properties required for denture base and other prosthetic applications, suffering from low resistance to impact, flexural weakness and fatigue (Asar et al., 2013).

The fracture of dentures is the most frequent problem when patients present with failures of their prostheses. Many of these fractures occur inside the mouth as a result of denture fatigue caused by mastication processes (Gurbuz et al., 2010). A study conducted in England and Wales found that approximately 1.75 million dentures failed due to fracture and nearly 1.0 million denture repairs were undertaken every year (Johnston et al., 1981). It is widely accepted that many materials suffer a loss of strength as a result of cyclical stress over a long period of time. Microcracks start to generate at the point of alternating stresses in the denture, propagate through the material and finally lead to fatigue failure after a certain period of time (Kelly, 1969; Yu et al., 2015). Flexural fatigue of PMMA has been determined as a cause of midline fractures of complete dentures (Vallittu et al., 1994b). According to Yu et al., the majority of fractures occurred in the midline of maxillary complete dentures, with the incidence being 2 to 3 times higher when compared to mandibular dentures (Yu et al., 2015). Additionally, acrylic resin dentures demonstrated flexing during functioning to a much greater degree than expected, as well as poor tissue adaptation (Kelly, 1969).

Various attempts have been made in the past to improve the mechanical properties of denture base acrylic resins by incorporating particles, wires, fibres or mesh aligned with the shape of the denture base (Andreopoulos and Papanicolaou, 1987; Im et al., 2017; Vallittu, 1996; Yoshida et al., 2011; Yu et al., 2017). One of the most notable developments was based on the chemical modification of conventional PMMA with rubber particles (butadiene-styrene) with sizes ranging from 1 µm to 5 µm,(Andreopoulos and Papanicolaou, 1987) marketed as a “high impact” variation. This has been successful to a certain extent in improving the impact strength and dimensional stability (Jagger et al., 2003; Jagger et al., 2002; Sasaki et al., 2016; Zheng et al., 2012). However, the incorporation of rubber decreases the flexural and fatigue strengths and the modulus of elasticity compared to conventional heat-polymerized acrylic resins (Jagger et al., 2003; Jagger et al., 1999; Jagger et al., 2002; Zheng et al., 2012).

Several studies have investigated clinical performance of metal-wire reinforced acrylic dentures (Im et al., 2017; Kim and Watts, 2004; Yoshida et al., 2011; Yu et al., 2017). Maxillary complete dentures made of acrylic resin reinforced with metal wire (Co-Co alloys) were placed under the ridge lap in the anterior region and in the anterior and posterior regions of the denture base. The tests showed that the wire reinforcement increased the flexural strength of the dentures (Yoshida et al., 2011). However, reinforcement of acrylic resin with metal wires often resulted in wire separation at the interface due to poor adhesion between the denture base resin and metal reinforcement (Kim and Watts, 2004; Yu et al., 2015). Further attempts were made to address this issue by improving the adhesion between the wire and resin through wire-surface treatment, however, it still proved largely inadequate (Kim and Watts, 2004). In addition, the addition of metal wire often resulted in unacceptable denture aesthetics and significantly increased the overall mass of the denture base (Yu et al., 2015).

Exploring substitutes for metal reinforcement, other studies have reported incorporation of micro-fibres such as aramid, ultrahigh molecular weight polyethylene, carbon, nylon, urethane oligomer and E-glass in the forms of chopped, flaked, continuous or woven constituents (Fajardo et al., 2011; Yu et al., 2015; Yu et al., 2017). Several studies concluded that glass-fibre reinforcement significantly increased flexural strength, flexural modulus and impact strength of acrylic dentures (Fajardo et al., 2011; Im et al., 2017; Kim and Watts, 2004; Vallittu et al., 1994b; Yoshida et al., 2011; Yu et al., 2015; Yu et al., 2017). Valletta et al. and Im et al. reported improved fatigue and fracture resistance from a complete denture made of acrylic resin reinforced with glass fibres with force magnitudes of 80 N, 100 N and 180 N applied to the occlusal surfaces of the test specimens with fatigue cyclic loading repeated at 300,000 masticatory cycles in a mastication simulator machine, the equivalent to real-life use for over a year (Im et al., 2017; Vallittu, 1996; Vallittu et al., 1994b). A clinical study investigated the orientation of the glass fibres in PMMA dentures and suggested that they should be placed close to the location of highest tensile stress to prevent any initiation of fracture. However, incorrect positioning of glass fibres could lead to a decrease in mechanical properties (Pan et al., 2013; Yoshida et al., 2011). Therefore, it is challenging to manufacture dentures with accurate fibre positioning and to maintain the mechanical properties consistently from a quality control point of view.

Recently, numerous investigations have focused on adding nanoparticles such as yttria-stabilized tetragonal zirconia polycrystals (Y-TZP) to improve the mechanical and physical properties of conventional heat-polymerized denture base resins (Gad et al., 2019b; Zhang et al., 2014; Zidan et al., 2019). This type of zirconia, called “ceramic steel”, possesses superior mechanical properties, good surface properties and high biocompatibility, thus making it an attractive option for many dental applications (Cavalcanti et al., 2009; Gad et al., 2016b; Trunec and Chlup, 2009). To date, the effect of zirconia nanoparticles on the flexural strength and fatigue loading cycles of HI PMMA has not been evaluated with specimens of a similar shape to a complete denture. Therefore, the aim of this study was to investigate the flexural strength properties of complete dentures made from HI PMMA heat-polymerized resin reinforced with zirconia nanoparticles with and without fatigue cyclic loading in a mastication simulator. The hypothesis was that HI PMMA heat-polymerized incorporated with zirconia nanoparticles with and without fatigue cyclic loading would have a significant positive effect on the flexural strength of the complete dentures.

9.3. MATERIALS AND EXPERIMENTAL METHOD

9.3.1. Materials

A commercially available Metrocryl HI denture base powder, PMMA (poly-methyl methacrylate), and Metrocryl HI (X-Linked) denture base liquid (MMA, methyl methacrylate) (Metrodent Limited, Huddersfield, UK) were selected as the denture base material. Yttria-stabilized zirconia (ZrO_2) (Sky Spring Nano Materials, Inc., Houston, Texas, USA) nanoparticles with an average size between 30 nm and 100 nm were chosen as the inorganic filler agent for fabricating the nanocomposite denture specimens, as shown in Table 9.1.

9.3.2. Preparation of complete removable dentures

9.3.2.1. Silanisation and selection of appropriate percentages of zirconia nanoparticles

According to a previous study (Zidan et al., 2019), the most appropriate weight percentages of zirconia nanoparticles were used in this study: 0% (control), 1.5 wt.%, 3.0 wt.%, 5.0 wt.%, 7.0 wt.%, and 10.0 wt.%. Three groups of complete dentures were prepared for this study and their compositions are described in Table 9.2. All had an acrylic resin powder-to-monomer ratio of 21 g:10 ml, in accordance with the manufacturer’s instructions. In the authors’ previous study (Zidan et al., 2019) with beam type PMMA-zirconia nanocomposite samples, it was determined that optimum flexural strength can be obtained by adding zirconia nanoparticles at approximately 3 wt.% and 5 wt.%.

Table 9.1. Materials used in making complete removable dentures

Materials	Trade name	Manufacturer	Lot. Number
High impact heat-curing acrylic denture base resin	HI Metrocryl	Metrodent Limited, Huddersfield, UK	Powder (22828) Liquid (103/4)
Yttria-stabilized zirconium oxide	Zirconium oxide	Sky Spring Nano Materials, Inc, Houston, TX, USA	8522-120315
Dental Plaster	Flasking plaster	Saint-Gobain, Formula, Newark, UK	0411217-3
High strength dental stone	Dentstone KD	Saint-Gobain, Formula, Newark, UK	085217-5
Type 4 Diestone	Metrostone	Metrodent Limited, Huddersfield, UK	032218-1
Addition cure silicone putty 1:1	Sheraduplica	Shera, Lemforde, Germany	Base (86392) Catalyst (86047)

Table 9.2. Weight percent zirconia in combination with acrylic resin powder as well as monomer content of the specimen groups.

Experimental Groups	Zirconia (wt.%)	Zirconia (g)	HI PMMA powder (g)	HI MMA monomer (ml)
Control	0.0	0.000	21.000	10.0
Nanocomposite-1	3.0	0.630	20.370	10.0
Nanocomposite-2	5.0	1.050	19.950	10.0

9.3.2.2. Preparation of denture base specimens

Maxillary edentulous master casts were duplicated using an addition-cure silicone putty to obtain a mould that was then used to produce thirty edentulous casts by pouring high-strength dental stone into the silicone mould. Two sheets of baseplate wax (Metro wax)

(Metrodent Limited) with a thickness of 3.50 mm were adapted onto the palatal surface on the edentulous cast, and then occlusal rim was placed on denture base wax. The maxillary master cast with occlusal rim was fixed on an articulator (John Winter) using dental plaster in preparation for setting the teeth. Then the maxillary anterior teeth (Artic 6M S10 shade BL3, Metrodent Limited) and maxillary posterior teeth (Artic 8M 10 30U shade A2, Metrodent Limited) were fixed onto the occlusal rim. Upon completing waxing of the denture base and teeth, the wax denture and plaster cast were removed from the articulator and placed in a flask filled with dental plaster and dental stones were place onto the teeth., after setting. The denture wax was then removed through dewaxing process.

The silane-treated zirconia and acrylic resin powders were weighed according to Table 9.2 using an electronic balance with an accuracy of three decimal points (Ohaus Analytical plus, Ohaus Corporation, Parsippany, NJ, USA). Where indicated, zirconia powder was added at the appropriate concentration to the acrylic resin monomer and mixed in a speed mixer (DAC 150.1 FVZK, High Wycombe) at 2,500 rpm for 5 min. Once mixed, the acrylic resin powder was then added to the solution, and mixed again in accordance with the manufacturer’s instruction, until a smooth, uniform mixture was obtained. The mixture was then packed into the flask, pressurised and immersed in a curing water bath for 6 hr to allow polymerisation.

The flask was then removed from the curing bath and left to cool 30 min at room temperature. The flask was then opened, and the denture removed. The denture was placed in an ultrasonic cleaning machine containing water (Elma) to remove any attached stone, trimmed using a tungsten carbide bur (D B Orthodontics), ground with an emery paper grit 40 (Norton, Saint-Gobain), and finally, polished with pumice powder in a polishing machine (Tavom). All thirty denture specimens were fabricated individually in the manner detailed above.

The specimens were manufactured into three groups of 10 dentures, with the respective quantities of nano-filler incorporated into each group (0 wt.%, 3 wt.% and 5 wt.% of zirconia). Furthermore, each group was again divided into 2 subgroups of 5 specimens for bending tests with and without fatigue loading.

9.3.3. Mechanical strength test

9.3.3.1. *Fatigue loading*

Fatigue cyclic loading was performed according to a previous study by Im et al.(Im et al., 2017) using a chewing simulator (CS-44.2 SD Mechatronik GmbH, Feldkirchen-Westerham, Germany) that simulated maxillary and mandibular movement in the mouth during mastication. Fifteen denture specimens, five from each group, were employed for fatigue tests. The specimens were stored in distilled water in an incubator at a temperature of 37±1°C for 7 days before applying the fatigue loading. The chewing simulator consisted of two test sample chambers. In one chamber, the denture was placed on a cast made of Type 4 Diestone fixed to a plastic sample cup. To avoid any contact between the palatal surface of the denture and cast during the test, a space of 1 mm was maintained between the specimen surface and the residual ridge of the cast as shown in Figure 9.1. To simulate the mastication motion, a stainless-steel T-shaped jig (50 mm length × 9.75 mm width) was fixed onto an antagonist holder. The upper bar faced the centre of midline of the denture and T-shaped jig was placed against the second premolar (full) and first molar (partial) teeth on each side at 1.6 Hz. The initial loading applied on the denture was 8 kg (78.48 N). The vertical movement of the upper bar was set at 2 mm and lateral movement at 0.2 mm, with a vertical speed of 30 mm/s. A total number of 250,000 mastication cycles were performed in 37°C distilled water to simulate approximately one year of use in an oral environment. All denture specimens were examined after fatigue tests to identify any cracks or failures.

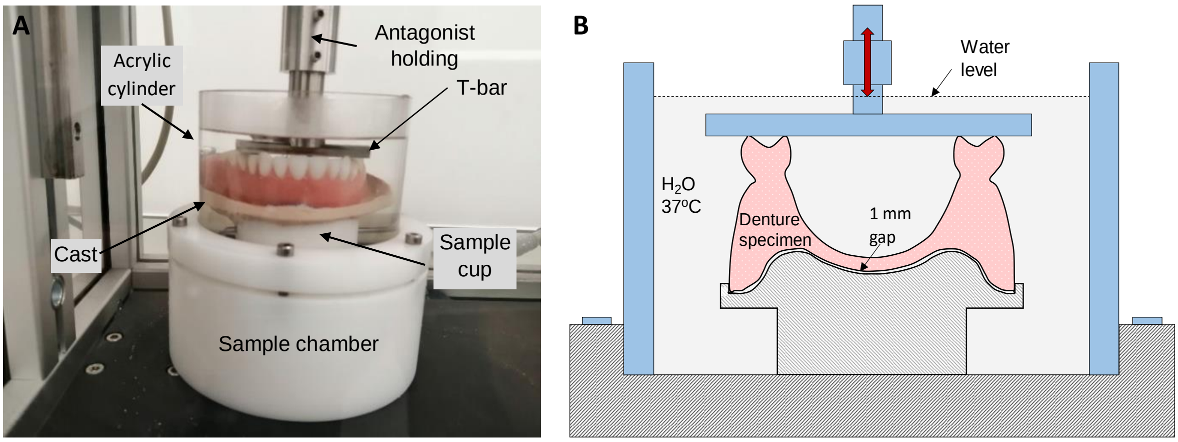

Figure 9.1. Photographs showing (A)Test set-up for mastication simulation under fatigue cyclic loading and (B) schematic diagram of mastication fatigue loading

9.3.3.2. Bending test

Thirty denture specimens with and without fatigue cyclic loading were subjected to three-point bending test in a Hounsfield universal testing machine (Hounsfield Tensometer, H10KS, Germany). The specimens were stored in distilled water at a temperature of 37±1°C for 7 days in an incubator before conducting the tests. The occlusal surface of the denture was placed within a specially designed specimen holder to prevent any movement of the dentures during the bending tests. The distance between the second molar teeth (last tooth on each side) acted as a supporting span with a length of 42.33 ± 0.2 mm. The loading head, made from stainless steel with a length of 70 mm and a tip diameter of 10 mm, was attached to the Hounsfield testing machine. The load was applied to the palatal fitting surface at a cross-over point between the palatal midline and the line connecting the centre of first molars on each side of the denture. After several pilot tests, it was found that this loading position provided a relatively flat surface with minimal chances of slipping. Furthermore, to avoid any slipping between the loading head and palatal surface, a small piece of emery paper with a thickness of 0.60 mm with a small hole at its centre was stuck by a double-sided sticky tape. The hole was aligned with the point of loading.

The thickness of the dentures was measured using a digital micrometer (Mitutoyo, Hampshire, UK) at the point of loading around the central palatal area. The average dimension was 3 ± 0.2 mm. The width of the load bearing area of the dentures was measured as 42 ± 0.2 mm, and the weight of all denture specimens were measured using an electronic digital scale (Machine Mart Limited, UK). A 10 KN load cell, a cross head speed of 5 mm/min and preload 10 N were used to record maximum fracture force (F) in Newtons during the bending tests. The equivalent flexural strength was calculated in MPa for all dentures specimens using Equation 9.1 (British Standards, 1989).

Figure 9.2 presents a picture and a schematic diagram of the bending test experimental set-up:

$$\sigma = \frac{3\mathrm{Fl}}{2\mathrm{bh}^2} \tag{9.1}$$

where F is the maximum force applied in N, l is the distance between the supports in mm, b is the width of load bearing area of the denture specimen in mm, and h is the thickness of the denture specimen in mm at the point of loading.

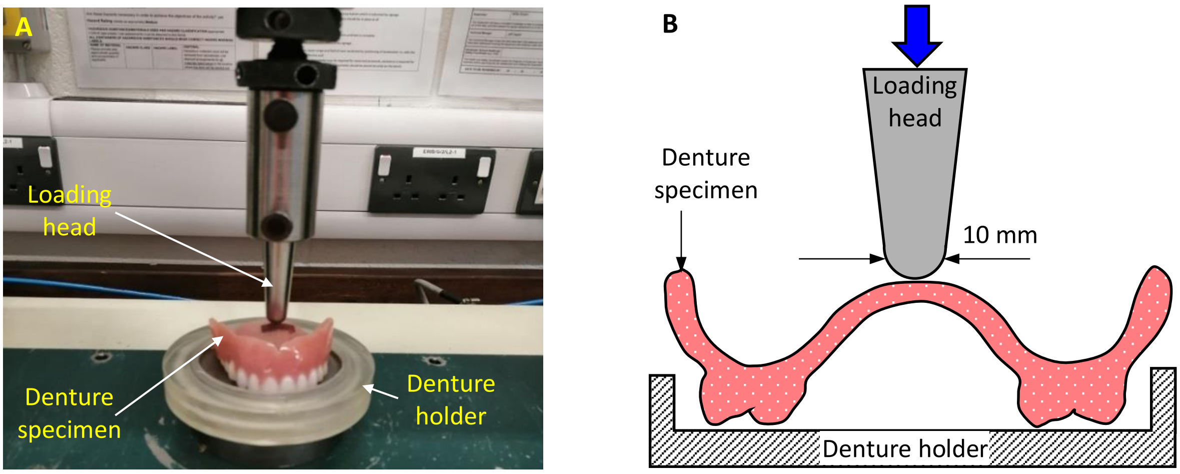

Figure 9.2. (A) Applying bending load on palatal surface of denture specimen in Hounsfield universal testing machine, (B) schematic diagram of loading condition.

9.3.4. Qualitative fractured surface analysis

Following fracture of the denture, the midline fractured surfaces from the bending tests of complete dentures were also studied using a scanning electron microscope (SEM) (Carl Zeiss Ltd, 40 VP, Smart SEM, Cambridge, UK) in order to identify the mechanism of failure. Part of the fractured specimens were mounted onto slotted aluminium stubs and coated with a thin layer of gold/palladium using a sputter coater. The stubs were then placed into a numbered specimen holder and loaded into the SEM for imaging using a secondary electron detector at an acceleration voltage of 2.0 kV.

9.3.5. Statistical analysis

The recorded results of bending with and without fatigue loading were calculated and statistically analysed using statistical software (SPSS statistics version 23, IBM, New York, NY, USA). Non-significant Shapiro-Wilk tests demonstrated that data from the bending strength tests was normally distributed and there was homogeneity of variance. A one-way analysis of variance (ANOVA) was used with the Bonferroni significant difference post-hoc test at a pre-set alpha value of 0.05. In addition, a Paired t-test analysis was applied to identify any significant difference between the groups at a pre-set alpha value of 0.05, with and without fatigue loading.

9.4. RESULTS

9.4.1. Weight and visual analysis of denture specimens

The mean weights of non-reinforced and reinforced complete dentures with 3 wt.% and 5 wt.% zirconia are listed in Table 9.3. The non-reinforced complete dentures were slightly heavier than the reinforced ones. However, the difference when compared to the reinforced dentures was negligible. This indicated that the addition of zirconia did not significantly change the weight of the dentures.

Table 9.3. Weight of complete dentures made of pure PMMA and zirconia impregnated PMMA

Weight of non-reinforced PMMA dentures (g) (Mean ± SD)	**Weight of reinforced PMMA dentures (g) (Mean ± SD)**	
Control Group 0 wt % of zirconia	3 wt % of zirconia	5 wt % of zirconia
20.1 ± 1.0	19.5 ± 0.2	19.5 ± 1.0

The colours of dentures made of 3 wt.% and 5 wt.% nanocomposites were a demonstrably lighter pink compared to the control group (HI acrylic resin), as shown in Figure 9.3. However, both 3 wt.% and 5 wt.% nanocomposite dentures appeared to display smoother and shinier surfaces in contrast to that of the control group.

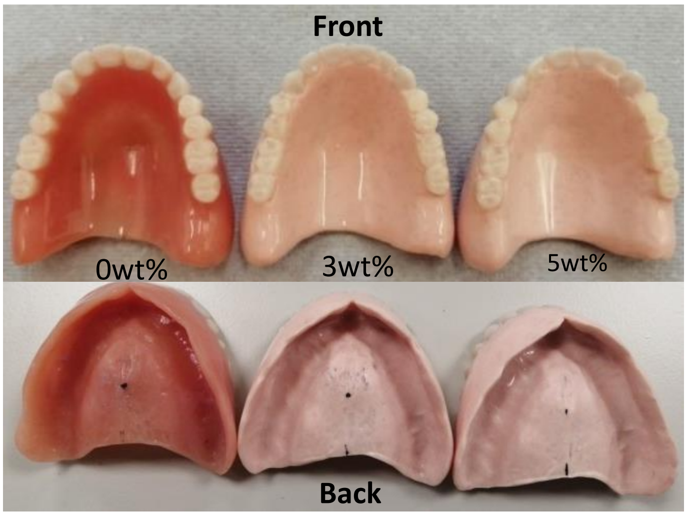

Figure 9.3. Photographs showing dentures from different specimen groups (a) control group (0 wt.% zirconia) (b) 3 wt.% zirconia and (c) 5 wt.% zirconia.

9.4.2. Cyclic Fatigue loading

Among the fifteen denture specimens that underwent fatigue cyclic loading tests in the mastication simulator, no dentures failed due to cracking or fracture. This indicated that all dentures, including the reinforced ones, would survive for at least a year in clinical service.

9.4.3. Equivalent Flexural strength

Force vs deflection curves of the different denture groups without any fatigue cyclic loading during the bending tests are presented in Figure 9.4 The peak breaking forces gradually increased with the increasing percentage of zirconia nanoparticles. Similar behaviour was also noticed for denture specimens following fatigue cyclic loading. One-way analysis of variance (ANOVA) of mean flexure strengths with and without fatigue loading is presented in Table 9.4 and Figure 9.5. The specimen groups containing 3 wt.% zirconia with and without fatigue cyclic loading showed a 7.45% and 19.55% increase in the equivalent flexural strength and maximum force respectively, when compared to the control group. In comparison, the specimen groups containing 5 wt.% zirconia with and without fatigue cyclic loading showed a 10.53% and 26.91% increase in the equivalent flexural strength. The highest increase in the mean value of strength was found for the group containing 5 wt. % zirconia (134.9 MPa) without fatigue cyclic loading, which also showed a significant difference ($p<0.05$) when compared to the control group (106.3 MPa). However, all the mean strengths of the dentures subjected to fatigue cyclic loading were slightly lower when compared to those of the dentures without any fatigue cyclic loading, but the decrease in mean values were not significant ($p>0.05$).

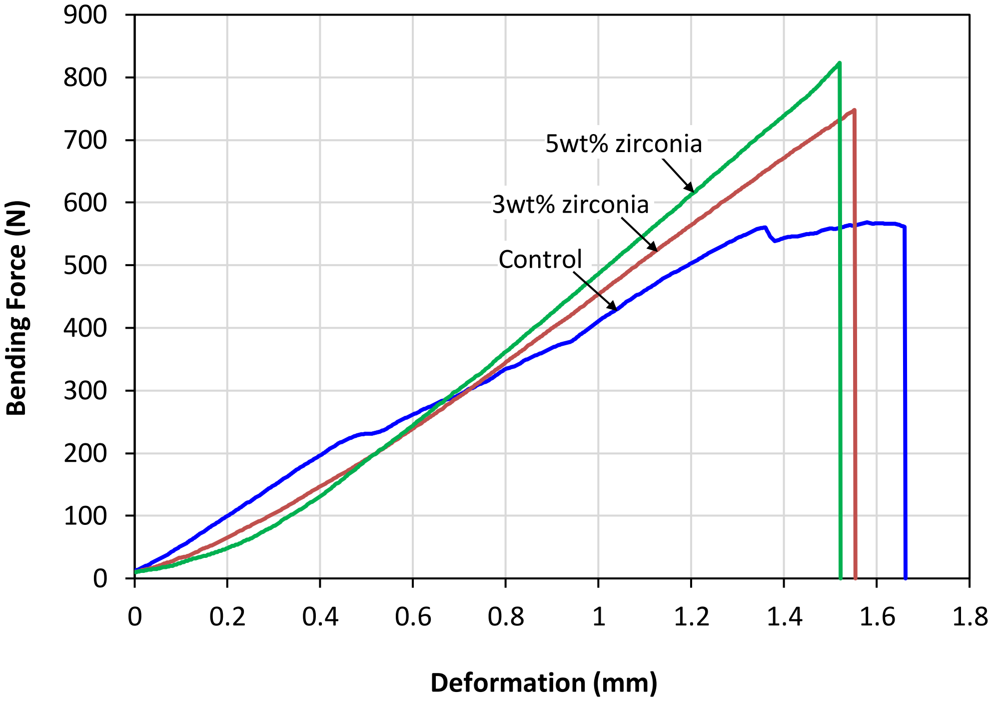

Figure 9.4. Line graph illustrating typical bending load vs deflection curves without fatigue loading for pure HI PMMA and zirconia reinforced nanocomposites.

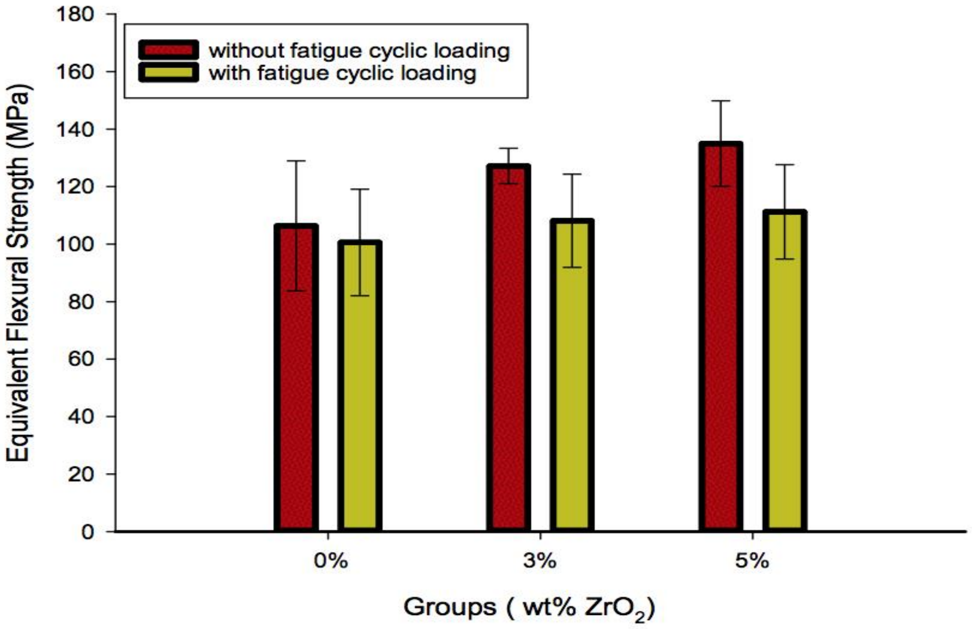

Figure 9.5. Bar chart showing equivalent flexural strengths of complete dentures with and without fatigue cyclic loading.

Table 9.4. Maximum force (N) and mean & SD of values the equivalent flexural strength (MPa) before and after fatigue cyclic loading for the test groups.

Weight percentage zirconia (wt.%)	**Without Fatigue Cyclic Loading**		**With Fatigue Cyclic Loading**	
	Maximum Force (N)	Equivalent flexural strength (MPa) & SD	Maximum Force (N)	Equivalent flexural strength (MPa) & SD
Control (0.0 %)	633.2	106.3 (21.3)^{Aa}	598.9	100.6 (17.4)^{Aa}
3.0 %	757.0	127.1 (5.8)^{Ab}	643.8	108.1 (15.2)^{Ab}
5.0 %	803.6	134.9 (13.9)^{Bc}	662.2	111.2 (15.45)^{Ac}

Note: Within a column, cells having similar (upper case) letters are not significantly different from the control group (0% zirconia content) and within a row values identified using the same lower-case letters are not significantly different; n = 5 specimens per group.

9.4.4. Failure modes of complete dentures

After the bending tests with and without fatigue cyclic loading, all 30 denture specimens were examined to identify the failure modes; these are listed in Table 9.5. The failure modes of the dentures can be broadly classified into two groups: complete fracture and incomplete fracture.

The first general mode of failure is referred to as midline fracture, wherein the denture was completely broken into two pieces along the midline in the palatal area, as shown in Figure 9.6. Midline fractures were identified in all groups except the control group with fatigue cyclic loading. The second failure mode can be divided in to two categories: localised fractures that occurred in the area where the load was applied on the denture with the compression head and cracks that occurred at the free end of the denture (Figure 9.6). Localised fractures occurred in only 10% of the specimens, which makes it a relatively uncommon failure mode. In contrast, cracks were observed in all specimen groups. This was very common among the failure modes, representing more than 50% of the failures. In addition, no fracture was seen at the anterior and posterior frameworks of the complete dentures as presented Figure 9.7, complete denture failure modes with and without fatigue cyclic loading.

Table 9.5. Failure modes of complete dentures with and without fatigue cyclic loading.

Failure modes	**Name of Failure modes**	**Control group (0 wt.% Zirconia)**		**3 wt.% Zirconia**		**5 wt.% Zirconia**	
		Without fatigue loading	With fatigue loading	Without fatigue loading	With fatigue loading	Without fatigue loading	With fatigue loading
Complete Fracture	Midline fracture	1	0	2	2	3	3
		Between central and lateral		One between central & lateral One between centrals	One between canine & first premolar One between central & lateral	Two. between centrals One through a central	One between centrals One through a lateral One between central & lateral
Incomplete fracture	Localised fracture	1	1	1	0	0	0
	Cracks	3	4	2	3	2	2

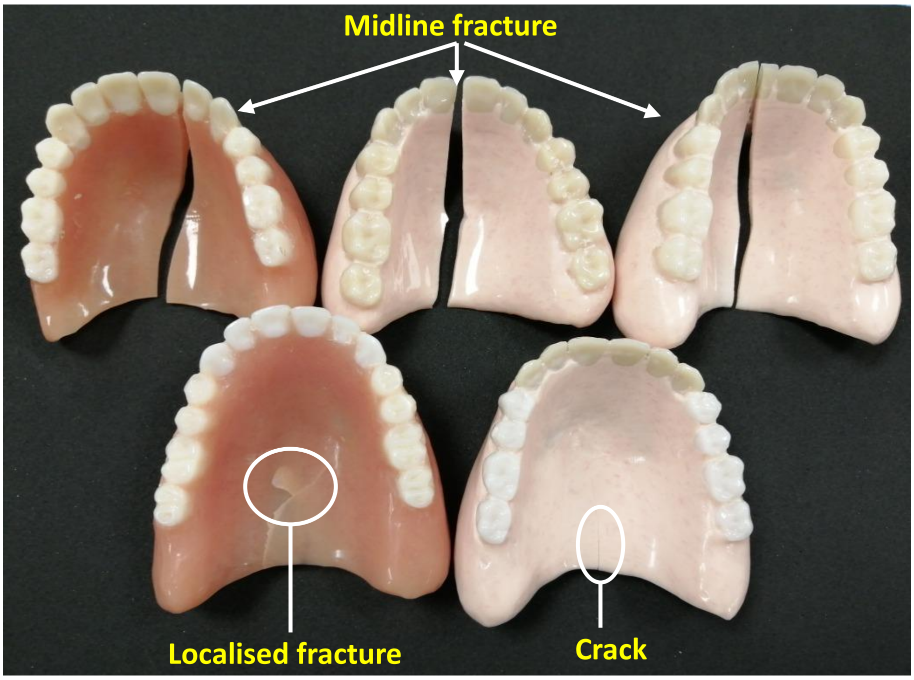

Figure 9.6. Photographs showing the failure modes observed in the dentures during the bending tests: Midline fracture, Localised fracture and Crack.

9.4.5. Fractured specimen analysis

Figure 9.8 shows fractured cross-sections of all three denture specimens (0 wt.%, 3 wt.%, 5 wt.% of zirconia) at the point of loading during the bending tests. All surfaces can be characterised by a pattern of globular-shaped peaks and valleys.

It appeared that the globular shapes would match with the peaks and valleys in the opposite surfaces of the two broken pieces. Although the surfaces did not show any large cracks or fractures, evidences of micro-cracks were present. Further magnified views of the surfaces at 1000× revealed patches of smooth surfaces along with rough surface areas. Figure 9.9 shows the characteristics of the rough and smooth surface areas at high magnification. Small voids were visible in all surfaces. The presence of zirconia nanoparticles was observed in the nanocomposites, particularly in the smooth surface regions. There was also evidence of zirconia particle clustering to a small degree, indicated by circles in Figure 9.9.

Loading	Groups	Specimen 1	Specimen 2	Specimen 3	Specimen 4	Specimen 5
Without fatigue loading	0wt% Zirconia 3wt% Zirconia 5wt% Zirconia					
With fatigue loading	0wt% Zirconia 3wt% Zirconia 5wt% Zirconia					

Figure 9.7. Complete denture failure modes with and without fatigue cyclic loading

Mag.	**0wt % Zirconia**	**3wt % Zirconia**	**5wt % Zirconia**
150×	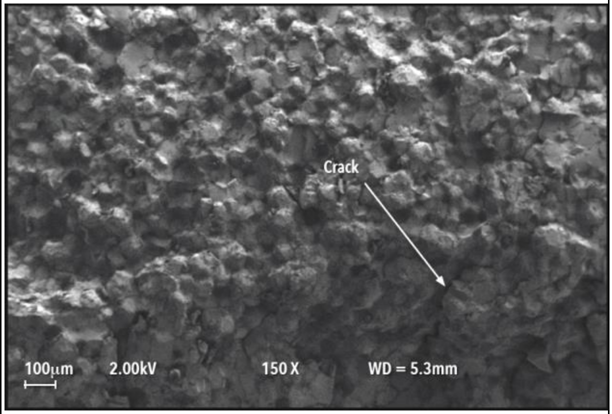	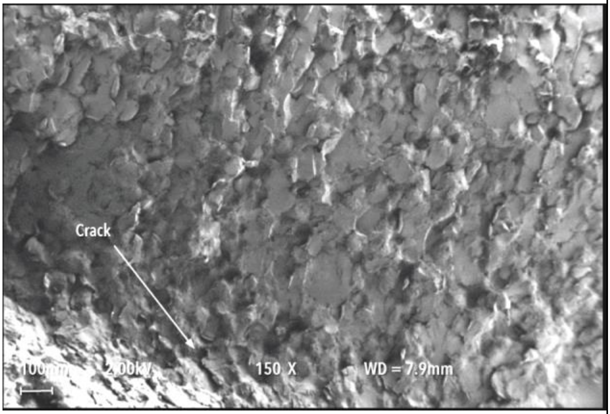	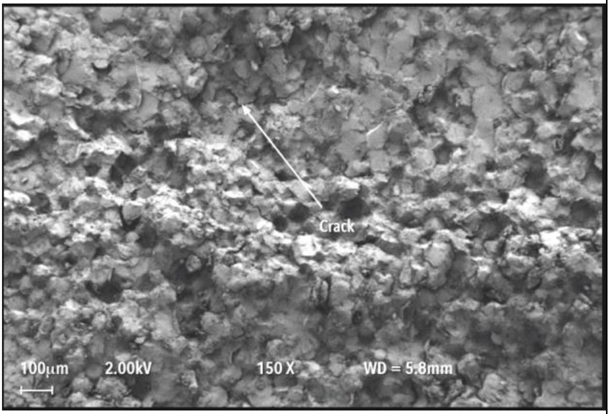
1,000×	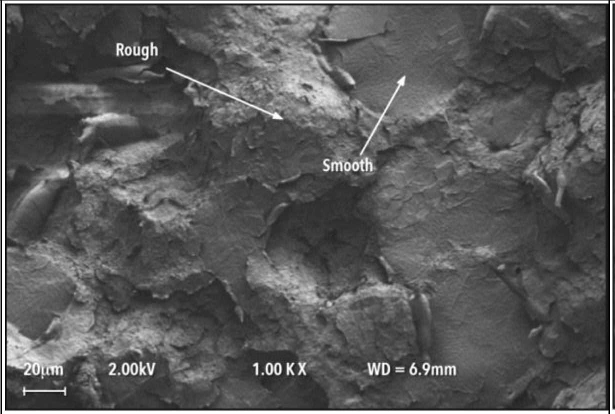	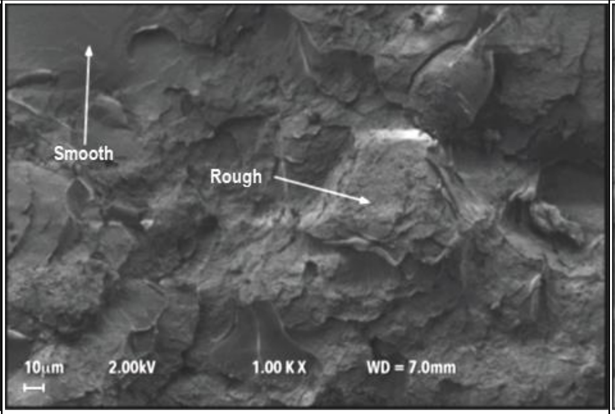	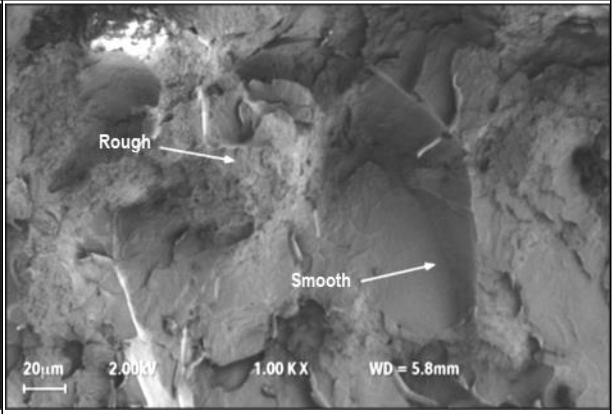

Figure 9.8. Fractured surfaces of denture specimens with fatigue cyclic loading during bending tests at different magnifications.

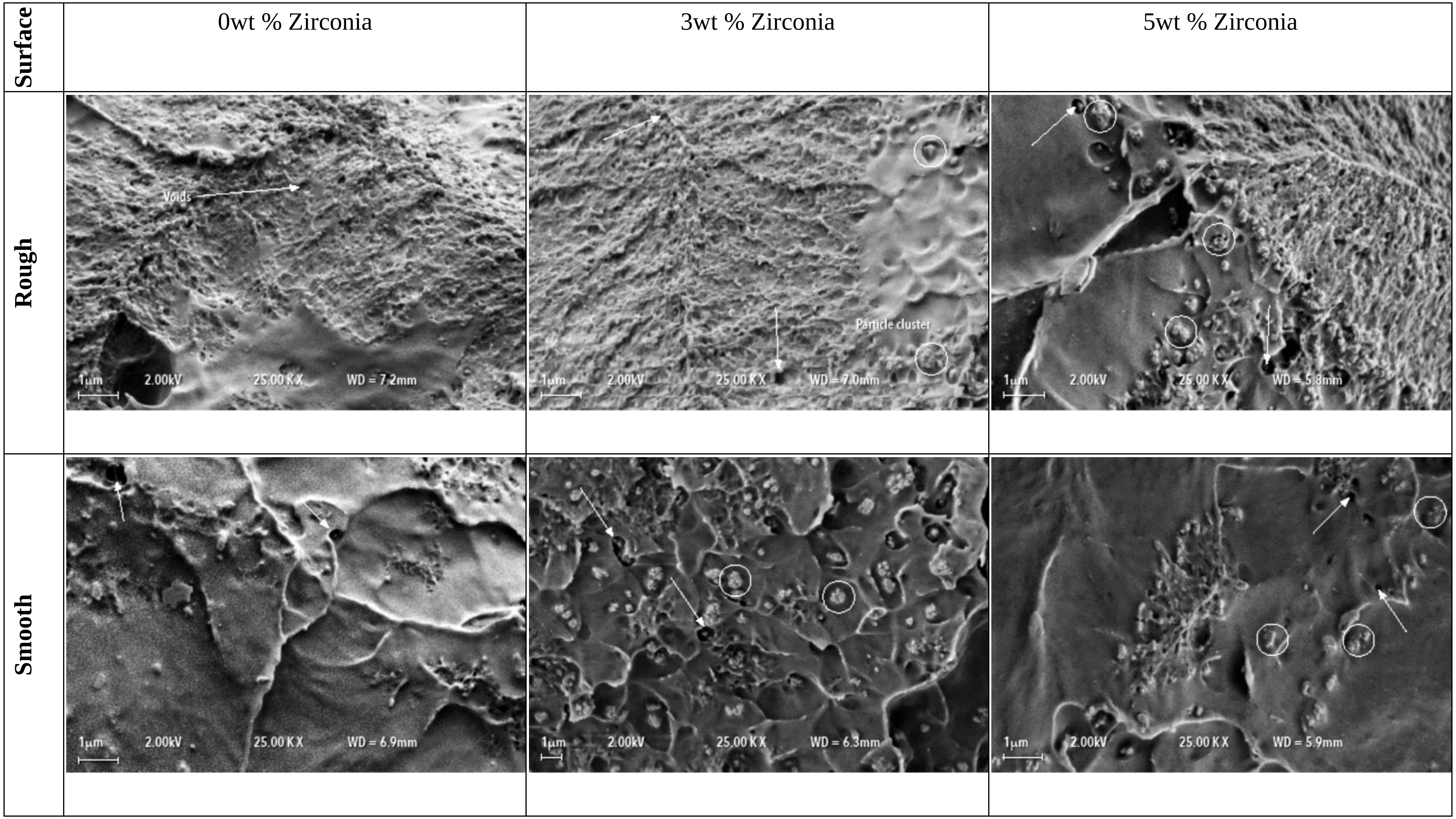

Figure 9.9. Fractured surfaces of dentures with fatigue cyclic loading during bending tests showing surface characteristics at 25,000×. Arrows indicate voids and circles indicate voids filled by zirconia particles.

9.5. DISCUSSION

This study evaluated the effect of fatigue cyclic loading on the equivalent flexural strength of complete (maxillary) dentures. The experimental data marginally supported the hypothesis of the study that without any fatigue cyclic loading the equivalent flexural strength of dentures manufactured of nanocomposite with 5 wt.% zirconia was significantly higher than the control group, but not significantly different from that with 3 wt.% zirconia.

The flexural strength of denture base materials is generally evaluated by a three-point bending test on a beam shape sample according to the British standard BS 2487:1989 (ISO 1567) using a beam shape sample (British Standards, 1989). The three-point bending, and the strength values are then calculated according to eq. 1. In this study, bending tests were conducted on real dentures in order to conduct experiments to as close a "real" situation as possible. Even though the loading arrangement for our experiments was same as that for a standardised beam shaped sample, the geometry was significantly different. Therefore, the calculated strength values were termed equivalent flexural strength. In a previous study, similar bending tests on actual dentures were conducted but no equivalent flexural strength was calculated, rather they measured other parameters such as toughness and stiffness. It should be noted that the equivalent flexural strength cannot be directly compared to the flexural strength values of the same materials in the authors' previous work (Zidan et al., 2019). However, improvements in equivalent flexural strength without fatigue cyclic loading for 5 wt.% (27.0 %) and 3 wt.% (19.55%) zirconia nanocomposite dentures when compared to the control group was comparable to the improvements in flexural strengths of the same nanocomposites when conducting three-point bending tests in the authors' previous work (Zidan et al., 2019). Additionally, using the equivalent flexural strength calculation whilst conducting bending tests directly on dentures could be considered more clinically relevant than standardised tests.

In this study, the increase in equivalent flexural strength with 3 wt.% and 5 wt.% of zirconia particles in HI PMMA could be related to the incorporation of nanoparticles with a size ranging from 30 nm to 100 nm, which is demonstrably smaller than HI PMMA powder particles (50 µm). The nanoparticles provide increased surface area to create stronger bonds between the acrylic matrix and the particles. However, the proportion of zirconia nanoparticles should be kept as relatively low as possible to ensure that they can be easily and uniformly embedded within the matrix resin without any significant particle clustering (Asar et al., 2013). An additional point to consider is a phenomenon called “transformation toughening”, which suggests nanoparticles are responsible for improving flexural strength by preventing or arresting crack propagation (Anusavice, 2003; Gad et al., 2018a; Zidan et al., 2019).

The surface of the hydrophobic polymer matrix does not wet or react well with the hydrophilic inorganic nano-fillers as result of the difference in surface energies (Asar et al., 2013). In order to improve wetting of the surfaces and adhesion bonding between the filler and matrix, the surface of hydrophobic fillers should be modified (Asar et al., 2013). According to previous studies, the application of silane treatment could play a major role in improving chemical bonds between fillers and polymer matrix, which could therefore increase fracture resistance (Yu et al., 2015; Yu et al., 2017). In this study, the surface of the zirconia nanoparticles was treated with a silane coupling agent that resulted in a strong adhesion between the surfaces of zirconia nanoparticles and PMMA matrix, thus leading to an improvement in the equivalent flexural strength of the nanocomposites (Gad et al., 2018a).

Furthermore, improved particle homogeneity in the HI MMA-zirconia nanoparticle mixture was ensured using a speed mixer machine, which was also thought to contribute to the improvement in the equivalent flexural strength. It is expected that a homogeneous distribution of zirconia particles would fill the spaces between linear chains of acrylic resin matrix. This would therefore restrict the segmental movements of the macromolecular chains and thus improve the flexural strength of the nanocomposite (Gad et al., 2019b).

After the application of fatigue loading cycles the hypothesis was rejected that, the nanocomposite dentures would display no statistically significant difference in equivalent flexural strength compared to the control group. However, 3 wt.% and 5 wt.% zirconia impregnated PMMA dentures showed a slight increase in equivalent flexural strength with fatigue cyclic loading. This implies that, under clinical conditions, the nanocomposite dentures would be either as good as, or better than, the control group.

After the fatigue cyclic loading in the mastication simulator for 250,000 cycles, denture specimens did not show any visible cracks or fracture failures, which was equivalent to a patient using a complete denture for approximately one year (Im et al., 2017). A mastication force of 40 N applied on the occlusal surface to each side of the premolar during simulation was similar to the chewing force on one side of the maxillary or mandibular complete dentures worn by a patient as reported in the literature (Im et al., 2017). Similar results were also found in the literature where the performance of acrylic resin denture reinforced with glass fibres and metal mesh was evaluated under a fatigue loading of 80N and 300,000 cycles. They concluded that the fatigue loading cycles might be insufficient to cause fatigue failure of the dentures (Im et al., 2017). This demonstrated agreement with this current study that no failure occurred after one year of fatigue loading cycles. However, this could be the reason for a decrease in flexural strength for all groups subjected to fatigue cyclic loading compared to that without fatigue cyclic loading. Generally, the fatigue strength of most materials decreased as a result of cyclic stress over a long period of time (Vallittu et al., 1994).

The mastication simulation did not fully represent the actual operation of dentures in a patient’s mouth. In clinical applications, the complete denture sits on flexible soft tissues in the mouth, and the load is applied on all occlusal surface areas during mastication. Furthermore, as indicated in previous studies, quantification of performance parameters such as fatigue weakening through applied force measurement was not conducted during the mastication tests (Kelly, 1969). In this study, only a qualitative performance evaluation was carried out by a pass or fail test under a certain number of fatigue cycles, which did not provide any information in relation to degradation behaviour over the time studied. Additionally, end of life tests of dentures through fracture were not conducted during the fatigue cycle as the unbroken dentures were needed to conduct the bending tests. Therefore, future research should focus on designing a new mastication simulator to simulate both maxillary and mandibular dentures with the facility to measure fatigue weakening force. Moreover, the fatigue cyclic loading could be increased to over 750,000 cycles, which is equivalent to three years of wearing a denture. It would also be interesting to continue the fatigue cyclic loading until the denture fails in order to differentiate the materials’ performances.

The classification of failure modes in this study was based on the location and propagation of fracture lines or cracks in the dentures from the point of loading or stress concentration at the palatal area. Only three types of failure were observed (midline fracture, crack and localised fracture) unlike the failures mentioned in the literature such as complete tooth failure and denture flange failure (Yu et al., 2015). In this study, both with and without fatigue cyclic loading, the fracture in the nanocomposite dentures started near the labial frenum and propagated either between the central, lateral and canine teeth or first premolar teeth from the polished surface toward the fitting surface, until it reached the loading point, thus resulting in a complete midline fracture. By comparison, one denture from the control group without fatigue cyclic loading showed a midline complete fracture. It is interesting to note that complete midline fractures occurred more frequently in the nanocomposite dentures than the control group. This could be explained by the fact that even though the addition of zirconia in PMMA could increase the equivalent flexural strength, at the same time it can also increase the overall brittleness of the denture.

The midline fracture might have occurred as result of the notch shape of the labial frenum, which is considered a potential weak point in the denture structure (Yu et al., 2017). Kelly et al. suggested that resistance to fatigue failure of dentures could be improved by eliminating contrasting surface contours such as deep notches at low frenal attachments during manufacture. Furthermore, acrylic resin should be carefully handled during denture fabrication as to avoid any contamination that could influence the presence of localised stress point (Kelly, 1969).

The SEM images of the denture specimens were also analysed after the bending tests without conducting any fatigue cyclic loading in the mastication simulation machine. No noticeable differences were observed in the failure mechanism of the dentures with and without the application of fatigue cyclic loading. Only the fractured surfaces from the dentures with fatigue cyclic loading are shown here to represent the worst-case scenario. It was also observed that the size of voids was of the same order as the size of the zirconia particles. Therefore, the particles would fill the empty spaces (Figure 9.9) and positively affect the strength of the denture. The SEM images also showed that the zirconia particles were fairly distributed within the PMMA matrix without significant particle clustering.

A limitation of this study is that several factors could contribute to the distributed results obtained for the equivalent flexural strengths. Even though the loading point on the denture was precisely measured and marked to obtain consistency throughout the experiments, it could be argued that the positioning of the loading head was not in the exact position every time during the bending tests. Emery paper was placed at the point of loading to avoid any major slipping of the loading head, but minor slipping could still also affect the results. Furthermore, although careful attention was given to make the denture specimens as identical as possible, any small variation during denture processing could affect the strength values. Only five specimens were tested for each group, however it could be argued that a larger sample size, for example ten, would give a better statistical distribution of the results.

HI PMMA with 3-5 wt. % of zirconia had only minor changes in the colour of the denture, which would therefore mean that it is aesthetically acceptable for clinical use. However, this may open opportunities for further investigation on adjusting its colour by adding natural biocompatible pigments. A general inspection of the specimens under standard illumination showed reduced translucent characteristics with increasing zirconia content, in line with the results found in the literature (Gad et al., 2019b). With zirconia-impregnated PMMA, the processing and manufacture of dentures for clinical application would avoid the issues faced with fibre or mesh reinforced dentures, such as longer processing times, incorrect positioning of the fibres within the denture, non-uniform distribution of fibres within the matrix, poor wetting of fibres across the smallest denture thickness and poor bonding between the fibres and the matrix due to lack of polymerisation (Pan et al., 2013).

9.6. CLINICAL IMPLICATIONS

This study suggested that maxillary complete removable dentures made of PMMA incorporating a small percentage (3-5 wt.%) of zirconia nanoparticles could additionally improve the equivalent flexural strength in clinical use when compared with the non-reinforced resin, leading to a longer operating life of the denture by resisting failure during mastication.

9.7. CONCLUSION

Removable complete dentures were made of High Impact (HI) heat-polymerized PMMA resin as a control group and HI PMMA reinforced with zirconia nanoparticles (3 wt.% and 5 wt.%) in order to compare their equivalent flexural strengths with and without applying fatigue loading. Higher equivalent flexural strengths were found for the specimens with 5 wt.% zirconia when the compared with 3 % zirconia and the control group, both with and without fatigue cyclic loading cycles. The specimens subjected to fatigue cyclic loading showed an observable decrease in the equivalent flexural strength, but these were not statistically significant when compared to the specimens without fatigue cyclic loading. The common failure modes in the dentures under bending were found to be midline fracture, localised fracture and cracking. Uniform distribution of zirconia particles was observed in the fractured specimens. Within the limitations of this study, it can be concluded that dentures made with 5% zirconia impregnated PMMA could have improved clinical longevity.

Chapter 10: Summary, Conclusions and Future Work

10.1. INTRODUCTION

Polymethyl methacrylate (PMMA) has been the most widely documented and used materials in prosthetic dentistry since 1937 (Ayad et al., 2008). HI PMMA acrylic resin reinforced with addition of rubber to conventional heat-cured acrylic resin has been successful in improving the impact strength of the denture base resins (Rodford, 1990). However, HI heat-cured PMMA resin has not been completely successful in improving all mechanical properties. One key weakness includes a reduction in stiffness or modulus of elasticity and hence the flexibility of the final denture base. Subsequently, its flexural strength for handling high impact has not been enhanced compared to the conventional heat-cured acrylic resins (Jagger et al., 2003; Zheng et al., 2012). The addition of zirconia (ZrO_2) nano particles (ZNP) in HI PMMA might produce a stronger denture base material with increased strength and fracture toughness. That same material may also exhibit a decrease of water sorption and solubility over a longer period than the conventional denture base materials. Figure 10.1 presents a summary of the properties evaluated for the nanocomposite through fundamental and functional characterisations.

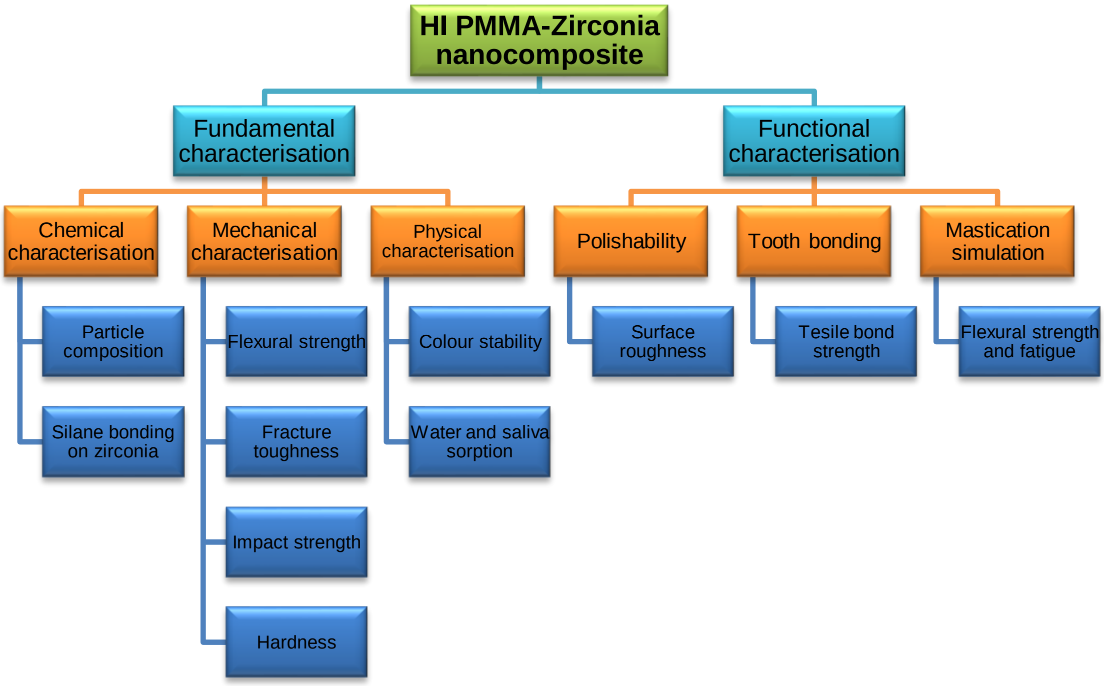

Figure 10.1. Characterisation summary of HI PMMA+ zirconia nanocomposite.

10.2. SELECTION OF THE METHODS

The methodologies for the preparation of specimens and their testing were carried out based on previous studies in the literature and relevant standards. However, due to technological advancements procedure for specimen preparation were altered to produce the best results with high consistency.

10.3. SUMMARY OF THE KEY FINDINGS

The first consideration for the present research was evaluating the mechanical properties of the HI PMMA-zirconia nanocomposites. This represents the conceptual stage of the material’s development. If a material does not meet certain strength requirements (defined by the relevant ISO specifications) there is no benefit of exploring potential patient acceptance of the material. Therefore, the first stage of testing explored whether the materials met the required standards for use as a dental material.

10.3.1. Chemical properties

Chapter 4 explored the effect of silane treatment of zirconia nanoparticles on flexural strength, flexural modulus and surface hardness of the HI PMMA denture base resin (control). The tests allowed to evaluate the properties of the nanocomposites in comparison with the HI PMMA denture base resins available on the market. The results of these experiments indicated that PMMA reinforced with silane treated ZNPs improved the flexural strength by 15% compared to the control group and by 40% compared to the nanocomposite with non-silanised zirconia. The flexural strengths of only the salinized and control groups met the British standard. These results were aligned with those by Zhang et al., who documented a significant increase in the flexural strength of PMMA with the addition of 2 wt.% and 3 wt.% of silanised zirconia and aluminium (Zhang et al., 2014). Use of silanised zirconia also increased surface hardness of the nanocomposite by 17% compared to the control group and 33% compared to non-silanised zirconia. Support for this finding can be found from a study by Lung et al., who found an increase in surface hardness of a dental resin reinforced with the silanised nano hydroxyapatite particles (Lung et al., 2016). The results also indicated an increase in flexural modulus, however only the nanocomposite group with silanised zirconia showed significantly higher value from that of the control group. The flexural modulus of both materials with added zirconia met the British Standard.

The improvements in mechanical properties mentioned above can be explained by the better adhesion between the zirconia and matrix facilitated by silanisation process, which forms a film of silane molecules around the filler particles, as confirmed by the FTIR analysis. The spectrum curve from the FTIR indicated the presence of the Zr-O-Si silanol groups that are produced by silane hydrolysis condensing with hydroxyl groups, forming a covalent bond.

These tests showed that the inclusion of silanised zirconia significantly improves the surface hardness and flexural strength of the composite. Flexural modulus was also increased with the addition of silanised zirconia, however, not significantly. These results suggest that the incorporation of silanised zirconia will improve the service life of the denture base owing to the improved mechanical properties resulted from enhancement of bonding between nanoparticles and HI PMMA.

10.3.2. Mechanical properties

With the strength of silanised zirconia-reinforced composites demonstrated, providing a ‘proof of concept’ for the inclusion of zirconia in denture base materials, it was then pertinent to examine how much zirconia to include in a potential denture. Chapter 5 explored the effect of incorporation of different weight percentages of zirconia on the flexural strength, flexural modulus and surface hardness, in addition to fracture toughness and impact strength. This can be viewed as finding the ‘sweet spot’, the ideal percentage of zirconia to be incorporated in the materials to be tested over longer periods of time.

Flexural strength was significantly enhanced (15%) by incorporation of 3 wt.% of zirconia nanoparticles versus the control. Furthermore, addition of zirconia at all loadings improved the flexural modulus, with 5 wt.% of zirconia resulting in the highest modulus. An explanation for the higher flexural strength and modulus values being observed at lower concentrations of zirconia is the uniformity of dispersion of nanoparticles (Gad et al., 2018a). At higher concentrations, zirconia nanoparticles tend to agglomerate, reducing the interfacial area between the zirconia and PMMA, thereby reducing the mechanical interlocking and flexibility. Similar findings can be found in the work of Alhareb et al., who observed a 16% increase in flexural strength with the reinforcement of PMMA with aluminium oxide and zirconia (Alhareb and Ahmad, 2011).

Fracture toughness decreased for all groups containing zirconia, except for the 5 wt.% group, which had an insignificant increase. However, of these reductions in fracture toughness, only the group with 10 wt.% zirconia was significantly different from the control. Although the impact strength of the composites was lowered by the addition of zirconia, for the groups containing 3 and 5 wt.% this reduction in impact strength was not significantly different from the control, with 5 wt.% showing the smallest decrease. The aforementioned tendency for agglomeration of nanoparticles can also be used to explain the decreases in fracture toughness observed in the present research. The agglomerations of nanoparticles may cause concentration of stresses in addition to restraining molecular movement, reducing the ability of the material to withstand the load. Furthermore, incorporation of zirconia, a hard ceramic, into the composite may increase the brittleness, thereby reducing the impact strength (Kundie et al., 2018).

Addition of any loading of zirconia increased the surface hardness of the composite compared to the control, with 7 and 10 wt.% groups significantly higher than the control in dry condition (day zero) and after a week immersion in water. However, following 45 days immersion in water the increase in hardness was not significantly higher than the control, with 3 and 5 wt.% groups showing the largest maintained increase. This increase in hardness can be attributed to the hardness of the tetragonal zirconia poly-crystals (Piconi and Maccauro, 1999). The softening observed after immersion may have been due to the leeching of residual monomers and water absorption (Hu et al., 2009).

In summation, the largest benefits in flexural strength and surface hardness were found with the addition of 3 wt.% zirconia, and the largest increases in fracture toughness and flexural modulus were found in the 5 wt.% group, which also saw the reduction in impact strength. These results suggest that the incorporation of between 3 and 5 wt.% of silanised zirconia would provide the optimum mechanical properties for a potential denture base.

10.3.3. Physical properties

Having established the mechanical stability of the material, and approximating the optimum loading of zirconia, Chapter 6 explored issues relating to longer-term use, sorption and solubility and those affecting patient acceptance, namely colour stability. This represents the second phase of testing, exploring the physical properties of the material over time.

Addition of zirconia lowered sorption after 90 days’ storage in both media, however these changes were not significant. 3 wt.% group had the lowest sorption in distilled water and 10 wt.% the lowest in saliva. After 180 days, addition of zirconia reduced solubility at all loadings in water compared to control group, however only 1.5 and 3 wt.% demonstrated lower solubility in saliva. None of these changes were statistically significant except for the increased solubility of 10 wt.% zirconia in saliva. It is important to state that all results for solubility in water, including the control, were above acceptable standards.

The lower water sorption values can be attributed to the long cure method of polymerisation increasing the degree of conversion and reducing voids (Garcia et al., 2010). A further explanation is the silane coupling agent provides better dispersion of the fillers throughout the polymer matrix which increasing the interfacial bonding between nanoparticles and PMMA matrix (Santos et al., 2002). The changes in solubility and sorption may be linked to the homogeneity of the material, with more homogenous materials absorbing less water and being less soluble (Pfeiffer and Rosenbauer, 2004). There was a correlation between the concentration of zirconia and the amount of sorption. This could have been due to the zirconia filling and voids in the PMMA resin, leaving less space for water to penetration. This was the explanation put forth by Alsharif et al, who observed higher silica loading resulted in the lowest mass change (Alsharif et al., 2013).

As the samples were immersed in water for a long time, sorption of water have been high enough to offset any mass lost by the leeching out of residual monomer (Dogan et al., 1995). The higher solubility in distilled water than saliva may be related to the higher amount of water absorbed providing an increased capacity for dissolution (Silva et al., 2008).

All loadings of zirconia negatively affected the colour and colour change of the material after storage for 180 days in both cleaners. Of these colour changes, the groups with 1.5 and 3 wt.% zirconia were clinically acceptable according to NBS unit standards, with 5 wt.% only slightly above the acceptable limit. The period of storage in this experiment (180 days) can be considered equivalent to 1.5 years' service, as one would expect the denture to be immersed in cleaner during sleep (approximately 8 hours a day). All colour change was in the form of whitening. A possible explanation for this is the sodium hypochlorite in Milton beaching the acrylic resin, as seen in previous studies (Goiato et al., 2013b). Davi et al. also found significant colour change when using cleaner with 1% sodium hypochlorite compared to less concentrated cleaners after 180 days (Davi et al., 2010). Further explanation from Hong links the colour change to residual monomer leaching out and the sorption of water (Hong et al., 2009). The changes in colour observed may also be attributed to the interaction of monomer with the glaze layer (Goiato et al., 2017).

Whilst two of the groups with zirconia were considered acceptable, there are some important caveats. Firstly, the increase in the colour changes suggests a loss of surface gloss. It has been reported that smoother surfaces prevent discolouring films from forming and facilitate plaque removal (Polyzois et al., 2013). In addition, it is important to note that the addition of zirconia at any loading drastically changed the colour of the composite prior to immersion, therefore although the colour change caused by the clearer may be acceptable, the issue of assessing the colour change caused by the incorporation of zirconia remains. One main limitation of the tests in this chapter was the small sample size, which should be increased to provide more representative data.

10.3.4. Polishability

Chapter 7 explores key issues relating to acceptance of the material by dental technicians, dentists and patients: polishing and surface roughness. Prior to polishing, all HI PMMA zirconia composites and control group had an unacceptably high surface roughness, However, all the nanocomposites showed lower Ra than the control group. After polishing one and two minute all experimental groups showed clinical acceptability ($Ra < 0.2\mu m$) of smooth surface, and the lower concentrations (1.5-5 wt.%) of zirconia provided values similar to the control group, which were recommended to prevent significant spread of microorganisms in the denture base nanocomposites. However, at high concentration of zirconia in group containing 10 wt.% was significantly increased the surface roughness in comparison to the control group. The group with 3 wt.% of zirconia was the smoothest for all groups, slightly better than of the control group.

Previous studies have similar findings: Ergun et al. found a significant increase in roughness with 20 wt.% of zirconia compared to 5 wt.% (Ergun et al., 2018). Al-Harbi et al., and Fouda et al. observed that the addition of nanodiamonds to PMMA in small concentrations (0.5 wt%) improved the smoothness of the surface, attributing this to the low ratio of small-size nanoparticles being able to fill in spaces in the polymeric chain (Al-Harbi et al., 2019; Fouda et al., 2019). SEM analysis results in chapter 7 indicated that the roughness of the samples with 7 and 10 wt.% zirconia was linked to clusters of nanoparticles visible on the composite surface. This supports the explanation that the reduction in the mechanical properties documented in Chapter 5 was due to the agglomeration of nanoparticles during mixing.

Another variable one must consider is the polishing method. While polishing was standardised for this experiment, many different techniques and products exist. The conventional polishing technique incorporating the use of pumice may also have attributed to high levels of polish that may not be achievable with other methods (Kuhar and Funduk, 2005).

10.3.5. Tooth bonding

Having concluded that the materials met the standards for both mechanical suitability and likelihood of patient acceptance, it was then necessary to investigate the use of the material for its intended purpose: a denture base. With the concept proven, Chapter 8 took the material and began testing it for its intended function– as a denture base to which artificial teeth are bound. The highest tensile bonding strength (TBS) value for central teeth was found in the group with 3 wt.% of zirconia and the highest for canine teeth was 1.5 wt.% zirconia, both of which were higher than the control of pure PMMA, although not significantly so.

The most common mode of failure was cohesive, fractures within the teeth. No pure adhesive failures at the interface between tooth and base were recorded. This indicates that the mechanical interlocking and chemical bonds between base and tooth were strong enough to maintain the denture's integrity, passing the TBS standards for a denture.

The lowest TBS results were found for the lateral teeth. One explanation for this is the relatively smaller contact areas and retention grooves resulting in less area of contact with the denture base. Cardash (1990) found that the highest TBS results were found in canines with vertical grooves that provided a larger surface area for bonding (Cardash et al., 1990).

There are multiple possible explanations for the reduction in tensile strength with the increased loading of zirconia. Firstly, one must consider the possibility that wax residue from the fabrication process might have remained on the teeth, leading to lower bonding strength (Spratley, 1987). It is also possible that the clustering of zirconia found at higher concentrations reduced the interaction between tooth and base (Zidan et al., 2019). Suzuki et al. showed that highly cross-linked resin teeth had poorer bonding to denture bases than conventional acrylic teeth (Suzuki et al., 1990). The addition of zirconia increased the hardness, and this may have affected the bond strength with, this could be related to hardness test in dry condition chapter 5. As most failure occurred within the teeth, it is fair to conclude that the bond strength was limited by the strength of the teeth, rather than the base materials (Andrade de Freitas et al., 2018). This is like the findings of Robison et al., who concluded that strength of the teeth defined bonding strength (Robison et al., 2016). No significant difference was found in TBS values between the control and lower loadings (1.5, 3 and 5 wt.%) of zirconia. However, composites with 7 and 10 wt.% of zirconia were had relatively poorer strength than the control. Again, composites with 3 and 5 wt.% zirconia offered the optimum results for a denture base.

10.3.6. Mastication simulation

Arriving at the conclusion that the material bonded well to artificial teeth, indicating its suitability for the intended function, the experiments of Chapter 9 explored the material with its intended form and function: the base of a denture, bonded to artificial teeth and used for mastication over a period of time. It was chosen to test denture based with 3 and 5 wt.% of zirconia as these loadings ranked highest across all previous experiments.

Flexural strength was highest in specimens with 5 wt% zirconia, both with and without fatigue loading. There was an insignificant decrease in flexural strength after fatigue cyclical loading. The improvements in equivalent flexural strength with the addition of zirconia were comparable to those seen in the three-point bending tests conducted in Chapter 5. The nanoparticles of zirconia are smaller than those of PMMA powder, providing an increased surface area resulting in stronger bonds between the matrix and the zirconia (Asar et al., 2013). As zirconia has demonstrated a tendency to cluster at higher concentrations, it is important to keep the concentration low enough to ensure uniform dispersal and embedding (Asar et al., 2013). Fracture resistance is improved by ‘transformation toughening’, whereby particles prevent crack propagation (Anusavice, 2003; Gad et al., 2018a; Zidan et al., 2019), and silane treatment improving the chemical bonds in the composite (Yu et al., 2015; Yu et al., 2017).

After fatigue loading simulation of a year of use, denture specimens did not show any visible cracks or fractures. The most common failure under bending (equivalent flexural strength) were midline fractures, localised fractures and cracking. Previous study conducted on denture base reinforced with glass fibres and metal mesh used (300,000 a fatigue cycles of 80 N) and the finding showed one year to be insufficient to cause fatigue failure of dentures (Im et al., 2017). However, this fatigue loading may have been the cause for the decrease in equivalent flexural strength following the mastication simulation. Generally, the fatigue strength of most materials decreased as a result of cyclic stress over a long period of time (Vallittu et al., 1994b).

10.4. CONCLUSIONS

From the results summary presented below, it can be concluded that the addition of zirconia at either 3 wt.% or 5 wt.% results in an improvement in the mechanical and physical properties of the HI PMMA as present in Table 10.1. Further improvement was also evidenced through functional tests such as polishability, mastication simulation and tooth bonding.

Addition of zirconia nanoparticles at low concentration (3 wt.% or 5 wt.%) in HI PMMA resin would provide the optimum mechanical properties for a potential denture base to reduce high incidence of fracture failure in clinical practice. However, the limitation of poor colour aesthetic (pale pink/white) needs to be addressed with the addition of biocompatible colour pigments.

Table 10.1. Summary table of test results of HI PMMA zirconia nanocomposite compared to the HI PMMA (control group).

Chapter Number	**Quality Tested**	**Control (pure HI PMMA)**	**Best HI PMMA-ZrO_2 nanocomposite percentage %**	**Improvement over control?**	**Significant difference from control**
4	Silanisation		3%	Yes	Yes
5	Flexural strength	(72.4 MPa)	3% (83.5 MPa)	Yes	Yes
	Flexural modulus	(1971 MPa)	5% (2419 MPa)	Yes	Yes
	Fracture toughness	(2.12 MPa $m^{1/2}$)	5% (2.14 MPa $m^{1/2}$)	Yes	No
	Impact strength	(10.0 kJ/m^2)	5% (9.05 kJ/m^2)	No	No
	Hardness in DW after 45 days	(15.5 kg/mm^2)	3% (17.3 kg/mm^2)	Yes	No
6	Sorption in DW after 90 days	(27.05 $\mu g/mm^3$)	3% (24.80$\mu g/mm^3$)	Yes	No
	Sorption in AS after 90 days	(25.17 $\mu g/mm^3$)	5% (23.77 $\mu g/mm^3$)	Yes	No
	Solubility in DW after 180 days	(8.01 $\mu g/mm^3$)	3% (3.78 $\mu g/mm^3$)	Yes	No
	Solubility in AS after 180 days	(-2.32 $\mu g/mm^3$)	3% (-3.03 $\mu g/mm^3$)	Yes	No
	Colour stability in DW after 180 days	(0.49 NBS unit)	3% (0.96 NBS unit)	No	Slight change
	Colour stability MIL	(1.01 NBS unit)	1.5% (2.76 NBS unit)	No	Noticeable change

	after 180 days				
	Colour stability STD after 180 days	(1.22 NBS unit)	1.5% (1.73 NBS unit)	No	Noticeable change
7	Surface Roughness after 1min polishing	(0.11 Ra (µm)	3% (0.11 Ra (µm)	No	No
	Surface Roughness after 2 min polishing	(0.12 Ra (µm)	3% (0.10 Ra (µm)	Yes	No
8	Tensile bond strength (Central)	(645.4 N)	3% (685.7 N)	Yes	No
	Tensile bond strength (Lateral)	(306.1 N)	1.5% (304.7 N)	No	No
	Tensile bond strength (Canine)	(496.7 N)	1.5% (514.0 N)	Yes	No
9	Equivalent Flexural Strength without fatigue	(106.3 MPa)	5 % (134.9 MPa)	Yes	Yes
	Equivalent Flexural Strength with fatigue	(100.6 MPa)	5 % (111.2 MPa)	Yes	No

10.5. FUTURE WORK AND RECOMMENDATIONS

Recommendations for future research:

Explore the use of zirconate silane coupling agent as an alternative to 3-trimethoxysilyl propyl methacrylate and the impact of this agent on the chemical bonding between the zirconia nanoparticles and acrylic resin.

Increasing the number of specimens in each group for experiments on sorption, solubility, colour stability and surface roughness to 10 or more in order to obtain a bigger group size, allowing the identification of statistical significance more easily.

Conduct experiments to evaluate elution and thermal expansion using artificial saliva to provide additional simulation of the oral environment.

Explore the impact of adding natural biocompatible colour pigments in HI PMMA+zirconia nanocomposite to provide a more aesthetically pleasing denture base.

Investigate the mechanical and physical properties of the nanocomposite with additional low concentrations of zirconia, especially at 2 wt.% and 4 wt.%. This will provide more data to allow for further refinement and optimisation of zirconia content.

Conduct further characterisation of the nanocomposite materials such as measuring gloss, opacity, wear resistance and thermal behaviour.

Explore the effects of different bonding method such as surface treatment of the teeth by monomer and adhesive, on the tensile bonding strength between the teeth and the nanocomposite. Further exploration of different bonding strength test, such as shear bonding, can also be carried out.

Employ the use of a newer mastication simulators to allow the simulation of chewing on both maxillary and mandibular dentures like in real life mastication. The number of cycles should also be increased to be equivalent to three years of use and continue testing until failure. Antimicrobial studies can also be conducted on optimisation of zirconia concentration to minimise the microbial activities on the surface.

References

Abdulwahhab, S. S. (2013). 'High-impact strength acrylic denture base material processed by autoclave', *J Prosthodont Res,* 57(4), pp. 288-93.

Abuzar, M. A., Bellur, S., Duong, N., Kim, B. B., Lu, P., Palfreyman, N., Surendran, D. & Tran, V. T. (2010). 'Evaluating surface roughness of a polyamide denture base material in comparison with poly (methyl methacrylate)', *J Oral Sci,* 52(4), pp. 577-81.

Agha, H., Flinton, R. & Vaidyanathan, T. (2016). 'Optimization of Fracture Resistance and Stiffness of Heat-Polymerized High Impact Acrylic Resin with Localized E-Glass FiBER FORCE(R) Reinforcement at Different Stress Points', *J Prosthodont,* 25(8), pp. 647-655.

Ahmed, M. A. & Ebrahim, M. I. (2014). 'Effect of Zirconium Oxide Nano-Fillers Addition on the Flexural Strength, Fracture Toughness, and Hardness of Heat-Polymerized Acrylic Resin', *World Journal of Nano Science and Engineering,* 04(02), pp. 50-57.

Alhareb, A., O & Ahmad, Z., A (2011). 'Effect of Al_2O3/ZrO_2 reinforcement on the mechanical properties of PMMA denture base', *Journal of Reinforced Plastics and Composites,* 30(1), pp. 86-93.

Akin, H., Kirmali, O., Tugut, F. & Coskun, M. E. (2014). 'Effects of different surface treatments on the bond strength of acrylic denture teeth to polymethylmethacrylate denture base material', *Photomed Laser Surg,* 32(9), pp. 512-6.

Alamoush, R.A., Silikas, N., Salim, N.A., Al-Nasrawi, S. and Satterthwaite, J.D., 2018. Effect of the composition of CAD/CAM composite blocks on mechanical properties. BioMed research international, 2018 (2018),pp.1-8.

Al-Dwairi, Z. N., Tahboub, K. Y., Baba, N. Z., Goodacre, C. J. & Ozcan, M. (2019). 'A Comparison of the Surface Properties of CAD/CAM and Conventional Polymethylmethacrylate (PMMA)', *J Prosthodont,* 28(4), pp. 452-457.

Al-Haddad, A., Vahid Roudsari, R. & Satterthwaite, J. D. (2014). 'Fracture toughness of heat cured denture base acrylic resin modified with Chlorhexidine and Fluconazole as bioactive compounds', *J Dent,* 42(2), pp. 180-4.

Al-Harbi, F. A., Abdel-Halim, M. S., Gad, M. M., Fouda, S. M., Baba, N. Z., AlRumaih, H. S. & Akhtar, S. (2019). 'Effect of Nanodiamond Addition on Flexural Strength, Impact Strength, and Surface Roughness of PMMA Denture Base', *J Prosthodont,* 28(1), pp. e417-e425.

Al-Mulla, M., Murphy, W., Huggett, R. & Brooks, S. (1989). 'Effect of water and artificial saliva on mechanical properties of some denture-base materials', *Dental Materials,* 5(6), pp. 399-402.

Alhareb, A. O., Akil, H. M. & Ahmad, Z. A. (2018). 'Effect of nitrile butadiene rubber/Al 2 O 3/YSZ fillers for PMMA denture base on the thermal and mechanical properties', *Journal of Thermal Analysis Calorimetry,* 134(2), pp. 941-951.

Alhavaz, A., Rezaei Dastjerdi, M., Ghasemi, A., Ghasemi, A. & Alizadeh Sahraei, A. (2017). 'Effect of untreated zirconium oxide nanofiller on the flexural strength and surface hardness of autopolymerized interim fixed restoration resins', *J Esthet Restor Dent*, 29(4), pp. 264-269.

Ali, I. L., Yunus, N. & Abu-Hassan, M. I. (2008). 'Hardness, flexural strength, and flexural modulus comparisons of three differently cured denture base systems', *J Prosthodont,* 17(7), pp. 545-9.

Alp, G., Johnston, W. M. & Yilmaz, B. (2019). 'Optical properties and surface roughness of prepolymerized poly(methyl methacrylate) denture base materials', *J Prosthet Dent,* 121(2), pp. 347-352.

Alshali, R. Z., Salim, N. A., Satterthwaite, J. D. & Silikas, N. (2015). 'Long-term sorption and solubility of bulk-fill and conventional resin-composites in water and artificial saliva', *J Dent,* 43(12), pp. 1511-8.

Alsharif, S. O., Hazizan, M. A., El-Aziz, N. A. A. & Ahmad, Z. A. (2013). Simulated Body Fluid Sorption and Solubility of Silica Reinforced Dental Resin Composites. *In:* Advanced Materials Research, 2013. Trans Tech Publ Ltd. 795(2013), pp. 626-630.

Altıncı, P. & Durkaya, P. (2016). 'Effects of thermocycling and various drinks on color stability of heat-polymerized acrylic resin', *Journal of Istanbul University Faculty of Dentistry,* 50(3), pp. 15-20.

Andrade de Freitas, S. L., Brandt, W. C., Miranda, M. E. & Vitti, R. P. (2018). 'Effect of Thermocycling, Teeth, and Polymerization Methods on Bond Strength Teeth-Denture Base', *Int J Dent,* 2018 (2018), pp. 1-5.

Andreopoulos, A. G. & Papanicolaou, G. C. (1987). 'Rubber-Modified Polymer Composites', *Journal of Materials Science,* 22(9), pp. 3417-3420.

Antonucci, J. M., Dickens, S. H., Fowler, B. O., Xu, H. H. & McDonough, W. G. (2005). 'Chemistry of Silanes: Interfaces in Dental Polymers and Composites', *J Res Natl Inst Stand Technol,* 110(5), pp. 541-58.

Anusavice, K. (2003). *Phillips' Science of Dental Materials 11th Edition*. USA: Saunders: Elsevier Inc., Maryland Heights, MO.

Anusavice, K. J., Shen, C. & Rawls, H. R. (2012). *Phillips' science of dental materials*: Elsevier Health Sciences.

Anusavice, K. J. S., Chiayi. Rawls, H. Ralph (2013). *Phillips' science of dental materials* (Twelfth edition. ed.): St. Louis, Missouri : Saunders.

Arikan, A., Ozkan, Y. K., Arda, T. & Akalin, B. (2005). 'An in vitro investigation of water sorption and solubility of two acetal denture base materials', *Eur J Prosthodont Restor Dent,* 13(3), pp. 119-22.

Asar, N. V., Albayrak, H., Korkmaz, T. & Turkyilmaz, I. (2013). 'Influence of various metal oxides on mechanical and physical properties of heat-cured polymethyl methacrylate denture base resins', *J Adv Prosthodont,* 5(3), pp. 241-7.

Ayad, N. M., Badawi, M. F. & Fatah, A. A. (2008). 'Effect of reinforcement of high-impact acrylic resin with zirconia on some physical and mechanical properties', *Rev Clin Pesq Odontol,* 4(3), pp. 145-51.

Ayaz, E. A., Altintas, S. H. & Turgut, S. (2014). 'Effects of cigarette smoke and denture cleaners on the surface roughness and color stability of different denture teeth', *J Prosthet Dent,* 112(2), pp. 241-8.

Ayaz, E. A. & Durkan, R. (2013). 'Influence of acrylamide monomer addition to the acrylic denture-base resins on mechanical and physical properties', *International Journal of Oral Science,* 5(4), pp. 229-235.

Barpal, D., Curtis, D. A., Finzen, F., Perry, J. & Gansky, S. A. (1998). 'Failure load of acrylic resin denture teeth bonded to high impact acrylic resins', *J Prosthet Dent*, 80(6), pp. 666-71.

Barron, D. J., Rueggeberg, F. A. & Schuster, G. S. (1992). 'A comparison of monomer conversion and inorganic filler content in visible light-cured denture resins', *Dent Mater,* 8(4), pp. 274-7.

Bartoloni, J. A., Murchison, D. F., Wofford, D. T. & Sarkar, N. K. (2000). 'Degree of conversion in denture base materials for varied polymerization techniques', *J Oral Rehabil,* 27(6), pp. 488-93.

Berger, J. C., Driscoll, C. F., Romberg, E., Luo, Q. & Thompson, G. (2006). 'Surface roughness of denture base acrylic resins after processing and after polishing', *J Prosthodont,* 15(3), pp. 180-6.

Bhardwaj, A., Bhardwaj, A., Misuriya, A., Maroli, S., Manjula, S. & Singh, A. K. (2014). 'Nanotechnology in dentistry: Present and future', *J Int Oral Health,* 6(1), pp.121-6.

Bonsor, S. J. & Pearson, G. J. (2013). *A clinical guide to applied dental materials*. London: Elsevier Churchill Livingstone.

British Standards. (1989). British Standard Specification for Denture base Polymers. London: British Standards Institution(BSI) BS 2487:1989 ISO 1567:1988, pp. 1-9.

British Standards. (2001). Dentistry-Denture base polymers. London.: British Standard Institution (BSI) BS EN ISO 1567:2001, pp. 1-28.

British Standards. (2008). Dentistry-Base polymers Part 1: Denture base polymers. London : Biritish Standards Institution (BSI) BS EN ISO 20795-1:2008, pp. 1-36.

British Standards. (2017). Dentistry-Artificial teeth for dental prostheses. London: British Standards Institution (BSI) BS EN ISO 22112: 2017, pp. 1-17.

Bural, C., Aktas, E., Deniz, G., Unlucerci, Y. & Bayraktar, G. (2011). 'Effect of leaching residual methyl methacrylate concentrations on in vitro cytotoxicity of heat polymerized denture base acrylic resin processed with different polymerization cycles', *J Appl Oral Sci,* 19(4), pp. 306-12.

Cardash, H. S., Applebaum, B., Baharav, H. & Liberman, R. (1990). 'Effect of retention grooves on tooth-denture base bond', *J Prosthet Dent,* 64(4), pp. 492-6.

Cardash, H. S., Liberman, R. & Helft, M. (1986). 'The effect of retention grooves in acrylic resin teeth on tooth denture-base bond', *J Prosthet Dent,* 55(4), pp. 526-8.

Carroll, C. E. & von Fraunhofer, J. A. (1984). 'Wire reinforcement of acrylic resin prostheses', *J Prosthet Dent,* 52(5), pp. 639-41.

Cavalcanti, A. N., Foxton, R. M., Watson, T. F., Oliveira, M. T., Giannini, M. & Marchi, G. M. (2009). 'Y-TZP ceramics: key concepts for clinical application', *Oper Dent,* 34(3), pp. 344-51.

Celebi, N., Yuzugullu, B., Canay, S. & Yucel, U. (2008). 'Effect of polymerization methods on the residual monomer level of acrylic resin denture base polymers', *Polymers for Advanced Technologies,* 19(3), pp. 201-206.

Cevik, P. & Yildirim-Bicer, A. Z. (2018). 'The Effect of Silica and Prepolymer Nanoparticles on the Mechanical Properties of Denture Base Acrylic Resin', *J Prosthodont,* 27(8), pp. 763-770.

Chaves, C. A., Regis, R. R., Machado, A. L. & Souza, R. F. (2009). 'Effect of ridge lap surface treatment and thermocycling on microtensile bond strength of acrylic teeth to denture base resins', *Braz Dent J,* 20(2), pp. 127-31.

Chow, W. S., Tham, W. L. & Ishak, Z. A. M. (2012). 'Improvement of Microstructure and Properties of Poly(methyl methacrylate)/Hydroxyapatite Composites Treated with Zirconate Coupling Agent', *Journal of Thermoplastic Composite Materials,* 25(2), pp. 165-180.

Christel, P., Meunier, A., Heller, M., Torre, J. P. & Peille, C. N. (1989). 'Mechanical properties and short-term in-vivo evaluation of yttrium-oxide-partially-stabilized zirconia', *J Biomed Mater Res,* 23(1), pp. 45-61.

Cierech, M., Wojnarowicz, J., Szmigiel, D., Baczkowski, B., Grudniak, A. M., Wolska, K. I., Lojkowski, W. & Mierzwinska-Nastalska, E. (2016). 'Preparation and characterization of ZnO-PMMA resin nanocomposites for denture bases', *Acta Bioeng Biomech,* 18(2), pp. 31-41.

Clancy, J. M. & Boyer, D. B. (1989). 'Comparative bond strengths of light-cured, heat-cured, and autopolymerizing denture resins to denture teeth', *J Prosthet Dent,* 61(4), pp. 457-62.

Clark, W. A. & Hsu, Y. T. (2014). 'The effect of autopolymerizing acrylic resin thickness on the bond strength of a repaired denture tooth', *J Prosthodont,* 23(7), pp. 528-33.

Clements, J. L., Tantbirojn, D., Versluis, A. & Cagna, D. R. (2018). 'Do denture processing techniques affect the mechanical properties of denture teeth?', *J Prosthet Dent,* 120(2), pp. 246-251.

Co, M. C. (1988). *Chroma Meter CR-200/CR-210/CR-221/CR-231. Hand Book.* Minotta GmbH., Ltd, (Vol. 3).

Colebeck, A. C., Monaco, E. A., Jr., Pusateri, C. R. & Davis, E. L. (2015). 'Microtensile bond strength of different acrylic teeth to high-impact denture base resins', *J Prosthodont,* 24(1), pp. 43-51.

Combe, E. C., Burke, F. T. & Douglas, W. H. (1999). *Dental biomaterials*: Kluwer Academic Publishers.

Consani, R. L., Folli, B. L., Nogueira, M. C., Correr, A. B. & Mesquita, M. F. (2016). 'Effect of Polymerization Cycles on Gloss, Roughness, Hardness and Impact Strength of Acrylic Resins', *Braz Dent J,* 27(2), pp. 176-80.

Craig, R. G., Powers, J. M. & Wataha, J. C. (2004). *Dental materials : properties and manipulation* (8th ed).: St. Louis, Mo. : Mosby.

Cunningham, J. L. (1993). 'Bond strength of denture teeth to acrylic bases', *J Dent,* 21(5), pp. 274-80.

Cunningham, J. L. & Benington, I. C. (1999). 'An investigation of the variables which may affect the bond between plastic teeth and denture base resin', *Journal of Dentistry,* 27(2), pp. 129-135.

da Silva, L. H., Feitosa, S. A., Valera, M. C., de Araujo, M. A. & Tango, R. N. (2012). 'Effect of the addition of silanated silica on the mechanical properties of microwave heat-cured acrylic resin', *Gerodontology,* 29(2), pp. e1019-23.

Davi, L. R., Peracini, A., Ribeiro Nde, Q., Soares, R. B., da Silva, C. H., Paranhos Hde, F. & de Souza, R. F. (2010). 'Effect of the physical properties of acrylic resin of overnight immersion in sodium hypochlorite solution', *Gerodontology,* 27(4), pp. 297-302.

de Souza Leão, R., de Moraes, S. L. D., de Luna Gomes, J. M., Lemos, C. A. A., da Silva Casado, B. G., do Egito Vasconcelos, B. C. & Pellizzer, E. P. (2019). 'Influence of addition of zirconia on PMMA: A systematic review', *Materials Science and Engineering: C,*(2019), pp. 1-8.

Denry, I. & Kelly, J. R. (2008). 'State of the art of zirconia for dental applications', *Dent Mater,* 24(3), pp. 299-307.

Diaz-Arnold, A. M., Vargas, M. A., Shaull, K. L., Laffoon, J. E. & Qian, F. (2008). 'Flexural and fatigue strengths of denture base resin', *J Prosthet Dent,* 100(1), pp. 47-51.

Dogan, A., Bek, B., Cevik, N. N. & Usanmaz, A. (1995). 'The Effect of Preparation Conditions of Acrylic Denture Base Materials on the Level of Residual Monomer, Mechanical-Properties and Water-Absorption', *Journal of Dentistry,* 23(5), pp. 313-318.

Durkan, R., Ayaz, E. A., Bagis, B., Gurbuz, A., Ozturk, N. & Korkmaz, F. M. (2013). 'Comparative effects of denture cleansers on physical properties of polyamide and polymethyl methacrylate base polymers', *Dent Mater J,* 32(3), pp. 367-75.

Elbishari, H. I. (2012). Characterisation of the effect of filler size on handling, mechanical and surface properties of resin composites. *PhD Doctoral dissertation*, The University of Manchester (United Kingdom)

Elshereksi, N. W., Ghazali, M. J., Muchtar, A. & Azhari, C. H. (2014). 'Perspectives for Titanium-Derived Fillers Usage on Denture Base Composite Construction: A

Review Article', *Advances in Materials Science and Engineering,* 2014(2014), p. 1-13.

Elshereksi, N. W., Ghazali, M. J., Muchtar, A. & Azhari, C. H. (2017). 'Studies on the effects of titanate and silane coupling agents on the performance of poly (methyl methacrylate)/barium titanate denture base nanocomposites', *J Dent,* 56(2017), pp. 121-132.

Ergun, G., Sahin, Z. & Ataol, A. S. (2018). 'The effects of adding various ratios of zirconium oxide nanoparticles to poly(methyl methacrylate) on physical and mechanical properties', *Journal of Oral Science,* 60(2), pp. 304-315.

European International Standard. (2000). Plastics-Detrmination of Charpy impact properties Part 1: Non-instrumented impact test. Switzerland: European International Standard Organization EN ISO 179-1:2000, pp. 1-20.

Fajardo, R. S., Pruitt, L. A., Finzen, F. C., Marshall, G. W., Singh, S. & Curtis, D. A. (2011). 'The effect of E-glass fibers and acrylic resin thickness on fracture load in a simulated implant-supported overdenture prosthesis', *J Prosthet Dent,* 106(6), pp. 373-7.

Fan, F. Q., Xia, Z. B., Li, Q. Y., Li, Z. & Chen, H. Q. (2013). 'ZrO_2/PMMA Nanocomposites: Preparation and Its Dispersion in Polymer Matrix', *Chinese Journal of Chemical Engineering,* 21(2), pp. 113-120.

Faot, F., Costa, M. A., Del Bel Cury, A. A. & Rodrigues Garcia, R. C. (2006). 'Impact strength and fracture morphology of denture acrylic resins', *J Prosthet Dent,* 96(5), pp. 367-73.

Farina, A. P., Cecchin, D., Soares, R. G., Botelho, A. L., Takahashi, J. M., Mazzetto, M. O. & Mesquita, M. F. (2012). 'Evaluation of Vickers hardness of different types of acrylic denture base resins with and without glass fibre reinforcement', *Gerodontology,* 29(2), pp. e155-60.

Ferracane, J. L. (2001). *Materials in dentistry : principles and applications* (2nd ed). Philadelphia: Lippincott Williams & Wilkins.

Figueroa, R. M. S., Conterno, B., Arrais, C. A. G., Sugio, C. Y. C., Urban, V. M. & Neppelenbroek, K. H. (2018). 'Porosity, water sorption and solubility of denture base acrylic resins polymerized conventionally or in microwave', *Journal of Applied Oral Science,* 26(2018), pp. 1-7.

Fouda, S. M., Gad, M. M., Ellakany, P., Al-Thobity, A. M., Al-Harbi, F. A., Virtanen, J. I. & Raustia, A. (2019). 'The effect of nanodiamonds on candida albicans adhesion and surface characteristics of PMMA denture base material - an in vitro study', *Journal of Applied Oral Science,* 27(2019), pp. 1-10.

Gad, M., ArRejaie, A. S., Abdel-Halim, M. S. & Rahoma, A. (2016a). 'The Reinforcement Effect of Nano-Zirconia on the Transverse Strength of Repaired Acrylic Denture Base', *Int J Dent,* 2016(2016), pp. 1-6.

Gad, M. M. & Abualsaud, R. (2019a). 'Behavior of PMMA Denture Base Materials Containing Titanium Dioxide Nanoparticles: A Literature Review', *Int J Biomater,* 2019(2019), p. 1-14.

Gad, M. M., Abualsaud, R., Rahoma, A., Al-Thobity, A. M., Al-Abidi, K. S. & Akhtar, S. (2018a). 'Effect of zirconium oxide nanoparticles addition on the optical and tensile properties of polymethyl methacrylate denture base material', *Int J Nanomedicine,* 13(2018), pp. 283-292.

Gad, M. M., Al-Thobity, A. M., Rahoma, A., Abualsaud, R., Al-Harbi, F. A. & Akhtar, S. (2019b). 'Reinforcement of PMMA Denture Base Material with a Mixture of ZrO_2 Nanoparticles and Glass Fibers', *Int J Dent,* 2019(2019), pp. 1-11.

Gad, M. M., Fouda, S. M., Al-Harbi, F. A., Napankangas, R. & Raustia, A. (2017). 'PMMA denture base material enhancement: a review of fiber, filler, and nanofiller addition', *Int J Nanomedicine,* 12(2017), pp. 3801-3812.

Gad, M. M., Rahoma, A. & Al-Thobity, A. M. (2018b). 'Effect of polymerization technique and glass fiber addition on the surface roughness and hardness of PMMA denture base material', *Dent Mater J,* 37(5), pp. 746-753.

Gad, M. M., Rahoma, A., Al-Thobity, A. M. & ArRejaie, A. S. (2016b). 'Influence of incorporation of ZrO_2 nanoparticles on the repair strength of polymethyl methacrylate denture bases', *Int J Nanomedicine*, 11(2016), pp. 5633-5643.

Gahlert, M., Gudehus, T., Eichhorn, S., Steinhauser, E., Kniha, H. & Erhardt, W. (2007). 'Biomechanical and histomorphometric comparison between zirconia implants with varying surface textures and a titanium implant in the maxilla of miniature pigs', *Clinical Oral Implants Research,* 18(5), pp. 662-668.

Garcia, L. D. R., Roselino, L. D. R., Mundim, F. M., Pires-de-Souza, F. D. P. & Consani, S. (2010). 'Influence of Artificial Accelerated Aging on Dimensional Stability of Acrylic Resins Submitted to Different Storage Protocols', *Journal of Prosthodontics-Implant Esthetic and Reconstructive Dentistry,* 19(6), pp. 432-437.

Goiato, M. C., Dos Santos, D. M., Baptista, G. T., Moreno, A., Andreotti, A. M., Bannwart, L. C. & Dekon, S. F. (2013a). 'Effect of thermal cycling and disinfection on colour stability of denture base acrylic resin', *Gerodontology,* 30(4), pp. 276-82.

Goiato, M. C., Freitas, E., dos Santos, D., de Medeiros, R. & Sonego, M. (2015). 'Acrylic Resin Cytotoxicity for Denture Base--Literature Review', *Adv Clin Exp Med,* 24(4), pp. 679-686.

Goiato, M. C., Nobrega, A. S., dos Santos, D. M., Andreotti, A. M. & Moreno, A. (2014). 'Effect of different solutions on color stability of acrylic resin-based dentures', *Braz Oral Res,* 28(1), pp. 1-7.

Goiato, M. C., Sônego, M. V., de Barros Carneiro, D., da Silva, E. V. F., da Rocha Bonatto, L., Rangel, E. C. & Dos Santos, D. M. (2017). 'Evaluation of a glaze polishing technique for pigmented denture acrylic resin submitted to thermocycling and disinfection', *Journal of International Oral Health,* 9(5), pp. 213-221.

Goiato, M. C., Zuccolotti, B. C., dos Santos, D. M., Sinhoreti, M. A. & Moreno, A. (2013b). 'Effect of intrinsic nanoparticle pigmentation on the color stability of denture base acrylic resins', *J Prosthet Dent,* 110(2), pp. 101-6.

Gungor, H., Gundogdu, M., Alkurt, M. & Yesil Duymus, Z. (2017). 'Effect of polymerization cycles on flexural strengths and microhardness of different denture base materials', *Dent Mater J,* 36(2), pp. 168-173.

Gungor, H., Gundogdu, M. & Yesil Duymus, Z. (2014). 'Investigation of the effect of different polishing techniques on the surface roughness of denture base and repair materials', *J Prosthet Dent,* 112(5), pp. 1271-7.

Gurbuz, O., Unalan, F. & Dikbas, I. (2010). 'Comparative study of the fatigue strength of five acrylic denture resins', *J Mech Behav Biomed Mater,* 3(8), pp. 636-9.

Hamza, T. A., Rosenstiel, S. F., Elhosary, M. M. & Ibraheem, R. M. (2004). 'The effect of fiber reinforcement on the fracture toughness and flexural strength of provisional restorative resins', *J Prosthet Dent,* 91(3), pp. 258-64.

Hatrick, C. D. (2011). *Dental materials : clinical applications for dental assistants and dental hygienists* (2nd ed). Maryland Heights, Mo. Saunders/Elsevier.

Hiramatsu, D. A., Moretti-Neto, R. T., Ferraz, B. F. R., Porto, V. C. & Rubo, J. H. (2011). 'Roughness and porosity of provisional crowns', *RPG. Revista de Pós-Graduação,* 18(2), pp. 108-112.

Ho, T. K., Satterthwaite, J. D. & Silikas, N. (2018). 'The effect of chewing simulation on surface roughness of resin composite when opposed by zirconia ceramic and lithium disilicate ceramic', *Dental Materials,* 34(2), pp. E15-E24.

Hong, G., Murata, H., Li, Y., Sadamori, S. & Hamada, T. (2009). 'Influence of denture cleansers on the color stability of three types of denture base acrylic resin', *J Prosthet Dent,* 101(3), pp. 205-13.

Honorez, P., Catalan, A., Angnes, U. & Grimonster, J. (1989). 'The effect of three processing cycles on some physical and chemical properties of a heat-cured acrylic resin', *The Journal of prosthetic dentistry,* 61(4), pp. 510-517.

Hu, Y. Q., Zhou, S. X. & Wu, L. M. (2009). 'Surface mechanical properties of transparent poly(methyl methacrylate)/zirconia nanocomposites prepared by in situ bulk polymerization', *Polymer,* 50(15), pp. 3609-3616.

Ilie, N., Hilton, T., Heintze, S., Hickel, R., Watts, D., Silikas, N., Stansbury, J., Cadenaro, M. & Ferracane, J. (2017). 'Academy of dental materials guidance—Resin composites: Part I—Mechanical properties', *Dental materials,* 33(8), pp. 880-894.

Im, S. M., Huh, Y. H., Cho, L. R. & Park, C. J. (2017). 'Comparison of the fracture resistances of glass fiber mesh- and metal mesh-reinforced maxillary complete denture under dynamic fatigue loading', *Journal of Advanced Prosthodontics,* 9(1), pp. 22-30.

Izumida, F. E., Ribeiro, R. C., Giampaolo, E. T., Machado, A. L., Pavarina, A. C. & Vergani, C. E. (2011). 'Effect of microwave disinfection on the surface roughness of three denture base resins after tooth brushing', *Gerodontology,* 28(4), pp. 277-82.

Jagger, D., Harrison, A., Jagger, R. & Milward, P. (2003). 'The effect of the addition of poly(methyl methacrylate) fibres on some properties of high strength heat-cured acrylic resin denture base material', *J Oral Rehabil,* 30(3), pp. 231-5.

Jagger, D. C., Harrison, A. & Jandt, K. D. (1999). 'The reinforcement of dentures', *J Oral Rehabil,* 26(3), pp. 185-94.

Jagger, D. C., Jagger, R. G., Allen, S. M. & Harrison, A. (2002). 'An investigation into the transverse and impact strength of "high strength" denture base acrylic resins', *J Oral Rehabil,* 29(3), pp. 263-7.

Jagger, R. (1978). 'Effect of the curing cycle on some properties of a polymethylmethacrylate denture base material', *Journal of oral rehabilitation,* 5(2), pp. 151-157.

Jang, D. E., Lee, J. Y., Jang, H. S., Lee, J. J. & Son, M. K. (2015). 'Color stability, water sorption and cytotoxicity of thermoplastic acrylic resin for non metal clasp denture', *J Adv Prosthodont,* 7(4), pp. 278-87.

Jar, P. Y., Lee, R., Shinmura, T. & Konishi, K. (1999). 'Rubber particle cavitation on toughness enhancement of SMI-modified poly (acrylonitrile-butadiene-styrene)', *Journal of Polymer Science Part B: Polymer Physics,* 37(14), pp. 1739-1748.

Jerolimov, V., Brooks, S. C., Huggett, R. & Bates, J. F. (1989). 'Rapid curing of acrylic denture-base materials', *Dent Mater,* 5(1), pp. 18-22.

John, J., Gangadhar, S. A. & Shah, I. (2001). 'Flexural strength of heat-polymerized polymethyl methacrylate denture resin reinforced with glass, aramid, or nylon fibers', *J Prosthet Dent,* 86(4), pp. 424-7.

Johnson, W. W. (1959). 'The history of prosthetic dentistry', *The Journal of Prosthetic Dentistry,* 9(5), pp. 841-846.

Johnston, E. P., Nicholls, J. I. & Smith, D. E. (1981). 'Flexure Fatigue of 10 Commonly Used Denture Base Resins', *Journal of Prosthetic Dentistry,* 46(5), pp. 478-483.

Jorge, J. H., Giampaolo, E. T., Vergani, C. E., Machado, A. L., Pavarina, A. C. & Carlos, I. Z. (2007). 'Biocompatibility of denture base acrylic resins evaluated in culture of L929 cells. Effect of polymerisation cycle and post-polymerisation treatments', *Gerodontology,* 24(1), pp. 52-7.

Kanie, T., Fujii, K., Arikawa, H. & Inoue, K. (2000). 'Flexural properties and impact strength of denture base polymer reinforced with woven glass fibers', *Dent Mater,* 16(2), pp. 150-8.

Karabela, M. M. & Sideridou, I. D. (2008). 'Effect of the structure of silane coupling agent on sorption characteristics of solvents by dental resin-nanocomposites', *Dent Mater,* 24(12), pp. 1631-9.

Karci, M., Demir, N. & Yazman, S. (2019). 'Evaluation of Flexural Strength of Different Denture Base Materials Reinforced with Different Nanoparticles', *J Prosthodont,* 28(5), pp. 572-579.

Kawai, N., Lin, J., Youmaru, H., Shinya, A. & Shinya, A. (2012). 'Effects of three luting agents and cyclic impact loading on shear bond strengths to zirconia with tribochemical treatment', *Journal of Dental Sciences,* 7(2), pp. 118-124.

Kelly, E. (1969). 'Fatigue failure in denture base polymers', *J Prosthet Dent,* 21(3), pp. 257-66.

Keyf, F. & Etikan, I. (2004). 'Evaluation of gloss changes of two denture acrylic resin materials in four different beverages', *Dent Mater,* 20(3), pp. 244-51.

Kim, H. H., Kim, M. J., Kwon, H. B., Lim, Y. J., Kim, S. K. & Koak, J. Y. (2012). 'Strength and cytotoxicity in glass-fiber-reinforced denture base resin with changes in the monomer', *Journal of Applied Polymer Science,* 126(S2), pp. E260-E266.

Kim, S. H. & Watts, D. C. (2004). 'The effect of reinforcement with woven E-glass fibers on the impact strength of complete dentures fabricated with high-impact acrylic resin', *J Prosthet Dent,* 91(3), pp. 274-80.

Kim, S. K., Park, J. M., Lee, M. H., Jung, J. Y., Li, S. P. & Wang, X. Y. (2009). 'Effects of chairside polishing and brushing on surface roughness of acrylic denture base resins', *Journal of Wuhan University of Technology-Materials Science Edition,* 24(1), pp. 100-105.

Kinloch, A.J. and Young, R.J., 1983. Fracture Behavior of Polymers Applied Science Pub.

Koksal, T. & Dikbas, I. (2008). 'Color stability of different denture teeth materials against various staining agents', *Dental Materials Journal,* 27(1), pp. 139-144.

Komine, F., Blatz, M. B. & Matsumura, H. (2010). 'Current status of zirconia-based fixed restorations', *J Oral Sci,* 52(4), pp. 531-9.

Korkmaz, T., Dogan, A., Murat Dogan, O. & Demir, H. (2010). 'The bond strength of a highly cross-linked denture tooth to denture base polymers: a comparative study', *J Journal of Adhesive Dentistry,* 13(1), pp. 1-8.

Koroglu, A., Ozdemir, T. & Usanmaz, A. (2009). 'Comparative Study of the Mechanical Properties of Fiber-Reinforced Denture Base Resin', *Journal of Applied Polymer Science,* 113(2), pp. 716-720.

Kuhar, M. & Funduk, N. (2005). 'Effects of polishing techniques on the surface roughness of acrylic denture base resins', *J Prosthet Dent,* 93(1), pp. 76-85.

Kundie, F., Azhari, C. H. & Ahmad, Z. A. (2018). 'Effect of nano-and micro-alumina fillers on some properties of poly(methyl methacrylate) denture base composites', *Journal of the Serbian Chemical Society,* 83(1), pp. 75-91.

Kurt, M., Saraç, Y. Ş., Ural, Ç. & Saraç, D. J. G. (2012). 'Effect of pre-processing methods on bond strength between acrylic resin teeth and acrylic denture base resin', Gerodontology, 29(2), pp. e357-e362.

Li, B. B., Xu, J. B., Cui, H. Y., Lin, Y. & Di, P. (2016). 'In vitro evaluation of the flexural properties of All-on-Four provisional fixed denture base resin partially reinforced with fibers', *Dent Mater J,* 35(2), pp. 264-9.

Liberman, R., Combe, E. C., Piddock, V., Pawson, C. & Watts, D. C. (1995). 'Development and assessment of an objective method of colour change measurement for acrylic denture base resins', *J Oral Rehabil,* 22(6), pp. 445-9.

Lung, C. Y., Sarfraz, Z., Habib, A., Khan, A. S. & Matinlinna, J. P. (2016). 'Effect of silanization of hydroxyapatite fillers on physical and mechanical properties of a bis-GMA based resin composite', *J Mech Behav Biomed Mater,* 54(2016), pp. 283-94.

MacGregor, A. R., Graham, J., Stafford, G. D. & Huggett, R. (1984). 'Recent experiences with denture polymers', *J Dent,* 12(2), pp. 146-57.

Machado, A. L., Bochio, B. C., Wady, A. F., Jorge, J. H., Canevarolo, S. V., Jr. & Vergani, C. E. (2012a). 'Impact strength of denture base and reline acrylic resins: An in vitro study', *J Dent Biomech,* 3(2012), pp. 1-7.

Machado, A. L., Breeding, L. C., Vergani, C. E. & da Cruz Perez, L. E. (2009). 'Hardness and surface roughness of reline and denture base acrylic resins after repeated disinfection procedures', *J Prosthet Dent,* 102(2), pp. 115-22.

Machado, A. L., Puckett, A. D., Breeding, L. C., Wady, A. F. & Vergani, C. E. (2012b). 'Effect of thermocycling on the flexural and impact strength of urethane-based and high-impact denture base resins', *Gerodontology,* 29(2), pp. e318-23.

Machado Cucci, A. L., Vergani, C. E., Giampaolo, E. T. & da Silveira Ferreira Afonso, M. C. (1998). 'Water sorption, solubility, and bond strength of two autopolymerizing acrylic resins and one heat-polymerizing acrylic resin', *The Journal of prosthetic dentistry,* 80(4), pp. 434-438.

Madfa, A. A., Al-Sanabani, F. A., Al-Qudami, N. H., Al-Sanabani, J. S. & Amran, A. G. (2014). 'Use of Zirconia in dentistry: an overview', *The Open Biomaterials Journal,* 5(1), pp.1-9.

Malacarne, J., Carvalho, R. M., de Goes, M. F., Svizero, N., Pashley, D. H., Tay, F. R., Yiu, C. K. & Carrilho, M. R. (2006). 'Water sorption/solubility of dental adhesive resins', *Dent Mater,* 22(10), pp. 973-80.

Mallakpour, S., Dinari, M. & Neamani, S. (2015). 'A facile and green method for the production of novel and potentially biocompatible poly (amide-imide)/ZrO_2–poly (vinyl alcohol) nanocomposites containing trimellitylimido-l-leucine linkages', *J Progress in Organic Coatings,* 86, pp. 11-17.

Mallakpour, S. & Ezhieh, A. N. (2017). 'Polymer Nanocomposites based on Modified ZrO_2 NPs and Poly(vinyl alcohol)/Poly(vinyl pyrrolidone) Blend: Optical, Morphological, and Thermal Properties', *Polymer-Plastics Technology and Engineering,* 56(10), pp. 1136-1145.

Mangal, U., Kim, J. Y., Seo, J. Y., Kwon, J. S. & Choi, S. H. (2019). 'Novel Poly(Methyl Methacrylate) Containing Nanodiamond to Improve the Mechanical Properties and Fungal Resistance', *Materials MDPI,* 12(20), p. 3438.

Manicone, P. F., Rossi Iommetti, P. & Raffaelli, L. (2007). 'An overview of zirconia ceramics: basic properties and clinical applications', *J Dent,* 35(11), pp. 819-26.

Matos, A. O., Costa, J. O., Beline, T., Ogawa, E. S., Assuncao, W. G., Mesquita, M. F., Consani, R. X. & Barao, V. A. (2018). 'Effect of Disinfection on the Bond Strength between Denture Teeth and Microwave-Cured Acrylic Resin Denture Base', *J Prosthodont,* 27(2), pp. 169-176.

McCabe, J. F. & Walls, A. (2009). *Applied Dental Materials* (9th ed). Hoboken: Wiley.

McNeme, S. J., von Gonten, A. S. & Woolsey, G. D. (1991). 'Effects of laboratory disinfecting agents on color stability of denture acrylic resins', *J Prosthet Dent,* 66(1), pp. 132-6.

Miettinen, V. M. & Vallittu, P. K. (1997). 'Water sorption and solubility of glass fiber-reinforced denture polymethyl methacrylate resin', *The Journal of Prosthetic Dentistry,* 77(5), pp. 531-534.

Mihai, L. L., Parlatescu, I., Gheorghe, C., Andreescu, C., Bechir, A., Pacurar, M. & Cumpata, C. N. (2014). 'In vitro Study of the Effectiveness to Fractures of the Aesthetic Fixed Restorations Achieved from Zirconium and Alumina', *Revista De Chimie,* 65(6), pp. 725-729.

Moffitt, A. R., Woody, R. D., Parel, S. M. & Miller, B. H. (2008). 'Failure modes with point loading of three commercially available denture teeth', *J Prosthodont,* 17(6), pp. 432-8.

Mohamed Hamouda, I. (2012). 'Current perspectives of nanoparticles in medical and dental biomaterials', *J Biomed Res,* 26(3), pp. 143-51.

Mohsen, N. M. & Craig, R. G. (1995). 'Effect of Silanation of Fillers on Their Dispersability by Monomer Systems', *Journal of Oral Rehabilitation,* 22(3), pp. 183-189.

Moslehifard, E., Robati Anaraki, M. & Shirkavand, S. (2019). 'Effect of adding TiO2 nanoparticles on the SEM morphology and mechanical properties of conventional heat-cured acrylic resin', *J Dent Res Dent Clin Dent Prospects,* 13(3), pp. 234-240.

Moussa, A. R., Dehis, W. M., Elboraey, A. N. & ElGabry, H. S. (2016). 'A Comparative Clinical Study of the Effect of Denture Cleansing on the Surface Roughness and Hardness of Two Denture Base Materials', *Open Access Maced J Med Sci,* 4(3), pp. 476-481.

Murray, M. D. & Darvell, B. W. (1993). 'The evolution of the complete denture base. Theories of complete denture retention--a review. Part 1', *Aust Dent J,* 38(3), pp. 216-9.

Nasution, H. & Arksornnukit, M. (2017). PMMA Demonstrated Higher Elastic Modulus and Nanohardness Compared with Polyamide Denture Base Materials. *In:* Key Engineering Materials, Trans Tech Publ Ltd, 751(2017), pp. 643-648.

Nejatian, T., Johnson, A. & Van Noort, R. (2006). Reinforcement of denture base resin. *In:* Advances in Science and Technology, Trans Tech Publ Ltd, 49(2006), pp. 124-129.

Neppelenbroek, K. H., Pavarina, A. C., Vergani, C. E. & Giampaolo, E. T. (2005). 'Hardness of heat-polymerized acrylic resins after disinfection and long-term water immersion', *J Prosthet Dent,* 93(2), pp. 171-6.

Oliveira, L. V., Mesquita, M. F., Henriques, G. E., Consani, R. L. & Fragoso, W. S. (2008). 'Effect of polishing technique and brushing on surface roughness of acrylic resins', *J Prosthodont,* 17(4), pp. 308-11.

Onwubu, S. C., Mdluli, P. S. & Singh, S. (2018). 'The effect of colloidal silica and diamond suspensions on the surface roughness of automatically finished heat-polymerized acrylic resin', *J Prosthet Dent,* 120(3), pp. 485- e1.

Ozyegin, L., Yesilbek, B., Bayrak, O. & Oktar, F. (2012). The Effect of Five Polishing Materials on the Surface Roughness of Acrylic and Composite Denture Resins. *In:* Key Engineering Materials, Trans Tech Publ Ltd, 493(2012), pp. 661-665.

Ozyilmaz, O. Y. & Akin, C. (2019). 'Effect of cleansers on denture base resins’ structural properties', *Journal of applied biomaterials & functional materials,* 17(1), pp. 1-9.

Palitsch, A., Hannig, M., Ferger, P. & Balkenhol, M. (2012). 'Bonding of acrylic denture teeth to MMA/PMMA and light-curing denture base materials: the role of conditioning liquids', *J Dent,* 40(3), pp. 210-21.

Parker, S., Riggs, P.D., Braden, M., Kalachandra, S. and Taylor, D.F., 1997. Water uptake of soft lining materials from osmotic solutions. Journal of dentistry, 25(3-4), pp.297-304.

Pan, Y. Y., Liu, F. W., Xu, D., Jiang, X. Z., Yu, H. & Zhu, M. F. (2013). 'Novel acrylic resin denture base with enhanced mechanical properties by the incorporation of PMMA-modified hydroxyapatite', *Progress in Natural Science-Materials International,* 23(1), pp. 89-93.

Patil, S. B., Naveen, B. H. & Patil, N. P. (2006). 'Bonding acrylic teeth to acrylic resin denture bases: a review', *Gerodontology,* 23(3), pp. 131-9.

Peracini, A., Davi, L. R., de Queiroz Ribeiro, N., de Souza, R. F., Lovato da Silva, C. H. & de Freitas Oliveira Paranhos, H. (2010). 'Effect of denture cleansers on physical properties of heat-polymerized acrylic resin', *J Prosthodont Res,* 54(2), pp. 78-83.

Perea, L., Matinlinna, J. P., Tolvanen, M., Lassila, L. V. & Vallittu, P. K. (2014). 'Monomer priming of denture teeth and its effects on the bond strength of composite resin', *J Prosthet Dent,* 112(2), pp. 257-66.

Pfeiffer, P. & Rosenbauer, E. U. (2004). 'Residual methyl methacrylate monomer, water sorption, and water solubility of hypoallergenic denture base materials', *J Prosthet Dent,* 92(1), pp. 72-8.

Piconi, C. & Maccauro, G. (1999). 'Zirconia as a ceramic biomaterial', *Biomaterials,* 20(1), pp. 1-25.

Pilatthadka, S., Vahalova, D. & Vosahlo, T. (2007). The zirconia: A new dental ceramic material. An overview. Prague Med Rep, 108(1), pp.5-12.

Polat, T. N., Karacaer, O., Tezvergil, A., Lassila, L. V. & Vallittu, P. K. (2003). 'Water sorption, solubility and dimensional changes of denture base polymers reinforced with short glass fibers', *J Biomater Appl,* 17(4), pp. 321-35.

Polychronakis, N. C., Polyzois, G. L., Lagouvardos, P. E. & Papadopoulos, T. D. (2015). 'Effects of cleansing methods on 3-D surface roughness, gloss and color of a polyamide denture base material', *Acta Odontol Scand,* 73(5), pp. 353-63.

Polyzois, G., Niarchou, A., Ntala, P., Pantopoulos, A. & Frangou, M. (2013). 'The effect of immersion cleansers on gloss, colour and sorption of acetal denture base material', *Gerodontology,* 30(2), pp. 150-6.

Precision, T. H. (2009). *Talysurf CLI 1000/2000 operator's. handbook.*

Precision, T. H. (2009). Talysurf CLI 3D Surface Profiling Systems. London: Taylor Hobson Limited.

Purnaveja, S., Fletcher, A. M., Ritchie, G. M., Amin, W. M., Moradians, S. & Dodd, A. W. (1982). 'Colour stability of two self curing denture base materials', *Biomaterials,* 3(4), pp. 249-50.

Rad, F. H., Ghaffari, T. & Tamgaji, R. (2017). 'Evaluation of the color stability of methyl methacrylate and nylon base polymer', *Journal of Dentistry,* 18(2), pp. 136-142.

Radford, D. R., Juszczyk, A. S. & Clark, R. K. (2014). 'The bond between acrylic resin denture teeth and the denture base: recommendations for best practice', *Br Dent J,* 216(4), pp. 165-7.

Rahal, J. S., Mesquita, M. F., Henriques, G. E. & Nobilo, M. A. (2004). 'Influence of chemical and mechanical polishing on water sorption and solubility of denture base acrylic resins', *Braz Dent J,* 15(3), pp. 225-30.

Rahim, T., Mohamad, D., Ismail, A. R. & Akil, H. M. (2011). 'Synthesis of nanosilica fillers for experimental dental nanocomposites and their characterisations', *J Physical Science,* 22(1), pp. 93-105.

Reis, A. F., Giannini, M., Lovadino, J. R. & Ambrosano, G. M. (2003). 'Effects of various finishing systems on the surface roughness and staining susceptibility of packable composite resins', *Dental Materials,* 19(1), pp. 12-18.

Reyes-Acosta, M. A., Torres-Huerta, A. M., Dominguez-Crespo, M. A., Flores-Vela, A. I., Dorantes-Rosales, H. J. & Ramirez-Meneses, E. (2015). 'Influence of ZrO_2 nanoparticles and thermal treatment on the properties of PMMA/ZrO_2 hybrid coatings', *Journal of Alloys and Compounds,* 643(2015), pp. S150-S158.

Robison, N. E., Tantbirojn, D., Versluis, A. & Cagna, D. R. (2016). 'Failure strengths of denture teeth fabricated on injection molded or compression molded denture base resins', *J Prosthet Dent,* 116(2), pp. 292-9.

Rodford, R. A. (1990). 'Further Development and Evaluation of High-Impact Strength Denture Base Materials', *Journal of Dentistry,* 18(3), pp. 151-157.

Saavedra, G., Valandro, L. F., Leite, F. P., Amaral, R., Oezcan, M., Bottino, M. A. & Kimpara, E. T. (2007). 'Bond strength of acrylic teeth to denture base resin after various surface conditioning methods before and after thermocycling', *International Journal of Prosthodontics,* 20(2), pp. 199-201.

Sabzi, M., Mirabedini, S. M., Zohuriaan-Mehr, J. & Atai, M. (2009). 'Surface modification of TiO2 nano-particles with silane coupling agent and investigation of its effect on the properties of polyurethane composite coating', *Progress in Organic Coatings,* 65(2), pp. 222-228.

Salim, S., Sadamori, S. & Hamada, T. (1992). 'The dimensional accuracy of rectangular acrylic resin specimens cured by three denture base processing method', *The Journal of Prosthetic Dentistry,* 67(6), pp. 879-881.

Santos, C., Clarke, R. L., Braden, M., Guitian, F. & Davy, K. W. (2002). 'Water absorption characteristics of dental composites incorporating hydroxyapatite filler', *Biomaterials,* 23(8), pp. 1897-904.

Santos, M., Soo, S. & Petridis, H. (2013). 'The effect of Parylene coating on the surface roughness of PMMA after brushing', *J Dent,* 41(9), pp. 802-8.

Saraç, D., Saraç, Y. Ş., Kurt, M. & Yüzbaşioğlu, E. . (2007). 'The effectiveness of denture cleansers on soft denture liners colored by food colorant solutions', *Journal of Prosthodontics,* 16(3), pp. 185-191.

Sasaki, H., Hamanaka, I., Takahashi, Y. & Kawaguchi, T. (2016). 'Effect of long-term water immersion or thermal shock on mechanical properties of high-impact acrylic denture base resins', *Dent Mater J,* 35(2), pp. 204-9.

Schneider, R. L., Curtis, E. R. & Clancy, J. M. (2002). 'Tensile bond strength of acrylic resin denture teeth to a microwave- or heat-processed denture base', *J Prosthet Dent,* 88(2), pp. 145-50.

Sideridou, I. D. & Karabela, M. M. (2009). 'Effect of the amount of 3-methacyloxypropyltrimethoxysilane coupling agent on physical properties of dental resin nanocomposites', *Dent Mater,* 25(11), pp. 1315-24.

Silva, E. M. d., Almeida, G. S., Poskus, L. T. & Guimarães, J. G. A. (2008). 'Relationship between the degree of conversion, solubility and salivary sorption of a hybrid and a nanofilled resin composite', *Journal of Applied Oral Science,* 16(2), pp. 161-166.

Silva, N. R. F. A., Sailer, I., Zhang, Y., Coelho, P. G., Guess, P. C., Zembic, A. & Kohal, R. J. (2010). 'Performance of Zirconia for Dental Healthcare', *Materials,* 3(2), pp. 863-896.

Singh, S., Palaskar, J. N. & Mittal, S. (2013). 'Comparative evaluation of surface porosities in conventional heat polymerized acrylic resin cured by water bath and microwave energy with microwavable acrylic resin cured by microwave energy', *Contemp Clin Dent,* 4(2), pp. 147-51.

Smith, D. C. (1962). 'Recent Developments and Prospects in Dental Polymers', *Journal of Prosthetic Dentistry,* 12(6), pp. 1066-78.

Sodagar, A., Bahador, A., Khalil, S., Shahroudi, A. S. & Kassaee, M. Z. (2013). 'The effect of TiO2 and SiO2 nanoparticles on flexural strength of poly (methyl methacrylate) acrylic resins', *J Prosthodont Res,* 57(1), pp. 15-9.

Sofya, P. A., Rahmayani, L. & Purnama, R. R. C. (2017). 'Effect of soft drink towards heat cured acrylic resin denture base surface roughness', *Padjadjaran Journal of Dentistry,* 29(1), pp. 58-63.

Spartalis, G. K., Cappelletti, L. K., Schoeffel, A. C., Michel, M. D., Pegoraro, T. A., Arrais, C. A., Neppelenbroek, K. H. & Urban, V. M. (2015). 'Effect of conventional water-bath and experimental microwave polymerization cycles on the flexural properties of denture base acrylic resins', *Dent Mater J,* 34(5), pp. 623-8.

Spratley, M. H. (1987). 'An investigation of the adhesion of acrylic resin teeth to dentures', *J Prosthet Dent,* 58(3), pp. 389-92.

Stafford, G. D., Bates, J. F., Huggett, R. & Handley, R. W. (1980a). 'A Review of the Properties of Some Denture Base Polymers', *Journal of Dentistry,* 8(4), pp. 292-306.

Stafford, G. D., Huggett, R. & Causton, B. E. (1980b). 'Fracture toughness of denture base acrylics', *J Biomed Mater Res,* 14(4), pp. 359-71.

Stoia, A. E., Sinescu, C., Negrutiu, M., Enescu, M., Rominu, R., Pielmusi, M., Tudor, A. & Rominu, M. (2010). 'Tensile Bond Strength of Acrylic Resin Teeth to Denture Base Repair Resin', *Advances in Communications, Computers, Systems, Circuits and Devices,* 32(2010), pp. 337- 41.

Suzuki, S., Sakoh, M. & Shiba, A. (1990). 'Adhesive bonding of denture base resins to plastic denture teeth', *J Biomed Mater Res,* 24(8), pp. 1091-103.

Taczała, J. & Sawicki, J. (2018). 'Bond between single artificial teeth and the base plate in removable denture metal framework', *Journal of Achievements in Materials Manufacturing Engineering,* 90(1), pp. 11-21.

Tham, W., Chow, W. & Ishak, Z. M. (2010a). 'The effect of 3-(trimethoxysilyl) propyl methacrylate on the mechanical, thermal, and morphological properties of poly (methyl methacrylate)/hydroxyapatite composites', *Journal of applied polymer science,* 118(1), pp. 218-228.

Tham, W., Chow, W. & Ishak, Z. M. (2010b). 'Simulated body fluid and water absorption effects on poly (methyl methacrylate)/hydroxyapatite denture base composites', *Express Polymer Letters,* 4(9), pp. 517-528.

Tham, W. L., Chow, W. S. & Ishak, Z. A. M. (2011). 'Effects of titanate coupling agent on the mechanical, thermal, and morphological properties of poly(methyl methacrylate)/hydroxyapatite denture base composites', *Journal of Composite Materials,* 45(22), pp. 2335-2345.

Thomas, T. C., Aswini. K., Mohamed, S., Krishnan, V., Mathew, A. & Manju, V. (2015). 'The effect on the flexural strength, flexural modulus and compressive strength of fibre reinforced acrylic with that of plain unfilled acrylic resin - an in vitro study', *J Clin Diagn Res,* 9(3), pp. ZC12-14.

Thongrakard, T. & Wiwatwarrapan, C. (2016). 'Tensile bond strength between auto-polymerized acrylic resin and acrylic denture teeth treated with MF-MA solution', *Journal of Advanced Prosthodontics,* 8(4), pp. 285-289.

Trunec, M. & Chlup, Z. (2009). 'Higher fracture toughness of tetragonal zirconia ceramics through nanocrystalline structure', *Scripta Materialia,* 61(1), pp. 56-59.

Tukmachi, M. S., Azeez, Z. A. & Mohammed, D. H. (2018). 'Evaluation of Bond Strength of Acrylic Artificial Teeth with Unreinforced and Nano Silica Reinforced Denture

Base Material after Chemical Disinfection', *Journal of Research in Medical and Dental Science,* 6(5), pp. 76-82.

Tuna, S. H., Keyf, F., Gumus, H. O. & Uzun, C. (2008). 'The evaluation of water sorption/solubility on various acrylic resins', *European journal of dentistry,* 2(3), pp. 191-197.

Umemoto, K. & Kurata, S. (1997). 'Basic study of a new denture base resin applying hydrophobic methacrylate monomer', *Dent Mater J,* 16(1), pp. 21-30.

Uzun, G., Hersek, N. & Tincer, T. (1999). 'Effect of five woven fiber reinforcements on the impact and transverse strength of a denture base resin', *J Prosthet Dent,* 81(5), pp. 616-20.

Vagkopoulou, T., Koutayas, S. O., Koidis, P. & Strub, J. R. (2009). 'Zirconia in dentistry: Part 1. Discovering the nature of an upcoming bioceramic', *Eur J Esthet Dent,* 4(2), pp. 130-51.

Vallittu, P. K. (1995). 'Bonding of resin teeth to the polymethyl methacrylate denture base material', *Acta Odontol Scand,* 53(2), pp. 99-104.

Vallittu, P. K. (1996). 'Comparison of the in vitro fatigue resistance of an acrylic resin removable partial denture reinforced with continuous glass fibers or metal wires', *J Prosthodont,* 5(2), pp. 115-21.

Vallittu, P. K. & Lassila, V. P. (1992). 'Reinforcement of acrylic resin denture base material with metal or fibre strengtheners', *J Oral Rehabil,* 19(3), pp. 225-30.

Vallittu, P. K., Lassila, V. P. & Lappalainen, R. (1994a). 'Acrylic resin-fiber composite—part I: The effect of fiber concentration on fracture resistance', *The Journal of Prosthetic Dentistry,* 71(6), pp. 607-612.

Vallittu, P. K., Lassila, V. P. & Lappalainen, R. (1994b). 'Transverse strength and fatigue of denture acrylic-glass fiber composite', *Dent Mater,* 10(2), pp. 116-21.

Van Noort, R. (2007). *An introduction to dental materials* (3rd ed). Edinburgh: Mosby.

Van Noort, R. & Barbour, M. (2013). *Introduction to Dental Materials*: Elsevier Health Sciences.

Vasiliu, M. P., Sachelarie, L., Tomită, D., Folescu, E. & Stadoleanu, C. (2016). Experimental Evaluation of Biocompatibility in Case of Acrylic Materials by Bio-Testing on Lab Animals. *In:* Key Engineering Materials, Trans Tech Publ Ltd, 695(2016), pp. 231-235.

Vichi, A., Louca, C., Corciolani, G. & Ferrari, M. (2011). 'Color related to ceramic and zirconia restorations: a review', *Dental materials,* 27(1), pp. 97-108.

Vojdani, M., Bagheri, R. & Khaledi, A. A. R. (2012). 'Effects of aluminum oxide addition on the flexural strength, surface hardness, and roughness of heat-polymerized acrylic resin', *Journal of Dental Sciences,* 7(3), pp. 238-244.

Volpato, C. Â. M., ´Altoé Garbelotto, L. G. D. Fredel, M. C & Bondioli, F (2011). Application of zirconia in dentistry. Advances in ceramics-electric and magnetic ceramics: Bioceramics, ceramics and environment, biological, mechanical and optical considerations. *Rijeka: InTech,* pp.397-420.

Wang, T., Tsoi, J. K. & Matinlinna, J. P. (2016). 'A novel zirconia fibre-reinforced resin composite for dental use', *J Mech Behav Biomed Mater,* 53(2016), pp. 151-160.

Wang, X. X., Song, X. M., Lin, M., Wang, H. T., Zhao, Y. L., Zhong, W. & Du, Q. G. (2007). 'Surface initiated graft polymerization from carbon-doped TiO_2 nanoparticles under sunlight illumination', *Polymer,* 48(20), pp. 5834-5838.

Whitehead, S., Shearer, A., Watts, D. & Wilson, N. (1995). 'Comparison of methods for measuring surface roughness of ceramic', *Journal of Oral Rehabilitation,* 22(6), pp. 421-427.

Williams, J. A., Billington, R. W. & Pearson, G. J. (2001). 'A long term study of fluoride release from metal-containing conventional and resin-modified glass-ionomer cements', *J Oral Rehabil,* 28(1), pp. 41-7.

Williams, J. G. & Cawood, M. J. (1990). 'European Group on Fracture - Kc and Gc Methods for Polymers', *Polymer Testing,* 9(1), pp. 15-26.

Wong, D. M., Cheng, L. Y., Chow, T. W. & Clark, R. K. (1999). 'Effect of processing method on the dimensional accuracy and water sorption of acrylic resin dentures', *J Prosthet Dent,* 81(3), pp. 300-4.

Yoshida, K., Takahashi, Y., Shimizu, H. & Dentistry, R. (2011). Effect of embedded metal reinforcements and their location on the fracture resistance of acrylic resin complete dentures. *J Journal of Prosthodontics,* 20(5), pp.366-371.

Yu, S. H., Cho, H. W., Oh, S. & Bae, J. M. (2015). 'Effects of glass fiber mesh with different fiber content and structures on the compressive properties of complete dentures', *J Prosthet Dent,* 113(6), pp. 636-44.

Yu, S. H., Oh, S., Cho, H. W. & Bae, J. M. (2017). 'Reinforcing effect of glass-fiber mesh on complete dentures in a test model with a simulated oral mucosa', *J Prosthet Dent,* 118(5), pp. 650-657.

Yu, W., Wang, X., Tang, Q., Guo, M. & Zhao, J. (2014). 'Reinforcement of denture base PMMA with ZrO_2 nanotubes', *J Mech Behav Biomed Mater,* 32(2014), pp.192-197.

Zappini, G., Kammann, A. & Wachter, W. (2003). 'Comparison of fracture tests of denture base materials', *J Prosthet Dent,* 90(6), pp. 578-85.

Zhang, X. Y., Zhang, X. J., Huang, Z. L., Zhu, B. S. & Chen, R. R. (2014). 'Hybrid effects of zirconia nanoparticles with aluminum borate whiskers on mechanical properties of denture base resin PMMA', *Dent Mater J,* 33(1), pp. 141-6.

Zhao, J., Milanova, M., Warmoeskerken, M. M. C. G. & Dutschk, V. (2012). 'Surface modification of TiO2 nanoparticles with silane coupling agents', *Colloids and Surfaces a-Physicochemical and Engineering Aspects,* 413, pp. 273-279.

Zheng, J. P., Wang, L., Hu, Y. M. & Yao, K. D. (2012). 'Toughening Effect of Comonomer on Acrylic Denture Base Resin Prepared via Suspension Copolymerization', *Journal of Applied Polymer Science,* 123(4), pp. 2406-2413.

Zidan, S., Silikas, N., Alhotan, A., Haider, J. & Yates, J. (2019). 'Investigating the Mechanical Properties of ZrO_2-Impregnated PMMA Nanocomposite for Denture-Based Applications', *Materials (MDPI),* 12(8), p. 1344.

Zoidis, P., Polychronakis, N., Lagouvardos, P., Polyzois, G. & Ngo, H. C. (2019). 'Evaluation of a Realistic Cleansing Protocol for Preventing Discoloration of Denture Resins', *J Prosthodont,* 28(1), pp. e89-e95.

Zuo, W., Feng, D., Song, A., Gong, H. & Zhu, S. (2016). 'Effects of organic-inorganic hybrid coating on the color stability of denture base resins', *J Prosthet Dent,* 115(1), pp. 103-8.

Appendix

CLUSTER FORMATION

From SEM analysis it was found that increasing zirconia concentration (wt%) caused an increase in cluster size in the PMMA-zirconia nanocomposite as shown in Figure A1.

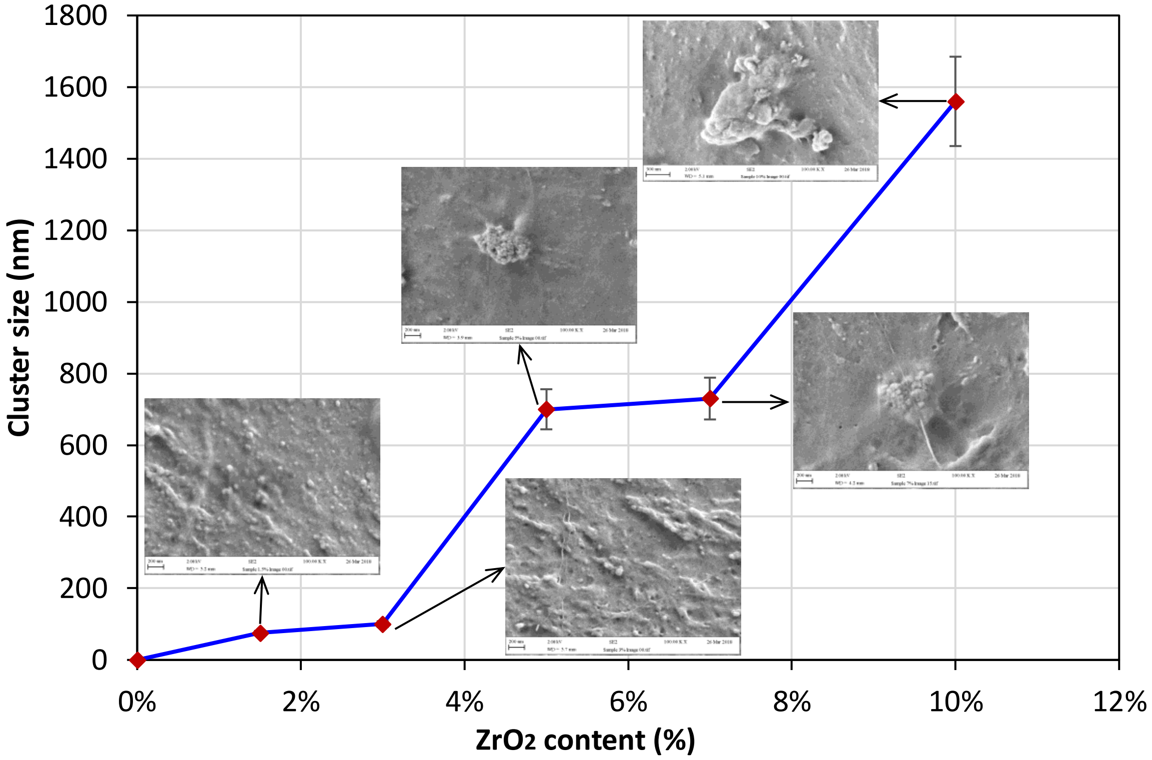

Figure A1. Variation in cluster size with zirconia concentrations in the nanocomposites

PUBLISHED PAPER FROM CHAPTER 5 AND CHAPTER 9

materials

Article

Investigating the Mechanical Properties of ZrO_2-Impregnated PMMA Nanocomposite for Denture-Based Applications

Saleh Zidan [1,*], Nikolaos Silikas [1], Abdulaziz Alhotan [1], Julfikar Haider [2] and Julian Yates [1]

[1] Dentistry, School of Medical Sciences, University of Manchester, Manchester M13 9PL, UK; Nikolaos.Silikas@manchester.ac.uk (N.S.); abdulaziz.alhotan@postgrad.manchester.ac.uk (A.A.); Julian.yates@manchester.ac.uk (J.Y.)
[2] School of Engineering, Manchester Metropolitan University, Manchester M1 5GD UK; j.haider@mmu.ac.uk
* Correspondence: saleh.zidan@postgrad.manchester.ac.uk; Tel.: 44-79-3309-6536

Received: 28 March 2019; Accepted: 20 April 2019; Published: 25 April 2019

Abstract: Acrylic resin PMMA (poly-methyl methacrylate) is used in the manufacture of denture bases but its mechanical properties can be deficient in this role. This study investigated the mechanical properties (flexural strength, fracture toughness, impact strength, and hardness) and fracture behavior of a commercial, high impact (HI), heat-cured denture base acrylic resin impregnated with different concentrations of yttria-stabilized zirconia (ZrO_2) nanoparticles. Six groups were prepared having different wt% concentrations of ZrO_2 nanoparticles: 0% (control), 1.5%, 3%, 5%, 7%, and 10%, respectively. Flexural strength and flexural modulus were measured using a three-point bending test and surface hardness was evaluated using the Vickers hardness test. Fracture toughness and impact strength were evaluated using a single edge bending test and Charpy impact instrument. The fractured surfaces of impact test specimens were also observed using a scanning electron microscope (SEM). Statistical analyses were conducted on the data obtained from the experiments. The mean flexural strength of ZrO_2/PMMA nanocomposites (84 ± 6 MPa) at 3 wt% zirconia was significantly greater than that of the control group (72 ± 9 MPa) ($p < 0.05$). The mean flexural modulus was also significantly improved with different concentrations of zirconia when compared to the control group, with 5 wt% zirconia demonstrating the largest (23%) improvement. The mean fracture toughness increased in the group containing 5 wt% zirconia compared to the control group, but it was not significant. However, the median impact strength for all groups containing zirconia generally decreased when compared to the control group. Vickers hardness (HV) values significantly increased with an increase in ZrO_2 content, with the highest values obtained at 10 wt%, at 0 day (22.9 $HV_{0.05}$) in dry conditions when compared to the values obtained after immersing the specimens for seven days (18.4 $HV_{0.05}$) and 45 days (16.3 $HV_{0.05}$) in distilled water. Incorporation of ZrO_2 nanoparticles into high impact PMMA resin significantly improved flexural strength, flexural modulus, fracture toughness and surface hardness, with an optimum concentration of 3–5 wt% zirconia. However, the impact strength of the nanocomposites decreased, apart from the 5 wt% zirconia group.

Keywords: PMMA; zirconia (ZrO_2); nanocomposite; denture base; flexural strength; impact strength; fracture toughness; hardness

1. Introduction

In practical applications, denture base materials experiences different types of stresses, such as compressive, tensile and shear, which can lead to premature failure. Intra-orally, repeated mastication over a period of time can lead to denture base fatigue failure. Extra-orally, denture bases can also experience high impact forces when dropped by accident [1,2]. Impact fractures occur extra-orally as a result of inadvertent denture damage [1,3]. The incidence of denture fracture is relatively high: 68% of dentures fail within three years of fabrication and the incidence in partial denture is greater than that of complete dentures [4,5]. Studies have also reported that 33% of the repairs in dental laboratories are as a result of de-bonded teeth, and 29% percent of fractures occur in the midline of the denture base, being seen more frequently in the upper than in the lower prosthesis [6,7]. The remaining 38% of fractures are caused by other types of failure [6,7].

High impact (HI) denture base resins are widely used in prosthetic dentistry. These materials are provided in either powder or liquid forms and are processed in the same manner as other heat-cured, poly-methyl methacrylate (PMMA) resins. HI resins are reinforced with butadiene-styrene rubber, with the rubber particles grafted to the poly-methyl methacrylate so that the particles are covalently bonded into the polymerized acrylic matrix in order to better absorb mechanical loads [4,8–10]. Incorporation of butadiene-styrene rubber into PMMA resins improves impact strength and dimensional stability [8,11,12]. However, such reinforcement can result in the reduction of mechanical properties, including flexural strength, fatigue strength and stiffness [8,11,13].

Many attempts have been made to improve the strength of denture base resins, including the addition of metal wires and plates made of either Co-Cr alloy or stainless steel. However, these materials present limitations contrary to the standard requirements, including poor adhesion between the acrylic resin and reinforcing metal. This separation can result in a reduction in overall mechanical strength within the prosthesis, as well as poor aesthetics. Additionally, metal-reinforced denture bases can become noticeably heavier [13,14]. Other attempts to improve denture base mechanical properties include fibre reinforcement to enhance fracture toughness, flexural and impact strength, and fatigue properties [13,15]. Different fibre types, such as ultra-high modulus polyethylene fibre (UHMPE), aramid fibre, nylon fibre, carbon fibre and glass fibre, have all been investigated [13,15,16]. UHMPE fibre does not demonstrate good adhesion to PMMA, and therefore, no significant increase in flexural properties has been demonstrated [17]. Carbon and aramid fibres are not practical materials because of difficulties in polishing the final prostheses, and resultant poor aesthetics [18]. However, nylon reinforcement enhances fracture resistance and structural elasticity of acrylic resins [15]. A study undertaken by Vallittu et al., on the flexural and transverse strength of heat-cured PMMA denture bases reinforced with a high concentration of continuous glass fibre demonstrated an improvement in these properties [19]. Additionally, silane coupling agents have been added to enhance adhesion between the polymer resin and glass fibres to improve mechanical strength, resulting in enhanced flexural and fatigue strength [19,20]. However, fibre orientation in the resin matrix is technically difficult to control and a random distribution could result in defects within the finished product [21].

In recent years, several investigations have focused on improving the mechanical properties of PMMA acrylic resins by adding nanomaterials, such as bio-ceramic nanoparticles, due to their special characteristics [22]. Zirconia (ZrO_2) is a bio-ceramic material that has been widely used for various dental applications, such as crowns and bridges, implant fixture “screws” and abutments, and orthodontic brackets [23]. Zirconia has a high flexural strength (900 to 1200 MPa), hardness (1200 HV), and fracture toughness (9–10 MPa $m^{1/2}$) [24]. Furthermore, zirconia shows excellent biocompatibility compared to other ceramic materials, such as alumina [22,24]. A number of studies found that reinforcement of conventional, heat-cured denture base resins with zirconia nanoparticles significantly improved mechanical properties such as flexural and impact strength, as well as surface hardness [22,25]. However, no systematic study on the effect of zirconia addition in the high impact (HI) heat-cured PMMA denture base material has been reported in the literature. Therefore, research is needed to identify an optimum amount of zirconia suitable for improving performance and life of HI PMMA denture bases.

The purpose of this study is to evaluate the effects of zirconia nanoparticle addition at low concentrations (up to 10%) to a commercially available, high-impact, PMMA denture base resin on selected mechanical properties such as flexural strength, impact strength, fracture toughness, hardness and fracture behaviour.

2. Material and Methods

2.1. Materials

A commercially available, Metrocryl HI denture base powder, (PMMA, poly-methyl methacrylate) and Metrocryl HI (X-linked) denture base liquid (MMA, methyl methacrylate) (Metrodent Limited, Huddersfield, UK) were selected as the denture base material. Yttria-stabilized zirconia (ZrO_2) nanoparticles (94% purity; Sky Spring Nano materials, Inc., Houston, TX, USA) were chosen as the inorganic filler agent for fabricating the nanocomposite denture base specimens.

2.2. Specimen Preparation

2.2.1. Silane Functionalization of Zirconia Nanoparticle Surfaces

Fifteen grams of zirconia nanoparticles and 70 mL of toluene solvent were deposited into a plastic container, which was then placed in a speed mixer (DAC 150.1 FVZK, High Wycombe, UK), and mixed at 1500 rpm for 20 min. Following the initial mixing, 7 wt% silane coupling agent (3-trimethoxysilyl propyl methacrylate; product no. 440159, Sigma Aldrich, Gillingham, UK) was added slowly over a period of 20 s. The mixture was then placed in the speed mixer at 1500 rpm for 10 min and divided equally into two tubes and spun in a centrifuge at 23 °C at 4000 rpm for 20 min. The supernatant (separated toluene) was removed, and the remaining silanized nanoparticles were transferred into a personal solvent evaporator (EZ-2 Elite, Genevac Ltd., SP Scientific Company, Ipswich, UK) for 3 h of drying at 60 °C.

2.2.2. Selection of Appropriate Percentages of Zirconia Nanoparticles

To determine the most appropriate weight percentages of zirconia nanoparticles for the current study, preliminary investigations were undertaken using 1.5 wt%, 10 wt% and 15 wt% mixtures. Based on these results and knowledge from relevant literature, a decision was made to utilize the following weight percentages of silanized zirconia nanoparticles in the denture base formulation: 0.0% (control), 1.5 wt%, 3.0 wt%, 5.0 wt%, 7.0 wt%, and 10.0 wt%. The composition details of the specimen groups used in this study are described in Table 1 (all used an acrylic resin powder:monomer ratio of 21 g:10 mL, in accordance with manufacturer's instructions).

Table 1. Weight percent zirconia in combination with acrylic resin powder as well as monomer content of the specimen groups. HI: High impact; PMMA: Poly-methyl methacrylate; MMA: methyl methacrylate.

Experimental Groups	Zirconia (wt%)	Zirconia (g)	HI PMMA Powder (g)	HI MMA Monomer (mL)
Control	0.0	0.000	21.000	10.0
1.5	1.5	0.315	20.685	10.0
3.0	3.0	0.630	20.370	10.0
5.0	5.0	1.050	19.950	10.0
7.0	7.0	1.470	19.530	10.0
10.0	10.0	2.100	18.900	10.0

2.2.3. Mixing of Zirconia with PMMA

The silane-treated zirconia and acrylic resin powders were weighed according to Table 1 using an electronic balance (Ohaus Analytical with accuracy up to 3 decimal points). The zirconia powder was added to the acrylic resin monomer and mixed by hand using a stainless-steel spatula to make sure all the powder was uniformly distributed within the resin monomer. The HI acrylic resin powder was then added to the solution, and mixing continued until a consistent mixture was obtained, according to the manufacturer's instruction. The mixing continued for approximately 20 min until the mixture reached a dough-like stage, which was suitable for handling. When the mixture reached a consistent dough-like stage (working stage), it was packed into a mould by hand. The moulds were made from aluminium alloy, which contained five cavities with a dimension of 65 mm (l) × 10 mm (w) × 2.50 mm (d) for producing flexural strength and hardness test samples. However, the cavity dimensions for the impact test was as follows: 80 mm (l) × 10 mm (w) × 4 mm (d) and fracture toughness was 40 mm (l) × 8 mm (w) × 4 mm (d). Before pouring the mixture into the mould, sodium alginate as a separating medium (John Winter, Germany) was applied to the surfaces of the mould for easy removal of the specimens. The mould was then closed and placed in a hydraulic press (Sirio P400/13045) under a pressure of 15 MPa in the first cycle, and then the pressure was released. Excess mixture was removed from the mould periphery, which was then re-pressed at room temperature for 15 min under the same pressure. The mould was then immersed in a temperature-controlled curing water bath for 6 h to allow polymerization. The curing cycle involved increasing the temperature to 60 °C over 1 h and maintained this temperature for 3 h. After this time, the temperature was increased to 95 °C over an additional 2 h to complete the heat polymerization cycle. The mould was removed from the curing bath and cooled slowly for 30 min at room temperature. The mould was then opened and the specimens were removed. The specimens were then trimmed using a tungsten carbide bur, ground with an emery paper and polished with pumice powder in a polishing machine (Tavom, Wigan, UK) in accordance with British International Standard Organization (BS EN ISO 20795-1:2008) and British Standard Specification for Denture Base Polymers (BS 2487: 1989 ISO 1567; 1988) [26,27].

2.3. Mechanical Characterization of the Nanocomposite

2.3.1. Flexural Strength Test

Flexural strength of the nanocomposite specimens was evaluated using a 3-point bend test in a universal testing machine (Zwick/Roell Z020 Leominster, UK) in accordance with British International Standard for Denture Base Polymers (2487: 1989) [27]. The dimensions of the specimens were 65 mm length × 10 ± 0.01 mm width × 2.50 ± 0.01 mm thickness. All specimens were stored in distilled water at a temperature of 37 ± 1 °C for 50 ± 2 h in an incubator before testing. The specimens were then removed from the distilled water and placed on a support jig. The loading plunger (diameter 7.0 mm) was fixed at the center of the specimen midway between two supports, which were parallel and separated by 50 ± 0.1 mm, and the diameter of the load supports were 3.20 mm. A 500 N load cell was used to record force and the load was applied using a cross-head speed of 5 mm/min. The maximum force (F) was recorded in newtons, and flexural strength was calculated in MPa for all specimens using the following equation [28]:

$$\sigma = \frac{3\mathrm{Fl}}{2\mathrm{bh}^2} \tag{1}$$

where F is the maximum force applied in N, l is the distance between the supports in mm, b is the width of the specimen in mm, and h is the height of the specimen in mm. The flexural modulus was determined as the slope of the linear portion of the stress/strain curve for each test run.

2.3.2. Fracture Toughness Test

Fracture toughness tests were conducted using a single edge span notch bending test on the Zwick universal testing machine in accordance with the British International Standard Organization (BS EN ISO 20795-1:2008) [26,29]. The dimensions of the specimens were 40 mm (l) × 8 mm (w) × 4 mm (h), and a notch was created in the middle of the specimens with a diamond blade and a saw to a depth of 3.0 ± 0.2 mm along a marked centre line. All specimens were then stored in distilled water and placed in an incubator at 37 ± 1 °C for 168 ± 2 h before testing. The specimens were removed from the water, dried by a towel and placed edgewise on the supports of the testing rig. The notch of the specimen was placed directly opposite to the load plunger (diameter 7 mm) and in the middle of the span between the two supports (32.0 ± 0.1 mm). The load cell was 500 N, and the cross-head speed was 1.0 mm/min. Fracture toughness was determined by increasing the force from zero to a maximum value in order to propagate a crack from the opposite side of the specimen to the impact point. The maximum force (P) in newtons to fracture was recorded in order to calculate the fracture toughness (K_{IC}) in MPa $m^{1/2}$ according to Equation (2) [29]:

$$K_{IC} = \frac{3PL}{2BW^{\frac{3}{2}}} \times Y \tag{2}$$

where W is the height of the specimen in mm, B is the width of the specimen in mm, L is the distance between the supports in mm, and Y is a geometrical function calculated by Equation (3).

$$Y = 1.93 \times \left(\frac{a}{w}\right)^{1/2} - 3.07 \times \left(\frac{a}{w}\right)^{\frac{3}{2}} + 14.53 \times \left(\frac{a}{w}\right)^{\frac{5}{2}} - 25.11 \times \left(\frac{a}{w}\right)^{\frac{7}{2}} + 25.80 \times \left(\frac{a}{w}\right)^{\frac{9}{2}} \tag{3}$$

where a is the depth of the notch.

2.3.3. Impact Test

The Charpy V-notch impact test (kJ/m^2) utilized a universal pendulum impact testing machine (Zwick/Roell Z020 Leominster). Specimen dimensions were 80 mm (l) × 10 ± 0.01 mm (w) × 4 ± 0.01 mm (h), in accordance with the European International Standard Organization (EN ISO 179-1:2000) [30]. The specimens were notched in the middle to a depth of 2.0 ± 0.2 mm, a notch angle of 45 ° and a notch radius of 1.0 ± 0.05 mm and were then stored in distilled water at 37 ± 1 °C for 168 ± 2 h in an incubator before testing. The specimens were then removed from the water and dried with a towel. Each specimen was placed in the machine and were supported horizontally at its ends (40 ± 0.2 mm), and the centre of the specimen (the un-notched surface) was hit by a free-swinging pendulum that was released from a fixed height. The pendulum load cell was 0.5 J and directly faced the centre of the specimen, as shown in Figure 1. When the test was started, the pendulum was released to strike the specimen, and the impact energy absorbed was recorded in joules (J). The Charpy impact strength (a_{iN}) (kJ/m^2) was calculated using Equation (4) [10,30]:

$$a_{iN} = \frac{E_c}{h * b_N} \times 10^3 \tag{4}$$

where E_c is the breaking energy in joules absorbed by breaking, h is the thickness in mm, and b_N is the remaining width in mm after notching.

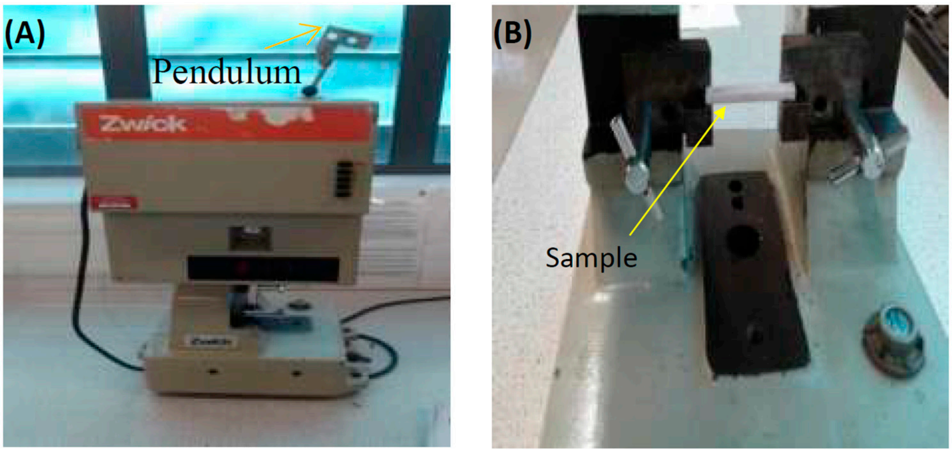

Figure 1. (**A**) Impact test machine and (**B**) position of sample in the machine before the test.

2.3.4. Hardness Test

The Vickers hardness ($HV_{0.05}$) of the specimens was measured using a micro-hardness testing machine (FM-700, Future Tech Corp, Tokyo, Japan). Specimens were 65 mm length × 10 mm width × 2.50 mm thickness, and the test load was fixed at 50 g for 30 s. The Vickers hardness was calculated by measuring the diagonals of the pyramid-shaped indentation impressed on the specimen. A total of three indentations were taken at different points in each specimen one side, and then a mean value was calculated. The mean hardness values for all the specimens were determined demonstrative of the materials in the dry condition at day 0. The specimens were then stored individually in 37 ± 1 °C distilled water for 7 d ± 2 h, and were then re-immersed for a total of 45 d ± 2 h. From the raw data, the mean hardness values for each sample group were calculated [31,32].

2.4. Scanning Electron Microscopy (SEM) Examination

The size and shape distribution of the PMMA powder and zirconia nanoparticles was analysed using a scanning electron microscope (SEM) (Carl Zeiss Ltd, 40 VP, Smart SEM, Cambridge, UK). The fractured surface was also studied to identify failure mechanism. Specimens were mounted onto aluminium stubs and sputter-coated with gold after which SEM visualization was performed using a secondary electron detector at an acceleration voltage of 2.0 kV.

2.5. Statistical Analyses

Flexural strength, modulus, impact strength, fracture toughness and Vickers hardness data were analysed using a statistical software (SPSS statistics version 23, IBM, New York, NY, USA). Non-significant Shapiro–Wilk and Levene tests showed that the data of flexural and fracture toughness were normally distributed and there was homogeneity of variance. The flexural and fracture toughness data were analysed using a one-way analysis of variance (ANOVA) with the Tukey honestly significant difference post-hoc test at a pre-set alpha of 0.05. Impact strength and hardness data demonstrated nonparametric distributions as evidenced by significant Shapiro–Wilk test results for two groups, and therefore the Kruskal–Wallis test was used to analyse the results as well as to compare the differences among the test groups at a pre-set alpha of 0.05. In addition, the Friedman's two-way analysis test was applied to identify any significant difference between the three immersion time groups ($p < 0.05$).

3. Results

3.1. Visual Analysis

SEM analysis revealed that the average particle size of the PMMA powder was approximately 50 µm with a range from 10 µm to 100 µm, as shown in Figure 2A. The rubber particles were also visible within the powder, with an average size of approximately 50 µm. The as-received, yttria-stabilized zirconia nanoparticles demonstrated an average size ranging between 30 nm and 60 nm for individual particles and 200 nm to 300 nm for clusters, as shown in Figure 2B.

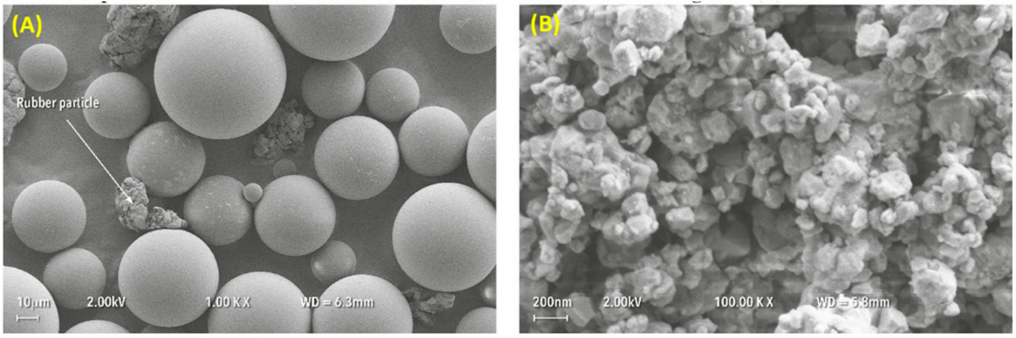

Figure 2. Particle size and shape distributions of (**A**) PMMA powder and (**B**) zirconia nanoparticles.

3.2. Mechanical Tests

3.2.1. Flexural Strength and Flexural Modulus

One-way analysis of variance (ANOVA) of flexural strength values presented in Table 2 show a significant difference ($p < 0.05$) for the specimen group containing 3 wt% zirconia. However, the mean values of flexural modulus showed a significant increase ($p < 0.05$) for all specimens, except that containing 7 wt% zirconia, which was not significantly different ($p > 0.05$) from the control group. The flexural strength data in the table demonstrates that an addition of zirconia nanoparticles to the HI PMMA gradually increased the strength up to 3 wt% and then gradually decreased for other compositions when compared to the control group (0 wt%). The highest value of flexural strength was recorded for the group containing 3 wt% zirconia (83.5 MPa) in comparison with the control group (72.4 MPa), representing a 15% increase in the flexural strength. However, a higher percentage of zirconia nanoparticles (7 wt% to 10 wt%) in the specimens reduced the strength, which was comparable to the control group. A similar behaviour was also found for the flexural modulus of the nanocomposites with increasing zirconia content (Table 2). However, a maximum value of the flexural modulus was reached at a zirconia content of 5 wt% (2419 MPa) when compared to the control group (1971 MPa), meaning an increase of 22.7%. Furthermore, even though at high zirconia content the modulus values decreased, they were still higher than those of the control group.

Table 2. Mean (MPa) Standard deviation (SD) values of flexural strength, flexural modulus and fracture toughness as well as median of impact strength (kJ/m^2) Interquartile range (IQR) for the test groups.

Zirconia Content (wt%)	Flexural Strength and SD (MPa)	Flexural Modulus and SD (MPa)	Impact Strength and (IQR) (kJ/m^2)	Fracture Toughness and (SD) (MPa m$^{1/2}$)
Control (0%)	72.4 (8.6) ^{A}	1971 (235) ^{A}	10.0 (2.69) ^{A}	2.12 (0.1) ^{A}
1.5	78.7 (6.9) ^{A}	2237 (117) ^{B}	7.03 (4.45) ^{A}	1.91 (0.2) ^{A}
3.0	83.5 (6.2) ^{B}	2313 (161) ^{B}	7.38 (4.50) ^{A}	1.97 (0.2) ^{A}
5.0	78.7 (7.2) ^{A}	2419 (147) ^{B}	9.05 (3.50) ^{A}	2.14 (0.1) ^{A}
7.0	72.2 (7.0) ^{A}	2144 (85) ^{A}	7.12 (1.50) ^{A}	1.86 (0.1) ^{A}
10.0	71.5 (5.7) ^{A}	2204 (91) ^{B}	5.89 (2.33) ^{B}	1.76 (0.8) ^{B}

Within a column, cells having similar (upper case) letters are not significantly different from the control (0% zirconia content) value. N = 10 specimens per group.

3.2.2. Fracture Toughness and Impact Strength

The mean values of the fracture toughness (Table 2) of the nanocomposites decreased significantly compared to that of the control group at the zirconia concentrations of 7% and 10% ($p < 0.05$). Furthermore, after the initial decrease of fracture toughness at 1.5 wt% zirconia, the values slightly increased in the groups containing 3 wt% and 5 wt% zirconia, but they were not statistically significant increases ($p > 0.05$). Table 2 shows that the best fracture toughness could be achieved at 5 wt% zirconia.

The values of the impact strength for all nanocomposite groups were not statistically significant ($p > 0.05$), as shown in Table 2. The median impact strength gradually decreased with the increase in zirconia content, except in the group containing 5 wt% zirconia, which showed the best impact strength (only 10% reduction compared to the control group). However, all measured impact strength values for the nanocomposites were lower than that for the control group.

3.2.3. Hardness

The median values of Vickers hardness in Table 3 show significant differences ($p < 0.05$) for the specimen groups containing 7 wt% and 10 wt% zirconia in both dry (0 day) and wet (7 days) conditions. From the graphical presentation of the hardness results (Figure 3), it is interesting to note that at lower zirconia contents (1.5–5.0%), the difference in hardness between dry and wet conditions was much lower than that at higher zirconia contents (7.0–10.0%). Furthermore, no significant difference was found between the hardness of the specimens stored in water for seven days and 45 days at all zirconia contents. This finding indicates that the hardness of the nanocomposites does not degrade over time in the wet condition at lower zirconia contents, particularly up to 3% zirconia.

Table 3. Vickers hardness (kg/mm^2) (median and interquartile range) after 0, 7 and 45 days of water immersion.

	Day Zero (Dry)	**7-Days Water- Immersion**	**45 Days Water-Immersion**
Weight Percent Zirconia	**Vickers Hardness (kg/mm^2) Median (IQR)**	**Vickers Hardness (kg/mm^2) Median (IQR)**	**Vickers Hardness (kg/mm^2) Median (IQR)**
Control (0.0%)	17.6 (1.7) ^{Aa}	15.2 (2.0) ^{Ab}	15.5 (3.3) ^{Ab*}
1.5%	18.9 (3.2) ^{Ab}	17.7 (1.1) ^{Ab}	17.0 (1.8) ^{Ab*}
3.0%	19.6 (4.0) ^{Ac}	17.8 (1.2) ^{Ac}	17.3 (2.8) ^{Ac}
5.0%	21.1 (3.1) ^{Ad}	17.9 (2.9) ^{Ad}	17.1 (2.2) ^{Ad*}
7.0%	21.7 (3.0) ^{Be}	19.4 (0.9) ^{Be}	16.8 (2.3) ^{Ae*}
10.0%	22.9 (2.9) ^{Bf}	18.4 (3.3) ^{Bf}	16.3 (1.2) ^{Af*}

Within a column, values identified using similar upper-case letters are not significantly different from the control group value; within rows values identified using the same lower-case letters are not significantly different; asterisks indicate significant differences between day 0 and 45 days; N = 5 specimens per experimental group.

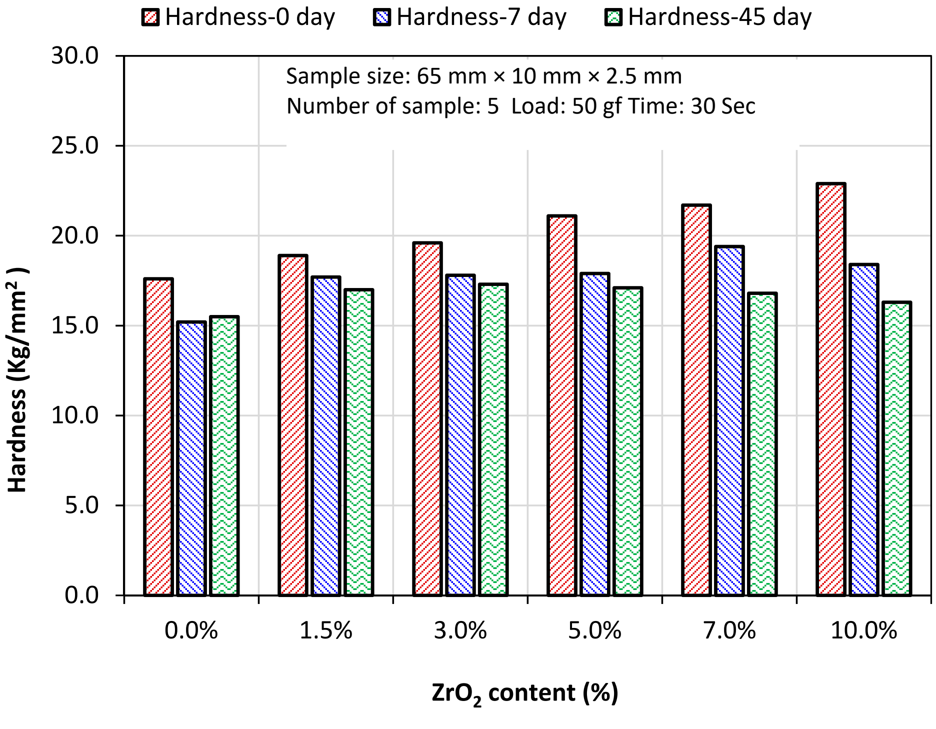

Figure 3. Vickers hardness median (kg/mm^2) after 0, 7, and 45 days of water immersion.

3.3. Microstructural Characteristics

The fractured surface of pure PMMA specimens displayed a smooth surface in small areas and revealed a ductile type failure behaviour exhibiting irregular and rough surface as is shown in Figure 4A. The composite fractured surface showed signs of cracks and particle clustering with small voids (Figure 4B). Figure 4C presents more clear fracture features and shows that the distribution of the nanoparticles was not uniform. The image highlights particle clustering in several places and voids on the fractured surface.

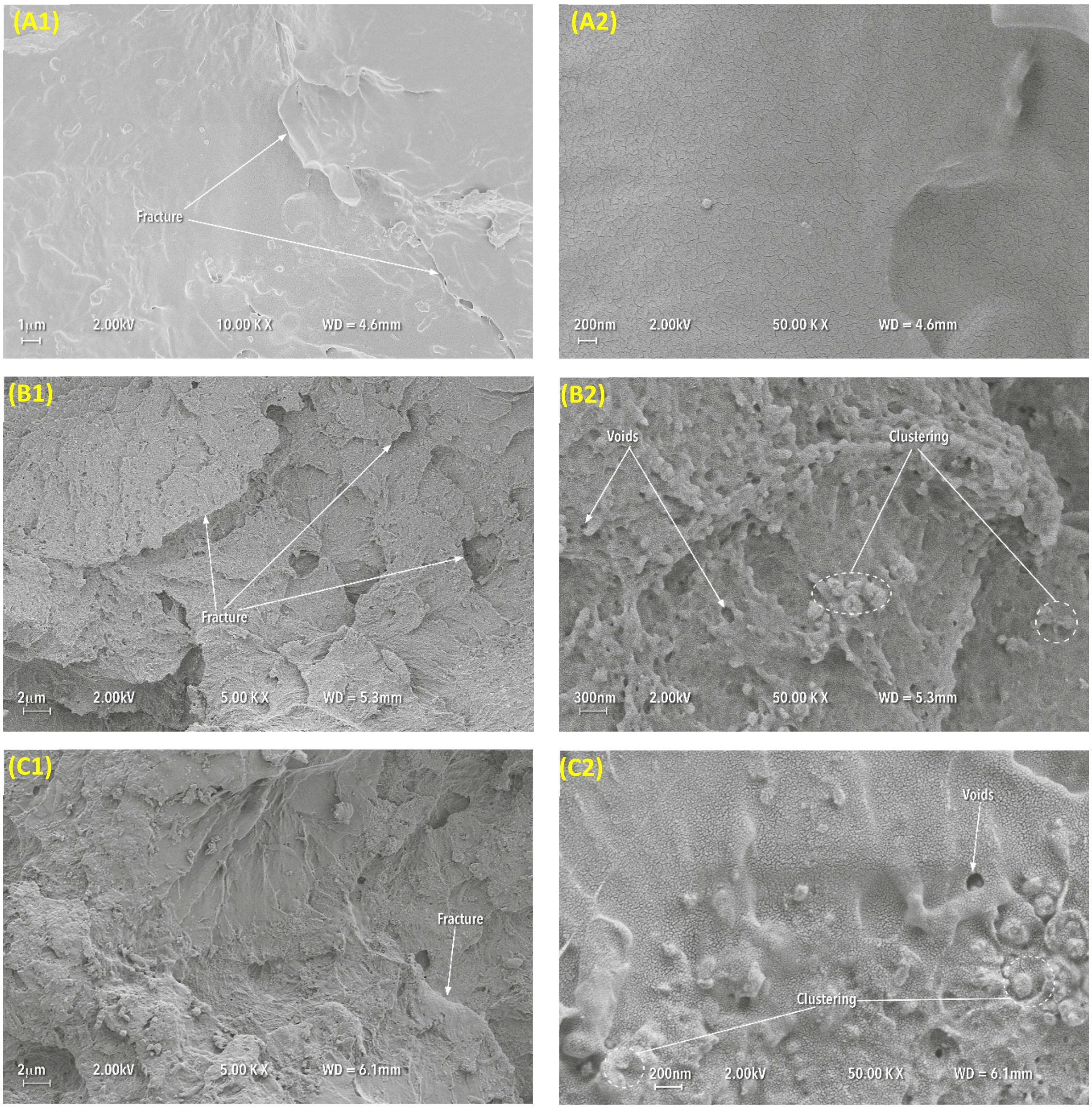

Figure 4. Representative SEM images of the fractured surfaces of impact strength test specimens at two different magnifications (1 at 10K and 2 at 50K for the control group (**A**) 0 wt%, (**B**) 5 wt% and (**C**) 10 wt% added zirconia, respectively).

4. Discussion

In this study, it was shown that combining zirconia nanoparticles to HI acrylic resin improved flexural strength and flexural modulus, which can lead to a reduction in different types of stresses encountered during the mastication process, including compressive, tensile and shear stresses [33]. However, the reinforced HI acrylic resin with lower concentration of zirconia (5%) did not show any significant difference from the control group on fracture toughness and impact strength.

The inorganic reinforcing nano-fillers have a large surface area that provides high surface energy, and this produces nanoparticles with a strong tendency to aggregate. This characteristic may decrease the chemical interaction between the nanoparticles and the base PMMA [22]. In this study, to enhance the chemical adhesion between the ZrO_2 nanoparticles and ZrO_2-PMMA, the surface of the ZrO_2 particles was treated with 7 wt% silane coupling agent (3-MPS) to create reactive functional groups. This could be responsible for improving the flexural properties of the nanocomposites at lower concentrations of zirconia nanoparticles. Moreover, the improvement in flexural strength and flexural modulus could be a result of the improved dispersion of the ZrO_2 nanoparticles when mixing with the speed mixer machine during the preparation stage. This improvement would decrease the agglomeration tendency in the composites. Additionally, the large interfacial area of the nanoparticles contributes to more contact points between the ZrO_2 and PMMA, thus enhancing mechanical interlocking and offers additional flexibility in the nanocomposites [34].

Only a few studies on the effect of adding ZrO_2 nanoparticles in HI heat-cured denture base acrylic resin are available in the literature. In contrast, investigators have worked on improving the mechanical properties of conventional heat-cured denture base acrylic resin by incorporating different types of fillers [35]. Alhareb et al. [36] showed a 16% increase in flexural strength value compared to control samples when PMMA was reinforced with Al_2O_3 and ZrO_2 with a filler concentration of 5 wt%. Moreover, the flexural modulus increased with an increase in Al_2O_3/ZrO_2 nanoparticle concentration [36]. The greater value of the modulus indicates a stiffer material [16], and this improvement can be explained by a homogenous distribution of the fillers within the polymer matrix. Vojdani et al. [3] evaluated the effect of adding Al_2O_3 particles to PMMA denture bases on flexural strength. They found that a 6% increase in flexural strength value with 2.5 wt% Al_2O_3 compared to a control group could be obtained. Zhang et al. [22] investigated the effect of hybrid ZrO_2 nanoparticles and micro-particles of aluminium borate whiskers (ABWS) at concentrations of 1 wt%, 2 wt%, 3 wt%, and 4 wt% on the flexural strength of PMMA denture base resin. They found that 2 wt% nano-ZrO_2 with a ZrO_2/ABWS ratio of 1:2 improved flexural strength by 32% when compared to a control group. These previous studies in the literature were in agreement with the results obtained in this study, which revealed that zirconia positively influenced the flexural properties of HI PMMA with an optimum zirconia concentration between 3 wt% and 5 wt%.

Fracture toughness (K_{IC}) is a critical stress intensity factor that provides information on crack formation [29] and the ability of a material to resist crack propagation [37]. The reduction of fracture toughness in the PMMA/ZrO_2 nanocomposites with increasing filler content could be due to a number of reasons, such as particle distribution in the polymer matrix, the type and size of the particles, the concentration of the added particles, and chemical reactions between the particles and polymer [15,35,38]. A high filler concentration leads to more filler-to-filler interactions than filler-to-matrix interactions; therefore, agglomeration may act as a point of stress concentration that could lead to non-uniform stress distribution. When applying the load, the agglomeration restrains the movement of molecular deformation and reduces the fracture toughness [38]. Sodagar et al. [39] determined that the incorporation of TiO_2 nanoparticles to the PMMA matrix causes agglomeration, which acts as a stress raiser in the centre of the matrix and reduces the mechanical properties of the polymer material with increasing concentrations of the TiO_2 nanoparticles. Fangqiang et al. [40] investigated the distribution of ZrO_2 particles in PMMA matrix using two strategies during mixing: Physical method and chemical method. The physical method was conducted by melt blending, high-energy ball milling or ultrasonic vibration. In the chemical method, when mixing nanoparticles with an MMA monomer, the inorganic ZrO_2 nanoparticles acted as a core, and the monomer as a shell structure by in situ polymerization of the monomers, known as grafting. The chemically modified nanoparticle surfaces with MMA enhanced the dispersion stability of the nanoparticles in the polymer matrix. Owing to a combined physical and chemical preparation, it was observed that the dispersion of ZrO_2 nanoparticles in the polymer matrix was enhanced and particle aggregation and phase separation decreased to a demonstrable extent. The results of the present study on fracture toughness are consistent with those reported in the study of Alhareb et al. [36], where a PMMA denture base reinforced with 5 wt% fillers (80/20 Al_2O_3/ZrO_2) showed an improvement in fracture toughness but an increase in zirconia concentration decreased toughness.

The incorporation of hard ZrO_2 ceramic into PMMA can increase brittleness in the specimens, which would reduce the impact strength. Additionally, the lack of adhesion due to poor chemical reaction at the interface between the particles and PMMA or the inhomogeneous distribution of the nanoparticles with frequent clustering could affect the impact strength negatively [25,36]. A study conducted by Gad et al. [25] evaluated the effect of the incorporation of ZrO_2 nanoparticles with varying concentrations (2.5 wt%, 5 wt% and 7 wt%) to PMMA denture bases on impact strength. The results showed that the impact strength decreased with an increase in ZrO_2 nanoparticle concentration. The finding of the impact strength in the present study is in agreement with that of the previous study, with the exception of the 5 wt% ZrO_2/PMMA nanocomposite results. This result can be explained by the fact that a concentration of 5 wt% might be the optimum quantity to improve particle distribution and reduce amalgamation. Asar et al. [35] investigated the influence of metal oxides, ZrO_2, TiO_3, and Al_2O_3, with 1% and 2% by volume on the impact strength of the PMMA acrylic resin. In contrast to the current study, the findings showed a slight increase in the values of impact strength with 2% ZrO_2 addition.

Denture base materials should also have adequate abrasion resistance to prevent high wear of the material by abrasive denture cleansers, food or general functional forces [41]. Greater hardness in the denture base will reduce abrasive wear. The improvement of hardness in the nanocomposites might be related to the inclusion of hard yttria-stabilized zirconia nanoparticles with fine grains, which are known as tetragonal zirconia poly-crystals (TZP). The size of the grains is dependent on the metastable nature of the tetragonal phase and can be important for providing improved mechanical properties in the nanocomposites, and this zirconia-yttria phase increases surface hardness to resist indentation [42]. However, the increase in surface hardness with the increase of the concentration of zirconia also reduces the impact strength, as seen in Table 3. The reason for hardness decrease after water immersion was described in a previous study conducted on acrylic resin denture base materials, where residual monomers release and water absorption occurring simultaneously caused the surface to become softened [43].

The finding of the present study is in agreement with a study by Yiqing et al. [43], who evaluated the hardness of PMMA/ZrO_2 nanocomposites with different ZrO_2 concentrations (0.5 wt%, 1 wt%, 2 wt%, 3 wt%, 4 wt%, 5 wt%, 7 wt% and 15 wt%) using indentation and pendulum hardness tests. They found that the hardness values were increased with an increase in the ratio of ZrO_2 to PMMA, with the highest value being 15 wt%. Zhang et al. [22] investigated the effect of zirconia nanoparticles and aluminium borate whiskers (ABW) in PMMA denture bases on the surface hardness at concentrations of 1 wt%, 2 wt%, 3 wt% and 4 wt%. The results showed an increase in surface hardness with an increase in ZrO_2/ABW content, and the optimum hardness was achieved at 3 wt% ZrO_2 nanoparticles. They suggested that the decrease in surface hardness with higher filler loading was caused by poor adhesion of the particles to the resin matrix and filler clustering within the matrix. In another study, the incorporation of aluminium oxide (Al_2O_3) with percentages of 0.5 wt%, 1 wt%, 2.5 wt% and 5 wt% to PMMA acrylic resin exhibited an improvement in Vickers hardness with an increase of Al_2O_3 filler concentrations [3].

The lower impact strength in the nanocomposites can be related to the presence of voids and clustering of the nanoparticles [22,36]. At high magnification, the SEM images showed voids on the fractured surface, and these voids could lead to the generation of stress concentration under loading and initiate crack propagation by crossing the HI PMMA/ZrO_2 nanocomposite matrix. At low magnification, the fractured surfaces of the nanocomposite specimens exhibited less ductile fracture compared to the control group with a large amount of fragment crack deformation, which formed an irregular surface. Furthermore, the distribution of ZrO_2 nanoparticles in the polymer matrix was not homogeneous with evidence of agglomerations, which could reduce the impact strength, particularly at high ZrO_2 concentrations (10 wt%).

5. Conclusions

With consideration to the limitations of this study, the following conclusions can be drawn:

1. The flexural strength of the high impact (HI) heat-cured PMMA denture base was significantly enhanced by the addition of zirconia nanoparticles with 3 wt% when compared to the pure acrylic material (control group).

2. The flexural modulus of the high impact (HI) heat-cured PMMA denture base was significantly enhanced compared to the control group by addition of zirconia nanoparticles with 1.5 wt%, 3 wt%, 5 wt% and 10 wt%. The 7 wt% of zirconia showed a non-significant enhancement compared to the control group.
3. The fracture toughness of the zirconia-reinforced PMMA was significantly decreased, particularly at 10 wt% ZrO_2 concentration. The fracture toughness was slightly increased at 5 wt%, but this was not significantly different compared to the control group.
4. For all zirconia contents, the impact strength of the nanocomposites was significantly lower than that of the control group. However, at 5 wt% and 3 wt% zirconia content, the proportion of reduction in impact strength was not significantly different from that of the control group.
5. Surface hardness continuously increased with increase of zirconia content, in the dry condition at day 0. However, in the wet condition after seven days, and 45 days surface hardness was decreased with all groups.
6. Addition of zirconia in PMMA between 3 wt% and 5 wt% zirconia would provide the optimum mechanical properties suitable for denture base applications.

Author Contributions: Conceptualization, J.Y. and S.Z.; Methodology, J.Y., S.Z., N.S., A.A. and J.H.; Validation, S.Z.; Formal Analysis, S.Z., J.H., N.S., and J.Y.; Investigation, S.Z; Data Curation, S.Z.; Writing—Original Draft Preparation, S.Z. and J.H.; Writing—Review & Editing, N.S., J.Y., J.H., S.Z., and A.A.; Visualization, S.Z. and J.H.; Supervision, J.Y., N.S. and J.H.; Project Administration, J.Y.

Funding: This research received no external funding.

Acknowledgments: The authors would like to thank the ministry of higher education of Libya for providing financial support for PhD study; Brian Daber from Department of Dental Biomaterial, University of Manchester; Paul Murphy from University Dental Hospital of Manchester; Michael Green and Hayley Andrews from the Faculty of Science and Engineering, Manchester Metropolitan University and Gary Pickles from School of Materials, University of Manchester, for supporting the experimental work.

Conflicts of Interest: The authors declare no conflict of interest.

Abbreviations

PMMA	Poly-methyl methacrylate
MMA	Methyl methacrylate
HI	High impact heat cured acrylic resin
HV	Vickers hardness
SD	Standard deviation
IQR	Interquartile range
SEM	Scanning Electron Microscope

References

1. Zappini, G.; Kammann, A.; Wachter, W. Comparison of fracture tests of denture base materials. *J. Prosthet. Dent.* **2003**, *90*, 578–585. [CrossRef]
2. Kanie, T.; Fujii, K.; Arikawa, H.; Inoue, K. Flexural properties and impact strength of denture base polymer reinforced with woven glass fibers. *Dent. Mater.* **2000**, *16*, 150–158. [CrossRef]
3. Vojdani, M.; Bagheri, R.; Khaledi, A.A.R. Effects of aluminum oxide addition on the flexural strength, surface hardness, and roughness of heat-polymerized acrylic resin. *J. Dent. Sci.* **2012**, *7*, 238–244. [CrossRef]
4. Sasaki, H.; Hamanaka, I.; Takahashi, Y.; Kawaguchi, T. Effect of long-term water immersion or thermal shock on mechanical properties of high-impact acrylic denture base resins. *Dent. Mater. J.* **2016**, *35*, 204–209. [CrossRef]
5. Jagger, D.C.; Harrison, A.; Jandt, K. The reinforcement of dentures. *J. Oral Rehabil.* **1999**, *26*, 185–194. [CrossRef]
6. Nejatian, T.; Johnson, A.; van Noort, R. Reinforcement of denture base resin. *Adv. Sci. Technol.* **2006**, *49*, 124–129. [CrossRef]

7. Agha, H.; Flinton, R.; Vaidyanathan, T. Optimization of Fracture Resistance and Stiffness of Heat-Polymerized High. Impact Acrylic Resin with Localized E-Glass FiBER FORCE(R) Reinforcement at Different Stress Points. *J. Prosthodont.* **2016**, *25*, 647–655. [CrossRef] [PubMed]
8. Jagger, D.; Harrison, A.; Jagger, R.; Milward, P. The effect of the addition of poly(methyl methacrylate) fibres on some properties of high strength heat-cured acrylic resin denture base material. *J. Oral Rehabil.* **2003**, *30*, 231–235. [CrossRef]
9. Stafford, G.; Bates, J.; Huggett, R.; Handley, R. A review of the properties of some denture base polymers. *J. Dent.* **1980**, *8*, 292–306. [CrossRef]
10. Abdulwahhab, S.S. High-impact strength acrylic denture base material processed by autoclave. *J. Prosthodont. Res.* **2013**, *57*, 288–293. [CrossRef]
11. Jagger, D.C.; Jagger, R.G.; Allen, S.M.; Harrison, A. An investigation into the transverse and impact strength of 'high strength' denture base acrylic resins. *J. Oral Rehabil.* **2002**, *29*, 263–267. [CrossRef]
12. Zheng, J.; Wang, L.; Hu, Y.; Yao, K. Toughening effect of comonomer on acrylic denture base resin prepared via suspension copolymerization. *J. Appl. Polym. Sci.* **2012**, *123*, 2406–2413. [CrossRef]
13. Kim, S.-H.; Watts, D.C. The effect of reinforcement with woven E-glass fibers on the impact strength of complete dentures fabricated with high-impact acrylic resin. *J. Prosthet. Dent.* **2004**, *91*, 274–280. [CrossRef]
14. Yu, S.-H.; Cho, H.-W.; Oh, S.; Bae, J.-M. Effects of glass fiber mesh with different fiber content and structures on the compressive properties of complete dentures. *J. Prosthet. Dent.* **2015**, *113*, 636–644. [CrossRef]
15. Gad, M.M.; Fouda, S.M.; Al-Harbi, F.; Näpänkangas, R.; Raustia, A.; Al-Harbi, F. PMMA denture base material enhancement: A review of fiber, filler, and nanofiller addition. *Int. J. Nanomed.* **2017**, *12*, 3801–3812. [CrossRef]
16. Uzun, G.; Hersek, N.; Tincer, T. Effect of five woven fiber reinforcements on the impact and transverse strength of a denture base resin. *J. Prosthet. Dent.* **1999**, *81*, 616–620. [CrossRef]
17. Köroğlu, A.; Özdemir, T.; Usanmaz, A. Comparative study of the mechanical properties of fiber-reinforced denture base resin. *J. Appl. Polym. Sci.* **2009**, *113*, 716–720. [CrossRef]
18. Kim, H.-H.; Kim, M.-J.; Kwon, H.-B.; Lim, Y.J.; Kim, S.-K.; Koak, J.-Y. Strength and cytotoxicity in glass-fiber-reinforced denture base resin with changes in the monomer. *J. Appl. Polym. Sci.* **2012**, *126*, E260–E266. [CrossRef]
19. Vallittu, P.K.; Lassila, V.P.; Lappalainen, R. Transverse strength and fatigue of denture acrylic-glass fiber composite. *Dent. Mater.* **1994**, *10*, 116–121. [CrossRef]
20. Vallittu, P.K.; Lassila, V.P.; Lappalainen, R. Acrylic resin-fiber composite—Part I: The effect of fiber concentration on fracture resistance. *J. Prosthet. Dent.* **1994**, *71*, 607–612. [CrossRef]
21. Pan, Y.; Liu, F.; Xu, D.; Jiang, X.; Yu, H.; Zhu, M. Novel acrylic resin denture base with enhanced mechanical properties by the incorporation of PMMA-modified hydroxyapatite. *Prog. Nat. Sci. Mater. Int.* **2013**, *23*, 89–93. [CrossRef]
22. Zhang, X.-Y.; Zhang, X.-J.; Huang, Z.-L.; Zhu, B.-S.; Chen, R.-R. Hybrid effects of zirconia nanoparticles with aluminum borate whiskers on mechanical properties of denture base resin PMMA. *Dent. Mater. J.* **2014**, *33*, 141–146. [CrossRef] [PubMed]
23. Wang, T.; Tsoi, J.K.-H.; Matinlinna, J.P. A novel zirconia fibre-reinforced resin composite for dental use. *J. Mech. Behav. Biomed. Mater.* **2016**, *53* (Suppl. C), 151–160. [CrossRef]
24. Kawai, N.; Lin, J.; Youmaru, H.; Shinya, A.; Shinya, A. Effects of three luting agents and cyclic impact loading on shear bond strengths to zirconia with tribochemical treatment. *J. Dent. Sci.* **2012**, *7*, 118–124. [CrossRef]
25. Gad, M.M.; Rahoma, A.; Al-Thobity, A.M.; ArRejaie, A.S. Influence of incorporation of ZrO_2 nanoparticles on the repair strength of polymethyl methacrylate denture bases. *Int. J. Nanomed.* **2016**, *11*, 5633–5643. [CrossRef]
26. British Standards. *Dentistry-Base polymers BS EN ISO 20795-1:2008*; Biritish Standards Institution (BSI): London, UK, 2008; p. 36.
27. British Standards. *British Standard Specification for Denture base Polymers BS 2487:1989 ISO 1567:1988*; Biritish Standards Institution (BSI): London, UK, 1989; p. 10.
28. Jerolimov, V.; Brooks, S.; Huggett, R.; Bates, J. Rapid curing of acrylic denture-base materials. *Dent. Mater.* **1989**, *5*, 18–22. [CrossRef]

29. Al-Haddad, A.; Roudsari, R.V.; Satterthwaite, J.D. Fracture toughness of heat cured denture base acrylic resin modified with Chlorhexidine and Fluconazole as bioactive compounds. *J. Dent.* **2014**, *42*, 180–184. [CrossRef] [PubMed]
30. European International Standard Organization. *European International Standard Organization (EN ISO 179-1:2000)*; International Organization for Standardization: Geneva, Switzerland, 2000.
31. Neppelenbroek, K.H.; Pavarina, A.C.; Vergani, C.E.; Giampaolo, E.T. Hardness of heat-polymerized acrylic resins after disinfection and long-term water immersion. *J. Prosthet. Dent.* **2005**, *93*, 171–176. [CrossRef]
32. Farina, A.P.; Cecchin, D.; Soares, R.G.; Botelho, A.L.; Takahashi, J.M.F.K.; Mazzetto, M.O.; Mesquita, M.F. Evaluation of Vickers hardness of different types of acrylic denture base resins with and without glass fibre reinforcement. *Gerodontology* **2012**, *29*, e155–e160. [CrossRef]
33. Li, B.B.; Bin Xu, J.; Cui, H.Y.; Lin, Y.; Di, P. In vitro evaluation of the flexural properties of All-on-Four provisional fixed denture base resin partially reinforced with fibers. *Dent. Mater. J.* **2016**, *35*, 264–269. [CrossRef]
34. Gad, M.M.; Abualsaud, R.; Rahoma, A.; Al-Thobity, A.M.; Al-Abidi, K.S.; Akhtar, S. Effect of zirconium oxide nanoparticles addition on the optical and tensile properties of polymethyl methacrylate denture base material. *Int. J. Nanomed.* **2018**, *13*, 283. [CrossRef]
35. Asar, N.V.; Albayrak, H.; Korkmaz, T.; Turkyilmaz, I. Influence of various metal oxides on mechanical and physical properties of heat-cured polymethyl methacrylate denture base resins. *J. Adv. Prosthodont.* **2013**, *5*, 241–247. [CrossRef]
36. Alhareb, A.O.; Ahmad, Z.A. Effect of Al_2O_3/ZrO_2 reinforcement on the mechanical properties of PMMA denture base. *J. Reinf. Plast. Compos.* **2011**, *30*, 86–93. [CrossRef]
37. Hamza, T.A.; Rosenstiel, S.F.; Elhosary, M.M.; Ibraheem, R.M. The effect of fiber reinforcement on the fracture toughness and flexural strength of provisional restorative resins. *J. Prosthet. Dent.* **2004**, *91*, 258–264. [CrossRef]
38. Kundie, F.; Azhari, C.H.; Ahmad, Z.A. Effect of nano-and micro-alumina fillers on some properties of poly (methyl methacrylate) denture base composites. *J. Serb. Chem. Soc.* **2018**, *83*, 75–91. [CrossRef]
39. Sodagar, A.; Bahador, A.; Khalil, S.; Shahroudi, A.S.; Kassaee, M.Z. The effect of TiO_2 and SiO_2 nanoparticles on flexural strength of poly (methyl methacrylate) acrylic resins. *J. Prosthodont. Res.* **2013**, *57*, 15–19. [CrossRef]
40. Fan, F.; Xia, Z.; Li, Q.; Li, Z.; Chen, H. ZrO_2/PMMA nanocomposites: Preparation and its dispersion in polymer matrix. *Chin. J. Chem. Eng.* **2013**, *21*, 113–120. [CrossRef]
41. Ali, I.L.; Yunus, N.; Abu-Hassan, M.I. Hardness, Flexural Strength, and Flexural Modulus Comparisons of Three Differently Cured Denture Base Systems. *J. Prosthodont.* **2008**, *17*, 545–549. [CrossRef]
42. Piconi, C.; Maccauro, G. Zirconia as a ceramic biomaterial. *Biomaterials* **1999**, *20*, 1–25. [CrossRef]
43. Hu, Y.; Zhou, S.; Wu, L. Surface mechanical properties of transparent poly(methyl methacrylate)/zirconia nanocomposites prepared by in situ bulk polymerization. *Polymer* **2009**, *50*, 3609–3616. [CrossRef]

materials

MDPI

Article

Evaluation of Equivalent Flexural Strength for Complete Removable Dentures Made of Zirconia-Impregnated PMMA Nanocomposites

Saleh Zidan [1,2,*], Nikolaos Silikas [1], Julfikar Haider [3], Abdulaziz Alhotan [1], Javad Jahantigh [1] and Julian Yates [1]

1 Dentistry, School of Medical Sciences, University of Manchester, Manchester M13 9PL, UK; nikolaos.silikas@manchester.ac.uk (N.S.); abdulaziz.alhotan@postgrad.manchester.ac.uk (A.A.); javad.jahantigh@mft.nhs.uk (J.J.); julian.yates@manchester.ac.uk (J.Y.)
2 Department of Dental Materials, Faculty of Dentistry, Sebha University, Sebha, Libya
3 Department of Engineering, Manchester Metropolitan University, Manchester M1 5GD UK; j.haider@mmu.ac.uk
* Correspondence: saleh.zidan@postgrad.manchester.ac.uk; Tel.: 44-79-3309-6536

Received: 2 May 2020; Accepted: 3 June 2020; Published: 5 June 2020

Abstract: High-impact (HI) polymethyl methacrylate (PMMA), obtained from modification of conventional PMMA, is commonly used in prosthodontics as a denture base material for improved impact resistance. However, it suffers from poor flexural strength properties. The aim of this study was to investigate the flexural strength of complete removable dentures made of HI heat-polymerised PMMA resin reinforced with zirconia nanoparticles at two different concentrations. The effect of fatigue loading on the flexural strength behaviour of the dentures was also investigated. A total of 30 denture specimens were fabricated from PMMA with different concentrations of zirconia nanoparticles: 0 (control), 3, and 5 wt.%. Ten specimens in each group were divided into two subgroups, with five specimens in each, to conduct both flexural strength and fatigue loading test of each of the subgroups. Fatigue loading was applied on the dentures using a mastication simulator and equivalent flexural strength was calculated with data from bending tests with and without fatigue cyclic loading. One-way analysis of variance (ANOVA) of the test data was conducted with the Bonferroni significant difference post-hoc test at a preset alpha value of 0.05. Paired *t*-test was employed to identify any difference between the specimens with and without the application of fatigue loading. The fractured surface of the denture specimens was examined with a scanning electron microscope (SEM). The bending tests demonstrated that the mean equivalent flexural strength of reinforced HI PMMA denture specimens with 5 wt.% zirconia nanoparticles increased significantly (134.9 ± 13.9 MPa) compared to the control group (0 wt.%) (106.3 ± 21.3 MPa) without any fatigue loading. The mean strength of the dentures with PMMA +3 wt.% zirconia also increased, but not significantly. Although the mean strength of all specimen groups subjected to fatigue loading slightly decreased compared to that of the specimen groups without any fatigue cyclic loading, this was not statistically significant. Denture specimens made of HI heat-polymerised PMMA reinforced with 5 wt.% zirconia nanoparticles had significantly improved equivalent flexural strength compared to that made of pure PMMA when the specimens were not subjected to any prior fatigue cyclic loading. In addition, the application of fatigue cyclic loading did not significantly improve the equivalent flexural strengths of all denture specimen groups. Within the limitations of this study, it can be concluded that the use of zirconia-impregnated PMMA in the manufacture of dentures does not result in any significant improvement for clinical application.

Keywords: denture base; high-impact PMMA; zirconia (ZrO_2); nanocomposite; flexural strength; fatigue loading

Materials **2020**, *13*, 2580; doi:10.3390/ma13112580 www.mdpi.com/journal/materials

1. Introduction

The acrylic resin polymethyl methacrylate (PMMA) is widely used for the manufacture of dental prostheses, including conventional removable complete or partial dentures and implant-supported prostheses [1]. Acrylic resins have many advantages, including acceptable aesthetic appearance, lightness, biocompatibility, and ease of processing in the laboratory for clinical use [2,3]. However, this material is still some way from possessing the ideal mechanical properties for denture base and other prosthetic applications, suffering from low resistance to impact, flexural weakness, and fatigue [4]. The fracture of dentures is the most frequent problem when patients present with failures of their prostheses. Many of these fractures occur inside the mouth as a result of denture fatigue caused by mastication processes [5]. It is widely accepted that many materials suffer a loss of strength as a result of cyclical stress over a long period of time. Microcracks start to generate at the point of alternating stresses in the denture, propagate through the material, and finally lead to fatigue failure after a certain period of time [3,6]. Flexural fatigue of PMMA has been determined as a cause of midline fractures of complete dentures [7]. Majority of fractures occurred in the midline of maxillary complete dentures, with the incidence being 2–3 times higher when compared to mandibular dentures [8,9]. Additionally, acrylic resin dentures demonstrated flexing during functioning to a much greater degree than expected, as well as poor tissue adaptation [6]. Various attempts have been made in the past to improve the mechanical properties of denture base acrylic resins by incorporating particles, wires, fibres, or mesh aligned with the shape of the denture base [10–14]. One of the most notable developments was based on the chemical modification of conventional PMMA with rubber particles (butadiene-styrene) with sizes ranging from 1 to 5 μm, marketed as a "high-impact" variation [14]. This has been successful, to a certain extent, in improving the impact strength and dimensional stability [15–18]. However, the incorporation of rubber decreases the flexural and fatigue strengths and the modulus of elasticity compared to conventional heat-polymerised acrylic resins [15,17–19]. Several in vitro studies have investigated performance of metal wire-reinforced acrylic dentures [10,11,13]. Maxillary complete dentures made of acrylic resin reinforced with metal wire (Cr–Co alloys) were placed under the ridge lap in the anterior region and in the anterior and posterior regions of the denture base. The tests showed that the wire reinforcement increased the flexural strength of the dentures [13]. However, reinforcement of acrylic resin with metal wires often resulted in wire separation at the interface due to poor adhesion between the denture base resin and metal reinforcement [20,21]. In addition, the addition of metal wire often resulted in unacceptable denture aesthetics and significantly increased the overall mass of the denture base [22].

Exploring substitutes for metal reinforcement, other studies have reported incorporation of microfibres such as aramid, ultrahigh molecular weight polyethylene, carbon, nylon, urethane oligomer and E-glass in the forms of chopped, flaked, continuous, or woven constituents [3,11,23]. Several studies concluded that glass-fibre reinforcement significantly increased flexural strength, flexural modulus, and impact strength of acrylic dentures [3,7,10,11,13,20,23]. Vallittu et al. and Im et al. reported improved fatigue and fracture resistance from a complete denture made of acrylic resin reinforced with glass fibres with force magnitudes of 80, 100, and 180 N applied to the occlusal surfaces of the test specimens with fatigue cyclic loading repeated at 300,000 masticatory cycles in a mastication simulator machine, the equivalent to real-life use for over a year [7,10,12]. A clinical study investigated the orientation of the glass fibres in PMMA dentures and suggested that they should be placed close to the location of highest tensile stress to prevent any initiation of fracture. However, incorrect positioning of glass fibres could lead to a decrease in mechanical properties [13,24]. Therefore, it is challenging to manufacture dentures with accurate fibre positioning and to maintain the mechanical properties consistently from a quality control point of view.

Recently, numerous investigations have focused on adding nanoparticles such as yttria-stabilised tetragonal zirconia polycrystals (Y-TZP) to improve the mechanical and physical properties of conventional heat-polymerised denture base resins [25–27]. This type of zirconia, called "ceramic steel", possesses superior mechanical properties, good surface properties, and high biocompatibility, thus making it an attractive option for many dental applications [28]. In the authors' previous study [26] with beam-type PMMA–zirconia nanocomposite samples, it was determined that optimum flexural strength can be obtained by adding zirconia nanoparticles at approximately 3 and 5 wt.%.

To date, the effect of zirconia nanoparticles on the flexural strength and fatigue loading cycles of HI PMMA has not been evaluated with specimens of a similar shape to a complete denture. Therefore, the aim of this study was to investigate the flexural strength properties of complete dentures made from HI heat-polymerised PMMA resin reinforced with zirconia nanoparticles with and without fatigue cyclic loading in a mastication simulator. The hypothesis was that HI heat-polymerised PMMA incorporated with zirconia nanoparticles with and without fatigue cyclic loading would lead to a significant increase in value of the flexural strength of the complete dentures.

2. Materials and Experimental Method

2.1. Materials

A commercially available Metrocryl HI denture base powder, PMMA (polymethyl methacrylate), and Metrocryl HI (X-Linked) denture base liquid (MMA, methyl methacrylate) (Metrodent Limited, Huddersfield, UK) were selected as the denture base material. Yttria-stabilised zirconia (ZrO_2) (94% purity; Sky Spring Nano Materials, Inc., Houston, TX, USA) nanoparticles with an average size between 30 and 100 nm were chosen as the inorganic filler agent for fabricating the nanocomposite denture specimens, as shown in Table 1.

Table 1. Materials used in making complete removable dentures.

Materials	Trade Name	Manufacturer	Lot. Number
High-impact heat-curing acrylic denture base resin	HI Metrocryl	Metrodent Limited, Huddersfield, UK	Powder (22828) Liquid (103/4)
Yttria-stabilised zirconium oxide	Zirconium oxide	Sky Spring Nano Materials, Inc., Houston, TX, USA	8522–120315
Dental plaster	Flasking plaster	Saint-Gobain, Formula, Newark, UK	0411217–3
High-strength dental stone	Dentstone KD	Saint-Gobain, Formula, Newark, UK	085217–5
Type 4 diestone	Metrostone	Metrodent Limited, Huddersfield, UK	032218–1
Addition cure silicone putty 1:1	Sheraduplica	Shera, Lemforde, Huddersfield, UK	Base (86392) Catalyst (86047)
3-Trimethoxysilyl propyl methacrylate	Silane coupling agent	Sigma Aldrich, Gillingham, UK	440159

2.2. Selection of Appropriate Percentages of Zirconia Nanoparticles

Three groups of complete dentures were prepared for this study by the first researcher and their compositions are described in Table 2. All had an acrylic resin powder-to-monomer ratio of 21 g:10 mL, in accordance with the manufacturer's instructions. The particle salinisation procedure can be found in [26].

Table 2. Weight percent zirconia in combination with acrylic resin powder as well as monomer content of the specimen groups.

Experimental Groups	Zirconia (wt.%)	Zirconia (g)	HI PMMA Powder (g)	HI MMA Monomer (mL)
Control	0.0	0.000	21.000	10.0
Nanocomposite-1	3.0	0.630	20.370	10.0
Nanocomposite-2	5.0	1.050	19.950	10.0

2.3. Preparation of Complete Removable Dentures

Maxillary edentulous master casts were duplicated using an addition cure silicone putty to obtain a mould that was then used to produce thirty edentulous casts by pouring high-strength dental stone into the silicone mould. Two sheets of baseplate wax (Metro wax, Metrodent Limited, Huddersfield, UK) with a thickness of 3.50 mm were adapted onto the palatal surface on the edentulous cast, and then the occlusal rim was placed on denture base wax. The maxillary master cast with occlusal rim was fixed on an articulator (John Winter, Halifax, UK) using dental plaster in preparation for setting the teeth. Then, the maxillary anterior teeth (Artic 6M S10 shade BL3, Metrodent Limited, Huddersfield, UK) and maxillary posterior teeth (Artic 8M 10 30U shade A2, Metrodent Limited, Huddersfield, UK) were fixed onto the occlusal rim. Upon completing waxing of the denture base and teeth, the wax denture and plaster cast were removed from the articulator and placed in a flask filled with dental plaster and dental stones were place onto the teeth, after setting. The denture wax was then removed through dewaxing process.

The silane-treated zirconia and acrylic resin powders were weighed according to Table 2, using an electronic balance with an accuracy of three decimal points (Ohaus Analytical plus, Ohaus Corporation, Parsippany, NJ, USA). Where indicated, zirconia powder was added at the appropriate concentration to the acrylic resin monomer and mixed in a speed mixer (DAC 150.1 FVZK, High Wycombe, UK) at 2500 rpm for 5 min. Once mixed, the acrylic resin powder was then added to the solution, and mixed again in accordance with the manufacturer's instruction, until a smooth, uniform mixture was obtained. The mixture was then packed into the flask, pressurised, and immersed in a curing water bath for 6 h to allow polymerisation.

The flask was then removed from the curing bath and left to cool 30 min at room temperature. The flask was then opened, and the denture removed. The denture was placed in an ultrasonic cleaning machine containing water (Elma Electronic, Bedford, UK) to remove any attached stone, trimmed using a tungsten carbide bur (D B Orthodontics, Yorkshire, UK), ground with an emery paper grit 40 (Norton, Saint-Gobain, Stafford, UK) and, finally, polished with pumice powder in a polishing machine (Tavom, Wigan, UK). All thirty denture specimens were fabricated individually in the manner detailed above.

2.4. Mechanical Strength Test

Fatigue cyclic loading was performed according to a previous study by Im et al. using a chewing simulator (CS-44.2 SD Mechatronik GmbH, Westerham, Germany) that simulated maxillary and mandibular movement in the mouth during mastication (Figure 1) [10].

Fifteen denture specimens, five from each group, were employed for fatigue tests. The upper bar faced the centre of midline of the denture and T-shaped jig was placed against the second premolar (full) and first molar (partial) teeth on each side at 1.6 Hz. The initial loading applied on the denture was 8 kg (78.48 N). The vertical movement of the T-bar was set at 2 mm and lateral movement at 0.2 mm, with a vertical speed of 30 mm/s. A total number of 250,000 mastication cycles were performed in 37 °C distilled water to simulate approximately one year of use in an oral environment.

Thirty denture specimens with and without fatigue cyclic loading were subjected to three-point bending test in a Hounsfield universal testing machine (Hounsfield Tensometer, H10KS, Birmingham, UK). The distance between the second molar teeth (last tooth on each side) acted as a supporting span with a length of 42.33 ± 0.2 mm. The load was applied to the palatal fitting surface at a crossover point between the palatal midline and the line connecting the centre of first molars on each side of the denture.

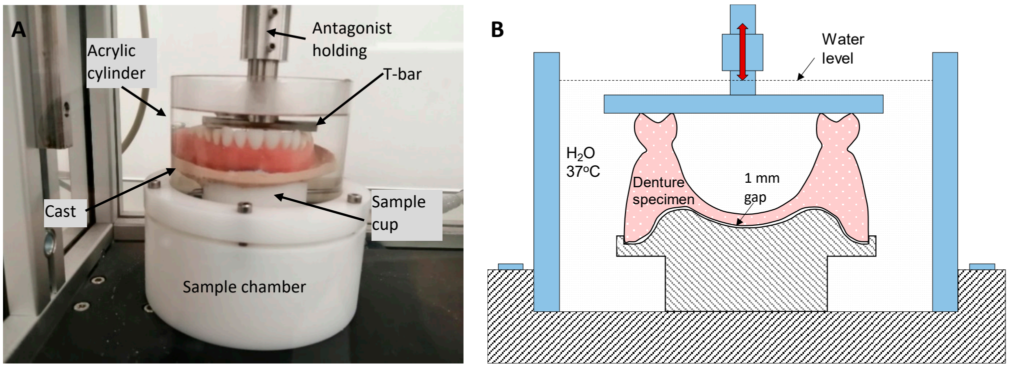

Figure 1. (**A**) Test setup for mastication simulation under fatigue cyclic loading and (**B**) schematic diagram of mastication fatigue loading.

The thickness of the dentures was measured using a digital micrometer (Mitutoyo, Andover, UK) at the point of loading around the central palatal area. The average dimension was 3 ± 0.2 mm. The width of the load bearing area of the dentures was measured as 42 ± 0.2 mm, and the weight of all denture specimens were measured using an electronic digital scale (Machine Mart Limited, Nottingham, UK). The equivalent flexural strength was calculated in MPa for all denture specimens using Equation (1) [29].

$$\sigma = \frac{3\mathrm{Fl}}{2\mathrm{bh}^2} \tag{1}$$

where F is the maximum force applied in N, l is the distance between the teeth supports in mm, b is the width of load bearing area of the denture specimen in mm, and h is the thickness of the denture specimen in mm at the point of loading.

Figure 2 presents a picture and a schematic diagram of the bending test experimental setup.

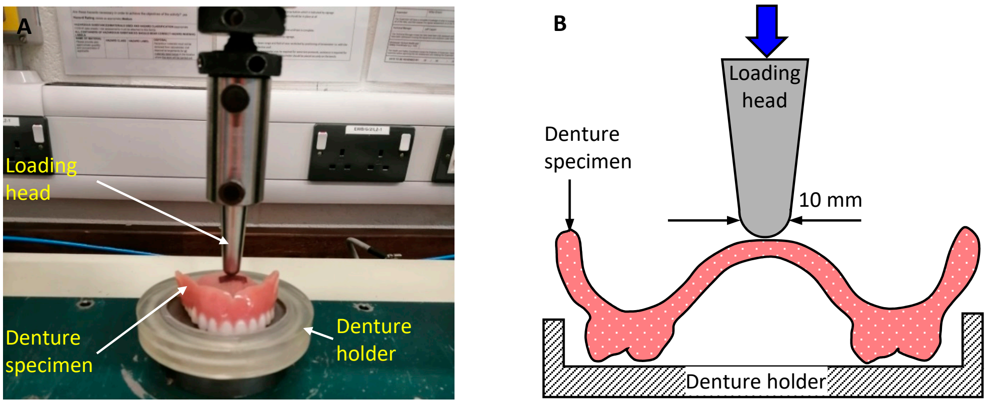

Figure 2. (**A**) Applying bending load on palatal surface of denture specimen in Hounsfield universal testing machine and (**B**) schematic diagram of loading conditions.

2.5. Fracture Behaviour Examination

Following fracture of the denture, the midline fractured surfaces from the bending tests of complete dentures were also studied using a scanning electron microscope (SEM) using a secondary electron detector at an acceleration voltage of 2.0 kV (Carl Zeiss Ltd., 40 VP, Smart SEM, Cambridge, UK) in order to identify the mechanism of failure. Part of the fractured specimens were mounted onto slotted aluminium stubs and coated with a thin layer of gold/palladium using a sputter coater.

2.6. Statistical Analysis

The recorded results of bending with and without fatigue loading were calculated and statistically analysed using statistical software (SPSS statistics version 23, IBM, New York, NY, USA). Non-significant Shapiro–Wilk tests demonstrated that data from the bending strength tests was normally distributed and there was homogeneity of variance. A one-way analysis of variance (ANOVA) was used with the Bonferroni significant difference post-hoc test at a preset alpha value of 0.05. In addition, a paired *t*-test analysis was applied to identify any significant difference between the groups at a preset alpha value of 0.05, with and without fatigue loading.

3. Results

3.1. Weight and Visual Analysis of Denture Specimens

The mean weights of non-reinforced and reinforced complete dentures with 3 wt.% and 5 wt.% zirconia are listed in Table 3. The non-reinforced complete dentures were slightly heavier than the reinforced ones. However, the difference when compared to the reinforced dentures was negligible. This indicated that the addition of zirconia did not significantly change the weight of the dentures.

Table 3. Weight of complete dentures made of pure polymethyl methacrylate (PMMA) and zirconia-impregnated PMMA.

Weight of Non-Reinforced PMMA Dentures (g) (Mean ± SD)	**Weight of Reinforced PMMA Dentures (g) (Mean ± SD)**	
Control Group 0 wt.% of zirconia	3 wt.% of zirconia	5 wt.% of zirconia
20.1 ± 1.0	19.5 ± 0.2	19.5 ± 1.0

3.2. Cyclic Fatigue Loading

Among the fifteen denture specimens that underwent fatigue cyclic loading tests in the mastication simulator, no dentures failed due to cracking or fracture. This indicated that all dentures, including the reinforced ones, would survive for at least a year in clinical service.

3.3. Equivalent Flexural Strength

Force versus deflection curves of the different denture groups without any fatigue cyclic loading during the bending tests are presented in Figure 3.

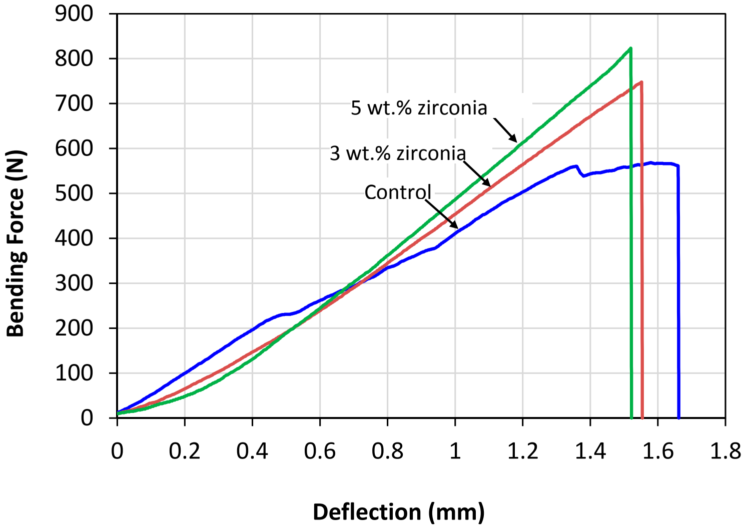

Figure 3. Typical bending load vs. deflection curves without fatigue cyclic loading for pure high impact (HI)-PMMA and zirconia-reinforced nanocomposites.

The peak breaking forces gradually increased with the increasing percentage of zirconia nanoparticles. Similar behaviour was also noticed for denture specimens following fatigue cyclic loading. One-way analysis of variance (ANOVA) of mean flexure strengths with and without fatigue loading is presented in Table 4.

Table 4. Maximum force (N) and mean and SD of values the equivalent flexural strength (MPa) before and after fatigue cyclic loading for the test groups.

	Without Fatigue Cyclic Loading		**With Fatigue Cyclic Loading**	
Weight Percent Zirconia	**Maximum Force (N)**	**Equivalent Flexural Strength (MPa) and SD**	**Maximum Force (N)**	**Equivalent Flexural Strength (MPa) and SD**
Control (0.0 %)	633.2	106.3 (21.3)^{Aa}	598.9	100.6 (17.4)^{Aa}
3.0 %	757.0	127.1 (5.8)^{Ab}	643.8	108.1 (15.2)^{Ab}
5.0 %	803.6	134.9 (13.9)^{Bc}	662.2	111.2 (15.45)^{Ac}

Note: Within a column, cells having similar (upper case) letters are not significantly different from the control group (0% zirconia content) and within a row values identified using the same lower-case letters are not significantly different; n = 5 specimens per group.

The specimen groups containing 3 wt.% zirconia with and without fatigue cyclic loading showed a 7.45% and 19.55% increase in the equivalent flexural strength and maximum force, respectively, when compared to the control group. In comparison, the specimen groups containing 5 wt.% zirconia with and without fatigue cyclic loading showed a 10.53% and 26.91% increase in the equivalent flexural strength. The highest increase in the mean value of strength was found for the group containing 5 wt.% zirconia (134.9 MPa) without fatigue cyclic loading, which also showed a significant difference ($p < 0.05$) when compared to the control group (106.3 MPa). However, all the mean strengths of the dentures subjected to fatigue cyclic loading were slightly lower when compared to those of the dentures without any fatigue cyclic loading, but the decrease in mean values were not significant ($p > 0.05$).

3.4. Failure Modes of Complete Dentures

After the bending tests with and without fatigue cyclic loading, all 30 denture specimens were examined to identify the failure modes; these are listed in Table 5. The failure modes of the dentures can be broadly classified into two groups: complete fracture and incomplete fracture.

Table 5. Failure modes of complete dentures with and without fatigue cyclic loading.

Failure Mode	**Name of Failure Modes**	**Control Group (0 wt.% Zirconia)**		**3 wt.% Zirconia**		**5 wt.% Zirconia**	
		Without Fatigue Loading	**With Fatigue Loading**	**Without Fatigue Loading**	**With Fatigue Loading**	**Without Fatigue Loading**	**With Fatigue Loading**
Complete fracture	Midline fracture	1	0	2	2	3	3
		Between central and lateral	-	One between central and lateral. One between centrals	One between canine and first premolar. One between central and lateral	Two between centrals. One through a central	One between centrals. One through a lateral. One between central and lateral
Incomplete fracture	Localised fracture	1	1	1	0	0	0
	Cracks	3	4	2	3	2	2

The first general mode of failure is referred to as midline fracture, where the denture was completely broken into two pieces along the midline in the palatal area, as shown in Figure 4. Midline fractures were identified in all groups except the control group with fatigue cyclic loading. The second failure mode can be divided in to two categories: localised fractures that occurred in the area where the load was applied on the denture with the compression head, and cracks that occurred at the free end of the denture. Localised fractures occurred in only 10% of the specimens, which makes it a relatively uncommon failure mode. In contrast, cracks were observed in all specimen groups. This was very common among the failure modes, representing more than 50% of the failures. In addition, no fracture was seen at the anterior and posterior frameworks of the complete dentures.

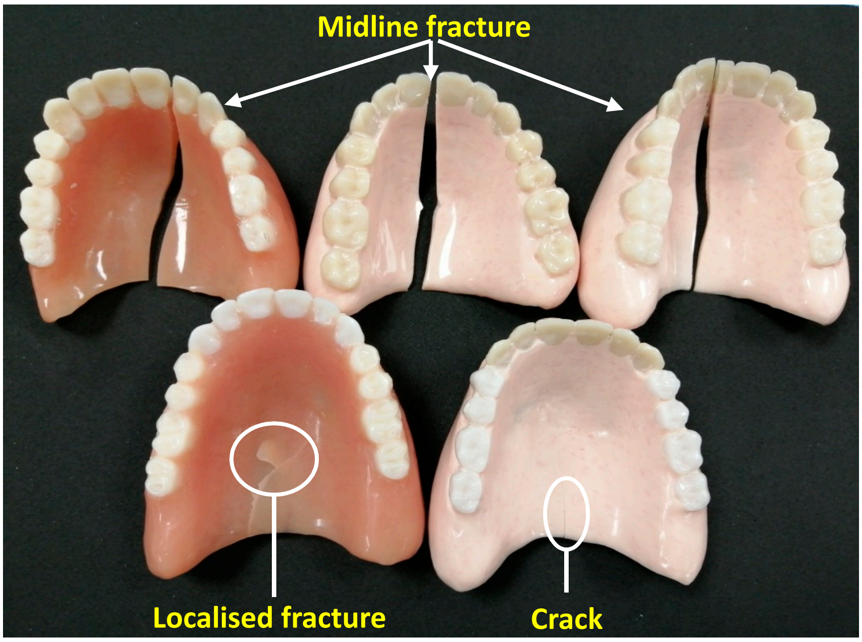

Figure 4. Failure modes observed in the dentures during the bending tests: midline fracture, localised fracture, and crack.

3.5. Fractured Specimen Analysis

Figure 5 shows fractured cross-sections of all three denture specimens (0, 3, 5 wt.% of zirconia) at the point of loading during the bending tests. All surfaces can be characterised by a pattern of globular-shaped peaks and valleys. It appeared that the globular shapes would match with the peaks and valleys in the opposite surfaces of the two broken pieces. Although the surfaces did not show any large cracks or fractures, evidences of microcracks were present. Further magnified views of the surfaces at 1000× revealed patches of smooth surfaces along with rough surface areas. Figure 6 shows the characteristics of the rough and smooth surface areas at high magnification. Small voids were visible in all surfaces. The presence of zirconia nanoparticles was observed in the nanocomposites, particularly in the smooth surface regions with indication of not fully homogeneous distribution. There was also evidence of zirconia particle clustering to a small degree, indicated by circles in Figure 6.

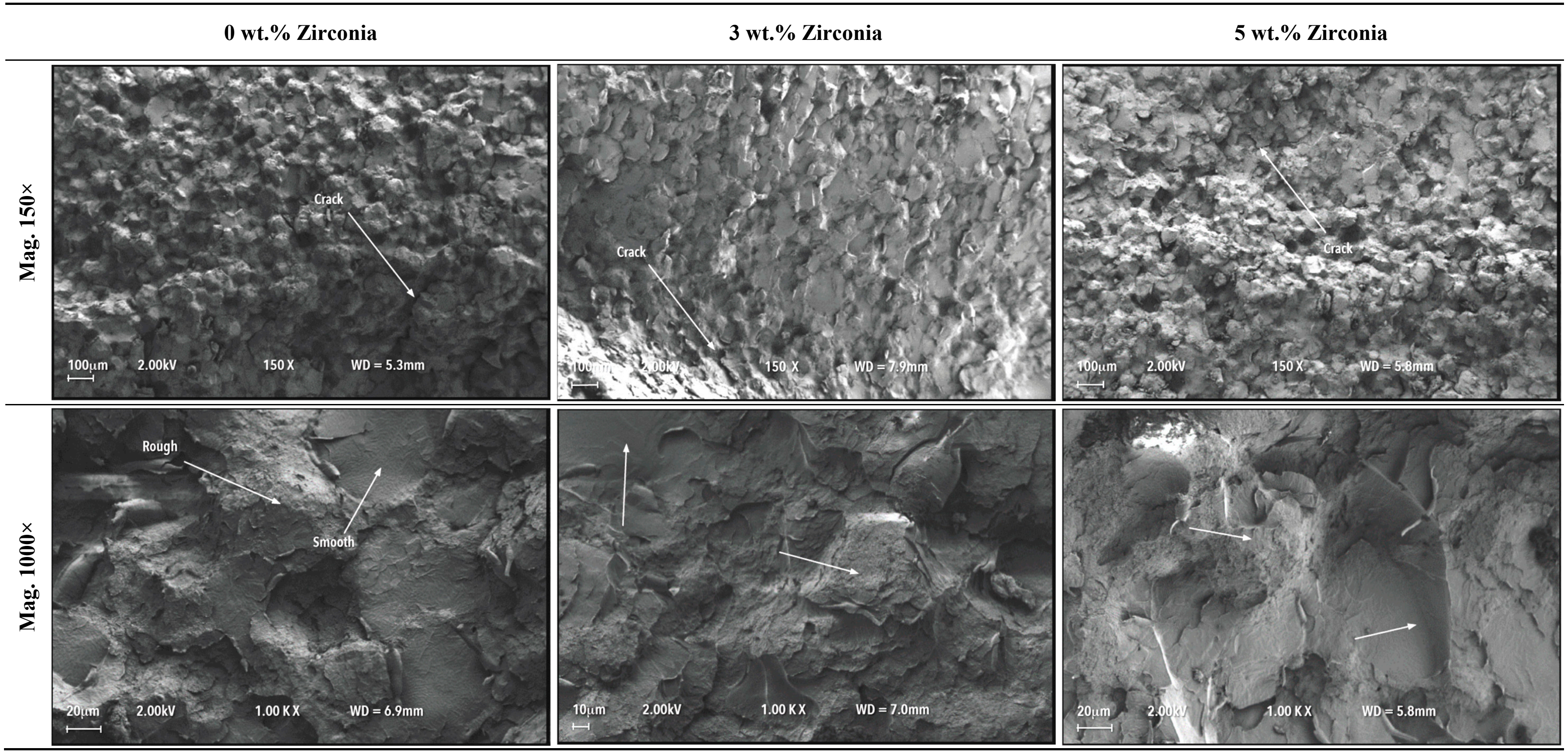

Figure 5. Fractured surfaces of denture specimens with fatigue cyclic loading during bending tests at different magnifications.

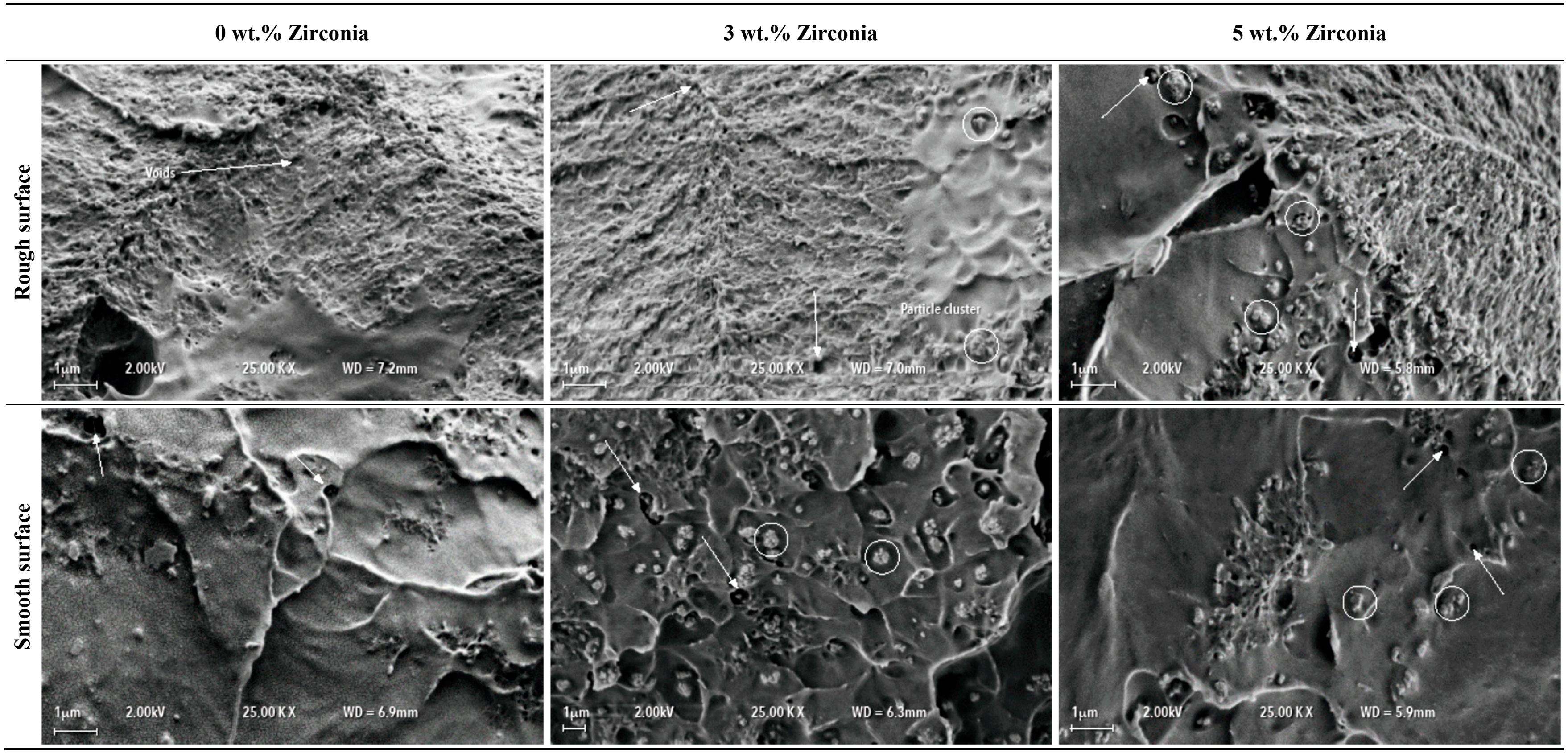

Figure 6. Fractured surfaces of dentures with fatigue cyclic loading during bending tests showing surface characteristics at 25,000×. Arrows indicate voids and circles indicate voids filled by zirconia particles.

4. Discussion

This study evaluated the effect of fatigue cyclic loading on the equivalent flexural strength of complete (maxillary) dentures. The experimental data marginally supported part of the hypothesis of the study that without any fatigue cyclic loading, the equivalent flexural strength of dentures manufactured of nanocomposite with only 5 wt.% zirconia was significantly higher than the control group, but not significantly different from that with 3 wt.% zirconia. However, the other part of the hypothesis, i.e., improvement in flexural strength of PMMA–zirconia denture base with zirconia particles after fatigue loading, was totally rejected.

The flexural strength of denture base materials is generally evaluated by a three-point bending test on a beam shape sample according to the British standard BS 20795-1:2013 (ISO 20795) using a beam shape sample according to Equation (1) [29]. In this study, bending tests were conducted on real dentures in order to conduct experiments to as close a "real" situation as possible. Additionally, using the equivalent flexural strength calculation whilst conducting bending tests directly on dentures could be considered more clinically relevant than standardised tests.

In this study, the increase in equivalent flexural strength with 3 and 5 wt.% of zirconia particles in HI-PMMA could be related to the incorporation of nanoparticles with a size ranging from 30 to 100 nm, which is demonstrably smaller than HI-PMMA powder particles (50 μm). The nanoparticles provide increased surface area to create stronger bonds between the acrylic matrix and the particles. However, the proportion of zirconia nanoparticles should be kept as relatively low as possible to ensure that they can be easily and uniformly embedded within the matrix resin without any significant particle clustering [4].

The surface of the hydrophobic polymer matrix does not wet or react well with the hydrophilic inorganic nanofillers as result of the difference in surface energies [4]. In order to improve wetting of the surfaces and adhesion bonding between the filler and matrix, the surface of hydrophobic fillers should be modified [4]. According to previous studies, the application of silane treatment could play a major role in improving chemical bonds between fillers and polymer matrix, which could therefore increase fracture resistance [3,11]. In this study, the surface of the zirconia nanoparticles was treated with a silane coupling agent that resulted in a strong adhesion between the surfaces of zirconia nanoparticles and PMMA matrix, thus leading to an improvement in the equivalent flexural strength of the nanocomposites [2].

Furthermore, improved particle homogeneity in the HI-MMA liquid zirconia nanoparticle mixture was ensured using a speed mixer machine, which was also thought to contribute to the improvement in the equivalent flexural strength. It is expected that a homogeneous distribution of zirconia particles would fill the spaces between linear chains of acrylic resin matrix. This would therefore restrict the segmental movements of the macromolecular chains and thus improve the flexural strength of the nanocomposite [25].

After the application of fatigue loading cycles, the hypothesis that the nanocomposite dentures would display no statistically significant difference in equivalent flexural strength compared to the control group was rejected. However, 3 and 5 wt.% zirconia-impregnated PMMA dentures showed a slight increase in equivalent flexural strength with fatigue cyclic loading. This implies that under clinical conditions, the nanocomposite dentures would be either as good as, or better than, the control group. A limitation of the study was that small number of specimens for each group was tested. A larger group size would help in distinguishing the difference between them more clearly.

After the fatigue cyclic loading in the mastication simulator for 250,000 cycles, denture specimens did not show any visible cracks or fracture failures, which was equivalent to a patient using a complete denture for approximately one year. A mastication force of 40 N applied on the occlusal surface to each side of the premolar during simulation was similar to the chewing force on one side of the maxillary or mandibular complete dentures worn by a patient as reported in the literature [10]. Similar results were also found in the literature where the performance of acrylic resin denture reinforced with glass fibres and metal mesh was evaluated under a fatigue loading of 80 N and 300,000 cycles.

They concluded that the fatigue loading cycles might be insufficient to cause fatigue failure of the dentures [10]. This demonstrated agreement with this current study that no failure occurred after one year of fatigue loading cycles. However, this could be the reason for a decrease in flexural strength for all groups subjected to fatigue cyclic loading compared to that without fatigue cyclic loading. Generally, the fatigue strength of most materials decreased as a result of cyclic stress over a long period of time [7].

The classification of failure modes in this study was based on the location and propagation of fracture lines or cracks in the dentures from the point of loading or stress concentration at the palatal area. Only three types of failure were observed (midline fracture, crack, and localised fracture) unlike the failures mentioned in the literature such as complete tooth failure and denture flange failure [3]. In this study, both with and without fatigue cyclic loading, the fracture in the nanocomposite dentures started near the labial frenum and propagated either between the central, lateral, and canine teeth or first premolar teeth from the polished surface toward the fitting surface, until it reached the loading point, thus resulting in a complete midline fracture. By comparison, one denture from the control group without fatigue cyclic loading showed a midline complete fracture. It is interesting to note that complete midline fractures occurred more frequently in the nanocomposite dentures than the control group. This could be explained by the fact that even though the addition of zirconia in PMMA could increase the equivalent flexural strength, it can, at the same time, also increase the overall brittleness of the denture.

The midline fracture might have occurred as result of the notch shape of the labial frenum, which is considered a potential weak point in the denture structure [11]. Kelly et al. suggested that resistance to fatigue failure of dentures could be improved by eliminating contrasting surface contours such as deep notches at low frenal attachments during manufacture. Furthermore, acrylic resin should be carefully handled during denture fabrication as to avoid any contamination that could influence the presence of localised stress point [6].

The SEM images of the denture specimens were also analysed after the bending tests without conducting any fatigue cyclic loading in the mastication simulation machine. No noticeable differences were observed in the failure mechanism of the dentures with and without the application of fatigue cyclic loading. Only the fractured surfaces from the dentures with fatigue cyclic loading are shown here to represent the worst-case scenario. It was also observed that the size of voids was of the same order as the size of the zirconia particles. Therefore, the particles would presumably fill the empty spaces (Figure 6) and positively affect the strength of the denture. The SEM images also showed that the zirconia particles were fairly distributed within the PMMA matrix without observable particle clustering.

With zirconia-impregnated PMMA, the processing and manufacture of dentures for clinical application would avoid the issues faced with fibre or mesh reinforced dentures, such as longer processing times, incorrect positioning of the fibres within the denture, non-uniform distribution of fibres within the matrix, poor wetting of fibres across the smallest denture thickness and poor bonding between the fibres and the matrix due to lack of polymerisation [24].

5. Clinical Implications

This study suggested that maxillary complete removable dentures made of PMMA incorporating a small percentage (5 wt.%) of zirconia nanoparticles could additionally improve the equivalent flexural strength when compared to pure PMMA but not clinically significant under the condition of fatigue loading during mastication.

6. Conclusions

Removable complete dentures were made of high-impact (HI) heat-polymerised PMMA resin as a control group and HI-PMMA reinforced with zirconia nanoparticles (3 and 5 wt.%) in order to compare their equivalent flexural strengths with and without applying fatigue loading. Higher equivalent flexural strengths were found for the specimens with 5 wt.% zirconia when the compared with that of 3 wt.% zirconia and the control group, only in cases without fatigue loading cycles. The specimens subjected to fatigue cyclic loading showed an observable decrease in the equivalent flexural strength, but these were not statistically significant when compared to the specimens without fatigue cyclic loading. Within the limitations of this study, it can be concluded that dentures made with zirconia-impregnated PMMA do not result in any significant improvements for clinical application. The common failure modes in the dentures under bending were found to be midline fracture, localised fracture, and cracking. Uniform distribution of zirconia particles was observed in the fractured specimens.

Author Contributions: Conceptualization, J.Y. and S.Z.; Methodology, J.Y., S.Z., N.S., J.J., and J.H.; Validation, S.Z.; Formal Analysis, S.Z., J.H., N.S., and J.Y.; Investigation, S.Z; Data Curation, S.Z. and A.A.; Writing—Original Draft Preparation, S.Z. and J.H.; Writing—Review & Editing, N.S., J.Y., J.H., and S.Z.; Visualization, S.Z. and J.H.; Supervision, J.Y., N.S. and J.H.; Project Administration, J.Y. All authors have read and agreed to the published version of the manuscript.

Funding: This research received no external funding.

Acknowledgments: The authors would like to thank the ministry of higher education of Libya for providing financial support for PhD study; David Watts and Brian Daber from Department of Dental Biomaterial, University of Manchester; Paul Murphy from University Dental Hospital of Manchester; Michael Green and Hayley Andrews from the Faculty of Science and Engineering, Manchester Metropolitan University and Gary Pickles from School of Materials, University of Manchester, for supporting the experimental work.

Conflicts of Interest: The authors declare no conflict of interest.

Abbreviations

PMMA	polymethyl methacrylate
MMA	methyl methacrylate
HI	high-impact heat cured acrylic resin
SD	standard deviation
SEM	scanning electron microscope

References

1. Diaz-Arnold, A.M.; Vargas, M.A.; Shaull, K.L.; Laffoon, J.E.; Qian, F. Flexural and fatigue strengths of denture base resin. *J. Prosthet. Dent.* **2008**, *100*, 47–51. [CrossRef]
2. Gad, M.; Abualsaud, R.; Rahoma, A.; Al-Thobity, A.M.; Al-Abidi, K.S.; Akhtar, S. Effect of zirconium oxide nanoparticles addition on the optical and tensile properties of polymethyl methacrylate denture base material. *Int. J. Nanomed.* **2018**, *13*, 283–292. [CrossRef]
3. Yu, S.-H.; Cho, H.-W.; Oh, S.; Bae, J.-M. Effects of glass fiber mesh with different fiber content and structures on the compressive properties of complete dentures. *J. Prosthet. Dent.* **2015**, *113*, 636–644. [CrossRef]
4. Asar, N.V.; Albayrak, H.; Korkmaz, T.; Turkyilmaz, I. Influence of various metal oxides on mechanical and physical properties of heat-cured polymethyl methacrylate denture base resins. *J. Adv. Prosthodont.* **2013**, *5*, 241–247. [CrossRef]
5. Stafford, G.D.; Smith, D.C. Flexural fatigue tests of some denture base polymers. *Br. Dent. J.* **1970**, *128*, 442–445. [CrossRef]
6. Kelly, E. Fatigue failure in denture base polymers. *J. Prosthet. Dent.* **1969**, *21*, 257–266. [CrossRef]
7. Vallittu, P.K.; Lassila, V.P.; Lappalainen, R. Transverse strength and fatigue of denture acrylic-glass fiber composite. *Dent. Mater.* **1994**, *10*, 116–121. [CrossRef]
8. Takahashi, T.; Gonda, T.; Maeda, Y. Influence of palatal morphology on strain in maxillary complete dentures: A preliminary report. *Int. J. Prosthodont.* **2012**, *25*, 619–621.
9. Prombonas, A.E.; Vlissidis, D.S. Comparison of the midline stress fields in maxillary and mandibular complete dentures: A pilot study. *J. Prosthet. Dent.* **2006**, *95*, 63–70. [CrossRef]
10. Im, S.-M.; Huh, Y.-H.; Cho, L.-R.; Park, C.-J. Comparison of the fracture resistances of glass fiber mesh- and metal mesh-reinforced maxillary complete denture under dynamic fatigue loading. *J. Adv. Prosthodont.* **2017**, *9*, 22–30. [CrossRef]

11. Yu, S.-H.; Oh, S.; Cho, H.-W.; Bae, J.-M. Reinforcing effect of glass-fiber mesh on complete dentures in a test model with a simulated oral mucosa. *J. Prosthet. Dent.* **2017**, *118*, 650–657. [CrossRef] [PubMed]
12. Vallittu, P.K. Comparison of the In Vitro Fatigue Resistance of an Acrylic Resin Removable Partial Denture Reinforced With Continuous Glass Fibers or Metal Wires. *J. Prosthodont.* **1996**, *5*, 115–121. [CrossRef] [PubMed]
13. Yoshida, K.; Takahashi, Y.; Shimizu, H. Effect of Embedded Metal Reinforcements and Their Location on the Fracture Resistance of Acrylic Resin Complete Dentures. *J. Prosthodont.* **2011**, *20*, 366–371. [CrossRef] [PubMed]
14. Andreopoulos, A.G.; Papanicolaou, G.C. Rubber-Modified polymer composites. *J. Mater. Sci.* **1987**, *22*, 3417–3420. [CrossRef]
15. Zheng, J.; Wang, L.; Hu, Y.; Yao, K. Toughening effect of comonomer on acrylic denture base resin prepared via suspension copolymerization. *J. Appl. Polym. Sci.* **2011**, *123*, 2406–2413. [CrossRef]
16. Sasaki, H.; Hamanaka, I.; Takahashi, Y.; Kawaguchi, T. Effect of long-term water immersion or thermal shock on mechanical properties of high-impact acrylic denture base resins. *Dent. Mater. J.* **2016**, *35*, 204–209. [CrossRef]
17. Jagger, D.; Harrison, A.; Jagger, R.; Milward, P. The effect of the addition of poly(methyl methacrylate) fibres on some properties of high strength heat-cured acrylic resin denture base material. *J. Oral Rehabil.* **2003**, *30*, 231–235. [CrossRef]
18. Jagger, D.C.; Jagger, R.G.; Allen, S.M.; Harrison, A. An investigation into the transverse and impact strength of "high strength" denture base acrylic resins. *J. Oral Rehabil.* **2002**, *29*, 263–267. [CrossRef]
19. Jagger, D.C.; Harrison, A.; Jandt, K.D. The reinforcement of dentures. *J. Oral Rehabil.* **1999**, *26*, 185–194. [CrossRef]
20. Kim, S.-H.; Watts, D.C. The effect of reinforcement with woven E-glass fibers on the impact strength of complete dentures fabricated with high-impact acrylic resin. *J. Prosthet. Dent.* **2004**, *91*, 274–280. [CrossRef]
21. Rached, R.; De Souza, E.M.; Dyer, S.R.; Ferracane, J.L. Dynamic and static strength of an implant-Supported overdenture model reinforced with metal and nonmetal strengtheners. *J. Prosthet. Dent.* **2011**, *106*, 297–304. [CrossRef]
22. Balch, J.H.; Smith, P.D.; Marin, M.A.; Cagna, D.R. Reinforcement of a mandibular complete denture with internal metal framework. *J. Prosthet. Dent.* **2013**, *109*, 202–205. [CrossRef]
23. Fajardo, R.S.; Pruitt, L.A.; Finzen, F.C.; Marshall, G.W.; Singh, S.; Curtis, D.A. The effect of E-Glass fibers and acrylic resin thickness on fracture load in a simulated implant-supported overdenture prosthesis. *J. Prosthet. Dent.* **2011**, *106*, 373–377. [CrossRef]
24. Pan, Y.; Liu, F.; Xu, D.; Jiang, X.; Yu, H.; Zhu, M. Novel acrylic resin denture base with enhanced mechanical properties by the incorporation of PMMA-modified hydroxyapatite. *Prog. Nat. Sci.* **2013**, *23*, 89–93. [CrossRef]
25. Gad, M.M.; Al-Thobity, A.M.; Rahoma, A.; Abualsaud, R.; Al-Harbi, F.A.; Akhtar, S. Reinforcement of PMMA Denture Base Material with a Mixture of ZrO_2 Nanoparticles and Glass Fibers. *Int. J. Dent.* **2019**, *2019*, 1–11. [CrossRef] [PubMed]
26. Zidan, S.; Silikas, N.; Alhotan, A.; Haider, J.; Yates, J. Investigating the Mechanical Properties of ZrO_2-Impregnated PMMA Nanocomposite for Denture-Based Applications. *Materials* **2019**, *12*, 1344. [CrossRef]
27. Zhang, X.-Y.; Zhang, X.-J.; Huang, Z.-L.; Zhu, B.-S.; Chen, R. Hybrid effects of zirconia nanoparticles with aluminum borate whiskers on mechanical properties of denture base resin PMMA. *Dent. Mater. J.* **2014**, *33*, 141–146. [CrossRef]
28. Cavalcanti, A.N.; Foxton, R.M.; Watson, T.F.; Oliveira, M.T.; Giannini, M.; Marchi, G.M. Y-TZP Ceramics: Key Concepts for Clinical Application. *Oper. Dent.* **2009**, *34*, 344–351. [CrossRef]
29. British Standards Institution. *Dentistry—Base Polymers, Part 1: Denture Base Polymers*; BSI EN ISO 20795-1:2013; British Standards Institution (BSI): London, UK, 2013; pp. 1–35.